Patent
Attorney's Docket No. 021565-060

IN THE UNITED STATES PATENT AND TRADEMARK OFFICE

In re Patent Application of	
Peter Waterhouse et al.	Group Art Unit: 1635
Application No.: 09/287,632	Examiner: ZARA JANE
Filed: April 7, 1999	Confirmation No.: 6526
For: METHODS AND MEANS FOR OBTAINING MODIFIED PHENOTYPES	

Declaration of Dr. Elizabeth Salisbury Dennis under 37 C.F.R. section 1.132

I, Elizabeth Salisbury Dennis, hereby declare that:

1. I am a citizen of Australia. I received a Ph. D. degree in 1968 from the University of Sydney, Australia. I am an author or co-author of approximately 200 peer-reviewed research papers in the field of plant molecular biology. A copy of my curriculum vitae is attached as Exhibit I.

2. My present position is Chief Research Scientist/CSIRO Fellow in the Division of Plant Industry of the Commonwealth Scientific and Industrial Research Organisation ("CSIRO"). My present work at CSIRO includes management and supervision of research projects in plant molecular biology, including research projects on gene silencing or that use gene silencing techniques.

3. I am very experienced in the field of molecular biology, including the field of post-transcriptional gene silencing and have authored and co-authored scientific publications in this field as listed in my curriculum vitae. I, together with others working with me, have incorporated introns in genetic constructs which were expressed in plant cells, and my research group was one of the first to do so. I am personally experienced with and familiar with the use of introns.

4. I have read US Patent Application No. 09/287,632 (the "Application") including the presently pending claims and the Office Action dated 8 February 2007 issued by the United States Patent and Trademark Office in connection with the Application.

5. I note that in the Office Action the Examiner alleged that "The claim(s) contain subject matter which was not described in the specification in such a way as to reasonably convey to one skilled in the relevant art that the inventor(s), at the time the application was filed, had possession of the claimed invention."

6. It is my understanding that the Examiner believes that the specification, claims

and the art do not adequately describe the distinguishing features or attributes shared by the members of the claimed genus of DNA constructs for gene silencing comprising the recited sense and antisense nucleotide sequences and further comprising an intron sequence, whereby any intronic sequence is inserted anywhere in the chimeric DNA, and whereby the DNA construct provides for the function claimed, namely reducing the phenotypic expression of a nucleic of interest in any plant cell or in any isolated eukaryotic cell.

7. I have been informed, and confirmed for myself, that the claimed subject matter recites that the intron is in the (transcribed) DNA region (for example claim 1, line 15), not "anywhere in the chimeric DNA" as mentioned by the Examiner in the Office Action, page 4, line 6.

8. The Examiner also asserts that the Application provides only two examples of chimeric constructs which contain an intron. From this, I understand that the Examiner believes that the Application does not describe a sufficient number of different possibilities for the chimeric dsRNA constructs claimed to allow a person skilled in the art to conclude that the inventors were in possession of the genus as broadly claimed.

9. In my view a person skilled in the art most relevant to the claimed subject matter is a person with a PhD in the field of molecular biology of eukaryotes with at least three years post doctoral research experience.

10. I disagree with the Examiner for the following reasons.

11. The Application teaches at least on page 23, lines 5 to 15 that the chimeric DNA constructs of the invention may comprise an intron in the transcribed region that encodes the double-stranded RNA molecule, that the inclusion of the intron enhances the efficiency of reduction of expression of the target nucleic acid of interest, and that the intron is preferably but not necessarily located in the spacer region. The Application also teaches on page 23, lines 13 to 15 that the intron in a "particularly preferred embodiment" is the *Flaveria trinervia* pyruvate orthophosphate dikinase 2 intron 2 as used in Example 6. It is clear to me that the teaching of the Application is not limited to this specific example or the particular intron. It is my firm opinion that on reading the Application, the person skilled in the art would have readily and immediately understood that the exemplified intron could be substituted for other introns well known in the art, and that other introns would function in the same manner. Moreover, the person skilled in the art would also have understood that the precise location of the intron in the transcribed region of the chimeric gene was not critical, given the fact that the intron would be spliced out of the transcribed RNA, yielding the RNA molecule comprising the double stranded RNA region. It is obvious to me and would be clear to the skilled person that splicing out of the intron would lead to the same RNA molecule irrespective of the position of the intron in the transcribed DNA region.

12. At the filing date of the application, numerous introns from a wide range of

eukaryotic organisms and genes were well known in the art and were well characterised. Furthermore, the mechanism of splicing of introns from primary transcripts was widely understood in the art. To evidence this, I refer to excerpts from a textbook widely used by post-graduate students during the years prior to 1998. These excerpts (Exhibit 2) describe the structure and function of introns including their splicing from primary RNA transcripts. (Molecular Biology of the Cell, second edition, pages 102; 486-487, 532-535.)

13. As commonly taught in the art, as evidenced in Exhibit 2, introns were first discovered and reported in 1977 and in the following years were shown to be present in many eukaryotic genes. In most eukaryotic genes, the protein encoding sequences (exons) were found to be interrupted by non-coding sequences (introns). It was known that to produce a protein, a gene encoding the protein was first transcribed into an RNA molecule (the primary transcript) by transcription of both the exons and introns. Before or during transport of the RNA molecule from the nucleus to the cytoplasm of the cell, a complex of RNA processing enzymes removes the intron sequences, thereby producing a shorter, mature RNA molecule, which is then ultimately translated in the cytoplasm. This process is commonly called intron splicing. The size of introns is commonly in the range of about 80 nucleotides to about 10 kilobases or more, and the internal sequence of introns is generally highly variable and not conserved. The only highly conserved sequences between introns are those required for intron removal. Consensus sequences have been identified at both ends of almost all introns that are important in intron splicing. These conserved sequences are located at the boundaries of the intron sequence at the 5' end (donor site) and at the 3' end (acceptor site). The pathway by which the introns are removed has also been elucidated and is illustrated for example in Exhibit 2, page 534, demonstrating the involvement of a spliceosome which contains proteins as well as small nuclear RNA molecules, conserved in eukaryotic species.

14. At the filing date of the application, a person of ordinary skill in the art would have been well aware of many different introns existed in eukaryote genes, that these introns were removed from the primary transcripts by a universally conserved RNA splicing pathway, and that the important structural features for the removal of introns from primary transcripts were highly conserved between different introns. Thus, a person of ordinary skill in the art would have appreciated the interchangeability of the intron that is specifically exemplified in the Application for any other intron sequence. Accordingly, given what was known at the filing date of the Application, a person of ordinary skill in the art would have appreciated from reading the Application that the chimeric DNA molecules of the invention could comprise any of a variety of introns and would have known of a wide variety of introns that could be used in place of the intron used in the example.

15. Furthermore, it is my opinion that the person skilled in the art when reading the Application would have realized that the exact location of the intron in the transcribed region of the chimeric gene encoding the dsRNA gene silencing molecules was not critical for the obtained gene silencing effect, as such intron

sequences are removed from the primary transcripts during splicing, and that the resultant spliced dsRNA molecule would be the same irrespective of the exact position of the intron in the transcribed region. Therefore, the chimeric genes would be expected to be functional irrespective of the position of the intron in the transcribed region.

16. Therefore it is my firm opinion that when the person skilled in the art is taught by the present application to include an intron in the chimeric DNA, it would have been immediately clear to such person that the teaching of the Application is not limited to the specific intron sequence which was exemplified, nor to the preferred location which was exemplified.

17. In support of my opinion expressed above, I am aware that many scientists have, subsequently, successfully used any of a variety of intron sequences in the transcribed region of the chimeric DNA by following the teaching of the Application as reported in Smith et al., (2000) (Exhibit 3). Examples of a number of such reports are attached as Exhibits 4 to 12. To me, this is clear and obvious evidence indicating that the teaching of the Application, in combination with the known art concerning introns, described the invention in sufficient manner to allow numerous others, skilled in the art, to make and use the invention.

18. In conclusion, it is therefore my opinion that a person of ordinary skill in the art would have concluded, judging at the filing date of the Application, that the Application adequately described all of the necessary features of the claimed subject matter in a manner sufficient to convey that the inventors were in possession of the invention as presently claimed.

I also declare that all statements made herein of my own knowledge are true and that all statements made on information and belief are believed to be true; and further that these statements were made with the knowledge that wilful false statements and the like so made are punishable by fine or imprisonment, or both, under Section 1001 of Title 18 of the United States Code and that such wilful false statements may jeopardise the validity of this application or any patent issued thereon.

August 6, 2002 _____

Date Elizabeth Salisbury Dennis

CURRICULUM VITAE

Name:	Elizabeth Salisbury DENNIS
Date of Birth:	10 December 1943
Place of Birth:	Sydney, Australia
Nationality:	Australian
Address:	CSIRO Plant Industry, Cnr Barry Drive and Clunies Ross Street, Black Mountain, Canberra, ACT 2601
Telephone:	W. (02) 6246 5061
Facsimile:	(02) 6246 5000
Email:	liz.dennis@csiro.au

Education:

1964	B.Sc. (Hons. 1st Class) Sydney University
1968	Ph.D. Sydney University Thesis entitled: "Studies on the *Bacillus subtilis* Genome" Supervisor Dr R.G. Wake

Academic Honours:

1980	Awarded Whiteley Prize for best zoological book on Papua New Guinea for "A Handbook of New Guinea Rodents" by J.I. Menzies and E.S. Dennis
1987	Elected Fellow of the Australian Academy of Technological Sciences and Engineering
1988	Pharmacia LKB/Biotechnology Medal of the Australian Biochemical Society for contributions to Biochemical Research
1995	Elected Fellow of the Australian Academy of Science
1997	Avon "Spirit of Achievement" Award
1998	Awarded Lemberg Medal of the Australian Society of Biochemistry & Molecular Biology
2000	Awarded the Inaugural Prime Minister's Prize for Science with Dr Jim Peacock
2002	Fellow of the American Society for the advancement of Science

Scholarships & Fellowships:

1961-64	Commonwealth Scholarship/Women's College Scholarship, University of Sydney
1965-68	Commonwealth Post Graduate Scholarship
1968-70	Post Doctoral Fellow, Anna Fuller Fund
1982-83	Fulbright Fellowship, Senior Scholar

Positions Held:

1968-70	Post Doctoral Fellow in laboratory of Dr Julius Marmur, Albert Einstein College of Medicine, New York, USA
1970-72	Lecturer in Microbiology then Lecturer in Biochemistry, University of Papua New Guinea
1972-74	Research Scientist, CSIRO Division of Plant Industry, Canberra
1974-76	Senior Lecturer in Biochemistry, University of Papua New Guinea
1976-present	Senior Research Scientist, Principal Research Scientist, Senior Principal Research Scientist, Chief Research Scientist, CSIRO Fellow - CSIRO Plant Industry, Canberra
1982-83	Visiting Fellow, Biochemistry Department, Stanford University, Laboratory of Dr Paul Berg

Societies:

Genetics Society of Australia (Committee Member 1978-1979)
Australian Society for Biochemistry and Molecular Biology
(President-Elect 1991, President 1992-93). Past President 1994.
International Society of Plant Molecular Biology (Board of Directors, 1990-93)
American Society of Plant Physiologists

Association with Universities:

Visiting Fellow:	Australian National University
Adjunct Professor:	Australian National University

Invited Speaker in International Meetings:

1974	U.S. Australia Meeting, "The Eukaryote Chromosome", Canberra, Australia
1981	XIII International Botanical Congress, Sydney, Symposium speaker
1982	Gordon Conference, Plant Molecular Biology, U.S.A.
1983	XV International Congress of Genetics (India) Agrigenetics Research Associates Meeting, Cancun, Mexico
1984	Arco-UCLA-Meeting, Cellular and Molecular Biology of Plant Stress, Keystone, U.S.A.
1985	1st International Congress of Plant Molecular Biology, Georgia, U.S.A., Symposium speaker Gordon Conference, Plant Molecular Biology, U.S.A. Agrigenetics Research Associates Meeting, Florida, U.S.A. German-Australia Meeting, "Biotechnology of Cereals", Germany
1986	Cold Spring Harbor Meeting on "Transposable Elements", Cold Spring Harbor, U.S.A.
1987	NATO Meeting, "Plant Molecular Biology, 1987", Copenhagen, Denmark FASEB Meeting, "Plant Gene Expression", Copper Mountain, U.S.A. International Meeting on "Plant Transposable Elements", Madison, Wisconsin, U.S.A. Agrigenetics Research Associates Meeting, Wisconsin, U.S.A.
1988	2nd International Congress of Plant Molecular Biology, Jerusalem, Symposium speaker
1989	Royal Society Meeting, "DNA Methylation and Gene Activity", London, U.K. 10th EMBO/EMBL Symposium, "Molecular Communication in Higher Plants",Heidelberg, F.R. Germany
1990	United Nations Industrial Development Organization International Centre for Genetic Engineering and Biotechnology, "Molecular & Genetic Approaches to Plant Stress" Delhi, India French-Australian Meeting, "Plant Molecular Biology", Versailles, France
1991	Keystone Symposium "Genetic Dissection of Plant Cell Processes", Keystone, USA. US:Australian Workshop, "Flowering", Hawaii, U.S.A. Society for Experimental Biology, "Biochemistry & Molecular Biology of Inducible Enzyzmes" Birmingham, U.K. 1st Queenstown Molecular Biology Meeting: Queenstown, New Zealand 3rd International Congress of Plant Molecular Biology, Tuscon, Arizona, U.S.A. - Symposium speaker
1992	International Workshop "Molecular Control of Flower Development and Plant Reproduction", Amsterdam, The Netherlands
1993	XV International Botanical Congress, Yokohoma, Japan, Symposium speaker "Frontiers of Gibberellin Research", Tokyo, Japan
1994	USA/Australian Workshop "Plants for the Future" Cairns, Australia
1995	8th International Congress on Isozymes, Brisbane, Australia 15th International on Plant Growth Regulators, Minneapolis, USA, Symposium speaker 3rd NIAR/COE Sympsium "Dynamics of Plant Genome Structure and Function", Tsukuka, Japan 10th FAOBMB Congress, Sydney, Australia, Symposium speaker
1997	Gordon Conference January 1997 "Low Temperature Effects in Plants", Ventura, California
1998	Molecular Physiology II "Genetic Engineering of Plants for Hostile Environments", Rothamstead, UK, Dec.

1999	"Genetic Control of Flowering" Symposium, Tsukuba, Japan, Nov.
2000	AAAS 2000 Genome Seminar, Washington, DC.
2001	John Innes Institute UK, EMBO Workshop - "The Molecular Basis of the Floral Transition".
2002	17th Long Ashton International Symposium, UK "New Frontiers in Plant Development: from Genes to Phenotype".
2003	XIX International Congress of Genetics – Melbourne August First International Symposium on Rice Functional Genomics – Shanghai China Frontiers in Plant Development Biology – Tokyo Japan Presentation to students at Okyama University
2004	International Conference on Arabidopsis, Germany, July International Plant Growth Substances, Canberra, August Wheat conference –. Fourth International Crop Science Congress, Brisbane, August

R&D Achievements in Collaborations with Industry:
Under Agrigenetics Corporation funding was part of a team which developed plant promoters which respond to anaerobic conditions and give high level expression. This resulted in patents which have been granted in the USA.

Extended this work with Wheat Industry Research Council Funding to develop a monocot promoter with high levels of expression for use in cereal transformation. This has also been patented.

Led a team funded by Gene Shears Pty Ltd to use ribozymes to develop a system for male sterility.

Played a role in the collaboration with Cotton Industry in developing genetically engineering cotton for use in Australia.

Led a team to develop a genetically engineered eucalypts for plantations. GIRD grant in collaboration with CSIRO, Forestry & APM, ANM, North Eucalypt, Technologies & Kimberly Clarke.

Program Leader in GrainGene in association with GRDC, AWB and CSIRO PI (Program 1).

Program Leader - Rice CRC (Program 2)

Leader of projects under CSIRO/Bayer

Board Member - Australian Genome Research Facility

Research Director - New South Wales Centre for Agricultural Genomics

Government Committees:

1986-91	Biotechnology Advisory Committee of the IR & D Board, Dept of Industry, Technology and Commerce, Australian Government
1985-87	Post Doctoral Awards Committee of CSIRO
1988	Member Australian Government Biotechnology Mission to the European Community
1989	Australian Government observer at European Community Biotechnology Action Program Meeting, "Plant Biotechnology in the European Community", Bad Honnef, West Germany
1990	Ad Hoc Genome Committee, DITAC "Plant Molecular Biology" Co-organizer French-Australian Meeting,
1993-94	Chairman, Multinational Coordinated Arabidopsis Genome Research Project
1994	Rice Biotechnology Working Group, Overseas Development Agency, UK Government

2000	Prime Minister's Science and Engineering Council

Journals:

1987-93	Editor "Advances in Plant Gene Research", Springer, Vienna, Austria
1990-93	Editor "Genetical Research", Cambridge, U.K.
1990-99	Editor "The Plant Journal", Blackwell & Bios, U.K., Foundation Editor
	Editorial Board "Molecular Breeding", Kluwer, Netherlands
	Editorial Board "Current Opinion in Plant Biology"

Research Interests:

Molecular basis of plant development particularly the initiation of flowering
Plant gene regulation
Molecular basis of plant response to stress

PUBLICATIONS - E.S. DENNIS

Also published as E.S. Goldring

1. **Dennis, E.S.** and Wake, R.G. (1965)
Clotting of milk by proteolytic enzymes
Biochim. Biophys. Acta 97, I59-162

2. **Dennis, E.S.** and Wake, R.G. (1966)
Autoradiography of the *Bacillus subtilis* chromosome
Journal of Molecular Biology, I5, 435-439

3. **Dennis, E.S.** and Wake, R.G. (1968)
The *Bacillus subtilis* genome: studies of its size and structure
In "Replication and Recombination of Genetic Material", 6I-70
(Eds. Peacock, W.J. and Brock, R.D.)
Australian Academy of Science, Canberra

4. **Goldring, E.S.** and Wake, R.G. (1968)
A comparison of the segregation of chromosomes within microcolonies developing from single *Bacillus subtilis* and *Bacillus megaterium* spores
Journal of Molecular Biology, 35, 647-650

5. Grossman, L.I., **Goldring, E.S.** and Marmur, J. (1969)
Preferential synthesis of yeast mitochondrial DNA in the absence of protein synthesis
Journal of Molecular Biology, 46, 367-376

6. **Goldring, E.S.**, Grossman, L.I., Krupnick, D., Cryer, D.R. and Marmur, J. (1970)
The petite mutation in yeast. Loss of mitochondrial deoxyribonucleic acid during induction of petites with ethidium bromide
Journal of Molecular Bioloy, 52, 323-335

7. **Goldring, E.S.,** Grossman, L.I. and Marmur, J. (1971)
Petite mutation in yeast. II. The isolation of mutants containing mitochondrial deoxyribonucleic acid of reduced size.
Journal of Bacteriology, I07, 377-381

8. Grossman, L.I., Cryer, D.R., **Goldring, E.S.** and Marmur, J. (1971)
The petite mutation in yeast. III. Nearest-neighbour analysis of mitochondrial DNA from normal and mutant cells
Journal of Molecular Biology, 62, 565

9. Peacock, W.J., Brutlag, D., **Goldring, E.S.,** Appels, R., Hinton, C.W. and Lindsley, D.L. (1974)
The organization of highly repeated DNA sequences in *Drosophila melanogaster* chromosomes
Cold Spring Harbor Symposium on Quantitative Biology. 38, 405-4I6

10. **Goldring, E.S.**, Brutlag, D.L. and Peacock, W.J. (1975)
Arrangement of the highly repeated DNA of *Drosophila melanogaster*
In "The Eukaryote Chromosome", 47-59
(Eds. Peacock, W.J. and Brock, R.D.)
Austalian National University Press, Canberra

11. Maddocks, I., Anders, E.M. and **Dennis, E.S.** (1976)
Donovanosis in Papua New Guinea
British Journal of Venereal Diseases, 52, 190-196

12. Price, M.A., Anders, E.M., Anders, R.F., Russell, D.A. and **Dennis, E.S.** (1976)
Cell-mediated immunologic status of healthy members of families with a history of leprosy
International Journal of Leprosy, 43, 307-3I3

13. Peacock, W.J., Appels, R., Gerlach, W.L. and **Dennis, E.S.** (1976)
DNA sequence probes - a new technique in plant breeding
CSIRO Division of Plant Industry Annual Report 1976, 41-45

14. Brutlag, D., Appels, R., **Dennis, E.S.** and Peacock, W.J. (1977)
Highly repeated DNA in *Drosophila melanogaster*
Journal of Molecular Biology, II2, 3I-47

15. **Goldring**, E.S. and Peacock, W.J. (1977)
Intramolecular heterogeneity of mitochondrial DNA of *Drosophila melanogaster*
Journal of Cell Biology, 73, 279-286

16. **Dennis**, E. and Menzies, J.I. (1978)
Systematics and chromosomes of New Guinea *Rattus*
Australian Journal of Zoology, 26, 197-206

17. Peacock, W.J., Lohe, A.R., Gerlach, W.L., Dunsmuir, P., **Dennis, E.S.** and Appels, R. (1978)
Fine structure and evolution of DNA in heterochromatin
Cold Spring Harbor Symposia on Quantitative Biology, 42, 112I-1135

18. Gerlach, W.L., Appels, R., **Dennis, E.S.** and Peacock, W.J. (1978)
Evolution and analysis of wheat genomes using highly repeated DNA sequences
Proc. 5th Int. Wheat Genetics Symposium, New Delhi, 1978, I, 8I-9I

19. **Dennis**, E. and Menzies, J.I. (1979)
A chromo A chromosomal and morphometric study of Papuan tree rats *Pogonomys* and *Chiruromys* (Rodentia, Muridae)
Journal Zoology. (Lond.) I89, 3I5-332

20. Schwinghamer, E.A. and **Dennis, E.S.** (1979)
Electron microscopic evidence for a multimeric system of plasmids in fast-growing *Rhizobium* spp.
Australian Journal of Biological Science, 32, 65I-662

21. Menzies, J.I. and **Dennis, E.S.** (1979)
"Handbook of New Guinea Rodents"
(Bernice P. Bishop Museum: Hawaii)
Wau Ecology Institute Handbook 6
(Wau Ecology Institute: Papua New Guinea)

22. Appels, R., Gerlach, W.L., **Dennis, E.S.**, Swift, H. and Peacock, W.J. (1980)
Molecular and chromosomal organization of DNA sequences coding for the ribosomal RNAs in cereals
Chromosoma (Berl.) 78, 293-3II

23. **Dennis, E.S.**, Gerlach, W.L. and Peacock, W.J. (1980)
Identical polypyrimidine-polypurine satellite DNAs in wheat and barley
Heredity, 44, 349-366

24. **Dennis, E.S.**, Dunsmuir, P. and Peacock, W.J. (1980)
Segmental amplification in a satellite DNA: Restriction enzyme analysis of the major satellite of *Macropus rufogriseus*
Chromosoma (Berl.) 79, I79-198

25. Peacock, W.J., **Dennis, E.S.**, Hilliker, A.J. and Pryor, A.J. (1980)
Differentiation of heterochromatin
In "Evolution and Speciation: Essays in Honour of M.J.D. White",78-l00
(Eds. Atchley, W.R. and Woodruff, D.S.)Cambridge University Press, New York

26. Peacock, W.J., Gerlach, W.L. and **Dennis, E.S.** (1981)
Molecular aspects of wheat evolution: Repeated DNA sequences
In "Wheat Science - Today and Tomorrow", 4l-60
(Eds. Evans, L.T. and Peacock, W.J.)Cambridge University Press, Cambridge

27. **Dennis, E.S.**, Peacock, W.J., White, M.J.D., Appels, R. and Contreras, N. (1981)
Cytogenetics of the parthenogenetic grasshopper *Warramaba virgo* and its bisexual relatives.VII: Evidence from repeated DNA sequences for a dual origin of *W. virgo*
Chromosoma (Berl.), 82, 453-469

28. Peacock, W.J., **Dennis, E.S.** and Gerlach, W.L. (1981)
Satellite DNA - change and stability
In "Chromosomes Today", 7, 30-41
Proc. 7th Int. Chromosome Conf., Oxford, 1980
(Eds. Bennett. MD., Bobrow, M. and Hewitt, G.) George Allen and Unwin, London

29. Peacock, W.J., **Dennis, E.S.**, Elizur, A. and Calaby, J.H. (1981)
Repeated DNA sequences and kangaroo phylogeny
Australian Journal of Biological Science, 34, 325-340

30. Peacock, W.J., **Dennis, E.S.**, Rhoades, M.M. and Pryor, A.J. (1981)
Highly repeated DNA sequence limited to knob heterochromatin in maize
Proceedings of the National Academy of Sciences, USA, 78, 4490-4494

31. Appels, R., **Dennis, E.S.**, Smyth, D.R. and Peacock, W.J. (1981)
Two repeated DNA sequences from the heterochromatic regions of rye (*Secale cereale*) chromosomes
Chromosoma (Berl.) 84, 265-277

32. Elizur, A., **Dennis, E.S.** and Peacock, W.J. (1982)
Satellite DNA sequences in the red kangaroo (*Macropus rufus*)
Australian Journal of Biological Science, 35, 313-325

33. Gerlach, W.L., Pryor, A.J., **Dennis, E.S.**, Ferl, R.J., Sachs, M.M. and Peacock, W.J. (1982)
cDNA cloning and induction of the alcohol dehydrogenase gene (*Adhl*) of maize
Proceedings of the National Academy of Sciences, USA, 79, 2981-2985

34. Peacock, W.J., **Dennis, E.S.** and Gerlach, W.L. (1982)
DNA sequence changes and speciation
In "Mechanisms of Speciation", 123-142
(Ed. Barigozzi, C.) Alan R. Liss, Inc., New York

35. White, M.J.D., **Dennis, E.S.**, Honeycutt, R.L., Contreras, N. and Peacock, W.J.(1982)
Cytogenetics of the parthenogenetic grasshopper *Warramaba virgo* and its bisexual relatives. IX. The ribosomal RNA cistrons
Chromosoma (Berl.) 85, 181-199

36. Sachs, M.M., Lorz, H., **Dennis, E.S.**, Elizur, A., Ferl, R.J., Gerlach, W.L., Pryor, A.J. and Peacock, W.J. (1982)
Molecular genetic analysis of the maize anaerobic response
In "Maize for Biological Research", 139-144(Ed. Sheridan, W.F.)
Plant Molecular Biology Association, Charlottesville, VA

37. Gerlach, W.L., Lörz, H., Sachs, M.M., Llewellyn, D., Pryor, A.J., **Dennis, E.S.** and Peacock, W.J. (1983)
The alcohol dehydrogenase genes of maize: A potential gene transfer system in plants
In "Manipulation and Expression of Genes in Eukaryotes", 213-220
Proc. Int. Conf. Monash University, 1982
(Eds. Nagley, P., Linnane, A.W., Peacock, W.J. and Pateman, J.A.)
Academic Press Australia

38. Sachs, M.M., Peacock, W.J., **Dennis, E.S.** and Gerlach, W.L. (1983)
Maize *Ac/Ds* controlling elements.
A molecular viewpoint. Maydica 28, 289-301

39. **Dennis, E.S.** and Peacock, W.J. (1983)
Knob heterochromatin DNA: organization and evolution
In "Genetics: New Frontiers. Vol. I Genetic Organization, Function and Regulation", 247-253
Proc. 15th Genetics Congr., New Delhi, 1983
(Eds. Chopra, V.L., Joshi, B.C., Sharma, R.P. and Bansal, H.C.)
Oxford and IBH Publishing Co., New Delhi

40. Gerlach, W.L., **Dennis, E.S.** and Peacock, W.J. (1983)
Molecular cytogenetics of wheat
In "Cytogenetics of Crop Plants", 191-212
(Eds. Swaminathan, M.S., Gupta, P.K. and Sinha, U.)
Macmillan IndiaLimited

41. Peacock, W.J., **Dennis, E.S.**, Gerlach, W.L., Llewellyn, D., Lorz, H., Pryor, A.J., Sachs, M.M., Schwartz, D. and Sutton, W.D. (1983)
Gene transfer in maize: controlling elements and the alcohol dehydrogenase genes
In "Advances in Gene Technology: Molecular Genetics of Plants and Animals", 311-325
Miami Winter Symp. 20
(Eds. Downey, K., Voellmy, R.W., Ahmad, F. and Schultz, J.)
Academic Press: New York
Reprinted in "Genetic Manipulation: Impact on Man and Society", 115-126 (1984)
(Eds. Arber, W., Illmensee, K., Peacock, W.J. and Starlinger, P.)
Cambridge University Press, Cambridge

42. **Dennis, E.S**., Gerlach, W.L., Pryor, A.J., Bennetzen, J.L., Inglis, A., Llewellyn, D., Sachs, M.M., Ferl, R.J. and Peacock, W.J. (1984)
Molecular analysis of the alcohol dehydrogenase (*Adh1*) gene of maize
Nucleic Acids Research, 12, 3983-4000

43. Howard, E.A. and **Dennis, E.S.** (1984)
Transposable elements in maize - the activator-dissociation (Ac-Ds) system
Australian Journal of Biological Science, 37, 307-314

44. **Dennis, E.S.**, Hohn, B., Hohn, Th., King, P.J., Schell, J. and Verma, D.P.S. (Eds.) (1984)
"Plant Gene Research - Basic Knowledge and Application" (Series)
Springer-Verlag, Wien

45. Peacock, W.J., **Dennis, E.S.**, Gerlach, W.L., Sachs, M.M. and Schwartz, D. (1984)
Insertion and excision of *Ds* controlling elements in maize
Cold Spring Harbor Symposia on Quanttative Biology, 49, 347-354

46. **Dennis, E.S.**, Waldron, J.C. and Peacock, W.J. (1984)
Genetic engineering and plant breeding
In "Pollination" 84, 98-101
Proc. Symposium, University of Melbourne, 1984 (Eds. Williams, E.G. and Knox, R.S.)
University of Melbourne, Parkville

47. Gerlach, W.L., **Dennis, E.S.** and Peacock, W.J. (1984)
Controlling elements in maize
Aust. CSIRO Divisional Annual Report 1983-84, 20-24

48. **Dennis, E.S.** and Peacock, W.J. (1984)
Knob heterochromatin homology in maize and its relatives
Journal of Molecular Evolution, 20, 341-350

49. **Dennis, E.S.**, Sachs, M.M., Gerlach, W.L. Finnegan, E.J. and Peacock, W.J. (1985)
Molecular analysis of the alcohol dehydrogenase 2 (Adh2) gene of maize
Nucleic Acids Research, 13, 727-743

50. Llewellyn, D., **Dennis, E.S.** and Peacock, W.J. (1985)
The alcohol dehydrogenase genes of maize: Expression studies in tobacco cells
In "Molecular Form and Function of the Plant Genome", 593-607
Proc. NATO Adv. Study Inst.-FEBS Adv. Course on Mol. Form and Function on the Plant Genome, Renesse, 1984
(Eds. Vloten-Doting, L. van, Groot, G.S.P. and Hall, T.C.)
Plenum Publishing Corporation, New York

51. Hohn, B. and **Dennis, E.S.** (Eds.) (1985)
"Genetic Flux in Plants", 253
"Plant Gene Research -Basic Knowledge and Application", 2
(Eds. **Dennis, E.S.**, Hohn, B., Hohn, Th., King, P.J., Schell, J. and Verma, D.P.S.)
Springer-Verlag, Wien

52. **Dennis, E.S.** and Berg, P. (1985)
Transcription from a plant gene promoter in animal cells
Nucleic Acids Research, 13, 7945-7957

53. Howard, E.A., Danna, K.J., **Dennis, E.S.** and Peacock, W.J. (1985)
Transient expression in maize protoplasts
In "Plant Genetics", 225-234
Proc. 3rd Annu. ARCO Plant Cell Res. Inst. - UCLA Symp.on Plant Biology, Keystone, Co., 1985
(Ed. Freeling, M.)
Alan R. Liss Inc., New York

54. Sachs, M.M., **Dennis, E.S.**, Ellis, J., Finnegan, E.J., Gerlach, W.L.,Llewellyn, D. and Peacock, W.J. (1985)
Adh1 and *Adh2*: Two genes involved in the maize anaerobic response
In "Cellular and Molecular Biology of Plant Stress", 217-226
UCLA Symp. Mol. Cell. Biol., New York, 1986, 22
Alan R. Liss Inc., New York

55. Brettell, R.I.S., **Dennis, E.S.**, Scowcroft, W.R. and Peacock, W.J. (1986)
Molecular analysis of a somaclonal mutant of maize alcohol dehydrogenase
Molecular and General Genetics, 202, 235-239

56. Peacock, W.J. and **Dennis, E.S.** (1986)
Plant gene engineering and plant agriculture
In "Biotechnology: Potentials and Limitations", 223-239
Report of the Dahlem Workshop, Berlin, 1985. Life Sciences Research Report 35
(Ed. Silver, S.)
Springer-Verlag, Berlin

57. **Dennis, E.S.**, Gerlach, W.L. and Peacock, W.J. (1986)
Excision of the *Ds* controlling element from the *Adh1* gene of maize
Maydica 31, 47-57

58. Sachs, M.M., **Dennis, E.S.**, Gerlach, W.L. and Peacock, W.J. (1986)
Two alleles of maize *alcohol dehydrogenase 1* have 3' structural and poly(A) addition polymorphisms
Genetics 113, 449-467

59. Landsmann, J., **Dennis, E.S.**, Higgins, T.J.V., Appleby, C.A., Kortt, A.A. and Peacock, W.J. (1986)
Common evolutionary origin of legume and non-legume plant haemoglobins
Nature (London) 324, 166-168

60. Gerlach, W.L., Sachs, M.M., Llewellyn, D.J., Finnegan, E.J. and **Dennis, E.S.** (1986)
Maize alcohol dehydrogenase: A molecular perspective
In "A Genetic Approach to Plant Biochemistry", 73-100
Series "Plant Gene Research - Basic Knowledge and Application"
(Eds. Blonstein, A.D. and King, P.J.)
Springer-Verlag, Wien

61. Appleby, C.A., Bogusz, D., **Dennis, E.S.**, Dudman, W.F., Fleming, A.I., Higgins, T.J., Kortt, A.A., Landsmann, J.,Peacock, W.J., Tjepkema, J.D., Trinick, M.J., Wittenberg, B.A.and Wittenberg, J.B. (1986)
The origin and survival of plant hemoglobin genes
Proc. 8th Aust. Nitrogen Fixation Conf., Adelaide, 1986, 77-78
AIAS Occ. Publ. 25
(Eds. Wallace, W. and Smith, S.E.)
Australian Institute of Agricultural Science, Parkville, Vic

62. Schwartz, D. and **Dennis, E.S.** (1986)
Transpose activity of the *Ac* controlling element in maize is regulated by its degree of methylation
Molecular and General Genetics, 205, 476-482

63. Ellis, J.G., Llewellyn, D.J., **Dennis, E.S.** and Peacock, W.J. (1987)
Maize *Adh-1* promoter sequences control anaerobic regulation: addition of upstream promoter elements from constitutive genes is necessary for expression in tobacco
EMBO Journal 6, 11-16

64. Llewellyn, D.J., Finnegan, E.J., Ellis, J.G., **Dennis, E.S.** and Peacock, W.J. (1987)
Structure and expression of an alcohol dehydrogenase 1 gene from *Pisum sativum* (cv. "Greenfeast")
Journal of Molecular Biology 195, 115-123

65. **Dennis, E.S.**, Walker, J.C., Ellis, J.G., Llewellyn, D.J., Singh, K., Peacock, W.J. and Wolstenholme, D. (1987)
Anaerobic regulation of the maize alcohol dehydrogenase gene
Proc. 9th Aust. Symp. on Anal. Chem., Sydney, 1987, 2, 925-928
(Anal. Chem. Div. R. Aust. Chem. Inst.: Melbourne)

66. Ellis, J.G., Llewellyn, D.J., Walker, J.C., **Dennis, E.S.** and Peacock, W.J. (1987)
The *ocs* element: A 16 base pair palindrome essential for activity of the octopine synthase enhancer
EMBO Journal, 6, 3203-3208

67. Walker, J.C., Howard, E.A., **Dennis, E.S.** and Peacock, W.J. (1987)
DNA sequences required for anaerobic expression of the maize alcohol dehydrogenase 1 gene
Proceedings of the National Academy of Sciences, USA, 84, 6624-6628

68. **Dennis, E.S.**, Brettell, R.I.S. and Peacock, W.J. (1987)
A tissue culture induced *Adh1* null mutant of maize results from a single base change
Molecular and General Genetics, 210, 181-183

69. Peacock, W.J., Wolstenholme, D., Walker, J.C., Singh, K., Llewellyn, D.J., Ellis, J.G. and **Dennis, E.S.** (1987)
Developmental and environmental regulation of the maize alcohol dehydrogenase 1 (*Adh1*) gene: Promoter-enhancer interactions
In "Plant Gene Systems and Their Biology", 263-277
(Eds. McIntosh, L. and Key, J.)
Alan R. Liss Inc., New York

70. **Dennis, E.S.**, Walker, J.C., Llewellyn, D.J., Ellis, J.G., Singh, K., Tokuhisa, J.G., Wolstenholme, D.R. and Peacock, W.J. (1987)
The response to anaerobic stress: Transcriptional regulation of genes for anaerobically induced proteins
In "Plant Molecular Biology", 407-417
(Eds. von Wettstein, D. and Chua, N.-H.)
Plenum Publishing Corporation, New York

71. Peacock, W.J., **Dennis, E.S.**, Finnegan, E.J., Peterson, T.A. and Taylor, B.H. (1987)
Aspects of the *Ac/Ds* transposable element system in maize
J. Cell Sci. Suppl. 7, 123-138

72. Howard, E.A., Walker, J.C., **Dennis, E.S.** and Peacock, W.J. (1987)
Regulated expression of an alcohol dehydrogenase 1 chimeric gene introduced into maize protoplasts
Planta 170, 535-540

73. Gerlach, W.L., **Dennis, E.S.**, Peacock, W.J. and Clegg, M.T. (1987)
The Ds1 controlling element family in maize and *Tripsacum*
Journal of Molecular Evolution, 26, 329-334

74. Walker, J.C., Llewellyn, D.J., Mitchell, L.E. and **Dennis, E.S.** (1987)
Anaerobically regulated gene expression; molecular adaptations of plants for survival under flooded conditions
Oxford Survey of Plant Molecular and Cell Biology, 4, 71-93

75. Bogusz, D., Appleby, C.A., Landsmann, J., **Dennis, E.S.**, Trinick, M.J. and Peacock, W.J. (1988)
Functioning haemoglobin genes in non-nodulating plants
Nature 331, 178-180

76. **Dennis, E.S.**, Sachs, M.M., Gerlach, W.L., Beach, L. and Peacock, W.J. (1988)
The *Ds1* transposable element acts as an intron in the mutant allele *Adh1-Fm335* and is spliced from the message
Nucleic Acids Research, 16, 3815-3828

77. **Dennis, E.S.**, Gerlach, W.L., Walker, J.C., Lavin, M. and Peacock, W.J. (1988)
Anaerobically regulated aldolase gene of maize: a chimaeric origin?
Journal of Molecular Biology, 202, 759-767

78. Landsmann, J., Llewellyn, D., **Dennis, E.S.** and Peacock, W.J. (1988)
Organ regulated expression of the *Parasponia andersonii* haemoglobin gene in transgenic tobacco plants
Molecular and General Genetics, 214, 68-73

79. Appleby, C.A., Bogusz, D., **Dennis, E.S.** and Peacock, W.J. (1988)
A role for haemoglobin in all plant roots?
Plant Cell and Environment, 11, 359-367

80. **Dennis, E.S.**, Finnegan, E.J., Taylor, B.H., Peterson, T.A., Walker, A.R. and Peacock, W.J. (1988)
Maize transposable elements: Structure, function, and regulation
In "Plant Transposable Elements", 101-113
(Ed. Nelson, O.) Plenum Publishing Corporation, New York

81. Trick, M., **Dennis, E.S.**, Edwards, K.J.R. and Peacock, W.J. (1988)
Molecular analysis of the alcohol dehydrogenase gene family of barley
Plant Molecular Biology, 11, 147-160

82. Appleby, C.A., Bogusz, D., **Dennis, E.S.**, Fleming, A.I., Landsmann, J. and Peacock, W.J. (1988)
The vertical evolution of plant hemoglobin genes
In "Nitrogen Fixation: Hundred Years After", 623-628
(Ed. Bothe, H., de Bruijn, F.J. and Newton, W.E.)
Gustav Fischer, Stuttgart: New York

83. Finnegan, E.J., Taylor, B.H., **Dennis, E.S.** and Peacock, W.J. (1988)
Transcription of the maize transposable element *Ac* in maize seedlings and in transgenic tobacco
Molecular and General Genetics,, 212, 505-509

84. Meeks-Wagner, D.R., **Dennis, E.S.**, Van, K.T.T. and Peacock, W.J. (1989)
Tobacco genes expressed during in vitro floral initiation and their expression during normal plant development
The Plant Cell, 1, 25-35

85. **Dennis, E.S.**, Walker, J.C., Llewellyn, D.J., Ellis, J.G., Singh, K., Tokuhisa, J.G., Wolstenholme, D.R. and Peacock, W.J. (1989)
The response to anaerobic stress: Transcriptional regulation of genes for anaerobically induced proteins
In "Environmental Stress in Plants", 231-245
NATO ASI Series, G19
(Ed. Cherry, J.H.) Springer-Verlag, Berlin Heidelberg

86. Finnegan, E.J., Taylor, B.H., Craig, S. and **Dennis, E.S.** (1989)
Transposable elements can be used to study cell lineages in transgenic plants
The Plant Cell, 1, 757-764

87. Huang, Y-.W. and **Dennis, E.S.** (1989)
Factors influencing stable transformation of maize protoplasts by electroporation

Plant Cell, Tissue Organ Culture, 18, 281-296

88. Taylor, B.H., Finnegan, E.J., **Dennis, E.S.** and Peacock, W.J. (1989)
The maize transposable element *Ac* excises in progeny of transformed tobacco
Plant Molecular Biology, 13, 109-118

89. Singh, K., Tokuhisa, J.G., **Dennis, E.S.** and Peacock, W.J. (1989)
Saturation mutagenesis of the octopine synthase enhancer: Correlation of mutant phenotypes with binding of a nuclear protein factor
Proceedings of the National Academy of Sciences, USA, 86, 3733-3737

90. Mitchell, L.E., **Dennis, E.S.** and Peacock, W.J. (1989)
Molecular analysis of an alcohol dehydrogenase (*Adh*) gene from chromosome 1 of wheat Genome, 32, 349-358

91. Osterman, J.C. and **Dennis, E.S.** (1989)
Molecular analysis of the *ADH1-C*m allele of maize
Plant Molecular Biology, 13, 203-212

92. Lawrence, G.J., Ellis, J.G., Finnegan, E.J., **Dennis, E.S.** and Peacock, W.J. (1989)
Tagging rust resistance genes in flax
In "Breeding Research: The Key to the Survival of the Earth", 535-538
Proc. 6th Int. Congress of SABRAO
(Eds. Iyama, S. and Takeda, G.)

93. Bouchez, D., Tokuhisa, J.G., Llewellyn, D.J., **Dennis, E.S.** and Ellis, J.G. (1989)
The ocs-element is a component of the promoters of several T-DNA and plant viral genes
EMBO Journal, 8, 4197-4204 .

94. Lechelt, C., Peterson, T., Laird, A., Chen, J., Dellaporta, S.L., **Dennis, E.S.**, Peacock, W.J. and Starlinger, P. (1989)
Isolation and molecular analysis of the maize *P* locus
Molecular and General Genetics, 219, 225-234

95. Lyon, B.R., Llewellyn, D.J., Huppatz, J.L., **Dennis, E.S.** and Peacock, W.J. (1989)
Expression of a bacterial gene in transgenic tobacco plants confers resistance to the herbicide 2,4-dichlorophenoxyacetic acid
Plant Molecular Biology, 13, 533-540

96. **Dennis, E.S.** and Brettell, R.I.S. (1990)
DNA methylation of maize transposable elements is correlated with activity
Phil. Trans. R. Soc. London. B 326, 217-229

97. Tokuhisa, J.G, Singh, K., **Dennis, E.S.** and Peacock, W.J. (1990)
A DNA-binding protein factor recognizes two binding domains within the octopine synthase enhancer element
The Plant Cell, 2, 215-224

98. Olive, M.R., Walker, J.C., Singh, K., **Dennis, E.S.**and Peacock, W.J. (1990)
Functional properties of the anaerobic responsive element of the maize *Adh1* gene
Plant Molecular Biology, 15, 593-604

99. Appleby, C.A., **Dennis, E.S.** and Peacock, W.J. (1990)
A primaeval origin for plant and animal haemoglobins?
Australian Systematic Botany 3, 81-89

100. Neale, A.D., Wahleithner, J.A., Lund, M., Bonnet, H.T., Meeks-Wagner, D.R., Peacock, W.J. and **Dennis, E.S.** (1990)
Floral explant specific clones include chitinase, β-1,3-glucanase, osmotin and extension
The Plant Cell, 2, 673-684

101. Bogusz, D., Llewellyn, D.J., Craig, S., **Dennis, E.S.**, Appleby, C.A. and Peacock, W.J.(1990)
Nonlegume hemoglobin genes retain organ-specific expression in heterologous transgenic plants
The Plant Cell, 2, 633-641

102. Lyon, B., Cousins, Y., Llewellyn, D., Huppatz, J., **Dennis, E.S.** and Peacock, W.J. (1990)
Genetic engineering of plants for resistance to the herbicide 2,4 D, "Genetic Engineering of crop Plants"
eds. Grierson, D. and Lycett, G., Butterworths, London, 67-77

103. Singh, K., **Dennis, E.S.**, Ellis, J.G., Llewellyn, D.J., Tokuhisa, J.G., Wahleithner, J.A. and Peacock, W.J. (1990)
OCSBF-1, a maize ocs enhancer binding factor: Isolation and expression during development
The Plant Cell, 2, 891-903

104. Olive, M.R., Walker, J.C., Singh, K., Ellis, J.G., Llewellyn, D., Peacock, W.J. and **Dennis**, E.S (1991)
The anaerobic responsive element
Plant Molecular Biology, 2, 673-68

105. Last, D.I., Brettell, R.I.S., Chamberlain, D.A., Chaudhury, A.M., Larkin, P.J., Marsh, E.L., Peacock, W.J. and **Dennis, E.S.** (1991)
pEmu: An improved promoter for gene expression in cereal cells
Theor. Appl. Gen., 81, 581-588

106. E.S. **Dennis** and D.J. Llewellyn, (Eds.) (1991)
Molecular Approaches to Crop Improvement.
Plant Gene Research - Basic Knowledge and Application
Springer-Verlag, Wien - New York, 7, 1-166

107. Christensen, T., **Dennis, E.S.**, Peacock, W.J., Landsmann, J. and Marcker, K.A. (1991)
Hemoglobin genes in non-legumes: Cloning and characterization of a *Casuarina glauca* hemoglobin gene.
Plant Molecular Biology, 16, 339-344

108. Brettell, R.I.S. and **Dennis, E.S.** (1991)
Reactivation of a silent *Ac* following tissue culture is associated with heritable alterations in its methylation pattern.
Molecular and General Genetics, 229, 365-372

109. Olive, M.R., Peacock, W.J. and **Dennis, E.S.** (1991)
The anaerobic responsive element contains two GC-rich sequences essential for binding a nuclear protein and hypoxic activation of the *Adh1* promotor
Nucleic Acids Research, 19, 7053-7060

110. Mooney, P.A., Goodwin, P.B., **Dennis, E.S.**, and Llewellyn, D.J., (1991)
Agrobacterium tumefaciens-gene transfer into wheat tissues
Plant Cell, Tissue and Organ Culture, 25, 209-218

111. Chapple, R. and **Dennis, E.S.**, (1991)
Research into gene mapping to reap a rich harvest
Australian Grain, 1, 12-14

112. Chaudhury, A.M., Craig, S., Bloemer, K.C., Farrell, L. and **Dennis, E.S.** (1992)
Genetic control of male fertility in higher plants
Australian Journal of Plant Physiology, 19, 419-26

113. Clarke, A.E., **Dennis, E.S.** and Mol, J. (1992)
Forefronts of flowering
The Plant Cell, 4, 867-870

114. Peacock, W.J., Bagnall, D., Burn, J., **Dennis**, E.,and Metzger, J. (1992)
DNA methylation controls flowering inititated by vernalization
Trans. Malaysian Soc. Plant Physiol. 3, 210-215

115. **Dennis, E.S.**, Olive, M., Dolferus, R., Millar, A., Peacock, W.J. and Setter, T.L. (1992)
Biochemistry and molecular biology of the anaerobic response
Society for Experimental Biology Seminar Series 49: Inducible Plant Proteins (Ed. Wray, J.L.) 231-245

116. **Dennis**. E.S., Millar, A., Dolferus, R., Olive, M., de Bruxelles, G., and Peacock, W.J. (1992)
Molecular analysis of the response to anaerobic stress
In "Adaptation of Vegetables and other Food Crops to Temperature & Water Stress" (Ed. C.G. Kuo), 59-67

117. **Dennis, E.S.**, (1992)
Manipulation of flowering and its biotechnological implications
The Third Biochemistry Alumni Guest Lecture,
University of Queensland

118. **Dennis, E.S.** and Bowman, J.L. (1993)
Manipulating floral organ identity
Current Biology 3, 90-93

119. Burn, J.E., Bagnall, D.J., Metzger, J.D., **Dennis, E.S.** and Peacock, W.J. (1993)
DNA methylation, vernalisation and the initiation of flowering
Proceedings of the National Academy of Sciences, USA, 90, 287-291

120. Finnegan, E.J., Lawrence, G.J., **Dennis, E.S.** and Ellis, J.G. (1993)
Behaviour of modified *Ac* elements in flax callus and regenerated plants
Plant Molecular Biology, 22, 625-633

121. Foley, R.C., Grossman, C., Ellis, J.G., Llewellyn, D.J., **Dennis, E.S.**, Peacock, W.J. and Singh, K.B. (1993)
Isolation of a maize bZIP protein sub family; candidates for the ocs-element transcription factor
The Plant Journal 3, 669-681

122. Finnegan, E.J., Brettell, R.I.S. and **Dennis, E.S.** (1993)
The role of DNA methylation in the regulation of plant gene expression
DNA Methylation: Molecular Biology and Biological Significance
(eds. J.P Jost and H.P. Saluz) Birkhauser Verlag Basel/Switzerland, 218-261

123. Lyon, B.R., Cousins, Y.L., Llewellyn, D.J. and **Dennis, E.S.** (1993)
Cotton plants transformed with a bacterial degradation gene are protected from accidental spray drift damage by the herbicide 2,4-dichlorophenoxyacetic acid
Transgenic Research 2, 162-169

124. Ellis, J.G., Tokuhisa, J.G., Llewellyn, D.J., Bouchez, D., Singh, K., **Dennis, E.S.** and Peacock, W.J. (1993)
Does the ocs-element occur as a functional component of the promoters of plant genes?
The Plant Journal 4, 433-443

125. Chaudhury, A.M., Letham, S., Craig, S. and **Dennis, E.S.** (1993)
amp1 - a mutant with high cytokinin levels and altered embryonic pattern, faster vegetative growth, constitutive photomorphogenesis and precocious flowering
The Plant Journal 4, 907-916

126. Finnegan, E.J., **Dennis, E.S.**, (1993)
Isolation and identification by sequence homology of a putative cytosine methyltransferase from *Arabidopsis thaliana*
Nucleic Acids Research., 21, 2383-2388

127. Burn, J.E., Smyth, D.R., Peacock, W.J.and **Dennis, E.S.** (1993)
Genes conferring late flowering in *Arabidopsis thaliana*
Genetica 90, 147-155

128. Harcourt, R., Southerton, S., Zhu, X., Llewellyn, D., Olive, M., Peacock, W J., **Dennis** E.S. (1993)
Genetic engineering for insect resistance in Eucalypts
Proceedings of the Second Canberra Meeting on *Bacillus thuringiensis*, Canberra, 1993 (ed. R J Akhurst) 85-95

129. **Dennis, E.S.** (Chair) (1993)
The multinational Coordinated *Arabidopsis thaliana* Genome Research Project Progress Report: Year three The Multinational Science Steering Committee
National Science Foundation USA 71pp

130. Chamberlain, D.A., Brettell, R.I.S., Last, D.I., Witrzens, B., McElroy, D., Dolferus, R. and **Dennis, E.S.** (1994)
The use of the Emu promoter with antibiotic and herbicide resistance genes for the selection of transgenic wheat callus and rice plants.
Australian Journal of Plant Physiology 21, 95-112

131. Chaudhury, A.M., **Dennis, E.S.** and Brettell, R.I.S., (1994)
Gene-expression following T-DNA transfer into plant cells is aphidicolin-sensitive.
Australian Journal of Plant Physiology 21, 125-31

132. Udvardi, M.K., Metzger, J.D., Krishnapillai, V., Peacock, W.J., and **Dennis, E.S.** (1994)
Cloning and sequencing of a full-length cDNA from *Thlaspi arvense* L. that encodes a cytochrome P-450
Plant Physiology 105, 755-756

133. Kyozuka, J., Olive, M., Peacock, W.J., **Dennis, E.S.**and Shimamoto, K. (1994)
Promotor elements required for developmental expression of the maize *Adh1* gene in transgenic rice
The Plant Cell, 6, 799-810

134. Burn, J., **Dennis, E.S.** and Peacock, W.J. (1994)
The mysteries of flowering
Today's Life Science, August 1994, 26-31

135. Brettell, R.I.S., Chamberlain, D.A., Drew, A.M., McElroy, D., Witrzens, B.and **Dennis, E.S.** (1994)
An assessment of methods for the genetic transformation of wheat.
In "Improvement of Cereal Quality by Genetic Engineering", Edited by. Robert J. Henry and John A. Ronalds, Plenum Press, New York 3-9

136. Millar, A.A., Olive, M.R. and **Dennis, E.S.** (1994)
The expression and anaerobic induction of alcohol dehydrogenase in cotton
Biochemical Genetics, 32, 279-300

137. McElroy, D., Zhang, W., Xu, D., Witrzens, B., Gubler, F., Jacobsen, J., Wu, R., Brettell, R.I.S. and **Dennis, E.S.** (1994)
Development of promoter systems for the expression of foreign genes in transgenic cereals
In "Improvement of Cereal Quality by Genetic Engineering" Edited by Robert J. Henry and John A. Ronalds, Plenum Press, New York 55-69

138. Hossain, M.A., McGee, J.D., Grover, A., **Dennis, E.S.**, Peacock, W.J. and Hodges, T.K. (1994)
Nucleotide sequence of a rice genomic pyruvate decarboxylase gene that lacks introns: A pseudo-gene?
Plant Physiology. 106, 1697-1698

139. Chaudhury, A.M., Lavithis, M., Taylor, P.E., Craig, S., Singh, M.B., Signer, E.R., Knox, R.B. and **Dennis, E.S.** (1994)
Genetic control of male fertility in *Arabidopsis thaliana.* structural analysis of premeiotic developmental mutants
Sexual Plant Reproduction. 7, 17-28

140. Dolferus, R., de Bruxelles, G., **Dennis, E.S.** and Peacock, W.J. (1994)
Regulation of the *Arabidopsis Adh* gene by anaerobic and other environmental stresses
Annals of Botany 74, 301-308

141. Chaudhury, A.M., Farrell, L.B., Chapple, R., Blömer, K., Craig, S. and Dennnis, E. S. (1994)
Genetic and molecular dissection of male-fertility in higher plants
In 'Genetic Control of Self-Incompatibility and Reproductive Development in Flowering Plants'. Eds. E.G. Williams, A.E. Clarke and R.B. Knox. Kluwer Academic Publishers, 403-422

142. Brettell, R.I.S., Olive, M.R. and **Dennis, E.S.** (1994)
Alcohol dehydrogenase in Maize Cell Cultures
In "Biotechnology in Agriculture and Forestry" Vol. 25 Maize
Edited by Y.P.S. Bajaj, Springer-Verlag Berlin Heidelberg, 445-455

143. Dolferus, R., Jacobs, M., Peacock, W.J. and **Dennis, E.S.** (1994)
Differential interactions of promoter elements in stress responses of the *Arabidopsis Adh* gene.
Plant Physiology 105, 1075-1087

144. Jacobsen-Lyon, K., Jensen, E.Ø., Jørgensen, J-E., Marcker, K.A., Peacock W.J. and **Dennis** E.S. (1995)
Symbiotic and Nonsymbiotic Hemoglobin Genes of *Casuarina glauca*
American Society of Plant Physiologists.
The Plant Cell 7, 213-223.

145. Harcourt, R., Kyozuka, J., Zhu, X., Southerton, S., Llewellyn, D., **Dennis**, E. and Peacock, J. (1995)
Genetic engineering for sterility in temperate plantation eucalypts
In "Eucalypt Plantations: Improving Fibre Yield and Quality" B.M. Potts, N.M.G. Borralho,

J.G. Reid, R.N. Cromer, W.N. Tibbits and C.A. Raymond (eds).
Emerging Technologies CRC for Temperate Hardwood Forestry - IUFRO Conference, Hobart, 1995, 403-405

146. Harcourt, R., Zhu, X., Llewellyn, D., **Dennis**, E. and Peacock J. (1995)
Genetic Engineering for Insect Resistance in Temperate Plantation Eucalypts
In "Eucalypt Plantations: Improving Fibre Yield and Quality" B.M. Potts, N.M.G. Borralho, J.G. Reid, R.N. Cromer, W.N. Tibbits and C.A. Raymond (eds).
Emerging Technologies CRC for Temperate Hardwood Forestry - IUFRO Conference, Hobart, 1995, 406-408

147. Mullins, K.V., Hartney, V.J., Llewellyn, D.J., Strauss, S. and **Dennis, E.S.** (1995)
Regeneration and Transformation of *Eucalyptus camaldulensis*
In "Eucalypt Plantations: Improving Fibre Yield and Quality" B.M. Potts, N.M.G. Borralho, J.B. Reid, R.N. Cromer, W.N. Tibbits and C.A. Raymond (eds).
Emerging Technologies CRC for Temperate Hardwood Forestry -IUFRO Conference, Hobart, 1995. 413-415

148. Southerton, S., Strauss, S., Olive, M., Zhu, X., Harcourt, R., Peacock, J. and **Dennis**, E. (1995)
Cloning and characterisation of a *Eucalyptus* floral meristem identity gene
In: "Eucalypt Planations: Improving Fibre Yield and Quality" B.M. Potts, N.M.G. Borralho, J.B. Reid, R.N. Cromer, W.N. Tibbits and C.A. Raymond (eds)
Emerging Technologies CRC for Temperate Hardwood Forestry -IUFRO Conference, Hobart, 1995, 424-426

149. Perriman, R., Bruening, G., **Dennis, E.S.** and Peacock, W.J. (1995)
Effective ribozyme delivery in plant cells
Proceedings of the National Academy of Sciences, USA, 92, 6175-6179

150. Peacock, J., Ming, L., Craig, S., **Dennis**, E and Chaudhury, A., (1995)
A mutagenesis programme for apomixis genes in *Arabidopsis*
Proceedings of an International Symposium on Induced Mutations and Molecular Techniques for Crop Improvement
International Atomic Energy Agency and the Food and Agriculture Organization for the United Nations, Vienna, 1995, 117-125

151. Grover, A., Hossain, M.A., Huq, M.E., McGee, J.D., Peacock, W.J., **Dennis, E.S.** and Hodges, T.K. (1995)
Studies on the alterations of Pdc gene expression in transgenic rice
Proceedings of the International Rice Research Conference - Fragile lives in fragile ecosystems.
International Rice Research Institute, Manila, Philippines, 911-921

152. Harcourt, R.L., Llewellyn, D., Morton, R., **Dennis, E.S.** and Peacock, W.J. (1996)
Effectiveness of Purified *Bacillus thuringiensis* Berliner Insecticidal Proteins in Controlling Three Insect Pests of Australian Eucalypt Plantations
Journal of Economic Entomology 89(6), 1392-1398

153. Chapple, R.M., Chaudhury, A.M., Blömer, K.C., Farrell, L.B. and **Dennis, E.S.** (1996)
Construction of a YAC contig of 2 megabases around the *MS1* gene in *Arabidopsis thaliana*
Australian Journal of Plant Physiology 23, 453-465

154. de Feyter, R., Young, M., Schroeder, K., **Dennis, E.S.** and Gerlach, W. (1996)
A ribozyme gene and an antisense gene are equally effective in conferring resistance to tobacco mosaic virus on transgenic tobacco
Molecular and General Genetics 250, 329-338

155. Mathews, A., Llewellyn, D.J., Wu, Y. and **Dennis** E.S. (1996)
Isolation and characterisation of full length cDNA clones of the giant taro (*Alocasia macrorrhiza*) trypsin/chymotrypsin inhibitor.
Plant Molecular Biology 30, 1035-1039

156. Chin-Atkins, A.N., Craig, S., Hocart, C.H., **Dennis, E.S.** and Chaudhury, A.M. (1996)
Increased endogenous cytokinin in the *Arabidopsis amp1* mutant corresponds with de-etiolation responses
Planta 198, 549-556

157. Andersson, C.R., Jensen, E.O., Llewellyn, D.J., **Dennis, E.S.** and Peacock, W.J. (1996)
A new hemogloblin gene from soybean: A role for hemoglobin in all plants.
Plant Biology. Proc. Nat. Acad. Sci. USA. 93, 5682-5687

158. **Dennis, E.S.**, Finnegan, E.J., Bilodeau, P., Chaudhury, A., Genger, R., Helliwell, C.A., Sheldon, C.C., Bagnall, D.J. and Peacock, W.J. (1996)
Vernalization and the initiation of flowering.
Seminars in Cell & Developmental Biology 7, 441-448

159. de Bruxelles, G.L., Peacock, W.J., **Dennis, E.S.** and Dolferus, R. (1996)
Abscisic Acid Induces the Alcohol Dehydrogenase Gene in *Arabidopsis*.
Plant Physiology. 111, 381-391

160. Millar, A.A. and **Dennis, E.S.** (1996)
Protein Synthesis during oxygen deprivation in cotton
Australian Journal of Plant Physiology. 23, 341-348

161. Finnegan, E.J., Peacock, W.J. and **Dennis, E.S.** (1996)
Reduced DNA methylation in *Arabidopsis thaliana* results in abnormal plant development
Proceedings of the National Academy of Sciences, USA, 93, 8449-8454

162. Millar A.A. and **Dennis, E.S.** (1996)
The alcohol dehydrogenase genes of cotton.
Plant Molecular Biology 31, 897-904

163. Hossain, M.A., Huq, E., Grover, A., **Dennis, E.S.**, Peacock, W.J. and Hodges, T.K. (1996)
Characterization of pyruvate decarboxylase genes from rice
Plant Molecular Biology 31, 761-770

164. Glover, J.A., Blömer, Farrell, L.B., Chaudhury, A.M. and **Dennis** E.S. (1996)
Searching for Tagged Male-Sterile Mutants of Arabidopsis
Plant Molecular Biology Reporter 14 330-342

165. Dolferus, R., Ellis, M., de Bruxelles, G., Trevaskis, B., Hoeren, F., **Dennis, E.S.** and Peacock, W.J. (1997)
Strategies of Gene Action in *Arabidopsis* during Hypoxia
Annals of Botany 79 (Supplement A): 21-31

166. Chaudhury, A.M., Ming, L., Miller, C., Craig, S., **Dennis**, E.S and Peacock, W.J. (1997)
Fertilization-independent seed development in *Arabidopsis thaliana*
Proceedings of the National Academy of Sciences, USA, 94, 4223-4228

167. Llewellyn, D., Lyon, B.R., Cousins, Y., Huppatz, J., **Dennis**, E. S., and Peacock W.J. (1997)
Genetic Engineering of plants for resistance to the Herbicide 2,4-D
Genetic Engineering of Crop Plants, Butterworths, London, 1990
Edited by G.W. Lycett & D. Grierson 6, 67-77

168. Kyozuka, J, Harcourt, R., Peacock, W.J. and **Dennis, E.S.** (1997)
Eucalyptus has functional equivalents of the *Arabidopsis AP1* gene

Plant Molecular Biology 35, 573-584

169. Andersson, C.R., Llewellyn, D.J., Peacock, W.J. and **Dennis, E.S.** (1997)
Cell-specific expression of the promoters of two nonlegume hemoglobin genes in a transgenic legume, *Lotus corniculatus*
Plant Physiology 113, 45-57

170. Dolferus, R., Osterman, J.C., Peacock, W.J. and **Dennis, E.S.** (1997)
Cloning of the *Arabidopsis* and rice formaldehyde dehydrogenase genes: Implications for the origin of plant ADH enzymes
Genetics 146, 1131-1141

171. McFadden, H., de Feyter, R., Murray, F., **Dennis**, E. S., and Peacock W.J. (1997)
Genetic engineering approaches to the improvement of cotton's tolerance to verticillium wilt
Proceedings of the Seventh National Verticillium Symposium, 6-10 October 1997, Athens, Greece, 187-191

172. Kloeckener-Gruissem, B. and **Dennis, E.S.** (1997)
Cloned Genes
In "Mutants of Maize", Edited by M.G. Neuffer, E.H. Coe and S.R. Wessler

173. Mullins, K.V., Llewellyn, D.J., Hartney, V.J., Strauss, S. and **Dennis, E.S.** (1997)
Regeneration and transformation of *Eucalyptus camaldulensis*
Plant Cell Reports 16, 787-791

174. **Dennis, E.S.**, Bilodeau, P., Burn, J., Finnegan E. J., Genger R., Helliwell C., Kang, B. J., Sheldoi C. C., and Peacock, W, J. (1997)
Methylation controls the low temperature induction of flowering in *Arabidopsis*
The Society for Experimental Biology 1025, 97-103.

175. Wu, Y., Llewellyn, D., Mathews, A. and **Dennis, E.S.** (1997)
Adaptation of *Helicoverpa armigera* (Lepidoptera: Noctuidae) to a proteinase inhibitor expressed transgenic tobacco
Molecular Breeding 3, 371-380.

176. Trevaskis, B., Watts, R.A., Andersson, C.R., Llewellyn, D.J., Hargrove, M.S., Olson, J.S., **Dennis, E.S.** and Peacock, W.J. (1997)
Two hemoglobin genes in *Arabidopsis thaliana*: the evolutionary origins of leghemoglobins
Proceedings of the National Academy of Sciences, USA, 94, 12230-12234.

177. Hartweck, L.M., Llewellyn, D.J. and **Dennis, E.S.** (1997)
The *Arabidopsis thaliana* genome has multiple divergent forms of phosphoinositol-specific phospholipase C
Gene 202, 151-156.

178. Murray, F.R., Llewellyn, D.J., Peacock, W.J. and **Dennis, E.S.** (1997)
Isolation of the glucose oxidase gene from *Talaromyces flavus* and characterisation of its role in the biocontrol of *Verticillium dahliae*.
Current Genetics 32, 367-375.

179. Chaudhury .A. M., Craig. S., **Dennis**. E. S. and Peacock. W.J. (1998)
Ovule and embryo development, apomixis and fertilization
Current Opinion in Plant Biology, 1, 26-31.

180. Witrzens, B., Brettell, R.I.S., Murray, F.R., McElroy, D. Li Z., and **Dennis, E.S.** (1998)
Comparison of three selectable marker genes for the transformation of wheat by microprojectile bombardment
Australian Journal of Plant Physiology 25, 39-44.

181. Finnegan E. J., Genger R. K., Kovac K., Peacock W.J., and **Dennis** E.S. (1998)
DNA methylation and the promotion of flowering by vernalization
Proceedings of the National Academy of Sciences, USA, 95, 5824-5829.

182. Hoeren F.U., Dolferus R., Wu Y., Peacock W.J., and **Dennis** E.S. (1998)
Evidence for a role for AtMYB2 in the induction of the Arabidopsis alcohol dehydrogenase gene (*ADH1*) by low oxygen
Genetics 149, 479-490.

183. Finnegan, E.J., Genger, R.K., Peacock, W.J. and **Dennis, E.S.**
DNA methylation in plants (1998)
Annual Review Plant Physiology and Plant Molecular Biology 49, 223-247.

184. Taylor, P.E., Glover, J.A., Lavithis, M., Craig, S., Singh, M.B., Knox, R.B., **Dennis, E.S.** and Chaudhury, A.M. (1998)
Genetic control of male fertility in *Arabidopsis thaliana*: structural analyses of postmeiotic developmental mutants
Planta 205, 492-505.

185. Helliwell, C.A., Sheldon, C.C., Olive, M. R., Walker, A. R., Zeevart, J. A. D., Peacock, W. J. and **Dennis, E.S.** (1998)
Cloning of the *Arabidopsis ent*-kaurene oxidase gene *GA3*
Proceedings of the National Academy of Sciences, USA, 95, 9019-9024.

186. Southerton, S. G., Strauss, S. H., Olive, M.R., Harcourt, R. L., Decroocq,V., Zhu, X., Llewellyn, D. J., Peacock. W. J., and **Dennis, E.S.** (1998)
Eucalyptus has a functional equivalent of the *Arabidopsis* floral meristem identity gene *LEAFY*
Plant Molecular Biology 37, 897-910.

187. de Feyter, R., McFadden, H., and **Dennis** E.S. (1998)
Five avirulence genes from *IXanthomonas campestris* pv. *malvacearum* cause geneotype-specific cell death when expressed transiently in cotton
Molecular Plant-Microbe Interactions 11, 698-701.

188. McFadden, H., Grover, A., de Feyter, R., Llewellyn, D. and **Dennis, E.S.** (1998)
Transgenic cotton expressing a gene for chitinase shows improved tolerance to Verticillium wilt in glasshouse trials
9th Australian Cotton Conference (Gold Coast, 11-14 August 1998) 591-597.

189. Rungis, D., Llewellyn, D., **Dennis, E.S.** and Lyon, B.R. (1998)
DNA markers: A new tool for improving the breeding of Australian cotton cultivars
9th Australian Cotton Conference (Gold Coast, 11-14 August 1998) 757-766.

190. Glover, J., Grelon M., Craig. S., Chaudhury A., and **Dennis, E.S.** (1998)
Cloning and characterisation of *MS5* from *Arabidopsis*: a gene critical in male meiosis
The Plant Journal 15, 345-356.

191. Murray, F., Llewellyn, D., McFadden, H., Last, D., **Dennis, E.S.** and Peacock, W.J.(1999)
Expression of the *Talaromyces flavus* glucose oxidase gene in cotton and tobacco reduces fungal infection, but is also phytotoxic
Molecular Breeding 5, 219-232.

192. Luo, M., Bilodeau, P., Koltunow, A., **Dennis, E.S.**, and Peacock, W.J. (1999)
Genes controlling fertilization-independent seed development in *Arabidopsis thaliana*
Proceedings of the National Academy of Sciences, USA, 96, 296-301.

193. Sheldon, C.C., Burn, J.E., Perez, P.P., Metzger, J., Edwards, J.A, Peacock, W.J. and **Dennis, E.S.** (1999)
The *FLF* MADS box gene: a repressor of flowering in Arabidopsis regulated by

vernalization and methylation
The Plant Cell 11, 445-458.

194. Bilodeau, P., Luo, M., **Dennis, E.S.**, Peacock, W.J. and Chaudhury, A. (1999)
Cloning and sequence analysis of two members of a novel gene family from Arabidopsis with homology to known proteins involved in hydroxylation and oxidation of an aromatic ring (accession nos. AF098945, AF098947)
Plant Physiology 119, 364-366.

195. Decroocq, V., Zhu, X., He, P.H., Llewellyn, D., Peacock, W.J. and **Dennis, E.S.** (1999)
Engineering reproductive sterility in Eucalypts
Proceedings 2nd International Wood Biotechnology Symposium (Canberra, 10-12 March 1997) 153-160.

196. Decroocq, V., Zhu, X. Kauffman, M., Kyozuka, J., Peacock, W.J., **Dennis, E.S.** and Llewellyn, D.J. (1999)
A *TM3*-like MADS-box gene from *Eucalyptus* expressed in both vegetative and reproductive tissues
Gene 228, 155-160.

197. Ellis, M.H., **Dennis, E.S.** and Peacock, W.J. (1999)
Arabidopsis roots and shoots have different mechanisms for hypoxic stress tolerance
Plant Physiology 119, 57-64.

198. Genger, R.K., Kovac, K.A., **Dennis, E.S.**, Peacock, W.J. and Finnegan, E.J. (1999)
Multiple DNA methyltransferase genes in *Arabidopsis thaliana*
Plant Molecular Biology 41, 269-278.

199. Helliwell, C.A., Poole, A., Peacock, W.J. and **Dennis, E.S.** (1999)
Arabidopsis *ent*-kaurene oxidase catalyzes three steps of gibberellin biosynthesis.
Plant Physiology 119, 507-510.

200. Llewellyn, D., Kyozuko, J., Floyd, R., Tanaka, H., Harcourt, R., Decroocq, V., He, P.H., Zhu, X. **Dennis, E.S.** and Peacock, W.J. (1999)
Transgenic eucalypts with insect resistance and herbicide tolerance
Proceedings 2nd International Wood Biotechnology Symposium (Canberra, 10-12 March 1997) 115-120.

201. Bilodeau, P., Udvardi, M.K., Peacock, W.J. and **Dennis, E.S.** (1999)
A prolonged cold treatment-induced cytochrome P450 gene from *Arabidopsis thaliana*
Plant Cell and Environment 22, 791-800.

202. Helliwell, C.A., Olive, Mark R., Gebbie, L., Forster, R., Peacock, W.J. and **Dennis, E.S.** (2000)
Isolation of an *ent*-kaurene oxidase cDNA from *Cucurbita maxima*
Australian Journal of Plant Physiology, 27, 1141-1149.

203. Harcourt, R.L., Kyozuka, J., Floyd, R.B., Bateman, K.S., Tanaka, H., Decroocq, V., Llewellyn, D.J., Zhu, X., Peacock, W.J. and **Dennis, E.S.** (2000)
Insect- and herbicide-resistant transgenic eucalypts
Molecular Breeding 6, 307-315.

204. Luo, M., Bilodeau, P., **Dennis, E.S.**, Peacock, W.J., and Chaudhury, A. (2000)
Expression and parent-of-origin effects for FIS2, MEA, and FIE in the endosperm and embryo of developing Arabidopsis seeds
Proceedings of the National Academy of Sciences USA, 97, 10637-10642.

205. Finnegan, E.J., Peacock, W.J. and **Dennis, E.S.** (2000)

DNA methylation, a key regulator of plant development and other processes.
Current Opinion in Genetics & Development 10, 217-223.

206. **Dennis, E.S.**, Dolferus, R., Ellis, M., Rahman, M., Wu, Y., Hoeren, F.U., Grover, A, Ismond, K.P., Good, A.G. and Peacock, W.J. (2000)
Molecular strategies for improving waterlogging tolerance in plants.
Journal of Experimental Botany, 51, 89-97.

207. Sheldon, C.C., Rouse, D.T., Finnegan, E.J., Peacock, W.J. and **Dennis, E.S.** (2000)
The molecular basis of vernalization: the central role of FLOWERING LOCUS C (FLC)
Proceedings of the National Academy of Sciences, USA, 97, 3753-3758.

208. Hughes, P., **Dennis, E.S.**, Whitecross, M., Llewellyn, D. and Gage, P. (2000)
The cytotoxic plant protein, beta-purothionin, forms ion channels in lipid membranes
Journal of Biological Chemistry 275, 823-827.

209. Quimio, C.A., Torrizo, L.B., Setter, T.L., Ellis,M., Grover, A., Abrigo, E.M., Oliva, N.O., Ella, E. S., Carpena, A.L., Ito, O., Peacock, W.J., **Dennis, E.S.** and Datta, S.K. (2000)
Enhancement of submergence tolerance in transgenic rice overproducing pyruvate decarboxylase
J. Plant Physiol. 156, 516-521.

210. **Dennis, E.S.**, Bagnall, D., Finnegan, E.J., Helliwell, C., King, R., MacMillan, C., Rouse, D., Sheldon, C.C., Tadege, M. and Peacock, W.J. (2000)
Flowering time, FLC, vernalization, demethylation and gibberellins
Flowering Newsletter 29, 5-13.

211. Sheldon, C.C., Finnegan, E.J., Rouse, D.T., Tadege,M., Bagnall, D.J., Helliwell, C.A., Peacock, W.J. and **Dennis, E.S.** (2000)
The control of flowering by vernalization
Current Opinion in Plant Biology 3, 418-422.

212. Finnegan, E.J., Bagnall, D.J., Helliwell, C.A., Rouse, D.T., Sheldon, C.C.,Tadege, M.,Peacock, W.J. and **Dennis, E.S.**(2000)
Encyclopedia of Life Sciences - "Vernalization" Article 2048.

213. Ellis, M.H., Millar, A.A., Llewellyn, D.J., Peacock, W.J. and **Dennis, E.S.** (2000)
Transgenic cotton (Gossypium hirsutum) over-expressing alcohol dehydrogenase shows increased ethanol fermentation but no increase in tolerance to oxygen deficiency
Aust. J. Plant Physiol., 27, 1041-1050.

214. Upadhyaya, N.M., Zhou, X., Wu, L., Ramm, K and **Dennis, E.S.**(2000)
The *tms2* Gene as a Negative Selection Marker in Rice
Plant Molecular Biology Reporter 18, 227-233, 2000.

215. Upadhyaya, N.M., Zhou, X.R., Zhu, Q.H., Eamens, A., Wang, M-B., Waterhouse, P.M., and **Dennis, E.S.**(2000)
Transgenic Rice
Transgenic Cereals, Edited by: L.O'Brien and R.J. Henry
American Association of Cereal Chemists, USA, pp 28-35.

216. Helliwell, C.A., Olive, M.R., Gebbie, L., Forster, R., Peacock, W.J., and **Dennis, E.S.** (2000)
Isolation of an *ent*-kaurene oxidase cDNA from *Cucurbita maxima*
Aust. J. Plant Physiol, 27, 1141-1149.

217. Nogue, F., Hocart, C., Letham, D.S., **Dennis, E.S.** and Chaudhury A.M. (2000)
Cytokinin synthesis is higher in the *Arabidopsis amp1* mutant
Plant Growth Regulation 32, 267-273.

218. Nogue, F., Grandjean, O., Craig, S., **Dennis, E.S.** and Chaudhury A.M. (2001)
Higher levels of cell proliferation rate and cyclin *CycD3* expression in the *Arabidopsis amp1* mutant
Plant Growth Regulation 32, 275-283.

219. Helliwell, C.A., Chin-Atkins, A.N., Wilson, I.W., Chapple, R., **Dennis, E.S.** and Chaudhury, A. (2001)
The Arabidopsis *AMP1* gene encodes a putative glutamate carboxypeptidase
The Plant Cell, 13, 2115-2125.

220. Adcock, G.J., **Dennis, E.S.**, Easteal S., et al (2001)
Mitochondrial DNA sequences in ancient Australians: Implications for modern human origins
P Natl Acad Sci USA 98, 537-542.

221. McFadden H.G., Lawrence G.J., **Dennis** E.S (2001)
Differential induction of chitinase activity in flax (Linum usitatissimum) in response to inoculation with virulent or avirulent strains of Melampsora lini, the case of flax rust
Australian Plant Path 30 (1): 27-30.

222. Adcock, G.J., **Dennis, E.S.**, Easteal S., Huttley, G.A., Jermiin, L.L., Peacock, W.J. and Thorne, A. (2001)
Human origins and ancient human DNA – Response
Science 292 (5552): 1656-1656.

223. Kishimoto, N., Sakai, H., Jackson, J., Jacobsen, S.E., Meyerowitz, E.M., **Dennis, E.S.** and Finnegan, E.Jean (2001)
Site specificity of the Arabidopsis METI DNA methyltransferase demonstrated through hypermethlation of the superman locus
Plant Molecular Biology 46: 171-183.

224. Hunt, P.W., Watts R.A., Trevaskis, B., Llewelyn D.J., Burnell, J., **Dennis, E.S.** and Peacock, W.J. (2001)
Expression and evolution of functionally distinct haemoglobin genes in plants
Plant Molecular Biology, 47, 677-692.

225. Watts, R.A., Hunt P.W., Hvitved, A.N., Hargrove, M.S., Peacock, W.J. and **Dennis, E.S.** (2001)
A hemoglobin from plants homologous to truncated hemoglobins of microorganisms
Proceedings of the National Academy of Sciences of the USA, 98, 10119-10124.

226. Chaudhury, A.M., Koltunow, A., Payne, T., Lou, M., Tucker, M.R., **Dennis, E.S.** and Peacock, W.J. (2001)
Control of Early Seed Development
Annu. Rev. Cell Dev. Biol. 17, 677-99.

227. Gocal, G.F.W., Sheldon, C.C., Gubler, F., Moritz, T., Bagnall, D.B., MacMillan, C.P., Li, S.F., Parish, R.W., **Dennis, E.S.**, Weigel, D. and King, R.W. (2001)
GAMYB-like Genes, Flowering and Gibberellin Signalling in Arabidopsis
Plant Physiology, 127,1682-1693.

228. Adcock, G.J., **Dennis, E.S.**, Esteal, S., Huttley, G.A., Jermin, L.S., Peacock, W.J., Thorne, A. (2001)
Mitochondrial DNA sequences in ancient Australians: Implications for modern human origins
Archaeol, Oceania 36, 163-174.

229. Helliwell, C.A., Sullivan, J.A., Mould, R.M., Gray, J.C., Peacock, W.J. and **Dennis, E.S.** (2001)
A plastid envelop location of Arabidopsis ent-kaurene oxidase links the plastid and endoplasmic reticulum steps of the gibberellin biosynthesis pathway
Plant Journal, 28, 1-9.

230. Rahman, M., Grover, A., Peacock, W.J., **Dennis, E.S.** and Ellis, M.H. (2001)
Effects of manipulation of pyruvate decarboxylase and alcohol dehydrogenase levels on the submergence tolerance of rice
Aust. J. Plant Physiol 28, 1-11.

231. Tadege, M., Sheldon, CC, Helliwell, CA, Stoutjesdijk, P., **Dennis, E.S.** and Peacock, W.J. (2001)
Control of flowering time by FLC orthologues in Brassica napus
The Plant Journal 28, 545-553.

232. Finnegan, E.J., Bagnall, D., Helliwell, C., Rouse, D., Sheldon, C., Tadege, M., Peacock, W.J., and **Dennis**, E. (2001)
Vernalization is the promotion of flowering in response to a prolonged period of growth at low temperatures.
Encyclopedia of Life Sciences. Nature Publishing Group. Macmillan Publishers.

233. Helliwell, C.A., Chandler, P.M., Poole, A., **Dennis, E.S.**, Peacock, W.J.(2001)
The CYP88A cytochrome P450, *ent*-kaurenoic acid oxidase, catalyzes three steps of the gibberellin biosyntheses pathway.
Proceedings of the National Academy of Science 98, 2065-2070.

234. Rouse, D.T., Sheldon, C.C., Bagnall, D.J., Peacock, W.J. and **Dennis, E.S.** (2002)
FLC, a repressor of flowering, is regulated by genes in difference inductive pathways
The Plant Journal 29, 1-10.

235. Shiao, T., Ellis, M.H., Dolferus, R., **Dennis, E.S.**, Doran, P.M. (2002)
Overexpression of Alcohol Dehydrogenase or Pyruvate Decarboxylase Improves Growth of Hairy Roots at Reduced Oxygen Concentrations.
Biotechnology and Bioengineering, 77, 455-461

236. Upadhyaya, N.M., Zhou, X.R., Zhu, Q.H., Ramm, K., Wu, L., Eamens, A., Sivakumar, R., Kato. T., Yun, D.W., Kumar, S., Narayana, K.K., Peacock, J.W., **Dennis, E.S.** (2002)
An *i*Ac/Ds gene and enhancer trapping system for insertional mutagenesis in rice.
Functional Plant Biology 29, 547-559.

237. Rungis, D., Llewellyn, D., **Dennis, E.S.**, Lyon, B.R. (2002)
Investigation of the chromosomal location of the bacterial blight resistance gene present in an Australian cotton (*Gossypium hirsutum* L) cultivar.
Australian Journal of Agricultural Research 53, 551-560.

238. Wu, Y., Llewellyn, D.J. and **Dennis, E.S.** (2002)
A quick and easy method for isolating good-quality RNA from cotton (*Gossypium hirsutum L.)* tissues
Plant Molecular Biology Reporter 20, 1-6.

239. Klok, E.J., Wilson, I.W., Wilson, D., Chapman, S.C., Ewing, R.M., Somerville, S.C., Peacock, W.J., Dolferus, R. and **Dennis, E.S.** (2002)
Expression Profile Analysis of the Low-Oxygen Response in Arabidopsis Root Cultures
The Plant Cell 14, 1-15.

240. Sheldon, C.C., Conn, A.B., **Dennis, E.S.**, and Peacock, W.J.(2002)
Different Regulatory Regions Are Required for the Vernalization-Induced Repression of FLOWERING LOCUS C and for the Epigenetic Maintenance of Repression
Plant Cell 14, 2527-2537.

241. Helliwell, C.A., Peacock, W.J. and **Dennis, E.S.** (2002)
Isolation and Functional Characterization of Cytochrome P450s in Gibberellin Biosynthesis Pathway
Methods in Enzymology 357, 381-388.

242. Hunt, P.W., Klok, E.J., Trevaskis, B., Watts, R.A., Ellis, M.H., Peacock, W.J. and **Dennis, E.S**. (2002)
Increased level of hemoglobin 1 enhances survival of hypoxic stress and promotes early growth in *Arabidopsis thaliana*
Proceedings of the National Academy of Science, USA 99, 17197-17202.

243. Upadhyaya, N.M., Zhu, Q., Eamens, A., and **Dennis, E.S.** (2002)
Rice Gene Machine: A Vehicle for Finding Functions of Cereal Genes
Asia Pacific Biotech News 6, 936-942.

244. Genger, R.K., Peacock, W.J., **Dennis, E.S**. and Finnegan, E.J. (2002)
Opposing effects of reduced DNA methylation on flowering time in *Arabidopsis thaliana*
Planta 216, 461-466

245. Dolferus, R., Klok, E.J., Delessert, C., Wilson, S., Ismond, K.P., Good, A.G., Peacock, W.J. and **Dennis, E.S.** (2003)
Enhancing the Anaerobic Response
Annals of Botany 91, 111-117

246. Oliver, S., **Dennis, E.S.** and Dolferus, R. (2003)
Cold-induced sterility in rice: a sweet affair
IREC Farmers' Newsletter, Large Area Edition, 164, Spring 2003

247. Ismond, K.P., Dolferus, R., De Pauw, M., **Dennis, E.S**. and Good, A.G. (2003)
Enhanced Low Oxygen Survival in Arabidopsis through Increased Metabolic Flux in the Fermentative Pathway
Plant Physiology 132, 1292-1302

248. Trevaskis, B., Bagnall, D.J., Ellis, M.H., Peacock, W.J. and **Dennis, E.S.** (2003)
MADS box genes control vernalization induced flowering in cereals
Proceedings of the National Academy of Sciences of the USA 100:22 13099-13104

249. Shinozaki, K., and **Dennis, E.S**. (2003)
Cell signalling and gene regulation – Global analyses of signal transduction and gene expression profiles (Editorial overview)
Current Opinion in Plant Biology 6, 405-409

250. Zhu, Q., Hoque, M.S., **Dennis, E.S**. and Upadhyaya, N (2003)
Ds tagging of *BRANCHED FLORETLESS 1 (BFLI)* that mediates the transition from spikelet to floret meristem in rice (*Oryza sativa* L)
BioMed Central Plant Biology 3:6

251. Tadege, M, Sheldon, C.C., Helliwell, C.A., Upadhyaya, N.M., **Dennis, E.S.** and Peacock, W.J. (2003)
Reciprocal control of flowering time by *OsSOC1* in transgenic *Arabidopsis* and by *FLC* in transgenic rice.
Plant Biotechnology Journal 1: 361-369

252. Santos, D.M., Dijo, J., Jacobs, M., **Dennis, E.S.** and Dolferus, R. (2003)
Approaches for the isolation of Arabidopsis adh1 regulator mutants using allyl alcohol selection
Russian Journal of Plant Physiology 50 (6): 762-773

253. Wang, M., Bian, X., Wu, L., Liu, L., Smith, N.A., Issenegger, D., Wu, R., Masuta,C., Vance, V.B. Watson, J.M., Rezaian, A., **Dennis, E.S.** and Waterhouse, P.M. (2004)
On the role of RNA silencing in the pathogenicity and evolution of viroids and viral satellites.
Proceedings of the National Academy of Sciences USA 101: 9, 3275-3280.

254. Finnegan, E.J., Sheldon, C.C., Jardinaud, F.M., Peacock, W.J. and **Dennis, E.S.** (2004)
A cluster of Arabidopsis genes with a co-ordinate response to an environmental stimulus
Current Biology 14: 911-916.

255. Zhu, Q., Ramm, K., Shivakkumar, R., **Dennis, E.S.** and Upadhyaya, N.M. (2004)
The *ANTHER INDEHISCENCE1* gene encoding a single MYB domain protein is involved in anther development in rice.
Plant Physiology 135: 1514-1525.

256. Upadhyaya, N., and **Dennis, E.S.** (2005)
New Lines on offer at rice mutant gene library
IREC Farmers' Newsletter 168, Rice R&D edition

257. **Dennis, E.S.** and Peacock, W.J. (2004)
Arabidopsis – what can crop breeders learn from a weed?
In: New Directions for a Diverse Planet, Proceedings 4th International Crop Science Congress (Brisbane, 26 September-1 October, 2004)

258. Delessert, C., Wilson, I., van der Straeten, D., **Dennis, E.S** and Dolferus, R. (2004)
Spatial and temporal analysis of the wounding response in Arabidopsis leaves
Plant Molecular Biology 55: 165-181

259. Eamens, A.L., Blanchard, C.L., **Dennis, E.S.** and Upadhyaya, M.M. (2004)
A bi-directional gene trap construct suitable for T-DNA and *Ds* mediated insertional mutagenesis in rice (*Oryza sativa* L.)
Plant Biotechnology Journal 2: 367-380

260. Upadhyaya, N.M., Zhu, Q-H., Hoque, M.S., Ramm, K., Shivakkumar, S., Smith, K.F., Pan, S-T., Li, S., Peng, K. and **Dennis, E.S.** (2004)
Dissociation (Ds) insertional mutagenesis using the transiently expressed transposase: improved constructs and their suitability for targeted saturation mutagenesis
Proceedings 2nd International Symposium on Rice Functional Genomics (Tucson, 15-17 November, 2004)

261. Hughes, P.A., Stevens, M.M., Park, H-W., Federici, B.A., **Dennis, E.S.** and Akhurst, R. (2005)
Response of larval *Chironomus tepperi* (Diptera: Chironomidae) to individual *Bacillius thuringiensis* var. *israelensis* toxins and toxin mixtures
Journal of Invertebrate Pathology 88:1 34-39

262. Rungis, D., Llewellyn, D., **Dennis, E.S.** and Lyon, B.R. (2005)
Simple sequence repeat (SSR) markers reveal low levels of polymorphism between cotton (*Gossypium hirsutum* L.) cultivars of Australian and American origin
Australian Journal of Agricultural Research 56: 301-307

263. Margis-Pinheiro M., Zhou X-R., Zhu Q-H., Dennis E.S. and Upadhyaya N.M. (2005)
Isolation and characterization of a *Ds*-tagged rice (*Oryza sativa* L.) GA responsive dwarf mutant defective in an early step of the gibberellin biosynthesis pathway.
Plant Cell Reports 23:819-833.

264. Chen, S, Helliwell, C.A., Wu, L., **Dennis, E.S.**, Upadhyaya, N., Zhang, R., Waterhouse, P.M. and Wang, M. (2005)
A novel T-DNA vector design conducive for selection of transgenic lines with simple transgene integration and stable transgene expression
Functional Plant Biology 32: 671-681

265. Wilson, I.W., Kennedy, G.C., Peacock, W.J. and **Dennis, E.S.** (2005)
Microarray analysis reveals vegetative molecular phenotypes of Arabidopsis flowering time

mutants
Plant Cell Physiology 46 : 1190-1201

266. Wu, Y., Llewellyn, D.J and **Dennis, E.S**. (2005)
Cycloheximide treatment of cotton ovules alters the abundance of specific classes of mRNAs and provides a method of generating novel ESTs for microarray expression profiling
Molecular Genetics and Genomics 274: 477 - 493

267. Oliver, S.N., Van Dongen, J.T., Alfred, S.C., Mamun, E., Zhao, X., Saini, H.S., Fernandes, S.F., Blanchard, C.L., Sutton, B.G., Geigenberger, P., **Dennis, E.S.**, and Dolferus, R. (2005)
Cold-induced repression of the rice anther-specific cell wall invertase gene *OSINV4* is correlated with sucrose accumulation and pollen sterility
Plant Cell and Environment 98:1534-1551

268. Luo, M., **Dennis,E.S.**, Berger,F., Peacock, W.J., and Chaudhury, A (2005)
MINISEED3 (*MINI3*), a *WRKY* family gene, and *IKU2*, a *LRR KINASE* gene, are regulators of endosperm development and seed size in *Arabidopsis*
Proceedings of the National Academy of Sciences 102: 17531-17536

269. Delessert, C., Wilson, I., Van Der Straeten, D., **Dennis, E.S.** and Dolferus, R. (2005)
The transcription factor ATAF2 represses the expression of pathogenesis-related proteins in Arabidopsis
Plant Journal 43, 745-757

270. Wu, Y., Machado, A., White, R.G., Llewellyn, D.J. and **Dennis, E.S.** 2006
Expression profiling identifies genes expressed early during lint fibre initiation in cotton
Plant Cell Physiology 47 (1): 107-127

271. Watts, R.A., Hargrove, M.S., Burnell, J.N., Olson, J.S. Peacock, W.J., and **Dennis, E.S.**
Variable oxygen binding and hexacoordination among plant hemoglobins
Plant Physiology (*submitted*)

272. Finnegan, E.J., Kovac, K.A., Jaligot, E.S., Sheldon, C.C., Peacock, W.J. and **Dennis, E.S.** (2005)
The down regulation of *FLOWERING LOCUS C* (*FLC*) in plants with low levels of DNA methylation and by vernalization occurs by distinct mechanisms
The Plant Journal 44, 420 - 42

273. Llewellyn, D., Batge, S., Poole, A. and **Dennis, E.S**.
Levels of the growth active Gibberellin, GA_1, and its antagonist ABA change inversely during cotton fibre development
Plant Physiology and Biochemistry (*submitted*)

274. Sheldon, C.C., Finnegan, E.J., Peacock, W.J. and **Dennis, E.S.** (2006)
Quantitative effects of vernalization on *FLC* and *SOC1* expression
The Plant Journal 45: 871-883

275. Hunt, P.W., Klok, E.J. Hebelstrup, K., Peacock, W.J. and **Dennis, E.S.**
GLB1, a class 1 haemoglobin gene is essential for plant survival following hypoxic stress
PLANTA (submitted)

276. Joshua A. Udall, Jordan M. Swanson, Karl Haller, Ryan A. Rapp, Michael E. Sparks, Jamie Hatfield, Yeisoo Yu, Yingru Wu, Caitriona Dowd, Aladdin B. Arpat, Brad A. Sickler, Thea A. Wilkins, Jin Ying Guo, Xiao Ya Chen, Jodi Scheffler, Earl Taliercio, Ricky Turley, Helen McFadden, Paxton Payton, Natalya Klueva, Randell Allen, Deshui Zhang, Candace Haigler, Curtis Wilkerson, Jinfeng Suo, Stefan R. Schulze, Margaret L. Pierce, Margaret Essenberg, HyeRan Kim, Danny J. Llewellyn, **Elizabeth S. Dennis**, David Kudrna, Rod Wing, Andrew H. Paterson, Cari Soderlund, and Jonathan F. Wendel (2006)
A global assembly of cotton ESTs
Genome Research 16:441-450

277. Andersson, C.R., Finnegan, E.J., Helliwell, C.A., Bagnall, D.J. Hughes, T., Peacock, W.J. and **Dennis, E.S.**
The *FLX* gene of Arabidopsis is required for high *FLC* Expression
Plant Physiology (under revision)

278. Zhu, Q-H., Ramm, K., Eamens, A.L. **Dennis, E.S.** and Upadhyaya, N.M. (2006)
Transgene structures suggest that multiple mechanisms are involved in T-DNA integration in plants
Plant Science 171: 308-322

279. Upadhyaya, N.M., Zhu, Q-H., Zhou, X-R., Eamens, A.L., Hoque, M.S., Ramm, K., Shivakkumar, R., Smith, K.F., Pan, S-T., Li, S, Peng, K., Kim, S.J. and **Dennis, E.S.** (2006)
Dissociation (*Ds*) constructs, mapped *Ds* launch pads and a transiently-expressed transposase system suitable for localized insertional mutagenesis in rice
Theoretical and Applied Genetics 112: 1326-1341.

280. Helliwell, C.A., Wood, C.C., Robertson, M., Peacock, W.J. and **Dennis, E.S.** (2006)
The Arabidopsis FLC protein interacts directly in vivo with *SOC1* and *FT* chromatin and is part of a high-molecular-weight protein complex
The Plant Journal 46:183-192

281. Trevaskis, B., Hemming, M.N., Peacock, W.J. and **Dennis, E.S.** (2006)
HvVRN2 Responds to Daylength, whereas HvVRN1 Is Regulated by Vernalization and Developmental Status
Plant Physiology 140: 1397 – 1405

282. Platten, J.D., Cotsaftis, O., Berthomieu, P., Bohnert, H., Davenport, R.J., Fairbairn, D.J. Horie, T., Leigh, R.A., Lin H-X., Luan, S., Mäser, P., Pantoja, O., Rodriguez-Navarro, A., Schachtman, D.P., Schroeder, J.I., Sentenac, H., Uozumi, N., Véry, A-A., Zhu, J-K., **Dennis, E.S.** and Tester, M. (2006)
Nomenclature for HKT transporters, key determinants of plant salinity tolerance
Trends in Plant Science 11: 372 - 374

283. Hebelstrup, Kim Henrik; Hunt, Peter; **Dennis, Elizabeth**; Jensen, Susie Bjerregaard; Jensen, Erik Østergaard (2006)
Hemoglobin is essential for normal growth of Arabidopsis organs
Physiologia Plantarum 127:1 157-166.

284. Amarasinghe, B.H.R., Faivre-Nitschke, E., Wu, Y., Udall, J.A., Dennis, E.S., Constable, G. and Llewellyn, D.J. (2006)
Genomic approaches to the discovery of promoters for sustained expression in cotton (*Gossypium hirsutim* L.) under field conditions: expression analysis in transgenic cotton and Arabidopsis of a Rubisco small subunit promoter identified using EST sequence analysis and cDNA microarrays

Plant Biotechnology 23, 437-450

285. Wood CC, Robertson M, Tanner G, Peacock, W.J., **Dennis, E.S.** and Helliwell, C.A. (2006)
The *Arabidopsis thaliana* vernalization response requires a polycomb-like protein complex that also includes VERNALIZATION INSENSITIVE 3
Proceedings of the National Academy of Sciences of America 103 (39): 14631-14636

286. Huang, S., Spielmeyer, W., Lagudah, E.S., James, R.A., Platten, J.D., **Dennis, E.S.** and Munns, R. (2006)
A Sodium Transporter (HKT7) Is a Candidate for *Nax1*, a Gene for Salt Tolerance in Durum Wheat
Plant Physiology 142: 1718 - 1727

287. **Dennis, E.S.,** Helliwell, C.A. and Peacock, W.J. (2006)
Vernalization – Spring into flowering
Developmental Cell 11: 1-7

288. Trevaskis, B., Tadege, M., Hemming, M., Peacock, W.J., **Dennis, E.S.** and Sheldon, C. (2007)
Short vegetative phase-like MADS-Box genes inhibit floral meristem identity in barley
Plant Physiology 143: 225-235

289. Byrt, C.S. Platten, J.D., Spielmeyer, W., James, R.A., Lagudah, E.S., **Dennis, E.S.**, Tester, M. and Munns, R. (2007)
HKT1;5-like Cation Transporters Linked to Na+ Exclusion Loci in Wheat, Nax2 and Kna1
Plant Physiology 143 : 1918-1928

290. Zhu Q-H., **Dennis, E.S.**, Upadhyaya, N.M. (2007)
Compact shoot and leafy head 1, a mutation affects leaf initiation and developmental transition in rice (*Oryza sativa* L.) 2007
Plant Cell Reports 26 : 421-427

291. Rahman, S., Morell, M., Topping, D., Bird, A., Zhongyi, L., **Dennis, E.S.** and Peacock, W.J. (2007)
Low Glycemic response cereals for enhanced human health
International Diabetes Monitor 19:21-25

292. Wu, Y., Llewellyn, D.J., White, R., Rugggiero, K. and **Dennis, E.S.** (2007)
Laser Capture Microdissection and cDNA microarrays used to generate gene expression profiles of the rapidly expanding fibre initial cells on the surface of cotton ovules
Planta doi 10.1007/s0045-007-0580-5

293. Wang, L., Wang, M-B., Tu J-X., Helliwell C.A., Waterhouse P.M., **Dennis E.S.**, Fu T-D., Fan Y-L (2007)
Cloning and characterisation of microRNAs from *Brassica napus*
FEBS Lett

294. Trevaskis, B., Hemming, M.N., **Dennis, E.S.**, Peacock, W.J., (2007)
The molecular basis of vernalization induced flowering in cereals
Trends Plant Sci

295. Sandra N. Oliver, Elizabeth S. Dennis and Rudy Dolferus.
ABA regulates apoplastic sugar transport in anthers and is a potential signal for cold-induced pollen sterility in rice.
Plant and Cell Physiology (PCP-2007-E-00096) in press

296. The Epigenetic Regulation of Flowering 2007-07-30 Current Opinion in Plant Science

Exhibit 2

MOLECULAR BIOLOGY OF THE CELL

SECOND EDITION

Bruce Alberts • Dennis Bray
Julian Lewis • Martin Raff • Keith Roberts
James D. Watson

Garland Publishing, Inc.
New York & London

TEXT EDITOR: Miranda Robertson

GARLAND STAFF

Managing Editor: Ruth Adams
Project Editor: Alison Walker
Production Coordinator: Perry Bessas
Designer: Janet Koenig
Copy Editors: Lynne Lackenbach and Shirley Cobert
Editorial Assistant: Māra Abens
Art Coordinator: Charlotte Staub
Indexer: Maija Hinkle

Bruce Alberts received his Ph.D. from Harvard University and is currently Chairman of the Department of Biophysics and Biochemistry at the University of California Medical School in San Francisco. *Dennis Bray* received his Ph.D. from the Massachusetts Institute of Technology and is currently a Senior Scientist in the Medical Research Council Cell Biophysics Unit at King's College London. *Julian Lewis* received his D.Phil. from Oxford University and is currently a Senior Scientist in the Imperial Cancer Research Fund Developmental Biology Unit, Dept. of Zoology, Oxford University. *Martin Raff* received his M.D. degree from McGill University and is currently a Professor in the Biology Department at University College London. *Keith Roberts* received his Ph.D. from Cambridge University and is currently Head of the Department of Cell Biology at the John Innes Institute, Norwich. *James D. Watson* received his Ph.D. from Indiana University and is currently Director of the Cold Spring Harbor Laboratory. He is the author of *Molecular Biology of the Gene* and, with Francis Crick and Maurice Wilkins, won the Nobel Prize in Medicine and Physiology in 1962.

Library of Congress Cataloging-in-Publication Data

Molecular biology of the cell / Bruce Alberts . . . [et al.].—2nd ed.
p. cm.
Includes bibliographies and index.
ISBN 0-8240-3695-6.—ISBN 0-8240-3696-4 (pbk.)
1. Cytology. 2. Molecular biology. I. Alberts, Bruce.
[DNLM: 1. Cells. 2. Molecular Biology. QH 581.2 M718]
QH581.2.M64 1989
574.87—dc19
DNLM/DLC
for Library of Congress 88-38275
CIP

Published by Garland Publishing, Inc.
136 Madison Avenue, New York, NY 10016

Printed in the United States of America

15 14 13 12 11 10 9 8 7 6 5 4 3 2

as *transfer RNAs* (*tRNAs*, see p. 103) or form the RNA components of ribosomes (rRNA, see p. 104) or smaller ribonucleoprotein particles.

The amount of RNA made from a particular region of DNA is controlled by *gene regulatory proteins* that bind to specific sites on DNA close to the coding sequences of a gene (see p. 557). In any cell at any given time, some genes are used to make RNA in very large quantities, while other genes are not transcribed at all. For an active gene, thousands of RNA transcripts can be made from the same DNA segment in each cell generation. Because each mRNA molecule can be translated into many thousands of copies of a polypeptide chain, the information contained in a small region of DNA can direct the synthesis of millions of copies of a specific protein. The protein *fibroin*, for example, is the major component of silk. In each silk gland cell, a single fibroin gene makes 10^4 copies of mRNA, each of which directs the synthesis of 10^5 molecules of fibroin—producing a total of 10^9 molecules of fibroin in just 4 days.

Eucaryotic RNA Molecules Are Spliced to Remove Intron Sequences[15]

In bacterial cells most proteins are encoded by a single uninterrupted stretch of DNA sequence that is copied without alteration to produce an mRNA molecule. In 1977 molecular biologists were astonished by the discovery that most eucaryotic genes have their coding sequences (called *exons*) interrupted by noncoding sequences (called *introns*). To produce a protein, the entire length of the gene, including both its introns and its exons, is first transcribed into a very large RNA molecule—the *primary transcript*. Before this RNA molecule leaves the nucleus, a complex of RNA processing enzymes removes all of the intron sequences, thereby producing a much shorter RNA molecule. After this *RNA processing* step, called **RNA splicing**, has been completed, the RNA molecule moves to the cytoplasm as an mRNA molecule that directs the synthesis of a particular protein (see Figure 3–13).

This seemingly wasteful mode of information transfer in eucaryotes is presumed to have evolved because it makes protein synthesis much more versatile. For example, the primary RNA transcripts of some genes can be spliced in various ways to produce different mRNAs, depending on the cell type or stage of development. This allows different proteins to be produced from the same gene. Moreover, because the presence of numerous introns facilitates genetic recombination events between exons, this type of gene arrangement is likely to have been profoundly important in the early evolutionary history of genes—speeding up the process whereby organisms evolve new proteins from parts of preexisting ones instead of evolving totally new sequences (see p. 602).

Sequences of Nucleotides in mRNA Are "Read" in Sets of Three and Translated into Amino Acids[16]

The rules by which the nucleotide sequence of a gene is translated into the amino acid sequence of a protein, the so-called **genetic code**, were deciphered in the early 1960s. The sequence of nucleotides in the mRNA molecule that acts as an intermediate was found to be read in serial order in groups of three. Each triplet of nucleotides, called a **codon**, specifies one amino acid. In principle, each RNA sequence can be translated in any one of three different *reading frames* depending on where the decoding process begins (Figure 3–14). In almost every case, only one of these reading frames will produce a functional protein. Since there are no punctuation signals except at the beginning and end of the RNA message, the reading frame is set at the initiation of the translation process and is maintained thereafter.

Since RNA is a linear polymer of four different nucleotides, there are $4^3 = 64$ possible codon triplets (remember that it is the *sequence* of nucleotides in the triplet that is important). However, only 20 different amino acids are commonly found in proteins, so that most amino acids are specified by several codons; that is, the genetic code is *degenerate*. The code (shown in Figure 3–15) has been highly conserved during evolution: with a few minor exceptions, it is the same in organisms as diverse as bacteria, plants, and humans.

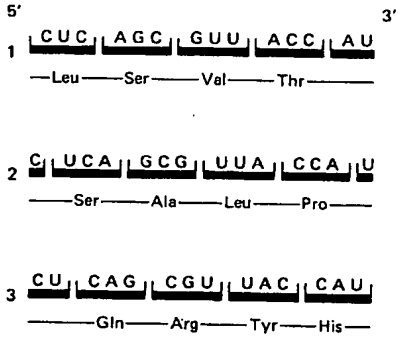

Figure 3–14 The three possible reading frames in protein synthesis. In the process of translating a nucleotide sequence into an amino acid sequence, the sequence of nucleotides in an mRNA molecule is read from the 5′ to the 3′ end in sequential sets of three nucleotides. In principle, therefore, the same RNA sequence can specify three completely different amino acid sequences, depending on the "reading frame."

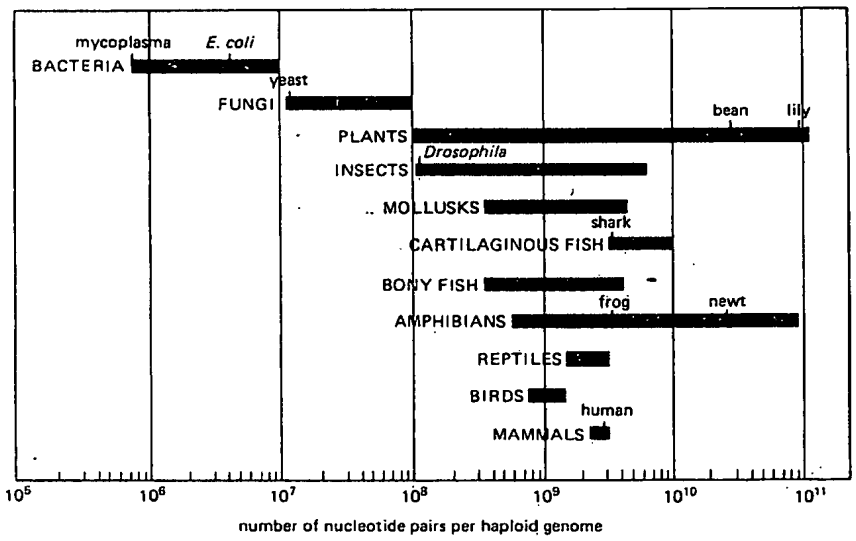

Figure 9–6 The amount of DNA in a haploid genome varies over a 100,000-fold range from the smallest procaryotic cell, the mycoplasma, to the large cells of some plants and amphibia. Note that the genome size of humans (3×10^9 nucleotide pairs) is much smaller than that of some other organisms.

about 10 times more complex than the fruit fly *Drosophila*, which is estimated to have about 5000 essential genes (see p. 510).

Whatever the nonessential DNA in higher eucaryotic chromosomes may do (see Chapter 10, p. 607), the data shown in Figure 9–6 make it clear that it is not a great handicap for a higher eucaryotic cell to carry a large amount of extra DNA. Indeed, even the essential coding regions are often interrupted by long stretches of noncoding DNA.

Each Gene Is a Complex Functional Unit for the Regulated Production of an RNA Molecule

The primary function of the genome is to produce RNA molecules. Selected portions of the DNA nucleotide sequence are copied into a corresponding RNA nucleotide sequence, which either (as mRNA) encodes a protein or forms a "structural" RNA, such as a tRNA or rRNA molecule. Each region of the DNA helix that produces a functional RNA molecule constitutes a **gene.**

Genes in a chromosome of a higher eucaryote can contain as many as 2 million DNA nucleotide pairs, and genes more than 100,000 nucleotide pairs in length are common (Table 9–1); yet only about 1000 nucleotide pairs are required to encode

Table 9–1 The Size of Some Human Genes in Thousands of Nucleotides

	Gene Size	mRNA Size	Number of Introns
β-Globin	1.5	0.6	2
Insulin	1.7	0.4	2
Protein kinase C	11	1.4	7
Albumin	25	2.1	14
Catalase	34	1.6	12
LDL receptor	45	5.5	17
Factor VIII	186	9	25
Thyroglobulin	300	8.7	36
Dystrophin*	more than 2000	17	more than 50

The size specified here for a gene includes both its transcribed portion and nearby regulatory DNA sequences. (Compiled from data supplied by Victor McKusick.)

*An altered form of this gene causes Duchenne muscular dystrophy.

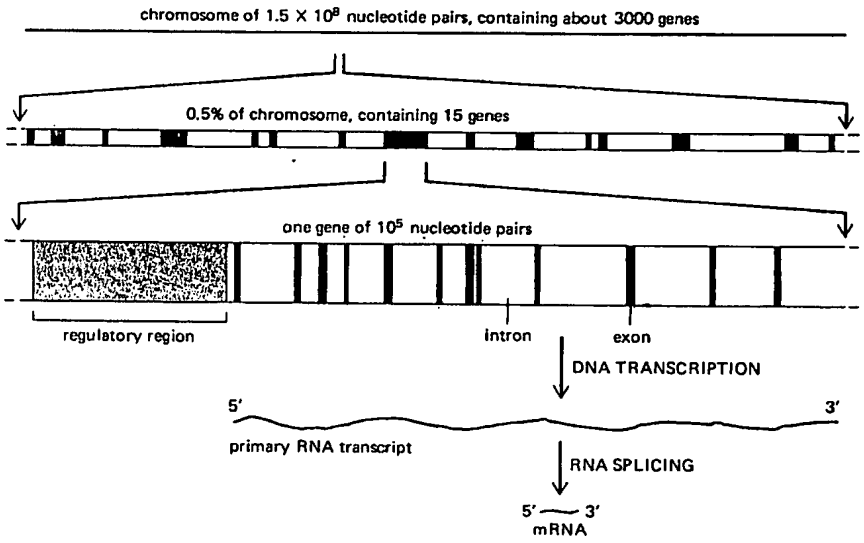

Figure 9–7 The organization of genes on a typical vertebrate chromosome. Proteins that bind to the DNA in regulatory regions determine whether a gene is transcribed; although often located on the 5′ side of a gene, as shown here, regulatory regions can also be located in introns, in exons, or on the 3′ side of a gene. The intron sequences are removed from the primary RNA transcripts that encode protein molecules to produce a messenger RNA (mRNA) molecule. The figure given here for the number of genes per chromosome is only a minimal estimate.

a protein of average size (one containing 300 to 400 amino acid residues). Most of the extra length consists of long stretches of noncoding DNA that interrupt the relatively short segments of coding DNA. The coding sequences are called **exons,** the intervening (noncoding) sequences are called **introns.** The RNA molecule (called a *primary RNA transcript*) synthesized from such a gene is altered to remove the intron sequences during its conversion to an mRNA molecule (see Figure 9–2) in the process of *RNA splicing* (see p. 531).

Large genes consist of a long string of alternating exons and introns, with most of the gene consisting of introns. In addition, each gene contains *regulatory DNA sequences,* which bind *gene regulatory proteins* that control transcription of the gene. Many regulatory sequences are located "upstream" (on the 5′ side) of the site where the RNA transcript begins, but they can also be located in introns, "downstream" (on the 3′ side) of the site where the RNA transcript ends, or even in exons. A typical vertebrate chromosome is illustrated schematically in Figure 9–7, along with one of its many genes.

Comparisons Between the DNAs of Related Organisms Distinguish Conserved and Nonconserved Regions of DNA Sequence[5]

Technical improvements in DNA sequencing are expected to allow the routine sequencing of stretches of chromosomal DNA that are millions of nucleotide pairs long, so that one can foresee the eventual determination of the sequence of all 3×10^9 nucleotides of the human genome. If more than 90% of this sequence is unimportant, however, it will be crucial to have some way of identifying the small proportion of sequence that is important. One way to achieve this is by the simultaneous sequencing of the corresponding regions of a related genome, such as that of the mouse. Human beings and mice are thought to have diverged from a common mammalian ancestor about 80×10^6 years ago, which is long enough for roughly two out of every three nucleotides to have been changed by random mutational events (see p. 220). Consequently, the only regions that will have remained closely similar (*conserved* regions) in the two genomes are those where mutations would impair function. (The organisms with these deleterious mutations would have been eliminated from the population by natural selection—see p. 221.) Thus, in general, *nonconserved* regions represent noncoding DNA—both between genes and in introns—whose DNA sequence is not critical for function. Conserved regions, in contrast, represent functionally important exons and regulatory regions. By revealing in this way the results of a very long natural "experiment," comparative DNA sequencing studies highlight the most interesting re-

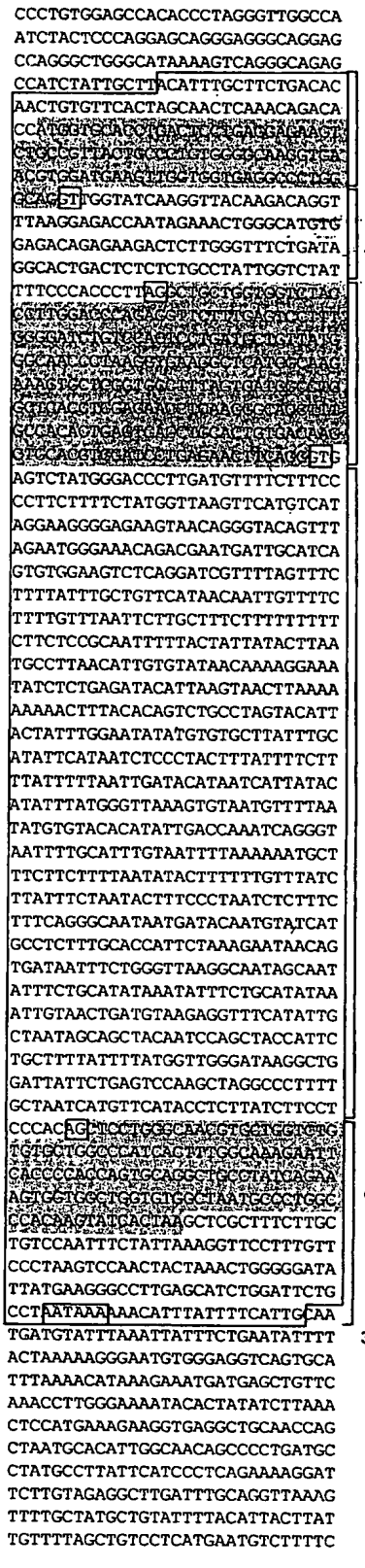

Figure 9–77 The transcribed portion of the human β-globin gene. The sequence of the DNA strand corresponding to the mRNA sequence is given, with the primary RNA transcript surrounded by a colored line and the nucleotides in the three coding regions (exons) shaded. Note that exon 1 includes a *5′-leader sequence* and that exon 3 includes a *3′-trailer sequence;* although these sequences are included in the mRNA, they do not code for amino acids. The highly conserved GT and AG nucleotides at the ends of each intron are boxed (see Figure 9–79), along with the cleavage and polyadenylation signal near the 3′ end of the gene (AATAAA, see Figure 9–75).

side of an intron sequence are joined to each other after the intron sequence has been cut out, this reaction is known as **RNA splicing.** RNA splicing occurs in the cell nucleus, out of reach of the ribosomes, and RNA is exported to the cytoplasm only when processing is complete (see p. 538).

Because most mammalian genes contain much more intron than exon sequence (see Table 9–1, p. 486), RNA splicing can account for the conversion of the very long nuclear hnRNA molecules (up to more than 50,000 nucleotides) to the much shorter cytoplasmic mRNA molecules (usually 500 to 3000 nucleotides).

Before discussing the distribution of introns in eucaryotic genes and some of their consequences for cell function, it is necessary to explain how intron sequences are recognized and removed by the splicing machinery.

hnRNA Transcripts Are Immediately Coated with Proteins and snRNPs[49]

Newly made RNA in eucaryotes, unlike that in bacteria, appears to become immediately condensed into a series of closely spaced protein-containing particles. These particles consist of about 500 nucleotides of RNA wrapped around an abundant protein complex that serves to condense and package each growing RNA transcript in a manner reminiscent of the DNA-protein complexes of nucleosomes. The resulting **hnRNP particles** (*heterogeneous nuclear ribonucleoprotein particles*) can be purified after nuclei have been treated with ribonucleases at levels just sufficient to destroy the linker RNA between them. The particles sediment at about 30S and have a diameter about twice that of nucleosomes (20 nm). Their protein core is correspondingly larger and more complex, being composed of a set of at least 8 different proteins of mass 34,000 to 120,000 daltons. Except for histones, the proteins in this core are the most abundant proteins in the cell nucleus. Those characterized thus far contain one or more copies of a short sequence of amino acids that is shared by many RNA-binding proteins (Figure 9–78).

The hnRNP particles are generally distorted by the standard spreading techniques used to view transcribing genes in the electron microscope (see Figure 9–70). These micrographs, however, reveal especially stable particles of a less common type on many RNA transcripts, whose location strongly implicates a role for them in RNA splicing. The stable particles form very quickly at the junctions between intron and exon sequences, and, as the RNA transcript elongates, these particles coalesce in pairs to form a larger assembly that is thought to be the *spliceosome* that catalyzes RNA splicing (Figure 9–79).

Biochemical analysis has revealed that the cell nucleus contains many complexes of proteins with small RNAs (generally RNAs of 250 nucleotides or less), which have arbitrarily been designated U1, U2,. . .,U12 RNAs. These complexes, called **small nuclear ribonucleoproteins (snRNPs),** resemble ribosomes in that each contains a set of proteins complexed to a stable RNA molecule. They are much smaller than ribosomes, however—about 250,000 daltons compared to 4.5 million daltons for a ribosome—and have higher protein-to-RNA ratios. Some proteins are present in several types of snRNPs, whereas others are unique to one type. This was first demonstrated using serum from patients with the disease *systemic lupus erythematosus,* who make antibodies directed against one or more snRNP proteins: a single antibody was found that binds the U1, U2, U5, and U4/U6 snRNPs, for example, suggesting that they all contain a common protein.

Figure 9–78 An amino acid sequence found in many eucaryotic RNA-binding proteins. This consensus—found in proteins from organisms as diverse as yeasts, *Drosophila*, and humans—is present in the proteins of hnRNP particles, in the protein bound to the poly-A tail of hnRNAs, in several snRNP proteins, and in the abundant nucleolar protein, nucleolin. When this sequence is found in a protein of unknown function, it suggests that the protein binds to RNA.

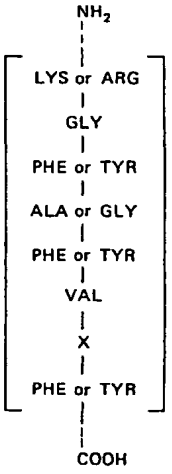

Individual snRNPs are believed to recognize specific nucleic acid sequences through RNA-RNA base-pair complementarity. Some mediate RNA splicing, some are involved in the cleavage reactions that generate the 3′ ends of some newly formed RNAs (see p. 596), while the function of others is unknown. The evidence for the role of snRNPs in RNA splicing comes from experiments on RNA processing *in vitro*.

Intron Sequences Are Removed as Lariat-shaped RNA Molecules[50]

Introns range in size from about 80 nucleotides to 10,000 nucleotides or more. They differ dramatically from exons in that their exact nucleotide sequences seem to be unimportant. Thus introns have accumulated mutations rapidly during evolution, and it is often possible to alter most of the nucleotide sequence of an intron without greatly affecting gene function. This has led to the suggestion that intron sequences have no function at all and are largely genetic "junk," a proposition we shall examine later (see p. 602). The only highly conserved sequences in introns are those required for intron removal. Thus there are consensus sequences at each end of an intron that are nearly the same in all known intron sequences, and these cannot be altered without affecting the splicing process that normally removes the intron sequence from the primary RNA transcript. These conserved boundary sequences at the **5′ splice site (donor site)** and the **3′ splice site (acceptor site)** are shown in Figure 9–80. The RNA breaking and rejoining reactions must be carried out precisely because an error of even one nucleotide would shift the reading frame in the resulting mRNA molecule and make nonsense of its message.

The pathway by which the intron sequences are removed from primary RNA transcripts has been elucidated by *in vitro* studies in which a pure RNA species containing a single intron is prepared by incubating an appropriately designed DNA fragment with a highly active, purified RNA polymerase (Figure 9–81). When these RNA molecules are added to a cell extract, they become spliced in a two-step enzymatic reaction that requires prolonged incubation with ATP, selected proteins in the extract, and the U1, U2, U5, and U4/U6 snRNPs; these components assemble into a large multicomponent ribonucleoprotein complex, or **spliceosome**. Characterization of the RNA species that appear as intermediates during the reaction, as well as the snRNPs required to produce them, led to the discovery

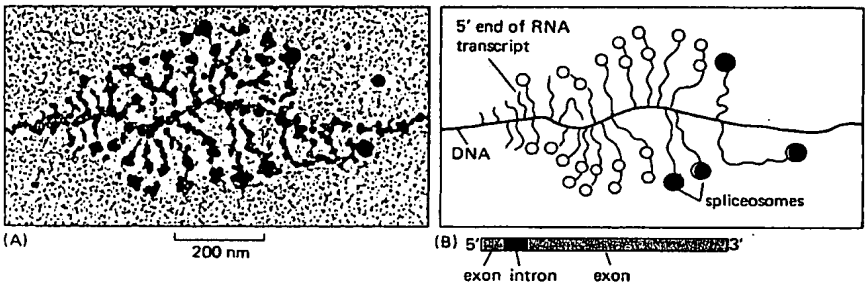

Figure 9–79 Electron micrograph of a chromatin spread showing large ribonucleoprotein particles assembling at the 5′ and 3′ splice sites to form a *spliceosome*. In the micrograph (A) a gene encoding a *Drosophila* chorion protein has been identified, so that the positions of the splice sites on the primary RNA transcript are known. (B) Most of the RNA transcripts have either one or two large RNP particles near their 5′ ends. When there are two particles on a transcript [open circles in (B)], they average 25 nm in diameter and occur at or very near the positions of the 5′ and 3′ splice sites for the single small intron sequence (228 nucleotides long) near the 5′ end of the transcripts. The more mature, longer transcripts on the two genes frequently display a single larger particle [colored circles in (B)] in the region of the intron, which probably results from the stable association of the two smaller particles and represents the assembled spliceosome. Since splicing occurs in some cases while the 3′ end of the RNA chain is still being transcribed, the poly A at the 3′ end of hnRNA molecules cannot be required for splicing. Most of the major hnRNP proteins have been removed from these transcripts by the spreading conditions used. (Adapted from Y.N. Osheim, O.L. Miller, and A.L. Beyer, *Cell* 43:143–151, 1985.)

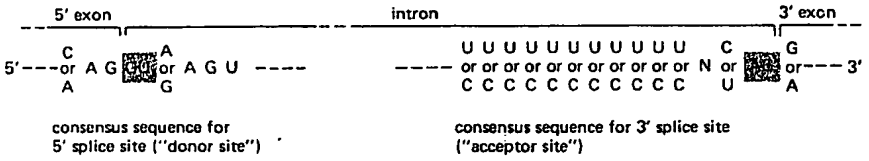

Figure 9–80 Consensus sequences for the 5′ and 3′ splice sites used in RNA splicing. The sequence given is that for the RNA chain; the nearly invariant GU and AG dinucleotides at either end of the intron are shaded in color (see also Figure 9–77).

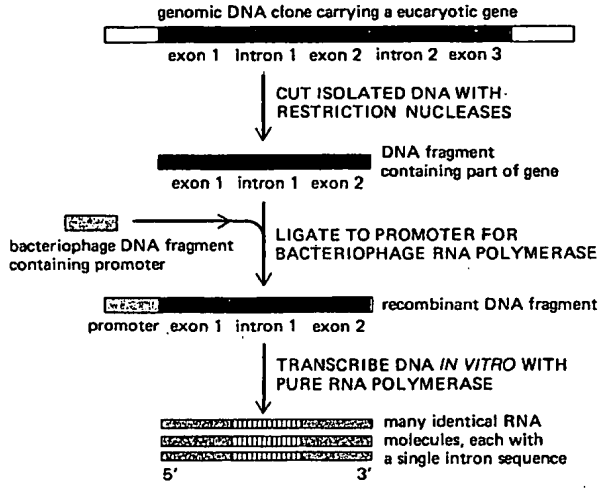

Figure 9–81 Outline of the procedure used to produce abundant amounts of pure RNA molecules for the analysis of RNA splicing *in vitro*. The method depends on the ability to produce large amounts of any desired DNA sequence by genetic engineering and DNA cloning (see p. 258) as well as on the availability of relatively simple RNA polymerases from bacteriophages T7 or SP6, which transcribe DNA with high efficiency *in vitro*. By coupling a eucaryotic DNA fragment to a bacteriophage promoter, a bacteriophage RNA polymerase can be used to generate *in vitro* large amounts of the RNA encoded by the eucaryotic DNA fragments. The 5′ cap present on hnRNAs can be incorporated into such RNAs by using a chemically synthesized, capped nucleotide to initiate the transcription process (not shown).

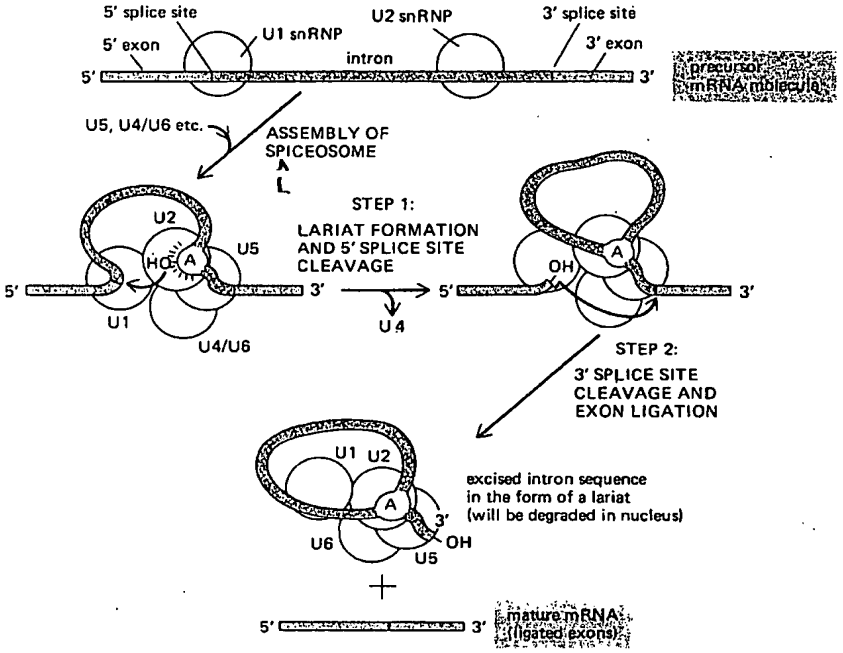

Figure 9–82 Catalysis of RNA splicing by a spliceosome formed from the assembly of U1, U2, U5, and U4/U6 snRNPs (shown as circles), plus other components (not shown). After assembly of the spliceosome, the reaction occurs in two steps: in step 1 a special A nucleotide in the intron sequence located close to the 3′ splice site attacks the 5′ splice site, which is cleaved; the cut 5′ end of the intron sequence joins covalently to this A nucleotide, forming the branched nucleotide shown in Figure 9–83. In step 2 the 3′-OH end of the first exon, which was exposed in the first step, adds to the beginning of the second exon, cleaving the RNA molecule at the 3′ splice site; the two exon sequences are thereby joined to each other and the intron sequence is released as a lariat. The complete spliceosome complex sediments at 60S, indicating that it is nearly as large as a ribosome. These splicing reactions occur in the nucleus and generate mRNA molecules from primary RNA transcripts (mRNA precursor molecules).

that the intron is excised in the form of a *lariat*, according to the splicing pathway shown in Figures 9–82 and 9–83.

Individual roles have been defined for several of the snRNPs. The U1 snRNP, for example, binds to the 5′ splice site, guided by a nucleotide sequence in the U1 RNA that is complementary to the nine-nucleotide splice-site consensus sequence (see Figure 9–80). Since RNA is capable of acting like an enzyme (see p. 105), either the RNA or the protein components of the spliceosome could be responsible for catalyzing the breakage and formation of covalent bonds required for RNA splicing.

Multiple Intron Sequences Are Usually Removed from Each RNA Transcript[51]

Because the spliceosome seems mainly to recognize a consensus sequence at each intron boundary, the *5′ splice site (donor site)* at the end of any one intron can in principle be joined to the *3′ splice site (acceptor site)* of any other intron in the splicing process. Thus, when the 5′ and 3′ halves of two different introns are experimentally combined, the resulting hybrid intron sequence is often recognized by the RNA-splicing enzymes and removed.

In view of this result, it is surprising that vertebrate genes can contain as many as 50 introns (see Table 9–1, p. 486). If any two 5′ and 3′ splice sites were mispaired for splicing, some functional mRNA sequences would be lost, with disastrous consequences. Somehow such mistakes are avoided: the RNA processing machinery normally guarantees that each 5′ splice site pairs only with the 3′ splice site that is closest to it in the downstream (5′-to-3′) direction of the linear RNA sequence (Figure 9–84). How this sequential pairing of splice sites is accomplished is not known, although the assembly of the spliceosome while the RNA transcript is still growing (see Figure 9–79) is presumed to play a major part in ensuring an orderly pairing of the appropriate splice sites. There is also evidence that the exact three-dimensional conformations adopted by the intron and exon sequences in the RNA transcript are important. We shall see, however—both below and in Chapter 10—that splicing can be controlled, and in selected cases the simple pattern of 5′-to-3′ splicing does not hold.

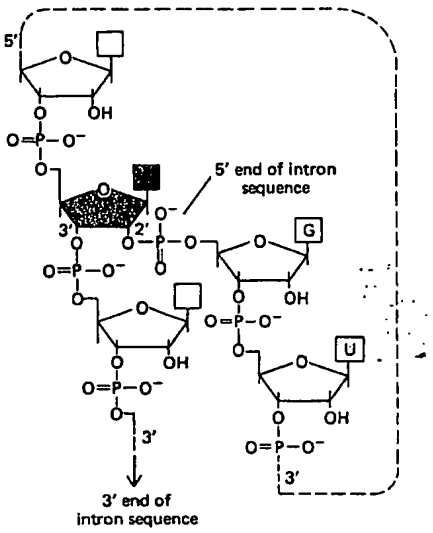

Figure 9–83 Structure of the branched RNA chain that forms during nuclear RNA splicing. The shaded A is the nucleotide highlighted in Figure 9–82, and the branch is formed in step 1 of the splicing reaction illustrated there. In this step the 5′ end of the intron sequence is cleaved and its phosphate group couples covalently to the 2′-OH ribose group of the A nucleotide, which is located about 30 nucleotides from the 3′ end of the intron sequence. The branched chain remains in the final excised intron sequence and is responsible for its lariat form (see Figure 9–82).

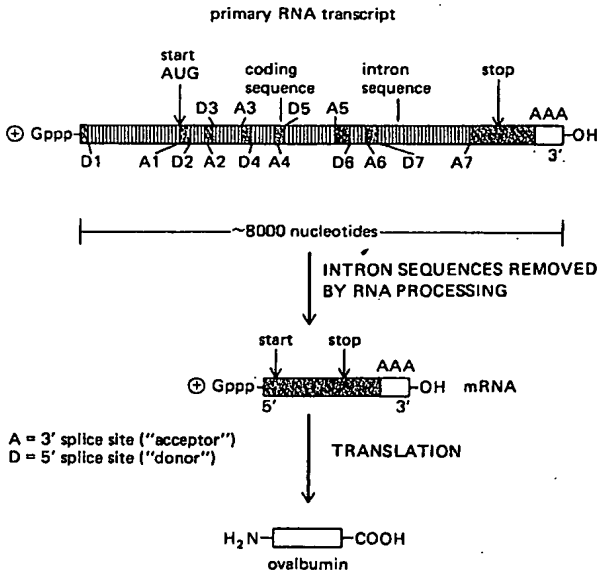

Figure 9–84 The primary RNA transcript for the chicken ovalbumin gene, showing the organized removal of seven introns required to obtain a functional mRNA molecule. The 5′ splice sites (donor sites) are denoted by D, and 3′ splice sites (acceptor sites) are denoted by A.

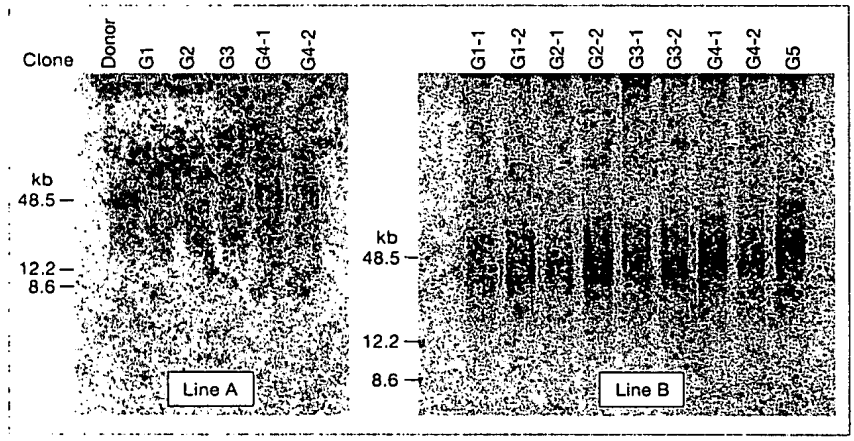

Figure 1 Telomere lengths in successive generations (G1–G5) of mice cloned from cumulus cells. Southern-blot analysis of terminal restriction-enzyme-cut fragments in five sequential generations shows that telomeres do not undergo incremental erosion in successive clonal generations. Genomic DNA isolated from peripheral-blood lymphocytes taken from representative animals from each generation was digested with the restriction enzyme *HinfI*, resolved on a pulse field gel, transferred to a solid support and probed with a 5′-^{32}P-labelled $(T_2AG_3)_3$ oligonucleotide. Peripheral blood lymphocytes were sampled on the same day. Ages of mice (in months) were: in line A, donor, 18; G1, 16; G2, 14; G3, 12; G4, 9; G5, 9; in line B, G1, 15.5; G2, 13; G3, 11; G4, 9; G5, 7. Suffix numbers (G4-1 and G4-2, for example) identify different pups of each generation.

was repeated with cumulus cells from adult G1 mice as nucleus donors to produce the next clonal generation, G2, and so on. Table 1 summarizes the results obtained following the reconstruction of 3,920 enucleated oocytes.

Previously, about 2% of enucleated oocytes receiving a cumulus cell nucleus developed to live-born pups[1]. This value is comparable to the cloning efficiency for G1 in lines A (1.5%) and B (4.2%). However, the success rate dropped in successive cloned generations: line A did not produce a G5 clone from 670 reconstructed oocytes; in line B, the only live-born G6 clone was cannibalized by her foster mother, thereby terminating the line. Mouse lines A and B therefore represent totals of 9 and 26 clones from their respective donors. Placental size was consistently in the range previously reported for cloned mice[2] and did not increase in successive generations (data not shown).

Do sequentially cloned mice show signs of accelerated ageing? We assessed the behaviour of these mice and determined telomere lengths to assess organismal and cellular measures of ageing, respectively. We evaluated learning ability in the Morris water maze and Krushinsky tests, as well as strength and agility, and also used other assays designed to monitor signs of premature ageing, such as a decline in activity in the home cage and loss of coordination[4]. All cloned mice were, by these criteria, normal compared with age-matched controls (data not shown); the G5 mouse is alive and healthy at 1.5 years.

We measured telomere length in peripheral blood lymphocytes of clones G1–G6 by Southern-blot analysis of terminal restriction-enzyme-digested fragments (Fig. 1) and found no evidence of shortened telomeres in the cloned mice. In fact, our results show that the telomeres lengthen with each generation. As representative animals of each generation were sampled simultaneously, we cannot rule out an age-related contribution to this increase (with younger mice having longer telomeres). In addition, long telomeres in mice are optimally studied by means of different assays such as quantitative fluorescence *in situ* hybridization[5]. We have detected telomerase activity in cumulus cells (data not shown); it is therefore possible that telomeres in these cells are unusually long, resulting in offspring with concomitantly longer telomeres.

Shortened[6] and lengthened[7] telomeres have been reported in cloned livestock but, unlike ours, those experiments involved only a single round of cloning. Our results on sequentially cloned mice verify that telomere shortening is not a necessary outcome of the cloning process[8]. However, as only 1–2% of reconstructed oocytes yield live-born clones, the possibility of selection for donor nuclei with the longest telomeres cannot be excluded. Further investigation is required into the consequences of nuclear transfer on telomere length and lifespan.

Table 1 Effect of sequential cloning on full-term development

Line	G1	G2	G3	G4	G5	G6	Total
A	2/131	1/228	1/263	5/238	0/670	-	9/1,530
	(1.5)	(0.4)	(0.4)	(2.1)	(0)		(0.6)
B	4/96	7/351	5/352	6/286	3/581	1/724	26/2,390
	(4.2)	(2.0)	(1.4)	(2.1)	(0.5)	(0.1)	(1.1)

Successive generations are represented as G1, G2 and so on for two independent mouse lines, A and B. The number of pups born live after cumulus-cell nuclear transfer is compared to successfully reconstructed oocytes (pups/oocytes), with the corresponding percentages in parentheses. Significant χ^2 comparisons were derived for G4 and G5 from line A, G1 and G5, G6 from line B, and G2, G3, G4 versus G6 from line B ($P < 0.05$).

Teruhiko Wakayama*†, Yoichi Shinkai‡, Kellie L. K. Tamashiro*, Hiroyuki Niida§, D. Caroline Blanchard||, Robert J. Blanchard||, Atsuo Ogura¶, Kentaro Tanemura¶, Makoto Tachibana‡, Anthony C. F. Perry#, Diana F. Colgan#, Peter Mombaerts#, Ryuzo Yanagimachi*

**Department of Anatomy and Reproductive Biology, John A. Burns School of Medicine, University of Hawaii, Honolulu, Hawaii 96822, USA*
‡Department of Cell Biology, Institute for Virus Research, Kyoto University, Sakyo-Ku, Kyoto 606-8507, Japan
§Life Sciences Division, Lawrence Berkeley National Laboratory, University of California, Berkeley, Cailfornia 94720, USA
||Bekesy Laboratory of Neurobiology, University of Hawaii, Honolulu, Hawaii 96822, USA
¶Department of Veterinary Science, National Institute of Infectious Disease, Tokyo 162-8640, Japan
#The Rockefeller University, 1230 York Avenue, New York, New York 10021, USA
†Present address: The Rockefeller University, 1230 York Avenue, New York, New York 10021, USA
e-mail: wakayat@mail.rockefeller.edu

1. Wakayama, T., Perry, A. C. F., Zuccotti, M., Johnson, K. R. & Yanagimachi, R. *Nature* 394, 369–374 (1998).
2. Wakayama, T. & Yanagimachi, R. *Nature Genet.* 22, 127–128 (1999).
3. Wakayama, T., Rodriguez, I., Perry, A. C. F., Yanagimachi, R. & Mombaerts, P. *Proc. Natl Acad. Sci. USA* 96, 14984–14989 (1999).
4. Tamashiro, K. L., Wakayama, T., Blanchard, R. J., Blanchard, D. C. & Yanagimachi, R. *Biol. Reprod.* 63, 328–334 (2000).
5. Zijlmans, J. M. *et al. Proc. Natl Acad. Sci. USA* 94, 7423–7428 (1997).
6. Shiels, P. G. *et al. Nature* 399, 316–317 (1999).
7. Lanza, R. P. *et al. Science* 288, 665–669 (2000).
8. Wilmut, I., Clark, J. & Harley, C. B. *Nature Biotech.* 18, 599–600 (2000).

Gene expression

Total silencing by intron-spliced hairpin RNAs

Post-transcriptional gene silencing (PTGS), a sequence-specific RNA degradation mechanism inherent in many life-forms, can be induced in plants by transforming them with either antisense[1] or co-suppression[2] constructs, but typically this results in only a small proportion of silenced individuals. Here we show that gene constructs encoding intron-spliced RNA with a hairpin structure can induce PTGS with almost 100% efficiency when directed against viruses or endogenous

genes. These constructs could prove valuable in reverse genetics, genomics, engineering of metabolic pathways and protection against pathogens.

Induction of PTGS by co-suppression and antisense methods that target the Nia-protease (*Pro*) gene sequence of potato virus Y (PVY)[3] cause silencing in 7% and 4% of independent transformants, respectively; induction of PTGS in these tobacco plants (*Nicotiana tabacum*) manifests as immunity[3,4] to the virus.

Using principles we developed for silencing constructs that express double-stranded RNA and inverted-repeat RNAs[3], we made a construct encoding a single self-complementary hairpin RNA (hpRNA) of the *Pro* sequence. The construct contains sense and antisense *Pro* sequences flanking an 800-nucleotide spacer fragment derived from the *uidaA* (GUS) gene (Fig. 1a). About 60% (25/43) of the plants that are transformed with this construct, many of which contained a single transgene copy, were immune to the virus. The spacer fragment contributed to the stability of the perfect inverted-repeat sequences, but it was not required for the specificity of the PTGS (Fig. 1a).

To test the effect of removing the loop region of hpRNA, we replaced the spacer with an intron sequence (Fig. 1a, b). The intron sequence provides stability to the DNA, but is spliced out during pre-mRNA processing[5] to produce loopless hpRNA. As a control, we made a sister construct in which the intron sequence was inserted in the reverse, non-splicing, orientation. When transformed into tobacco, 22 of 34 (65%) reverse-intron plants were immune, a similar frequency to plants transformed with the GUS spacer construct. Amazingly, we found that 22 of 23 plants transformed with the construct containing the functional intron were immune to the virus.

To test whether this enhancement by the sense-intron construct was a general phenomenon, we made two hpRNA constructs against the endogenous Δ12-desaturase (*Fad2*) gene of *Arabidopsis*, which catalyses the conversion of oleic to linoleic acid in the seed[6,7]; one construct contained an intron and the other a non-intron spacer region. We found that 69% (44/63) of the transgenic plants with the non-intron spacer region construct showed PTGS of the Δ12-desaturase gene, but that 100% (30/30) of plants transformed with the intron construct showed silencing of this gene.

How does the presence of this intron enhance silencing efficiency? The process of intron excision from the construct by the spliceosome might help to align the complementary arms of the hairpin in an environment favouring RNA hybridization, promoting the formation of a duplex. Alternatively, splicing may transiently increase the amount of hairpin RNA by facilitating, or retarding, the hairpin's passage from the nucleus, or by creating a smaller, less nuclease-sensitive loop.

Our PVY constructs contained intron-2 from the *Pdk* gene of *Flaveria*[8], whereas the Δ12-desaturase construct contained intron-1 from the *Arabidopsis Fad2* gene (Fig. 1b). PVY constructs were controlled by the constitutive CaMV35S (ref. 9) promoter and produced hpRNA containing the PVY coding-region sequence (700 nucleotides); the desaturase gene construct used the seed-specific napin promoter[10] to produce hpRNA representing 120 nucleotides of the 3′-untranslated region of the Δ12-desaturase gene.

We believe that constructs encoding intron-hpRNA should efficiently induce PTGS for a wide range of genes in a variety of circumstances and could become as useful to plant biology as RNAi[11,12] is to the study of nematodes and *Drosophila*. The transgene design might also have application in organisms in which RNAi has been obtained by injection of double-stranded RNA.

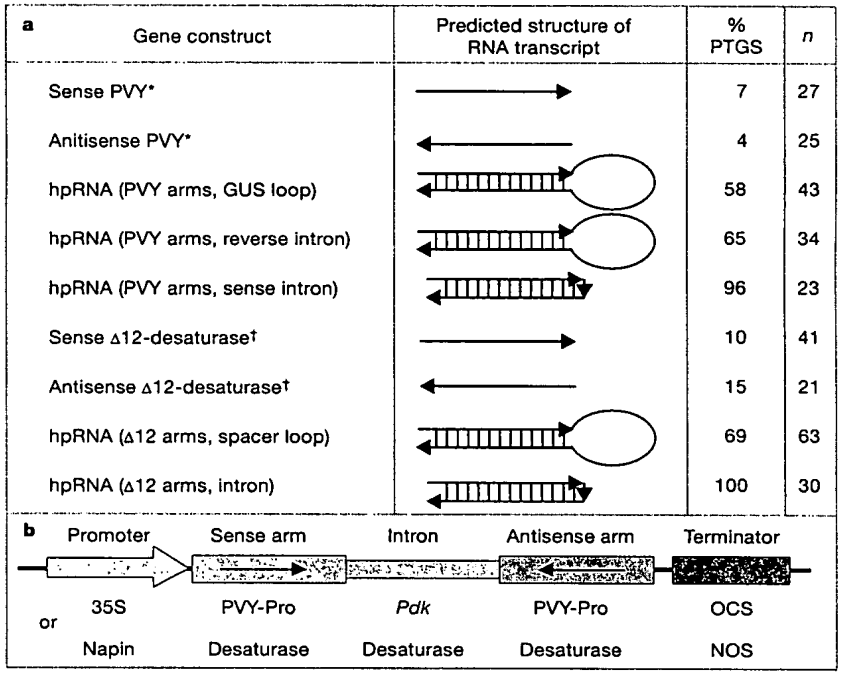

Figure 1 Efficiency of induction of post-transcriptional gene silencing (PTGS) by different gene constructs and the predicted structure of RNA transcribed from the transgenes. **a**, PTGS efficiency measured for potato virus (PVY) and Δ12-desaturase genes as the percentage of independent transgenic plants immune to PVY and the percentage of plants with enzyme activity reduced by more than 20% compared with wild type, respectively. In the predicted structures of RNA transcripts, right- and left-pointing arrows represent sense and antisense orientation of sequences, respectively; small vertical arrows represent splice-junction sequences remaining after the intron has been spliced out. Vertical lines in the predicted structures indicate duplex formation. Asterisks, data from ref. 3; daggers, data from ref 7; hpRNA, hairpin RNA; *n*, number of independent transformants; GUS, β-glucuronidase. **b**, Design of intron-containing hairpin constructs. OCS, octopine synthase; NOS, nopaline synthase.

Neil A. Smith, Surinder P. Singh, Ming-Bo Wang, Peter A. Stoutjesdijk, Allan G. Green, Peter M. Waterhouse
CSIRO Plant Industry, Canberra, ACT 2601, Australia
e-mail: peter.waterhouse@pi.csiro.au

1. Hamilton, A. J., Lycett, G. W. & Grierson, D. *Nature* **346**, 284–287 (1990).
2. Jorgensen, R. A. *Science* **268**, 689–691 (1995).
3. Waterhouse, P. M., Graham, M. W. & Wang, M.-B. *Proc. Natl Acad. Sci. USA* **95**, 13959–13964 (1998).
4. Waterhouse, P. M., Smith, N. A. & Wang, M.-B. *Trends Plant Sci.* **4**, 452–457 (1999).
5. Wang, M.-B., Upadhyaya, M. N., Brettel, R. I. S. & Waterhouse, P. M. *J. Genet. Breed.* **51**, 325–334 (1997).
6. Okuley, J. *et al. Plant Cell* **6**, 147–158 (1994).
7. Cartea, M. E., Migdal, M., Galle, A. M., Pelletier, G. & Guerche, P. *Plant Sci.* **136**, 181–194 (1998).
8. Rosche, E. & Westhoff, P. *Plant Mol. Biol.* **29**, 663–678 (1995).
9. Gleave, A. P. *Plant Mol. Biol.* **20**, 1203–1207 (1992).
10. Stalberg, K., Ellerstrom, M., Josefsson, L. G. & Rask, L. *Plant Mol. Biol.* **23**, 671–683 (1993).
11. Fire, A. *et al. Nature* **391**, 806–811 (1998).
12. Sharp, P. A. *Genes Dev.* **13**, 139–141 (1999).

The Plant Journal (2001) 27(6), 581–590

TECHNICAL ADVANCE

Construct design for efficient, effective and high-throughput gene silencing in plants

S. Varsha Wesley[1,†], Christopher A. Helliwell[1,†], Neil A. Smith[1,†], MingBo Wang[1], Dean T. Rouse[1], Qing Liu[1], Paul S. Gooding[1], Surinder P. Singh[1], David Abbott[1], Peter A. Stoutjesdijk[1], Simon P. Robinson[1], Andrew P. Gleave[2], Allan G. Green[1] and Peter M. Waterhouse[1,*]

[1]*CSIRO Plant Industry, PO Box 1600 Canberra ACT 2601, Australia, and*

[2]*HortResearch, Mt Albert Research Centre, Private Bag 92 169, Auckland, New Zealand*

Received 6 February 2001; revised 18 May 2001; accepted 1 June 2001.

*For correspondence (fax +61 262465000; e-mail peterw@pi.csiro.au).

†These authors contributed equally to this work.

Summary

Post-transcriptional silencing of plant genes using anti-sense or co-suppression constructs usually results in only a modest proportion of silenced individuals. Recent work has demonstrated the potential for constructs encoding self-complementary 'hairpin' RNA (hpRNA) to efficiently silence genes. In this study we examine design rules for efficient gene silencing, in terms of both the proportion of independent transgenic plants showing silencing, and the degree of silencing. Using hpRNA constructs containing sense/anti-sense arms ranging from 98 to 853 nt gave efficient silencing in a wide range of plant species, and inclusion of an intron in these constructs had a consistently enhancing effect. Intron-containing constructs (ihpRNA) generally gave 90–100% of independent transgenic plants showing silencing. The degree of silencing with these constructs was much greater than that obtained using either co-suppression or anti-sense constructs. We have made a generic vector, pHANNIBAL, that allows a simple, single PCR product from a gene of interest to be easily converted into a highly effective ihpRNA silencing construct. We have also created a high-throughput vector, pHELLSGATE, that should facilitate the cloning of gene libraries or large numbers of defined genes, such as those in EST collections, using an *in vitro* recombinase system. This system may facilitate the large-scale determination and discovery of plant gene functions in the same way as RNAi is being used to examine gene function in *Caenorhabditis elegans*.

Keywords: PTGS, RNAi, genomics, vector, ihpRNA, Gateway.

Introduction

The ultimate goal of current genome projects is to identify the biological function of every gene in the genome. Whole genomes of several organisms (including *Arabidopsis*, http://www.arabidopsis.org), have been completely sequenced, providing a wealth of information. The functions of some of the genes have been identified directly by the appropriate assay, or have been inferred by homology to genes of known function in other organisms. Loss-of-function mutants, from insertional mutagenesis or transposable elements, have also been very informative about the role of some of these genes (AzpirozLeehan and Feldmann, 1997; Martienssen, 1998), particularly in the large-scale analysis of the yeast genome (Ross-Macdonald *et al.*, 1999). However, the functions of a large proportion of genes remain unknown.

Injection or ingestion of dsRNA into nematodes can trigger specific RNA degradation, in a process known as RNA-interference (RNAi; Fire *et al.*, 1998). This process facilitates targeted post-transcriptional gene silencing (PTGS) and has recently been harnessed to study the function of over 4000 genes on chromosomes I and III

(a)

Construct	Predicted RNA structure	PTGS	*n*
Adj-hp RNA	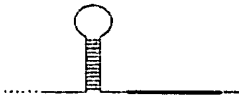	25 %	8
hpRNA		85 %	14
sRNA		30 %	10

(b)

hpRNA		55 %	234
ihpRNA		90 %	243
ihpRNA overhang	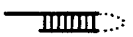	80 %	48
ihpRNA spacer		89 %	36

Figure 1. The predicted RNA structure and efficacy of gene-silencing constructs.
(a) Three constructs, controlled by Ubi1 promoter, silencing GUS in rice. Thick lines indicate a 560 nt GUS sequence; grey lines indicate non-GUS sequences; dashed grey lines indicate intron-junction sequences left after splicing; and short lines within the stem of hairpin structures indicate base pairing. Numbers in PTGS column indicate the percentage of plants showing GUS silencing; *n* = number of plants in each treatment.
(b) Silencing efficacy of four different construct types with sequences as depicted in (a), except the thick lines in hpRNA and ihpRNA represent the various different target sequences in Table 1; and the thick lines in iphRNAoverhang and iphRNAspacer represent PVY Pro sequences. The percentage PTGS of hpRNA and ihpRNA, and iphRNAoverhang and iphRNA spacer, are the average percentage silencing of these types of constructs reported in Table 1 and the percentage of plants showing immunity to PVY, respectively.

in *Caenorhabditis elegans* (Fraser *et al.*, 2000; Gonczy *et al.*, 2000). We discovered that transgenes designed to express double-stranded or single-stranded self-complementary (hairpin) RNA have a similar post-transcriptional silencing effect in plants (Wang and Waterhouse, 2000; Waterhouse *et al.*, 1998) and that, in at least two examples, almost 100% of plants transformed with an intron-containing hairpin RNA construct showed silencing (Smith *et al.*, 2000). These results led us to ask whether hpRNA technology might be exploited for gene discovery in plants. We have sought to design and evaluate generic intron–hpRNA constructs that might enable plant gene-discovery studies on a scale that matches those in nematodes.

Results

Location of silence-inducing sequences in hairpin RNA constructs

Constructs encoding RNAs with regions of self-complementarity efficiently induce gene silencing. We have previously shown that the sequences in the duplex stem in hpRNAs direct gene silencing (Smith *et al.*, 2000; Waterhouse *et al.*, 1998), whereas the results of Hamilton *et al.* (1998) suggest that single-stranded RNA sequences adjacent to a potential hairpin-forming structure give sequence specificity to silencing. The latter arrangement (adj-hpRNA) could be easily incorporated into gene-silencing vectors as the sequence encoding the hairpin RNA could be generic to the vector, while the specificity of the silencing would be accomplished by simply inserting a single copy of target gene sequence. In contrast, hpRNA constructs require two copies of the target sequence in an inverted-repeat orientation, in order to produce duplex RNA. To compare the relative efficacy of the designs, various GUS-silencing constructs, under the control of the Ubi1 promoter and associated intron, were made (Figure 1a) and super-transformed into GUS-expressing rice. Histochemical staining of the transformed plants showed that the adj-hp RNA construct gave no higher frequency of silenced lines than conventional co-suppression (sRNA), but the hpRNA construct gave many more silenced lines (Figure 1a). This suggested that the hpRNA was the design of choice.

Examination of the stained rice Ubi-hpGUS plants and a similar 35S-hpGUS construct in tobacco (Figure 2f) showed that the silencing was evenly distributed throughout the plant. Analysis of RNAs in the tobacco plants for the presence of GUS-derived small (≈21 nt) RNAs showed a perfect correlation between the presence of these molecules and the presence of the 35S-hpGUS construct and silencing of the target GUS gene (Figure 3). This confirms that the silencing was due to PTGS; such small RNAs are a hallmark of PTGS (Hamilton and Baulcombe, 1999; Waterhouse *et al.*, 2001)

Intron-spliced hpRNA vectors

We have found that it is necessary to include a spacer region between the arms of hpRNA constructs for stability of the inverted repeat DNA in *Escherichia coli*. However, replacing the spacer (loop) region of hpRNA constructs with a functional intron sequence increases the proportion of independent silenced lines recovered from approximately 50 to about 100% (Smith *et al.*, 2000). In these experiments, the targets were potato virus Y (PVY) and the *FAD2* Δ12-desaturase gene of *Arabidopsis*. The constructs were designed such that their pre-mRNA should splice to

form hpRNAs with small loops (Figure 4). The PVY construct should give an hpRNA comprising a 730 nt stem and a 6 nt loop; the hpRNA from the Δ12-desaturase construct should contain a 120 nt stem and a 21 nt loop. Although the PVY construct contained only two and four bases of original exon sequence 5′ and 3′ of the intron, respectively, the intron was still functional. RT–PCR and sequencing of transgene mRNA in plants containing the *Hin*dIII intron fragment (Figure 4) showed that the intron was cleaved out, leaving the predicted splice junction (data not shown).

The Δ12-desaturase result (100% of independent plants showing silencing despite having a 21 nt loop in the hpRNA) showed that the intron-enhanced silencing was not solely due to the tightness of the hairpin loop. Therefore we wondered whether this could be exploited to make a generic intron-spliced hpRNA (ihpRNA) vector into which the gene, or gene fragment, of choice could be directionally cloned to make sense and anti-sense arms. The vector pHANNIBAL (Figures 4 and 5), and a sister vector, pKANNIBAL (with bacterial ampicillin and kanamycin resistance genes, respectively), were designed so that a PCR fragment could be inserted in the sense orientation into the *Xho*I.*Eco*RI.*Kpn*I polylinker and in the anti-sense orientation in the *Cla*I.*Hin*dIII.*Bam*HI.*Xba*I polylinker. This may be accomplished either by two separate PCR reactions with the appropriate single sites introduced with each primer, or by a single PCR using primers each introducing two restriction sites (e.g. primer 1, *Xba*I.*Xho*I.xxx; primer 2, *Cla*I.*Kpn*I.xxx). The construct will produce an hpRNA with a loop of 30–50 bases depending on which restriction sites are used to insert the targeting gene sequences.

The efficacy of pHANNIBAL was tested in *Arabidopsis* targeting the pigment biosynthesis gene chalcone synthase (*CHS*); the ethylene signalling gene *EIN2*; and the flowering repression gene *FLC1*. These genes were chosen because their mutant alleles have been reported in *Arabidopsis* to give distinct phenotypes. The *tt4* (CS85) EMS mutant (Koornneef *et al.*, 1990) produces inactive CHS, resulting in reduced production of flavonoid pigments in both the stem and seed coat. The mutant *ein2* (Alonso *et al.*, 1999) is insensitive to ethylene and grows well on media containing 1-aminocyclopropane-1-carboxylic acid, whereas wild-type plants develop a very stunted appearance when grown on such media. The mutant *flc1* (Amasino *et al.*, 2000) flowers earlier than wild-type *Arabidopsis*.

A 741 nt piece of CHS coding region was amplified from *A. thaliana* (Landsberg *erecta*) using primers that added an *Xho*I and a *Kpn*I site on the ends of one product and an *Xba*I and *Bam*HI site on the ends of the other product. These two amplification products were then directionally cloned into pHANNIBAL (Figure 5). Similar cloning strategies were adopted for a 600 nt sequence from *EIN2*, and both a 650 nt and a 400 nt sequence from *FLC1*. As controls, sense and anti-sense constructs of CHS and an anti-sense construct of FLC1 were also generated. All the constructs were subcloned into the binary vector pART27 and transformed into *Arabidopsis*.

Only two of the 19 plants transformed with the CHS co-suppression construct, and none of the 25 plants transformed with the CHS anti-sense construct, showed any obvious evidence of silencing. Whereas over 90% (21 of 23) of the plants transformed with the CHS-HANNIBAL constructs showed pronounced silencing (Table 1). The seed colours of most of these lines were virtually indistinguishable, to the naked eye, from seed of the *tt4*(CS85) mutant (Figure 2a). Examination of the seed under a light microscope revealed that the degree of pigmentation was generally uniform in the cells of the coat of an individual seed, and among seeds of the same line (Figure 2b,c). There was a perceptible difference in the levels of pigmentation between the different lines. The relative flavonoid content of seed from three lines selected to span the range of seed colour in the plant lines transformed with CHS-HANNIBAL, and from the co-suppression line giving the lightest coloured seed were 7, 23, 47 and 75%, respectively. The *tt4* (CS85) and wild-type seed had values of 0 and 100%, respectively.

Sixty-four independent lines transformed with the EIN-HANNIBAL construct were obtained. The progeny from 42 of the lines showed Mendelian segregation for normal and stunted growth when grown on ACC medium, whereas all wild-type plants showed a stunted morphology on this medium (Table 1; Figure 2e).

The transgenic progeny of every one of the 31 independent plants transformed with the FLC1-HANNIBAL constructs flowered earlier and made fewer leaves, prior to flowering, than wild-type plants (Table 1; Figures 2d and 6). The transgenic progeny from the majority of the plants transformed with the FLC1 anti-sense construct had similar leaf numbers and flowering times to those of wild-type plants. The flowering time and leaf number provided an easy measurement of the degree of silencing in individual lines. Only two of the 31 FLC1-HANNIBAL plant lines did not flower in less than 25 days after germination, whereas only two anti-sense plant lines flowered in less than 30 days. This suggests that ihpRNA constructs not only give an increased proportion of silenced transformants than anti-sense constructs, but also give more profound levels of silencing. However, even the most profoundly silenced FLC1-HANNIBAL line flowered 1 day later than the *flc* mutant, suggesting that it was not quite the equivalent of a null allele.

Collectively, pHANNIBAL-based constructs (which are driven by the constitutive 35S promoter) have been

made for five different genes (*CHS*, *EIN2*, *FLC1*, PVY-Pro and polyphenol oxidase – *PPO*). Similar intron-containing constructs targeting seed specifically against two different genes (Δ12- and Δ9-desaturase) in *Arabidopsis* and/or cotton have been tested for their silencing efficiency. Intron-less hpRNA, anti-sense and co-suppression constructs have also been used in many of these gene/host combinations. The results are summarized in Table 1. The ihpRNA constructs were effective, with arm lengths ranging from 98 to 853 nt, giving 66–100% (average 90%) independent silenced transformants. Intron-free hpRNA constructs gave 48–69% (average 58%) silenced

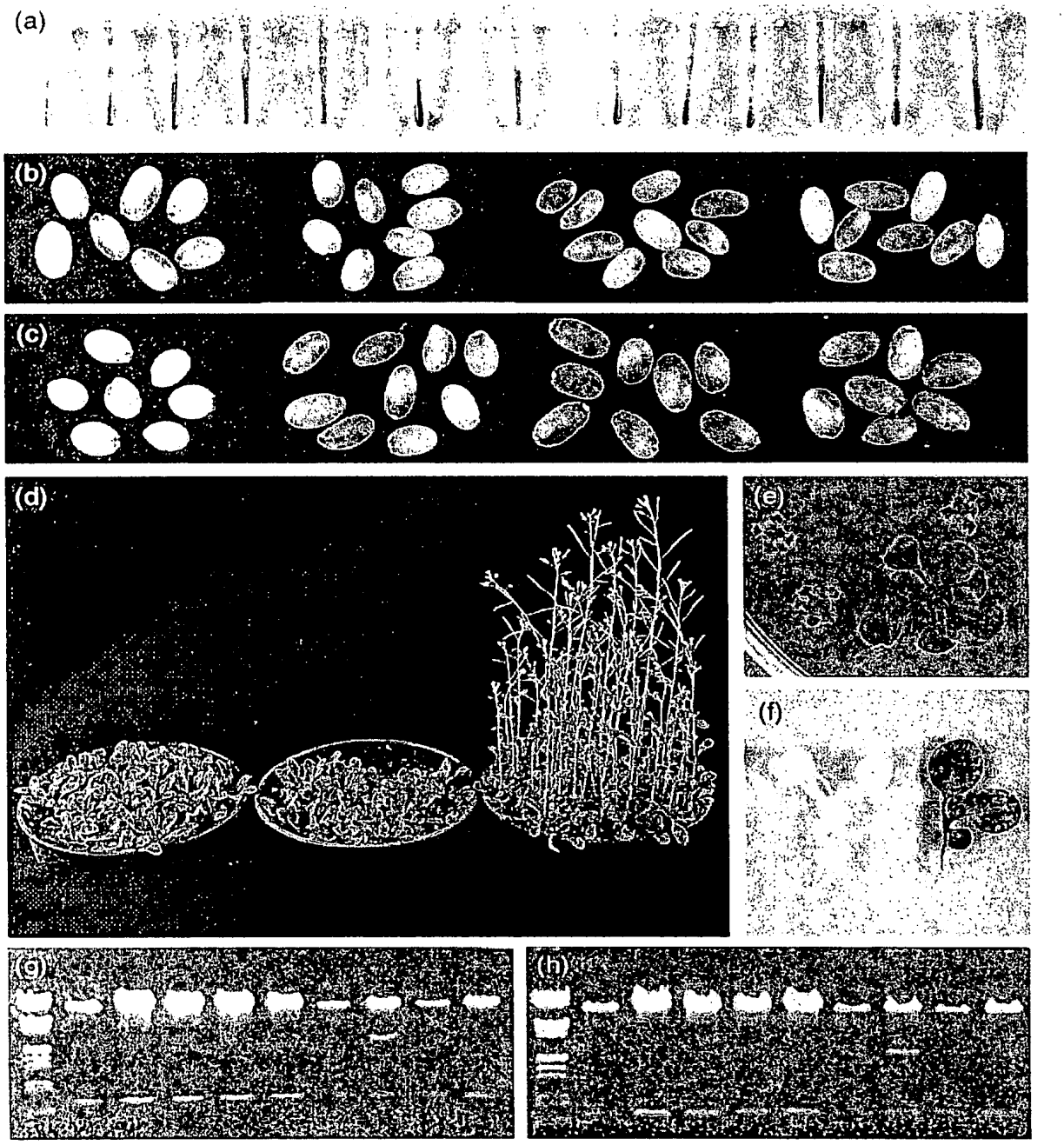

transformants, and conventional co-suppression or anti-sense constructs gave 0–30% (average 13 and 12%, respectively) silenced transformants. The intron-spliced or intron-free hpRNA constructs were effective when targeted against the coding, 5′ untranslated or 3′ untranslated regions of the mRNA. Taken together, these results indicate that ihpRNA constructs consistently give the most efficient silencing under a wide range of conditions.

Effect of intron location and unbalanced arms in pHANNIBAL

Intron-spliced hpRNA constructs appear to give a higher proportion of silenced transformants than intron-free hpRNA constructs. One explanation for this might be that the process of intron-splicing aligns the arms of the hpRNA, facilitating their duplex formation in the spliceosome complex, whereas the arms of hpRNAs have to find their self-complementarity by random, but tethered, collisions. If there is a threshold of duplex RNA required for PTGS in plants, then facilitating more efficient duplex RNA formation from ihpRNA might raise the level in low transgene-expressing plants such that PTGS is enabled. Similar levels of transcription of non-spliced hpRNA might produce lower steady-state levels of duplex RNA that are insufficient for PTGS. The same threshold theory could also be applied for the tighter loop of ihpRNA, giving more nuclease-stable and higher steady-state duplex RNA levels than the larger looped hpRNA. To test the validity of these possibilities, a construct was made in which a spacer region was inserted between one of the arms and the intron in a PVY ihpRNA construct (Figure 1b). This spacer region should impede alignment of the arms during the splicing process and produce a spliced hpRNA with a large loop. When plants transformed with the construct were challenged with PVY, 32 out of 36 independent transformants were immune to the virus. This suggests that the majority of the intron-enhanced silencing efficiency is not due to better alignment of the RNA arms or by presence of a tighter ssRNA loop. It may also explain why the GUS–hpRNA construct so efficiently silenced GUS in the rice plants reported in Figure 1(a), as this construct contained an intron in the 5′ untranslated leader sequence of the ubiquitin promoter.

A common feature of our hpRNA constructs has been the use of matched-length arms. These constructs should produce hpRNA with only a few unpaired 5′ nucleotides. If pHANNIBAL is to be used as a generic vector for inserts from gene libraries, occasionally a restriction site within the PCR fragment will be common to the one used to clone into the polylinker. This will sometimes lead to the unintended construction of an hpRNA with unmatched arm length. To investigate whether this was an important attribute, a pHANNIBAL construct was made (using the

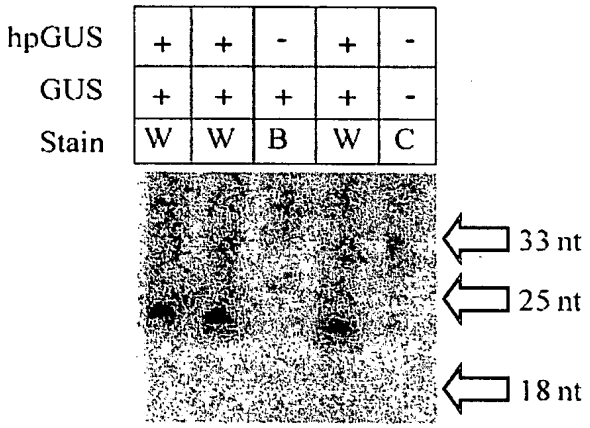

Figure 3. Detection of short (≈22 nt) GUS-derived RNAs in tobacco plants showing hpRNA-mediated GUS silencing.
Total RNA (20 μg each), isolated from tobacco plants showing independent segregation of a 35S GUS transgene and a 35S hpGUS transgene, was separated in a 15% denaturing polyacrylamide gel, blotted onto a Hybond-N membrane and hybridized with *in vitro*-transcribed ^{32}P-labelled GUS RNA. The presence (+) or absence (–) of the target GUS and/or the 35S hpGUS transgene in the plant, from which the sample was taken, is indicated above each track. The phenotype of each of these plants after incubation with X-glucuronide and removal of chlorophyll with ethanol is also indicated. Silenced lines are white (W), unsilenced lines blue (B). The non-transgenic control is designated (C). Sizes indicated on the filter were determined by migration of DNA oligonucleotides.

Figure 2. Silenced phenotypes in ihpRNA transformed plants and recombinase cloning into pHELLSGATE.
(a) *Arabidopsis* seed samples from left to right: five independent CHS-ihpRNA lines; wild-type seed; *tt4*CHS mutant; three CHS-anti-sense lines and three CHS-co-suppression lines. The anti-sense and co-suppression lines were chosen as those showing the lightest seed-coat pigmentation.
(b) *Arabidopsis* seed samples from four independent CHS-ihpRNA lines, chosen to reflect the range of seed-coat pigmentation, viewed under a light microscope.
(c) Four companion seed samples to (b) from left to right: *tt4*CHS mutant; the two anti-sense-silenced lines from Table 1; and wild-type seed.
(d) Three pots of *Arabidopsis* plant lines 25 days after germination. From left to right: wild-type; earliest-flowering anti-sense; and FLC1-pHANNIBAL-transformed line.
(e) *Arabidopsis* transformed with EIN2-pHANNIBAL growing on 50 μM ACC. The larger, vigorous plantlet is an ethylene-insensitive EIN2-pHANNIBAL plant; the small plantlets are ethylene-sensitive wild-type plants.
(f) X-glucuronide-stained transgenic GUS tobacco plantlets segregating for presence (left) or absence (right) of the GUS-hpRNA transgene.
(g,h) Agarose gel of restriction enzyme-digested plasmid preparations from nine individual colonies recovered from *E. coli* transformed with a pHELLSGATE/400ntPCR-product recombination reaction. *Xho*I digestion (g) will release the 400 nt sense arm but not the ccdB fragment, and *Xba*I digestion (h) will release the 400 nt anti-sense arm but not the other ccdB fragment. Left-hand track in both gels contains size markers.

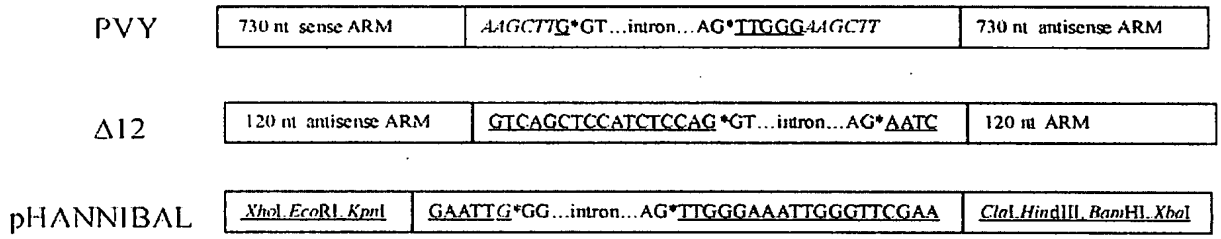

Figure 4. Splice junctions, loop regions and self-complementarity of ihpRNA constructs: PVY, Δ12-desaturase, and pHANNIBAL.
Nucleotides underlined have no complement in the hpRNA and should form a loop structure. *, splice point; *Hin*dIII site in PVY-ihpRNA construct shown in italics.

PVY–Pro sequence) that should produce a hpRNA with a stem of 400 nt and 5′ region of 300 unpaired nucleotides (Figure 1b). When 48 independent transformed plants, containing this construct, were challenged with PVY, 38 (≈80%) of them were immune to the virus. This shows that an unpaired 5′ extension of hpRNA does not abolish its ability to induce silencing, although its efficiency may be slightly reduced.

High-throughput vector

With the completion of the *Arabidopsis* genome project; the advent of micro-array technology; and the ever-increasing investigation into plant metabolic, perception and response pathways, a rapid, targeted way of silencing genes would be of major assistance. The high incidence and degree of silencing in plants transformed with pHANNIBAL constructs suggest that it could form the basis of a high-throughput silencing vector. However, one of the major obstacles in using pHANNIBAL for a large number of defined genes or a library of undefined genes would be cloning the hairpin arm sequences for each gene in the correct orientations.

Attempts to clone PCR products of sense and anti-sense arms, together with the appropriately cut pHANNIBAL vector as a single-step four-fragment ligation, failed to give efficient or reproducible results (data not shown). Therefore a construct (pHELLSGATE) was made (Figure 5) to take advantage of Gateway technology which facilitates easy cloning of PCR fragments (http://www.invitrogen.com/content.cfm). With this technology, a PCR fragment is generated (bordered with recognition sites attB1 and attB2) which is directionally recombined *in vitro* into a plasmid containing attP1 and attP2 sites using the commercially available recombinase preparation.

The pHELLSGATE vector was designed such that a single PCR product from primers with the appropriate attB1 and attB2 sites would be recombined into it simultaneously to form the two arms of the hairpin (Figure 5). The *ccdB* gene, which is lethal in standard *E. coli* strains such as DH5α (but not in DB3.1), was placed in the locations to be replaced by the arm sequences, ensuring that only recombinants containing both arms would be recovered. Placing a chloramphenicol-resistance gene within the intron gives a selection to ensure the retention of the intron in the recombinant plasmid. The pHELLSGATE vector was tested using 200 and 400 nt PCR products for two different genes. Many bacterial colonies were obtained on chloramphenicol-containing plates spread with DH5α bacteria, transformed with the *in vitro* recombination reaction. Analysis of 24 colonies transformed with the 400 nt reaction and 36 colonies from the 200 nt reaction showed that, in both cases, all but one of the colonies contained the desired recombinant plasmid (Figure 2g,h). This was confirmed by sequence analysis (data not shown). These results show that this vector facilitates the rapid, efficient and simple production of hpRNA constructs. pHELLSGATE is a binary vector, with a high-copy-number origin of replication for ease of handling. Recombinant pHELLSGATE constructs can be directly transformed into *Agrobacterium* for transformation into plants. This system should lend itself to high-throughput applications.

Discussion

Now that the genomes of a number of species have been completely sequenced, the challenge is to understand the functions and interplay of genes in an organism. The use of chemical mutagens, transposons and T-DNA tagging have been very useful in screening for mutants of individual genes. However, with these undirected methods it is often slow and laborious work to identify each mutant and to track down the gene responsible. RNAi has revolutionized the study of genes in *C. elegans* and *Drosophila*, with two groups recently reporting the systematic analysis of over 4000 genes on chromosomes I and III in *C. elegans* (Fraser *et al.*, 2000; Gonczy *et al.*, 2000). By way of comparison, chromosome 2 of *Arabidopsis* has been entirely sequenced (Lin *et al.*, 2000) and the presence of 4037 genes has been predicted. Yet to undertake a systematic analysis

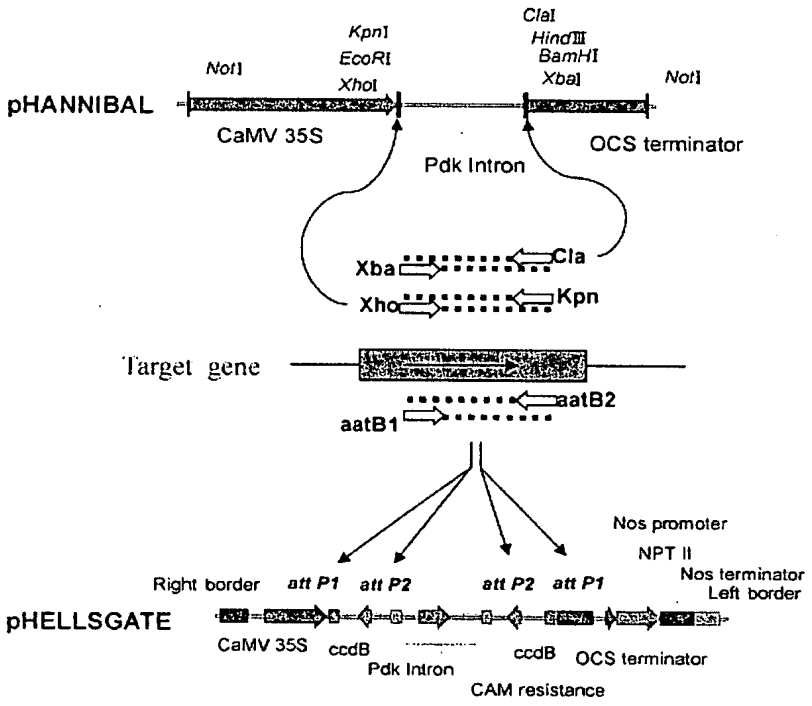

Figure 5. Maps and cloning strategies for pHANNIBAL and pHELLSGATE.
PCR products from the target gene are cloned into the polylinkers of pHANNIBAL conventionally; restriction sites added by the primers ensure the correct orientation of the resulting sense and anti-sense arms. The attB1 and attB2 sequences on a single PCR product facilitate the recombination of one sense-orientated and one anti-sense-orientated molecule into each molecule of pHELLSGATE when incubated with BP clonase. The complete sequences and annotations for pHANNIBAL and pHELLSGATE have been lodged at EMBL (Acc No: AJ311872 and AJ311874).

Table 1. Efficiency of hpRNA, co-suppression and anti-sense constructs at silencing a range of genes in a range of plant species

Gene	Species	Prom	Intron	Target	Arm (nt)	GenBank Acc No.	Co-ordinates	ihp RNA	hp RNA	Sense	Anti-sense
PPO	Tobacco	35S	Pdk	ORF	572	AX028815	172–844	21/30		5/54	
GUS	Tobacco	35S		ORF	800	S69414	1–800		23/48		
PVY	Tobacco	35S	Pdk	ORF	730	U09509	6278–7008	23/24	25/43	2/27	1/25
EIN2*	*Arabidopsis*	35S	Pdk	ORF	600	AF141202	538–1123	42/64			
FLC1*	*Arabidopsis*	35S	Pdk	ORF	650	AY034083	1–650	16/16			2/13
FLC1*	*Arabidopsis*	35S	Pdk	ORF	400	AY034083	250–650	15/15			
CHS	*Arabidopsis*	35S	Pdk	ORF	741	AF112086	248–1075	21/23		2/19	0/25
Δ12	*Arabidopsis*	Napin	Δ12a	3′ UTR	120	L26296	1243–1363	30/30	44/63	4/41	3/21
Δ12	Cotton	Lectin		ORF	853	X97016	68–921		17/29		7/30
Δ12	Cotton	Δ12c	Δ12c	5′ UTR	98	X97016	1–98	26/26			
Δ9	Cotton	Lectin		ORF	514	X95988	24–538		15/26		4/30
GUS	Rice	Ubi		ORF	560	S69414	1–560	12/14		3/10	1/8
Average percentage of silenced plants								90	58	13	12

The type of promoter (Prom), type of intron, length of arms and details of how to find the specific sequences of the arms for various gene-silencing constructs are shown. The last four columns show the number of primary independent transformants (or transformed lines where progeny were analysed) showing silencing/the number of transgenic plants produced from the primary transformation experiment.
*Silencing analysis was done on the progeny of the primary transformed plants.

of these genes using the conventional plant technologies of insertional mutagenesis would require vast resources. It has been calculated that to have a 90% chance of finding just one specific single gene (of about 1 kb) in *Arabidopsis* using T-DNA insertional mutagenesis would require the generation of about 350 000 independent transformants (Krysan *et al.*, 1999). The work described in this paper facilitates a directed silencing which, when combined with the efficient, non-tissue culture transformation method for *Arabidopsis* (Clough and Bent, 1998), provides the tools that make the challenge of mirroring in plants, the gene discovery under way in nematodes, more feasible.

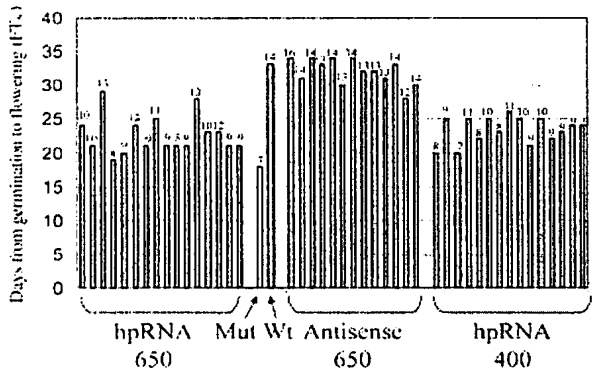

Figure 6. Flowering time in transgenic progeny from independent FLC1-pHANNIBAL and FLC1-anti-sense transformed C24 *Arabidopsis* lines.
Flowering time (FT_{50}) and leaf number (in figures above each column) for transgenic progeny from 16 and 15 independent plant lines transformed with pHANNIBAL constructs containing 650 and 400 nt arms of FLC1 sequence, respectively; 13 independent plants transformed with a conventional, 35S-driven, anti-sense construct containing the appropriate 650 nt of FLC1; the flc-13 mutant (white bar); and wild-type plants (cross-hatched bar). Wild-type plants were transgenic for GUS and kanamycin resistance, to allow the plants to be grown under identical conditions. The standard error for leaf numbers did not exceed 0.7 of 1 day for any plant line.

Using hpRNA constructs, we have obtained silenced plants for every gene that we targeted, irrespective of whether it was a viral gene, transgene or endogenous gene, and the silencing appears to be uniform within tissues in which the hpRNA is expressed. With ihpRNA constructs the efficiency averaged about 90%, and arms of 400–800 nt appear to be stable and effective. High levels of silencing were obtained with constructs having unmatched arm lengths, with arms as long as 853 nt or as little as 98 nt, and with arm sequences derived from coding, 3′ or 5′ untranslated regions of the target gene. These results suggest that ihpRNA constructs will be effective in a wide range of circumstances, and augur well for the generic use of the technology. The silencing was much more profound with ihpRNA constructs than either anti-sense or co-suppression constructs; some ihpRNA transformants were close to exhibiting a complete knock-out of the target endogenous gene. However, most of the ihpRNA plants showed dramatically reduced but detectable levels of target gene activity. This variation in degree of silencing in the ihpRNA plants may be a useful feature for gene discovery and genomics: complete silencing of genes required for basic cell function or development will probably be embryo-lethal and therefore not easily recovered using traditional tagging approaches, whereas the reduced gene expression caused by hpRNA constructs may give viable plants with phenotypes indicative of the role of the target gene.

Although the pHANNIBAL construct should be very useful for studying a modest number of genes (e.g. 10–50), such as in a metabolic pathway, it would not be feasible with normal resources to use it for hundreds to thousands of genes. However, the pHELLSGATE vector has the potential to facilitate making large numbers of gene ihpRNA constructs rapidly and efficiently. The simple steps required, namely PCR, incubation of the PCR product with the vector and recombinase, selection of recombinant plasmid, and then transformation into *Agrobacterium*, are steps that could easily be automated. The templates for PCR could be the defined genes in an EST library using standard forward and reverse primers. Alternatively, given that ihpRNA constructs with arms as small as 98 nt give effective silencing, oligosynthesizers could be automated to systematically synthesize oligonucleotides of each computer-identified gene along a chromosome, or for genes for which no function is known, and pass these primers into an automated ihpRNA production system.

It has been shown that RNAi in *Drosophila* is directed by 21 nt dsRNA oligomers derived from the inducing dsRNA (Elbashir *et al.*, 2001; Zamore *et al.*, 2000). Similar 21–25 nt RNAs have also been found associated with PTGS in plants (Hamilton and Baulcombe, 1999; Waterhouse *et al.*, 2001). It is tempting to speculate that the minimum region of homology between an mRNA and the arms of an effective hpRNA will also be 21–25 nt. If so, this rule would allow the design of hpRNAs to silence a single member of a gene family, as such unique sequences are present in most gene families. Also, by choosing conserved regions, it may be possible to silence whole gene families using a single construct. However, these rules remain to be proven.

Experimental procedures

Plasmid construction

Standard gene cloning methods (Sambrook *et al.*, 1989) were used to make the gene constructs. The plasmids for dicot transformation were derived from pART7 and pART27 (Gleave, 1992), and those for monocot transformation were derived from pVec4 (Wang *et al.*, 1997, Wang *et al.*, 1998). The accession numbers of the gene sequences, and the co-ordinates of the sequences used in the hpRNA, co-suppression and anti-sense constructs, are shown in Table 1. The annotated sequences of pHANNIBAL, pKANNIBAL and pHELLSGATE are lodged with EMBL and have accession numbers AJ311872, AJ311873 and AJ311874, respectively. Constructs made in pHANNIBAL were subcloned as *Not*I fragments into pART27, then introduced into *Agrobacterium* strains AGL1 or LBA4404 either by electroporation or tri-parental mating. pHELLSGATE was maintained in *E. coli* strain DB3.1 (Invitrogen, Carlsbad, CA, USA) in which the *ccdB* gene is not lethal.

Plant transformation

Nicotiana tabaccum (W38), cotton and rice were transformed essentially as described by Ellis *et al.* (1987), Cousins *et al.* (1991) and Wang *et al.* (2001), respectively. *Arabidopsis* was transformed by the dipping method of Clough and Bent (1998).

Analysis of transgenic plants

Northern blot analysis for the presence or absence of short RNAs was performed essentially as described by Wang *et al.* (2001).

Polyphenol oxidase (PPO) activity was measured using an oxygen electrode essentially as described by Robinson and Dry (1992). Rice and tobacco were tested for GUS activity using the histochemical stain X-glucuronide essentially as described by Jefferson *et al.* (1987). The reactions of plants to potato virus Y were analysed as described by Waterhouse *et al.* (1998). The activity of EIN2, which is required in the ethylene perception pathway, was observed by growing plants on media containing 1-aminocyclopropane-1-carboxylic acid (ACC) as described by Alonso *et al.* (1999). To identify lines silenced for EIN1, at least 30 progeny of each transformed line were germinated and grown on ACC-containing media.

To measure the effect of silencing FLC1, 20–30 seeds from each transgenic C24 *Arabidopsis* line, the transposon mutant flc13 (Sheldon *et al.*, 2000), and a control GUS line, were germinated and grown on kanamycin plates as described by Sheldon *et al.* (2000). The plants were scored daily over a 40-day period for the appearance of flowers. Flowering time (FT_{50}) for each line was taken as the number of days after germination for 50% of the plants to show flowering. After flowering, the number of leaves of 10 randomly selected plants was counted for each line.

Chalcone synthase (CHS) activity was monitored by visual observation of stem and leaf colour in plants grown under high light, and by unaided or microscope-assisted visual observation of seed-coat colour. The seeds were collected after they had matured and dried on the plant. The relative flavonoid concentrations in seeds were determined by measuring extracts for absorbance between 490 and 530 nm in a Spectramax 340-PC (Molecular Devices Corporation, Sunnyvale, CA, USA). Duplicate extracts were made from 25 mg seed of each line, essentially as described by Gerats *et al.* (1982). The average absorbance value for each line was mathematically transformed to give relative values such that the *tt4* and wild-type seed became values of 0 and 100%, respectively.

The activity of Δ12- and Δ9-desaturase activity during lipid synthesis was estimated from the relative proportions of individual fatty acids in mature seed, as determined by routine methods for GC analysis of fatty acid methyl esters.

Unless otherwise stated, plants were considered to be showing silencing when they showed obvious appropriate phenotypic differences from wild-type plants, or when they had a gene activity that was reduced by at least 20%.

AttB primers, PCR and recombination reaction for introduction of sequences into pHELLSGATE

Primers with attB1 and attB2 sequences were purchased from Life Technologies. Polymerase chain reactions (PCR) and *in vitro* BP clonase recombination reactions were carried out according to the manufacturer's instructions (Invitrogen). The recombination reaction product was either electroporated or heat-shocked into RbCl-treated DH5α *E. coli*.

Acknowledgements

Many thanks to Tony Arioli, Sharon Abrahams and Liz Dennis for helpful discussions, and to Geoff Ellacott for excellent technical assistance.

References

Alonso, J.M., Hirayama, T., Roman, G., Nourizadeh, S. and Ecker, J.R. (1999) EIN2, a bifunctional transducer of ethylene and stress responses in *Arabidopsis*. *Science*, **284**, 2148–2152.

Amasino, R.M., Schomburg, F.M., Michaels, S.D., Sung, S.-B. and Scortecci, K. (2000) International Patent Application WO 00/50615.

AzpirozLeehan, R. and Feldmann, K.A. (1997) T-DNA insertion and mutagenesis in *Arabidopsis*: going back and forth. *Trends Genet.* **13**, 152–156.

Clough, S.J. and Bent, A.F. (1998) Floral dip: a simplified method for *Agrobacterium*-mediated transformation of *Arabidopsis thaliana*. *Plant J.* **16**, 735–743.

Cousins, Y.L., Lyon, B.R. and Llewellyn, D.J. (1991) Transformation of an Australian cotton cultivar: prospects for cotton improvement through genetic engineering. *Aust. J. Plant Physiol.* **18**, 481–494.

Elbashir, S.M., Lendeckel, W. and Tuschl, T. (2001) RNA interference is mediated by 21- and 22-nucleotide RNAs. *Genes Dev.* **15**, 188–200.

Ellis, J.G., Llewellyn, D.J., Dennis, E.S. and Peacock, W.J. (1987) Maize *Adh1* promoter sequences control anaerobic regulation: addition of upstream promoter elements from constitutive genes is necessary for expression in tobacco. *EMBO J.* **6**, 11–16.

Fire, A., Xu, S., Montgomery, M.K., Kostas, S.A., Driver, S.E. and Mello, C.C. (1998) Potent and specific genetic interference by double stranded RNA in *Caenorhabditis elegans*. *Nature*, **391**, 806–811.

Fraser, A.G., Kamath, R.S., Zipperlen, P., Martinez-Campos, M., Sohrmann, M. and Ahringer, J. (2000) Functional genomic analysis of *C. elegans* chromosome I by systematic RNA interference. *Nature*, **408**, 325–330.

Gerats, A.G.M., de Vlaming, P., Doodeman, M., Al, B. and Schram, A.W. (1982) Genetic control of the conversion of dihydroflavonols and anthocyanins in flowers of *Petunia hybrida*. *Planta*, **155**, 364–368.

Gleave, A.P. (1992) A versatile binary vector system with a T-DNA organisational structure conducive to efficient integration of cloned DNA into the plant genome. *Plant Mol. Biol.* **20**, 1203–1207.

Gonczy. P., Echeverri, C., Oegema, K., *et al.* (2000) Functional genomic analysis of cell division in *C. elegans* using RNAi of genes on chromosome III. *Nature*, **408**, 331–336.

Hamilton, A.J. and Baulcombe, D.C. (1999) A species of small antisense RNA in post-transcriptional gene silencing in plants. *Science*, **286**, 950–952.

Hamilton, A.J., Brown, S., Han, Y.H., Ishizuka, M., Lowe, A., Solis, A.G.A. and Grierson, D. (1998) A transgene with repeated DNA causes high frequency post-transcriptional suppression of ACC-oxidase gene expression in tomato. *Plant J.* **15**, 737–746.

Jefferson, R.A., Kavanagh, T.A. and Bevan, M.W. (1987) GUS fusion: β-glucuronidase as a sensitive and versatile gene fusion marker in higher plants. *EMBO J.* **6**, 3901–3907.

Koornneef, M., Bosma, T.D.G., Hanhart, C.J., van der Veen, J.H. and Zeevaart, J.A.D. (1990) The isolation and characterization of gibberellin-deficient mutants in tomato. *Theor. Appl. Gen.* **80**, 852–857.

Krysan, P.J., Young, J.C. and Sussman, M.R. (1999) T-DNA as an insertional mutagen in *Arabidopsis*. *Plant Cell*, **11**, 2283–2290.

Lin, X.Y., Kaul, S.S., Rounsley, S. *et al.* (2000) Sequence and analysis of chromosome 2 of the plant *Arabidopsis thaliana*. *Nature*, **402**, 761–768.

Martienssen, R. (1998) Functional genomics: probing plant gene

function and expression with transposons. *Proc. Natl Acad. Sci. USA*, 95, 2021–2026.

Robinson, S.P. and Dry, I.B. (1992) Broad bean leaf polyphenol oxidase is a 60-kilodalton protein susceptible to proteolytic cleavage. *Plant Physiol.* 99, 317–323.

Ross-Macdonald, P., Coelho, P.S.R., Roemer, T. *et al.* (1999) Large-scale analysis of the yeast genome by transposon tagging and gene disruption. *Nature*, **402**, 413–418.

Sambrook, J., Fritsch, E.F. and Maniatis, T. (1989) *Molecular Cloning: A Laboratory Manual*, 2nd edn. Cold Spring Harbor, NY: Cold Spring Harbor Laboratory Press.

Sheldon, C.C., Rouse, D.T., Finnegan, E.J., Peacock, W.J. and Dennis, E.S. (2000) The molecular basis of vernalization: the central role of FLOWERING LOCUS C (FLC). *Proc. Natl Acad. Sci. USA*, 97, 3753–3758.

Smith, N.A., Singh, S.P., Wang, M.-B., Stoutjesdijk, P., Green, A. and Waterhouse, P.M. (2000) Total silencing by intron-spliced hairpin RNAs. *Nature*, **407**, 319–320.

Wang, M.-B. and Waterhouse, P.M. (2000) High-efficiency silencing of a β-glucuronidase gene in rice is correlated with repetitive transgene structure but independent of DNA methylation. *Plant Mol. Biol.* **43**, 67–82.

Wang, M.-B., Li, Z.-Y., Matthews, P.R., Upadhyaya, N.M. and Waterhouse, P.M. (1998) Improved vectors for *Agrobacterium tumefaciens*-mediated transformation of monocot plants. *Acta. Hort.* **461**, 401–407.

Wang, M.-B., Upadhyaya, N.M., Brettell, R.I.S. and Waterhouse, P.M. (1997) Intron-mediated improvement of a selectable marker gene for plant transformation using *Agrobacterium tumefaciens*. *J. Genet. Breed.* **51**, 325–334.

Wang, M.-B., Wesley, S.V., Finnegan, E.J., Smith, N.A. and Waterhouse, P.M. (2001) Replicating satellite RNA induces sequence-specific DNA methylation and truncated transcripts in plants. *RNA*, **7**, 16–28.

Waterhouse, P.M., Graham, M.W. and Wang, M.-B. (1998) Virus resistance and gene silencing in plants can be induced by simultaneous expression of sense and antisense RNA. *Proc. Natl Acad. Sci. USA*, **95**, 13959–13964.

Waterhouse, P.M., Wang, M.-B. and Lough, T. (2001) Gene silencing as an adaptive defence against viruses. *Nature*, **441**, 834–842.

Zamore, P.D., Tuschl, T., Sharp, P.A. and Bartel, D.P. (2000) RNAi: double-stranded RNA directs the ATP-dependent cleavage of mRNA at 21–23 nucleotide intervals. *Cell*, **101**, 25–33.

EMBL database accession numbers: AJ311872 and AJ311874.

Exhibit 5

The Plant Cell, Vol. 14, 2059–2069, September 2002, www.plantcell.org © 2002 American Society of Plant Biologists

Double Jeopardy: Both Overexpression and Suppression of a Redox-Activated Plant Mitogen-Activated Protein Kinase Render Tobacco Plants Ozone Sensitive

Marcus A. Samuel and Brian E. Ellis[1]

Biotechnology Laboratory, University of British Columbia, Vancouver, British Columbia, V6T 1Z3 Canada

In plants, the role of mitogen-activated protein kinase (MAPK) in reactive oxygen species (ROS)–based signal transduction processes is elusive. Despite the fact that ROS can induce MAPK activation, no direct genetic evidence has linked ROS-induced MAPK activation with the hypersensitive response, a form of programmed cell death. In tobacco, the major ROS-induced MAPK is salicylate-induced protein kinase (SIPK). We found through gain-of-function and loss-of-function approaches that both overexpression and RNA interference–based suppression of SIPK render the plant sensitive to ROS stress. Transgenic lines overexpressing a nonphosphorylatable version of SIPK were not ROS sensitive. Analysis of the MAPK activation profiles in ROS-stressed transgenic and wild-type plants revealed a striking interplay between SIPK and another MAPK (wound-induced protein kinase [WIPK]) in the different kinotypes. During continuous ozone exposure, abnormally prolonged activation of SIPK was seen in the SIPK-overexpression genotype, without WIPK activation, whereas strong and stable activation of WIPK was observed in the SIPK-suppressed lines. Thus, one role of activated SIPK in tobacco cells upon ROS stimulation appears to be control of the inactivation of WIPK.

INTRODUCTION

Mitogen-activated protein kinase (MAPK) modules form a key part of the eukaryotic signal transduction network that links environmental inputs to a wide range of modifications of cellular functions, ranging from cell division to cell death. In plants, MAPK signaling has been implicated in defense against pathogens and herbivores, in cellular responses to auxin, abscisic acid, and other phytohormones, in cell cycle control, in the induction of programmed cell death, and in responses to abiotic stresses such as UV light and ozone (Zhang and Klessig, 1997; Kovtun et al., 1998; Romeis et al., 1999; Heimovaara-Dijkstra et al., 2000; Samuel et al., 2000; Nishihama et al., 2001; Yang et al., 2001; Miles et al., 2002).

A variety of stress responses have been found to involve the rapid activation of a specific subset of plant MAPKs, notably Arabidopsis MPK6 (Ichimura et al., 2000; Kovtun et al., 2000; Nühse et al., 2000; Yuasa et al., 2001) and its orthologs in other species, such as salicylic acid–induced protein kinase (SIPK) in tobacco (Zhang and Klessig, 1998a, 1998b; Romeis et al., 1999; Mikolajczyk et al., 2000; Samuel et al., 2000; Zhang et al., 2000) and salt stress-induced MAPK (SIMK) in alfalfa (Cardinale et al., 2000). Because many biotic and abiotic stressors (virus infection, treatment with microbial elicitors, wounding, and osmotic stress) elicit a very rapid oxidative burst in plant cells, the apparent convergence of disparate stress signals on this particular MAPK node may be related to the sensitive response of MPK6/SIPK to redox perturbation.

Exposure to ozone immediately creates an oxidizing environment in plant tissues and triggers an array of cellular responses, including the accumulation of antioxidants, elicitation of pathogenesis-related proteins, deposition of phenols, induction of ethylene synthesis, suppression of primary metabolic activities such as photosynthesis, and eventually cell death (Darrall, 1989; Schraudner et al., 1992; Conklin and Last, 1995; Sharma and Davis, 1997; Tuomainen et al., 1997). Ozone enters the plant mesophyll through the stomata and diffuses through inner air spaces. In the cell wall and plasmalemma, it is converted spontaneously to reactive oxygen species (ROS) by contact with either water or membrane components (Sharma and Davis, 1997). The ozone-induced cell death process is influenced by the interaction of multiple signaling molecules, including salicylic acid, jasmonic acid, and ethylene (Orvar and Ellis, 1997; Overmyer et al., 2000; Rao et al., 2000).

One of the earliest responses elicited by ozone and other ROS generators in plants is the activation of specific MAPKs (Samuel et al., 2000; Desikan et al., 2001). The primary ROS-activated tobacco MAPK has been identified as the 46-kD

[1]To whom correspondence should be addressed. E-mail bee@interchange.ubc.ca; fax 604-822-2114.

Article, publication date, and citation information can be found at www.plantcell.org/cgi/doi/10.1105/tpc.002337.

SIPK; a second MAPK, the 44-kD wound-induced protein kinase (WIPK), usually responds more weakly (Kumar and Klessig, 2000; Samuel et al., 2000).

The rapid activation of these MAPKs suggests that their action on downstream targets could be important for the modulation of the cellular response to increased oxidative damage, but direct evidence for that role is lacking in plants. No intracellular substrates have been identified for either SIPK or WIPK, nor have loss-of-function genotypes been assessed for their ability to control redox stress. Stable overexpression or suppression of SIPK or WIPK in transgenic tobacco apparently did not result in the alteration of its activity (Yang et al., 2001). By contrast, transient overexpression of SIPK or its upstream activator, NtMEK2, in an active form has been shown to lead to the activation of either SIPK or both SIPK and WIPK, with associated induction of defense genes and hypersensitive response (HR)–like cell death (Yang et al., 2001; Zhang and Liu, 2001). This finding suggests that SIPK may play a role as a positive regulator in the cell death pathway.

The previously reported inability to produce SIPK-suppressed lines, and the lack of phenotype or alteration of SIPK activity reported for overexpression lines (Yang et al., 2001), have suggested that the normal functioning of this kinase may be essential for cell survival. However, we report here, using RNA interference (RNAi) technology, the recovery and analysis of transgenic tobacco plants in which SIPK is either overexpressed ectopically or largely eliminated. These plants display distinctive ozone response phenotypes that confirm the importance of SIPK activation for the effective control of ROS damage and also reveal an unexpected interplay between the activities of SIPK and WIPK.

RESULTS

Infiltration of fully grown tobacco leaves with a suspension of *Agrobacterium tumefaciens* cells carrying a SIPK-FLAG overexpression construct resulted in the accumulation of the epitope-tagged SIPK protein in the infiltrated tissue within 48 h. In unstressed cells, endogenous SIPK was not phosphorylated at the TXY motif found in the activation loop of the kinase, as indicated by the absence of any signal in the control lane of a protein gel blot (Figure 1C) prepared using an anti-pMAPK antibody that specifically recognized the doubly phosphorylated protein. In the infiltrated tissue, however, at least a portion of the pool of SIPK became activated by 48 h after infiltration, with even greater activation observed by 72 h. In the same period, the infiltrated zones showed signs of tissue collapse, and by 96 h, these zones became completely necrotic (Figure 1A).

When leaves were coinfiltrated with Agrobacterium carrying the SIPK-FLAG overexpression construct plus an RNAi construct that targeted SIPK, both expression and activation of SIPK-FLAG were suppressed completely (Figures 1B and 1C). The cell death induced by the overexpression of SIPK-FLAG in the infiltrated zones also was eliminated (Figure 1A).

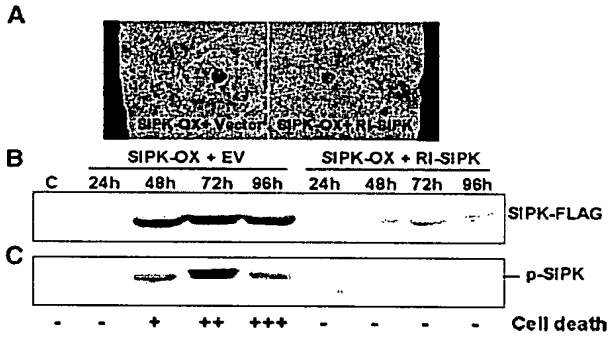

Figure 1. Post-Transcriptional Gene Silencing-Induced Suppression of Cell Death Triggered by Transient Overexpression of SIPK.

Coinfiltration with Agrobacterium containing the SIPK-FLAG construct along with the SIPK-RI construct inhibited the cell death process induced by transient overexpression of SIPK-FLAG alone **(A)**. Protein samples extracted at different times after infiltration of the constructs were immunoblotted with either anti-FLAG antibody **(B)** or phospho-MAPK-specific antibody (anti-pERK) **(C)**. −, +, ++, and +++ indicate the extent of visible lesions appearing in the infiltrated zones. EV, agrobacterium carrying empty vector.

The cell death associated with the spontaneous activation of SIPK in overexpression (OX) transgenic cells suggested that it might be difficult to recover stably transformed lines using this construct, but cocultivation of tobacco leaf discs with the appropriate Agrobacterium culture and selection on kanamycin yielded a number of transgenic lines that were found to ectopically express a range of levels of SIPK-FLAG (Figure 2A). No spontaneous activation of SIPK was detected in these lines, all of which displayed normal growth and development phenotypes.

Transformation of tobacco leaf discs with the SIPK-RI construct also yielded stable transgenic lines, although with a sharply reduced frequency. In the recovered RI lines, silencing of endogenous SIPK expression was observed to varying degrees, ranging from partial reduction in both SIPK mRNA and protein to elimination of both products (Figures 3B and 3C). The specificity of this silencing was shown by the continued expression in most of the recovered RI lines of the closely related *NTF4* MAPK gene, whose cDNA sequence is 89% identical to that of *SIPK* (Figure 3D). The RI lines again showed largely normal growth and development phenotypes, although the most severely suppressed lines showed some modest tendency to dwarfing (data not shown).

Plants of both the OX and RI lines showed no signs of spontaneous cell death under normal growth conditions. However, exposure of mature OX or RI leaves to levels of ozone that caused no visible injury to wild-type plants (500 parts per billion [ppb]) resulted in the rapid appearance of small necrotic lesions on leaves of both the transgenic

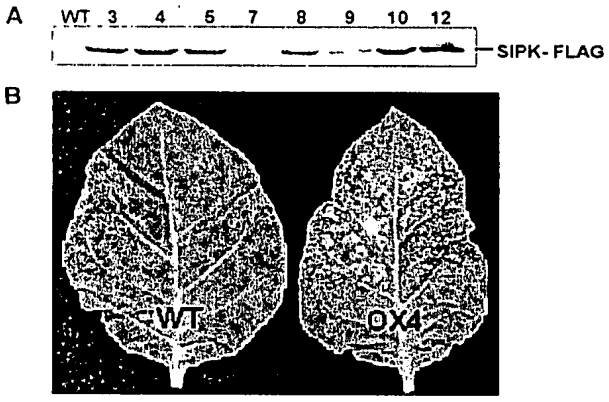

Figure 2. Transgenic Tobacco Plants Overexpressing SIPK-FLAG Show Increased Ozone Sensitivity.

(A) Proteins (40 μg) extracted from leaves of the different OX lines ectopically expressing SIPK-FLAG were immunoblotted using anti-FLAG antibody.

(B) Transgenic tobacco line OX4 and wild-type tobacco (Xanthi-nc) plants (n = 25) were exposed to ozone (500 ppb) for 8 h. The treated leaves were photographed 24 h after exposure.

WT, wild type.

genotypes (Figures 2B and 3E). The kinetics of this oxidative stress damage were quite different. Lesions consistently appeared on the leaves of OX plants as early as 4 to 6 h, but visually similar lesions only appeared on RI leaves ~24 h later. In plants challenged with lower ozone concentrations (250 ppb), an analogous pattern was observed except that the necrotic responses were delayed until 48 h (OX) and 72 h (RI) (data not shown). When leaf discs prepared from the wild-type, OX, and RI genotypes were assayed for the loss of membrane integrity and associated ion leakage resulting from ozone exposure (500 ppb), differential timing of the damage response also was observed (Figure 4).

To assess in situ the relative levels of hydrogen peroxide accumulation induced by ozone exposure, control and ozone-treated leaf halves were infiltrated with 3,3′-diaminobenzidine solution. The staining patterns revealed no detectable levels of hydrogen peroxide in untreated leaves of any of the genotypes or in leaves of wild-type plants after 8 h of ozone exposure. However, strong 3,3′-diaminobenzidine staining was observed in both the OX and RI lines after ozone treatment (Figure 4B).

The observation that overexpression of SIPK-FLAG in infiltrated leaves was accompanied by the spontaneous activation of MAPK and by cell death raised the question of whether activation of the ectopically expressed protein was necessary for the induction of cell death. Therefore, site-directed mutagenesis was used to create a version of SIPK-FLAG in which the TEY motif found in the activation loop of SIPK had been converted to an AEF sequence. This modification yielded a kinase that retained a low level of basal activity when the recombinant protein was assayed in vitro against myelin basic protein (Figure 5A), but it could not be activated further through dual phosphorylation of the activation loop by upstream MAPK kinases. Unlike the SIPK-FLAG construct, when transiently expressed in tobacco leaves, the SIPK(AEF)-FLAG construct failed to cause cell death in the infiltrated zone (data not shown).

Stably transformed tobacco plants expressing high levels of SIPK(AEF)-FLAG also were recovered readily after Agrobacterium cocultivation, and these plants displayed no visibly altered phenotype. Despite accumulating similar levels of the epitope-tagged kinase (Figure 5B), the ozone sensitivity of these SIPK(AEF) transgenic lines did not differ from that of wild-type plants (data not shown). This finding indicates that the heightened ozone sensitivity observed in SIPK-OX transgenic lines requires not only that the ectopically expressed kinase be expressed at high levels within the plant cell but that it have the capacity to become activated.

The activation status of both SIPK and WIPK in tobacco tissue extracts can be assessed either on protein gel blots using a phosphospecific antibody or by immunoprecipitation with antibodies that discriminate between SIPK and WIPK, followed by in gel or in vitro kinase activity assays. When the various transgenic and wild-type tobacco lines were monitored during a 30-min period of ozone exposure, striking differences in the pattern of kinase activation were observed among these genotypes (Figure 6).

As reported previously (Samuel et al., 2000), ozone treatment led to the rapid activation of SIPK in leaves of wild-type plants. This was accompanied by a much weaker activation of the smaller kinase, WIPK (Figure 6A). In the OX4 genotype, ozone exposure also led to SIPK activation, but the level of activation appeared to be depressed relative to the wild-type response, despite the presence of far greater amounts of ectopically expressed SIPK in the OX cells (Figures 6B and 6C). No activation of WIPK was detected in the OX tissue samples.

The SIPK(AEF) genotype presented a kinase activation profile that was very similar to that of the wild type. This indicates that flooding the cell with a nonactivatable version of SIPK (a potential dominant-negative form) does not interfere with the ability of the upstream MAPK cascade elements to transmit oxidant-induced signals to their cognate MAPKs.

Exposure of the RI genotype to ozone, on the other hand, yielded a very different MAPK activation profile. Very weak or no SIPK activation was detected, as would be predicted for a genotype in which SIPK expression has been suppressed by post-transcriptional gene silencing (Figures 6A and 6C). Instead, ozone exposure produced strong and specific activation of WIPK. The identity of these highly activated kinases in ozone-treated leaves of each genotype was confirmed through immunoprecipitation of the 30-min ozone-treated protein extracts with either SIPK- or WIPK-specific antibodies, followed by in gel kinase assays (Figures 6D and 6E).

Aside from the unexpected massive activation of WIPK, the stability of that activation also was strikingly different in

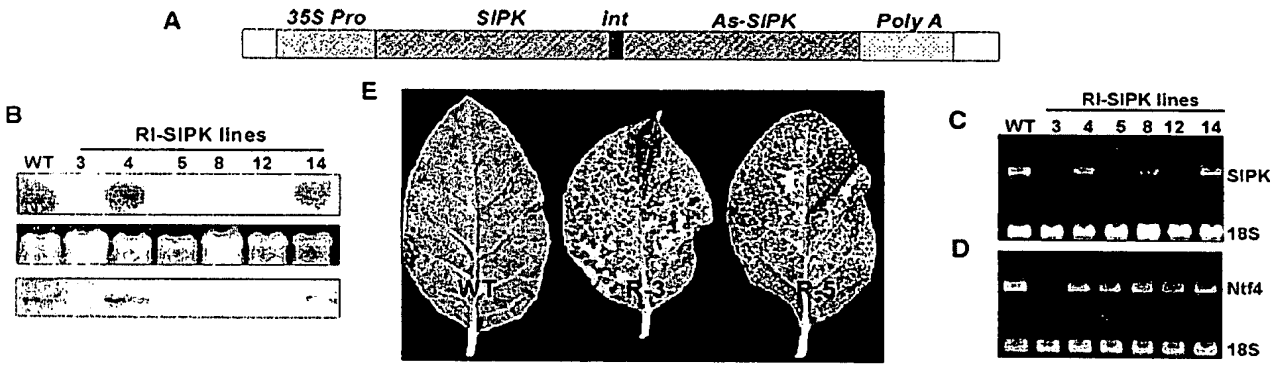

Figure 3. SIPK-Suppressed Lines Also Are Sensitive to Ozone.

(A) RNAi construct under the control of the 35S promoter of *Cauliflower mosaic virus*.

(B) SIPK is suppressed in four of the six PCR-positive lines. RNA gel blot analysis was performed using total RNA (15 μg) extracted from wild-type and SIPK-RI lines and probed with the radiolabeled C-terminal fragment of the *SIPK* ORF. Autoradiography revealed essentially no SIPK mRNA in four of the six PCR-positive lines (top). Ethidium bromide staining of the gel showed equal loading of RNA (middle). Immunoblot analysis of protein samples from the same lines indicated the absence of detectable amounts of SIPK protein in all four SIPK-suppressed lines (bottom).

(C) Similar results were observed when reverse transcriptase–mediated PCR was conducted using *SIPK*-specific primers.

(D) *NTF4* gene expression in the SIPK-suppressed lines was analyzed by reverse transcriptase–mediated PCR using gene-specific primers.

(E) SIPK-suppressed lines R3 and R5 display ozone-sensitive phenotypes. Plants (n = 15) of SIPK-suppressed tobacco transgenic lines R3 and R5, together with wild-type plants, were exposed to ozone (500 ppb) for 8 h per day for 2 days. The treated leaves were photographed 24 h after the end of 2 days of exposure.

WT, wild type.

this genetic background. Normally, when oxidants trigger a rapid activation of SIPK, it is a transient response. The activation is effectively lost within 1 h, even under conditions of continuous oxidant stimulus, as seen in Figure 7A (wild-type lane). However, in the RI genotype, WIPK was not only activated rapidly but the pool of this MAPK remained continuously active for up to 8 h after the initiation of the response (Figure 7A, RI lane). Although normally there is far less WIPK than SIPK present in tobacco leaves (Zhang and Klessig, 1998b), the high activation signal observed in the RI tissue extracts did not appear to reflect increased levels of WIPK protein in this genotype compared with wild-type plants, as assessed by protein gel blot analysis (Figure 7C).

Interestingly, kinase activation by ozone in the OX genotype also was prolonged abnormally, relative to that seen in ozone-treated wild-type plants, but in this case, the active kinase was SIPK rather than WIPK (Figure 7B). In addition, unlike the hyperactivated WIPK pool, the extended activation of SIPK in the OX line was more transient and disappeared within 4 h. This is approximately the time at which visible lesions began appearing on ozone-treated OX leaves.

Examination of the temporal response of the two genes (*GST* [glutathione *S*-transferase] and *cAPX* [cytosolic ascorbate peroxidase]) whose expression was induced strongly by ozone treatment revealed that the loss of SIPK signaling in the RI genotype resulted in a delayed response in the expression of both genes. In the OX line, the prolonged activation of SIPK signaling resulted in the suppression of *GST* induction, whereas *APX* gene expression was unaffected (Figures 8A and 8B).

DISCUSSION

Plant cells must deal constantly with ROS from a range of sources, including photooxidation, mitochondrial electron transport, flavin oxidase by-products, and environmental insults such as UV light, ozone, and ionizing radiation. Against this background, ROS pulses ("oxidative bursts") also can occur within cells, usually as very early responses to localized challenges to cellular integrity such as wounding and pathogen assault. These pulses may serve in multiple functions, including activation of redox protection mechanisms, modulation of intracellular signal transduction pathways, and transmission of systemic signals to neighboring cells.

A severe oxidative challenge that overwhelms local protective measures ultimately will lead to cell death. The archetype for this outcome is the HR response induced during incompatible host–pathogen interactions. Similar lesions are induced by exposure to increased levels of ozone or UV light. The exact process by which cellular integrity fails is unclear, but the notion that HR represents a form of genetically programmed cell death is supported by the identification of nu-

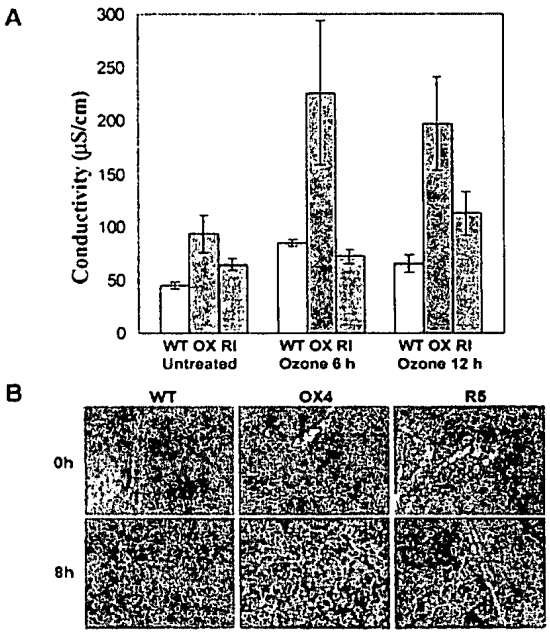

Figure 4. Quantitation of Ozone-Induced Cell Death and Hydrogen Peroxide Accumulation in SIPK Kinotypes.

(A) Ion leakage from leaf discs (five each) of the third and fourth leaves of wild-type, OX4, and RI5 lines was assessed as an indicator of the loss of membrane integrity 6 and 12 h after the initiation of ozone exposure (500 ppb). The data presented are means and standard deviations from three independent experiments.

(B) 3,3'-Diaminobenzidine staining to detect hydrogen peroxide accumulation in ozone-treated leaves of SIPK kinotypes.

WT, wild type.

merous mutants affected in the process of lesion formation (Richberg et al., 1998).

The correlation of ROS pulses with the cell death process has been described extensively. Treatments such as chilling, wounding, pathogen infection, UV irradiation, and ozone exposure rapidly induce ROS accumulation in plant cells, followed later by lesion development. However, despite these correlative observations, a functional link between ROS accumulation and local lesion formation has yet to be defined.

It is striking that so many stresses that elicit ROS accumulation in plant cells consistently appear to activate MAPK modules as one of their earliest effects (Seo et al., 1995; Zhang and Klessig, 1998b; Allan et al., 2001; Desikan et al., 2001; Orozco-Cardenas et al., 2001). The MAPK observed most consistently to be activated by both applied stresses and ROS is SIPK in tobacco (Samuel et al., 2000; Miles et al., 2002) or its apparent orthologs in other species, such as MPK6 in Arabidopsis (Kovtun et al., 2000; Yuasa et al., 2001) and SIMK in alfalfa (Cardinale et al., 2000). This pattern suggests that SIPK activation might play an important role in determining the response and ultimate fate of the stressed cells.

Links between ROS-associated cell death and MAPK signaling have been reported for a number of nonplant systems. Hydrogen peroxide–induced cell death in cultured mammalian oligodendrocyte cells is inhibited by PD98059, a specific inhibitor of MEK, the upstream kinase of the ERK1/2 MAPK (Bhat and Zhang, 1999), whereas delayed and prolonged activation of p44 and p42 MAPKs is critical for genistein-induced programmed cell death in rat primary cortical neurons (Linford et al., 2001). Similarly, delayed and persistent activation of ERK1/2 is associated with glutamate-induced oxidative cytotoxicity in neuronal cell lines (Stanciu et al., 2000).

There also is evidence that ROS-activated MAPKs may play analogous roles in plant cells. Cell death induced in Arabidopsis cell suspension cultures by treatment with a bacterial elicitor (harpin) is inhibited when the cells are treated with the MEK inhibitor PD98059 (Desikan et al., 1999), whereas pretreatment of tobacco cells with staurosporine, a general protein kinase inhibitor, suppresses the cell death normally induced by exposure to fungal elicitors (Suzuki et al., 1999).

Genetic manipulation experiments also have implicated MAPK activation in the cell death process. In Arabidopsis plants overexpressing constitutively active forms of the MAPK kinases AtMEK4 and AtMEK5 under the control of an inducible promoter, HR-like lesions appeared after induction with dexamethasone, and lesion formation was preceded by the activation of endogenous MAPKs and the accumulation of hydrogen peroxide (Ren et al., 2002). Transient overexpression of a constitutively active form of a MAPK kinase (NtMEK2) in tobacco also led to the sustained activation of MAPKs, identified

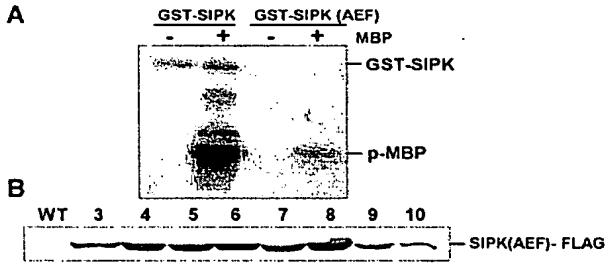

Figure 5. Activity and Expression of Mutagenized SIPK.

(A) The recombinant SIPK activation loop mutant is less active than wild-type SIPK. Myelin basic protein (MBP)-phosphorylating activities of SIPK and SIPK(AEF) were measured by incubating recombinant proteins (5 μg) with 5 μg of MBP, as described in Methods. The phospho-MBP product was visualized through autoradiography after SDS-PAGE fractionation.

(B) SIPK(AEF) transgenic lines show high expression of the transgene product. Proteins (40 μg) extracted from the different lines overexpressing SIPK(AEF)-FLAG were fractionated by SDS-PAGE and immunoblotted using anti-FLAG antibody.

WT, wild type.

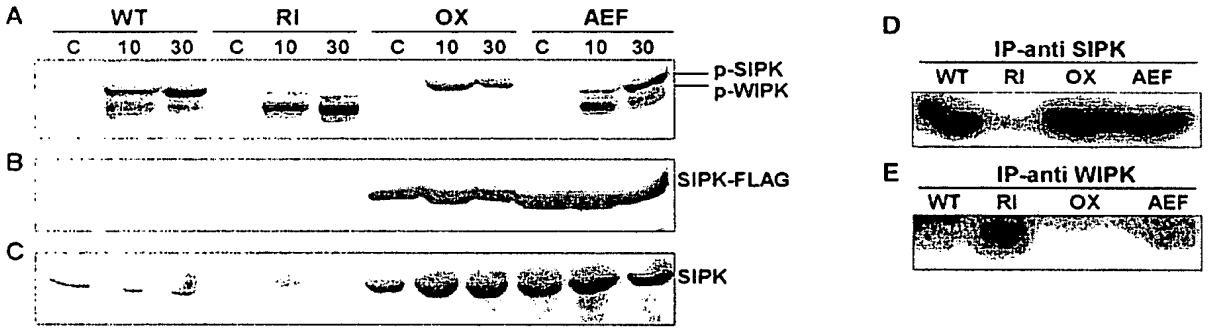

Figure 6. Differential Ozone-Induced Activation of SIPK and WIPK in SIPK Kinotypes.

(A) Crude protein extracts prepared from ozone-exposed tissues from T1 lines of the different SIPK kinotypes (RI5, OX4, and AEF8) and the wild type were resolved on a 10% polyacrylamide gel, blotted, and probed with an anti-phospho-ERK antibody to recognize phospho-MAPK forms.
(B) The same blot was probed subsequently using an anti-FLAG antibody to detect ectopic expression of the transgene product in the different kinotypes.
(C) A replicate protein gel blot was analyzed using a SIPK-specific antibody, revealing high expression of SIPK forms in the overexpressor lines and its absence in the SIPK-suppressed lines.
(D) and **(E)** Protein samples prepared from ozone-exposed (30 min) tissues from the different kinotypes were immunoprecipitated with either SIPK-specific **(D)** or WIPK-specific **(E)** antibodies. The immunoprecipitates were subjected to an in gel kinase assay, as described in Methods.
WT, wild type.

as SIPK and WIPK, and to the death of the infiltrated tissue (Yang et al., 2001). Transient overexpression of SIPK itself was shown subsequently to result in the formation of HR-like lesions, but only in young leaves (Zhang and Liu, 2001).

We have confirmed that ectopic SIPK overexpression leads to the appearance of high levels of the activated kinase in Agrobacterium-infiltrated tobacco tissue and to rapid cell death (Figure 1). On the other hand, when stably transformed tobacco plants were produced that overexpressed epitope-tagged SIPK (Figure 2), they displayed no visible phenotype. When exposed to ozone, however, the transgenic SIPK-OX plants proved to be much more sensitive than the nontransgenic parental line, indicating that ROS-induced cell death was controlled less effectively in the overexpression genotype.

Although this pattern is consistent with the results of NtMEK2 or SIPK-OX transient expression, its physiological relevance remains uncertain, because we know little about the effects of the accumulation of nonphysiological levels of active signal components on cellular function. To unambiguously identify a functional relationship between ROS activation of SIPK and ROS-induced cell death, we turned to the creation of defined loss-of-function mutants.

The modification of SIPK function in transgenic tobacco plants using either conventional gene-silencing methods (cosuppression and antisense-mediated suppression) or overexpression of dominant-negative forms proved ineffective (Yang et al., 2001) (data not shown). However, expression of an intron-containing "hairpin RNA" (Smith et al., 2000) designed to target a unique tract within the SIPK coding sequence yielded a number of transgenic plants in which SIPK expression was suppressed severely and specifically through post-transcriptional gene silencing. Loss of SIPK had no obvious phenotypic consequences for plants grown under normal greenhouse conditions.

Given the sensitivity of SIPK-OX lines to ozone, it might have been predicted that the absence of this kinase would have no effects, or perhaps even positive effects, on the ozone sensitivity of the SIPK-RI lines. Instead, after ozone treatments that induced no visible damage on wild-type plants, the SIPK-RI lines developed numerous lesions on their middle leaves within 24 h. Thus, the inability of the suppressed genotype to generate and activate SIPK compromises the cell's ability to manage ROS stress and to control cell death, although apparently on a different time scale from that observed in SIPK-OX plants.

Which facet of ROS-stress management has been compromised in SIPK-OX and SIPK-RI plants is not clear. No constitutive hydrogen peroxide accumulation was detected in any of the genotypes, suggesting that their heightened ozone sensitivity is not the consequence of a preexisting accumulation of ROS. Instead, it appears that alteration of the normal ozone-induced MAPK activation process, through either unregulated overexpression or suppression, creates an inability to cope with increased redox stress. Examination of the transcriptional activity of two genes whose mRNAs accumulate rapidly after ozone exposure showed that the response of both genes was affected differently (Figure 8).

Expression of *cAPX*, which encodes a major ROS-scavenging enzyme, was induced less effectively by ozone in RI plants, whereas it was unaffected in the OX line. Antisense suppression of *cAPX* was shown previously to create hypersensitivity to both ozone (Orvar and Ellis, 1997) and pathogens (Mittler

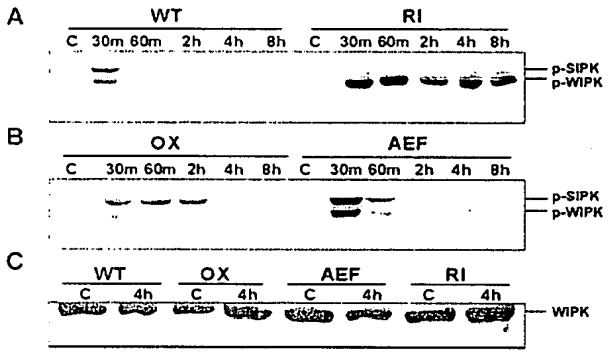

Figure 7. Loss of SIPK Has Differential Effects on the Expression of Ozone-Induced Genes and Leads to the Hyperactivation of WIPK.

(A) and **(B)** Extended ozone exposure reveals strong and prolonged activation of WIPK in the RI line. A temporal profile of the phosphorylation status of SIPK and WIPK was generated through anti-pERK immunoblotting of crude proteins extracted from tissues of either wild-type and RI lines **(A)** or OX and AEF lines **(B)** exposed to ozone for different times (0 to 8 h).

(C) Alteration of SIPK does not lead to changes in the amount of WIPK. Protein extracts from untreated and 4-h ozone-treated tissues from different kinotypes were immunoblotted with anti-WIPK antibody. WT, wild type.

et al., 1999) in transgenic tobacco plants. On the other hand, ozone-induced expression of *GST*, a general cellular protectant, was suppressed strongly in the *OX* line, but its expression was delayed markedly in the RI line. In Arabidopsis, both hydrogen peroxide and ozone induce GST expression (Clayton et al., 1999; Grant et al., 2000), and this expression has been demonstrated to require the activity of an unidentified 48-kD MAPK and calcium ion influx. Calcium channel activity also is essential for the ROS activation of SIPK in tobacco (Samuel et al., 2000).

The delayed response of the antioxidant genes in the RI line could result in increased early accumulation of ROS (Figure 4B), which could lead to a necrotic cell death process. In the OX line, although the *cAPX* gene response to ozone appeared to be normal, the antioxidant response clearly was unable to contain the increasing ROS levels associated with extended SIPK activation (Figure 4B). MAPK activation has been linked previously to increased ROS accumulation in Arabidopsis (Ren et al., 2002). A broader comparison of transcript profiles should generate useful insights into other connections between the transmission of redox signals by SIPK and the ability of the cell to avoid oxidative cell death.

Another aspect of the link between SIPK activation and cell death is revealed in the pattern of MAPK activation in ROS-stressed plants. The activation of SIPK by ozone occurred within 10 min in SIPK-OX plants but was not reversed for 4 h, by which time cell death already was becoming visible. This outcome is similar to the association of the prolonged activation of mammalian ERK with the induction of programmed cell death in neurons (Stanciu et al., 2000). Considered together with the results of the transient expression experiments, this finding demonstrates that the unregulated continuous activity of SIPK within plant cells profoundly affects normal homeostatic mechanisms.

The absence of SIPK in the SIPK-RI genotype also led to premature cell death under redox stress conditions, but in this case, the hyperactivated species observed was WIPK rather than SIPK. There have been other indications that WIPK plays a central role in plant stress signaling. This gene was identified originally on the basis of its rapid and transient induction upon wounding of tobacco leaves (Seo et al., 1995), and the gene product was shown later to be activated transiently by wounding (Seo et al., 1999) and by various other stresses (Romeis et al., 1999; Zhang et al., 2000). WIPK activation usually is accompanied by the activation of SIPK, but SIPK and WIPK do not always respond in unison; some oxidative stresses appear to activate SIPK preferentially and leave WIPK unaffected (Kumar and Klessig, 2000; Samuel et al., 2000).

WIPK activity, either alone or together with SIPK, has been suggested to be involved in the induction of cell death in cultured tobacco cells by specific fungal elicitor treatments (Zhang et al., 2000). Pretreatment of the elicited cells with staurosporine and K252A (protein kinase inhibitors) completely suppressed both WIPK activation and cell death. However, transient overexpression of WIPK did not result in its activation and failed to induce cell death in infiltrated tobacco leaves, unlike overexpression of SIPK (Zhang and Liu, 2001). In another study, the stable overexpression of WIPK in transgenic tobacco was accompanied by the constitutive expression of protease inhibitor II and the accumulation of methyl jasmonate

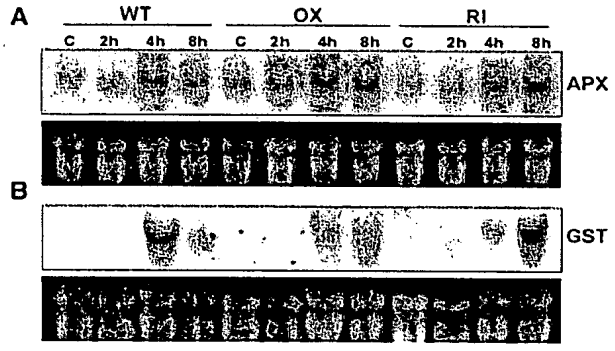

Figure 8. Alteration of SIPK Signaling Affects the Expression of GST and cAPX.

RNA gel blot analysis of the accumulation of cAPX **(A)** and GST mRNA **(B)** in wild-type, SIPK-overexpressing, and SIPK-suppressed transgenic tobacco. Plants were exposed to ambient air (C) or 500 ppb of ozone for 2, 4, and 8 h, and total RNA was harvested from the third and fourth leaves.
WT, wild type.

(Seo et al., 1999), but the oxidative stress sensitivity of the WIPK-OX lines was not reported.

How SIPK elimination leads to the prolonged hyperactivation of WIPK is unknown, but various possibilities suggest themselves. If NtMEK2 is the sole upstream MAPK kinase responsible for the activation of both SIPK and WIPK, these two MAPKs may normally compete for binding to NtMEK2. However, basal levels of SIPK in unstimulated tobacco cells are much higher (10-fold) than those of WIPK (Zhang and Klessig, 1998b). In the absence of competition from SIPK, activation of WIPK by NtMEK2 activation in SIPK-RI cells may be much more efficient than usual. This scenario also might explain why WIPK remains largely inactivated in ozone-treated SIPK-OX tissues in which an excess of SIPK is present. However, although this model accounts for WIPK hyperactivation, it does not necessarily explain why that activation is prolonged abnormally.

Alternatively, one of the normal roles of activated SIPK may be the direct or indirect regulation of WIPK activity. Both dual-specificity phosphoprotein phosphatases (MKP) and Ser/Thr phosphatases have been implicated in inactivating MAPK pathways in mammalian and plant models (Brondello et al., 1997; Meskiene et al., 1998; Ulm et al., 2001; Westermarck et al., 2001). If SIPK activity is required for the induction or activation of a protein phosphatase that normally acts upon phospho-WIPK, the absence of SIPK from oxidant-stressed SIPK-RI cells would create a situation in which WIPK could be activated by its cognate MAPK kinase but could not be inactivated subsequently.

In this regard, it is interesting that Arabidopsis plants in which a dual-specificity phosphatase (AtMKP-1) has been mutated by T-DNA insertional mutagenesis display increased activation of an unidentified ~49-kD MAPK and are more susceptible to ROS-generating stresses (e.g., UV light) (Ulm et al., 2001). On the other hand, MP2C, an alfalfa Ser/Thr phosphatase belonging to the PP2C class, has been shown to be a negative regulator of the MAPK pathway involving stress-activated MAPK, an apparent ortholog of WIPK (Meskiene et al., 1998). Both classes of protein phosphatase could be involved in cross-regulation mechanisms. Resolution of this question, and of the relative importance of the loss of SIPK activity versus the enhancement of WIPK activity in controlling oxidant-induced cell death, will require the development and analysis of other relevant single and multiple loss-of-function genotypes. These studies are now under way.

METHODS

Plant Material and Treatment

Tobacco (*Nicotiana tabacum*) plants of all genotypes were grown for 6 weeks in soil under controlled environmental conditions (25/20°C, 16-h-light/8-h-dark cycle) and then exposed to ozone (500 parts per billion) and harvested as described previously (Orvar and Ellis, 1997).

Recombinant Protein Production

The open reading frame (ORF) of salicylate-induced protein kinase (*SIPK*) was amplified by reverse transcriptase–mediated (RT) PCR using gene-specific primers and RNA isolated from untreated leaves of tobacco cv Xanthi-nc. The amplicon was cloned in frame into the expression vector pGEX 4T-3. Mutations in the activation loop of SIPK were introduced using a PCR-mediated approach, taking advantage of the unique NheI restriction site close to the activation loop. The mutational primers were designed so that the mutant form would code for AEF instead of TEY at amino acid positions Thr-218 and Tyr-220.

The *SIPK*(AEF) gene construct then was cloned into pGEX 4T-3. The recombinant glutathione *S*-transferase (GST) fusion proteins were expressed in *Escherichia coli* BL21 cells by induction with 0.1 mM isopropylthio-β-galactoside for 4 h at 25°C, followed by purification according to the manufacturer's protocol (Amersham Pharmacia). The different constructs were sequenced to confirm the changes and the absence of mismatches.

Intron-Spliced Hairpin Loop RNA–SIPK Construct

The double-stranded RNA interference construct was tailored through a PCR-mediated approach using the N-terminal sequence of the *SIPK* ORF. A minimal intron based on the splice junctions and flanking regions of the fourth intron of *AtMPK6* (the Arabidopsis ortholog of SIPK) was incorporated into the sense-strand primer. The sense strand then was amplified using a primer combination that generated an EcoRI cleavage site and intron-XbaI sequence on the opposite ends of the product, whereas the antisense strand was amplified using a primer combination that added BamHI and XbaI sites on the opposite ends of the product. These two products were directionally cloned into EcoRI-BamHI–processed Bin19/pRT101 through a triple ligation, which placed the RNA interference construct under the control of the 35S promoter of *Cauliflower mosaic virus* (Figure 3A).

Binary Vector Construction and Plant Transformation

The different SIPK overexpression constructs were tagged with a C-terminal FLAG epitope through a PCR-mediated approach, followed by ligation into the plant expression vector Bin19/pRT101, which contains an *nptII*-selectable marker. All of the constructs were sequenced to confirm the presence of appropriate changes. The recombinant binary vector was used to transform competent *Agrobacterium tumefaciens* (EHA105) cells by a freeze-thaw transformation procedure.

Agrobacterium-mediated transformation of tobacco (cv Xanthi-nc) was performed using a leaf disc cocultivation procedure. Transformants were selected on half-strength Murashige and Skoog (1962) culture medium containing 50 mg/L kanamycin. Surviving plantlets were screened by PCR using 35S forward and gene-specific reverse primer combinations. Positive transformants then were screened by protein gel blot analysis (see below) using an anti-FLAG antibody for the SIPK overexpression lines and anti-SIPK antibodies to assess the RI suppression lines.

The confirmed transgenic lines were transferred to soil and grown to maturity, and seeds were collected. The T1 seeds were germinated on half-strength Murashige and Skoog (1962) medium with 50 mg/L kanamycin, and antibiotic-resistant plants were transferred to soil and grown under controlled conditions.

Transient Transformation Using Agrobacterium Infiltration

Four- to 6-week-old wild-type tobacco plants (cv Xanthi-nc) were used for infiltration experiments as described previously (Yang et al., 2001). This involved leaf infiltration with a mixed culture (OD of 0.4 at 600 nm) of Agrobacterium EHA105 containing the SIPK-FLAG overexpression construct plus an equal population of Agrobacterium containing either the empty vector or the SIPK-RI construct. At the indicated times (Figure 1), the infiltrated area was cut from the leaf, frozen in liquid nitrogen, and stored at −80°C until further analysis.

RNA Gel Blot and RT-PCR Analysis

Total RNA (15 μg) was resolved on 1% agarose-formaldehyde gels, blotted, and probed as described previously (Orvar and Ellis, 1997). The 600-bp C-terminal fragment of the *SIPK* ORF and PCR-amplified fragments of the cytosolic ascorbate peroxidase (*cAPX*) and *GST* were used as probes. Gene-specific primers were used to amplify the ORFs of *cAPX* (forward, 5′-AGAACAATTGCTATGGGTAAGTG-3′; reverse, 5′-GCAAGCTTAAGCTTCAGCAAAT-3′) and *GST* (forward, 5′-ATGGCGATCAAAGTCCATGGTA-3′; reverse, 5′-TTTTTGCAGCTTCTCCAATCCC-3′) using cDNA as the template.

The cDNA was synthesized from total RNA extracted from control and ozone-exposed tissues of the different genotypes/treatments using a first-strand cDNA synthesis kit (Invitrogen, Carlsbad, CA). RT-PCR was performed using gene-specific primers designed to target either *SIPK* (25 cycles) or *NTF4* (30 cycles). The number of cycles was adjusted so that the amplification was within the linear range. As an internal control, 18S ribosomal cDNA was amplified using a 1:4 ratio of 18S-specific primers to competitor's DNA fragments provided by Ambion (Austin, TX).

Protein Extraction and Protein Gel Blot Analysis

Total protein extracts were prepared (40 to 80 μg) and used for protein gel blot analysis as described previously (Samuel et al., 2000). A primary antibody dilution of 1:1000 was used for anti-pERK (New England Biolabs, Beverly, MA), and a dilution of 1:5000 was used for anti-SIPK, anti-wound-induced protein kinase (WIPK) (Seo et al., 1999; Y. Ohashi, personal communication), and anti-FLAG (Sigma) antibodies.

Immune Complex Kinase Assay

Immunoprecipitations were performed as described previously (Samuel et al., 2000) using 250 μg of extracted protein together with 5 μg of either anti-SIPK or anti-WIPK antibodies. The immunoprecipitates were analyzed in an in gel kinase assay as described previously using myelin basic protein as the substrate (Zhang and Klessig, 1997).

In Vitro Kinase Assays

GST fusion proteins (5 μg) of the wild-type and mutant SIPK(AEF) were incubated with 5 μg of myelin basic protein and 10 μCi of γ-^{32}P–labeled ATP (>5000 Ci/mmol) (Amersham Pharmacia) in a 20-μL reaction mixture (20 mM Hepes, pH 7.5, 5 mM $MgCl_2$, 1 mM EGTA, 5 mM β-mercaptoethanol, 2 mM Na_3VO_4, and 20 mM β-glycerophosphate) at 30°C for 30 min. The reaction was stopped with 6 × SDS loading buffer, and the samples were resolved on a 15% polyacrylamide gel, blotted onto a nylon membrane, and visualized by autoradiography.

Ion-Leakage Assay

Five leaf discs (9 mm) were cut from each of the third and fourth leaves of ozone-exposed and untreated plants of the wild type, OX4, and RI5 lines. The 10 leaf discs were incubated in 5 mL of deionized water at 25°C on a gyratory shaker at 110 rpm for 4 h, and the conductivity of the solution was measured as described previously (Mittler et al., 1999).

In Situ Staining for Hydrogen Peroxide

Hydrogen peroxide was visualized in situ by 3,3′-diaminobenzidine staining performed essentially according to Torres et al. (2002). Leaf halves were collected after 8 h of ozone exposure (500 parts per billion) and vacuum infiltrated with the 3,3′-diaminobenzidine (1 mg/mL) solution. Infiltrated leaves were placed under high humidity until brown precipitation was observed (5 to 6 h) and then fixed with a solution of ethanol:lactic acid:glycerol (3:1:1, v/v) for 2 days, followed by further clearing in methanol. Unless indicated otherwise, all experiments were repeated with consistent results.

Upon request, all novel materials described in this article will be made available in a timely manner for noncommercial research purposes. No restrictions or conditions will be placed on the use of any materials described in this article that would limit their use for noncommercial research purposes.

ACKNOWLEDGMENTS

We thank Y. Ohashi for providing the anti-WIPK and anti-SIPK antibodies and H. Hall for assistance with the 3,3′-diaminobenzidine staining experiments. Funding for this research was provided by the Natural Sciences and Engineering Research Council of Canada.

Received February 13, 2002; accepted May 15, 2002.

REFERENCES

Allan, A.C., Lapidot, M., Culver, J.N., and Fluhr, R. (2001). An early tobacco mosaic virus-induced oxidative burst in tobacco indicates extracellular perception of the virus coat protein. Plant Physiol. **126,** 97–108.

Bhat, N.R., and Zhang, P. (1999). Hydrogen peroxide activation of multiple mitogen-activated protein kinases in an oligodendrocyte cell line: Role of extracellular signal-regulated kinase in hydrogen peroxide-induced cell death. J. Neurochem. **72,** 112–119.

Brondello, J.M., Brunet, A., Pouyssegur, J., and McKenzie, F.R. (1997). The dual specificity mitogen-activated protein kinase phosphatase-1 and -2 are induced by the p42/p44 MAPK cascade. J. Biol. Chem. **272,** 1368–1376.

Cardinale, F., Jonak, C., Ligterink, W., Niehaus, K., Boller, T., and Hirt, H. (2000). Differential activation of four specific MAPK pathways by distinct elicitors. J. Biol. Chem. **275,** 36734–36740.

Clayton, H., Knight, M.R., Knight, H., McAinsh, M.R., and Hetherington, A.M. (1999). Dissection of the ozone-induced calcium signature. Plant J. **17,** 575–579.

Conklin, P.L., and Last, R.L. (1995). Differential accumulation of antioxidant mRNAs in *Arabidopsis thaliana* exposed to ozone. Plant Physiol. **109,** 203–212.

Darrall, N.M. (1989). The effect of air pollutants on physiological processes in plants. Plant Cell Environ. **12,** 1–30.

Desikan, R., Clarke, A., Atherfold, P., Hancock, J.T., and Neill, S.J. (1999). Harpin induces mitogen-activated protein kinase activity during defence responses in *Arabidopsis thaliana* suspension cultures. Planta **210,** 97–103.

Desikan, R., Hancock, J.T., Ichimura, K., Shinozaki, K., and Neill, S.J. (2001). Harpin induces activation of the Arabidopsis mitogen-activated protein kinases AtMPK4 and AtMPK6. Plant Physiol. **126,** 1579–1587.

Grant, J.J., Yun, B.W., and Loake, G.J. (2000). Oxidative burst and cognate redox signalling reported by luciferase imaging: Identification of a signal network that functions independently of ethylene, SA and Me-JA but is dependent on MAPKK activity. Plant J. **24,** 569–582.

Heimovaara-Dijkstra, S., Testerink, C., and Wang, M. (2000). Mitogen-activated protein kinase and abscisic acid signal transduction. Results Probl. Cell Differ. **27,** 131–144.

Ichimura, K., Mizoguchi, T., Yoshida, R., Yuasa, T., and Shinozaki, K. (2000). Various abiotic stresses rapidly activate Arabidopsis MAP kinases ATMPK4 and ATMPK6. Plant J. **24,** 655–665.

Kovtun, Y., Chiu, W.-L., Tena, G., and Sheen, J. (2000). Functional analysis of oxidative stress-activated mitogen-activated protein kinase cascade in plants. Proc. Natl. Acad. Sci. USA **97,** 2940–2945.

Kovtun, Y., Chiu, W.L., Zeng, W., and Sheen, J. (1998). Suppression of auxin signal transduction by a MAPK cascade in higher plants. Nature **395,** 716–720.

Kumar, D., and Klessig, D.F. (2000). Differential induction of tobacco MAP kinases by the defense signals nitric oxide, salicylic acid, ethylene, and jasmonic acid. Mol. Plant-Microbe Interact. **13,** 347–351.

Linford, N.J., Yang, Y., Cook, D.G., and Dorsa, D.M. (2001). Neuronal apoptosis resulting from high doses of the isoflavone genistein: Role for calcium and p42/44 mitogen-activated protein kinase. J. Pharmacol. Exp. Ther. **299,** 67–75.

Meskiene, I., Bogre, L., Glase, W., Balog, J., Brandstotter, M., Zwerger, K., Ammerer, G., and Hirt, H. (1998). MP2C, a plant protein phosphatase 2C, functions as a negative regulator of mitogen-activated protein kinase pathways in yeast and plants. Proc. Natl. Acad. Sci. USA **95,** 1938–1943.

Mikolajczyk, M., Awotunde, O.S., Muszynska, G., Klessig, D.F., and Dobrowolska, G. (2000). Osmotic stress induces rapid activation of a salicylic acid-induced protein kinase and a homolog of protein kinase ASK1 in tobacco cells. Plant Cell **12,** 165–178.

Miles, G.P., Samuel, M.A., and Ellis, B.E. (2002). Suramin inhibits oxidant-induced MAPK signalling in plants. Plant Cell Environ. **25,** 521–527.

Mittler, R., Herr, E.H., Orvar, B.L., van Camp, W., Willekens, H., Inze, D., and Ellis, B.E. (1999). Transgenic tobacco plants with reduced capability to detoxify reactive oxygen intermediates are hyperresponsive to pathogen infection. Proc. Natl. Acad. Sci. USA **96,** 14165–14170.

Murashige, T., and Skoog, F. (1962). A revised medium for rapid growth and bioassays with tobacco tissue culture. Physiol. Plant. **15,** 473–497.

Nishihama, R., Ishikawa, M., Araki, S., Soyano, T., Asada, T., and Machida, Y. (2001). The NPK1 mitogen-activated protein kinase kinase kinase is a regulator of cell-plate formation in plant cytokinesis. Genes Dev. **15,** 352–363.

Nühse, T.S., Peck, S.C., Hirt, H., and Boller, T. (2000). Microbial elicitors induce activation and dual phosphorylation of the *Arabidopsis thaliana* MAPK 6. J. Biol. Chem. **17,** 7521–7526.

Orozco-Cardenas, M., Narvaez-Vasquez, J., and Ryan, C. (2001). Hydrogen peroxide acts as a second messenger for the induction of defense genes in tomato plants in response to wounding, systemin, and methyl jasmonate. Plant Cell **13,** 179–191.

Orvar, B.L., and Ellis, B.E. (1997). Transgenic tobacco plants expressing antisense RNA for cytosolic ascorbate peroxidase show increased susceptibility to ozone injury. Plant J. **11,** 1297–1305.

Overmyer, K., Tuominen, H., Kettunen, R., Betz, C., Langebartels, C., Sandermann, H., Jr., and Kangasjärvi, J. (2000). Ozone-sensitive Arabidopsis *rcd1* mutant reveals opposite roles for ethylene and jasmonate signaling pathways in regulating superoxide-dependent cell death. Plant Cell **12,** 1849–1862.

Rao, M.V., Lee, H., Creelman, R.A., Mullet, J.E., and Davis, K.R. (2000). Jasmonic acid signaling modulates ozone-induced hypersensitive cell death. Plant Cell **12,** 1633–1646.

Ren, D., Yang, H., and Zhang, S. (2002). Cell death mediated by MAPK is associated with hydrogen peroxide production in Arabidopsis. J. Biol. Chem. **277,** 559–565.

Richberg, M.H., Aviv, D.H., and Dangl, J.L. (1998). Dead cells do tell tales. Curr. Opin. Plant Biol. **1,** 480–485.

Romeis, T., Piedras, P., Zhang, S., Klessig, D.F., Hirt, H., and Jones, J. (1999). Rapid Avr9- and Cf-9-dependent activation of MAP kinases in tobacco cell cultures and leaves: Convergence of resistance gene, elicitor, wound, and salicylate responses. Plant Cell **11,** 273–287.

Samuel, M.A., Miles, G.P., and Ellis, B.E. (2000). Ozone treatment rapidly activates MAP kinase signalling in plants. Plant J. **22,** 367–376.

Schraudner, M., Ernst, D., Langebartels, C., and Sandermann, H. (1992). Biochemical responses to ozone. III. Activation of the defense-related proteins β-1,3-glucanase and chitinase in tobacco leaves. Plant Physiol. **99,** 1321–1328.

Seo, S., Okamoto, M., Seto, H., Ishizuka, K., Sano, H., and Ohashi, Y. (1995). Tobacco MAP kinase: A possible mediator in wound signal transduction pathways. Science **270,** 1988–1992.

Seo, S., Sano, H., and Ohashi, Y. (1999). Jamonate-based wound signal transduction requires activation of WIPK, a tobacco mitogen-activated protein kinase. Plant Cell **11,** 289–298.

Sharma, Y.K., and Davis, K.R. (1997). The effects of ozone on antioxidant responses in plants. Free Radical Biol. Med. **23,** 480–488.

Smith, N.A., Singh, S.P., Wang, M.B., Stoutjesdijk, P.A., Green, A.G., and Waterhouse, P.M. (2000). Total silencing by intron-spliced hairpin RNAs. Nature **407,** 319–320.

Stanciu, M., Wang, Y., Kentor, R., Burke, N., Watkins, S., Kress, G., Reynolds, I., Klann, E., Angiolieri, M.R., Johnson, J.W., and DeFranco, D.B. (2000). Persistent activation of ERK contributes to glutamate-induced oxidative toxicity in a neuronal cell line and primary cortical neuron cultures. J. Biol. Chem. **275,** 12200–12206.

Suzuki, K., Yano, A., and Shinshi, H. (1999). Slow and prolonged activation of the p47 protein kinase during hypersensitive cell

death in a culture of tobacco cells. Plant Physiol. **119,** 1465–1472.

Torres, M.A., Dangl, J.L., and Jones, J.D.G. (2002). Arabidopsis gp91^{phox} homologues *AtrbohD* and *AtrbohF* are required for accumulation of reactive oxygen intermediates in the plant defense response. Proc. Natl. Acad. Sci. USA **99,** 517–522.

Tuomainen, J., Betz, C., Kangasjärvi, J., Ernst, D., Yin, Z., Langebartels, C., and Sandermann, H. (1997). Ozone induction of ethylene emission in tomato plants: Regulation by differential transcript accumulation for the biosynthetic enzymes. Plant J. **12,** 1151–1162.

Ulm, R., Revenkova, E., di Sansebastiano, G.P., Bechtold, N., and Paszkowski, J. (2001). Mitogen-activated protein kinase phosphatase is required for genotoxic stress relief in Arabidopsis. Genes Dev. **15,** 699–709.

Westermarck, J., Li, S.P., Kallunki, T., Han, J., and Kahari, V.M. (2001). p38 mitogen-activated protein kinase-dependent activation of protein phosphatases 1 and 2A inhibits MEK1 and MEK2 activity and collagenase 1 (MMP-1) gene expression. Mol. Cell. Biol. **21,** 2373–2383.

Yang, K.Y., Liu, Y., and Zhang, S. (2001). Activation of a mitogen-activated protein kinase pathway is involved in disease resistance in tobacco. Proc. Natl. Acad. Sci. USA **98,** 741–746.

Yuasa, T., Ichimura, K., Mizoguchi, T., and Shinozaki, K. (2001). Oxidative stress activates ATMPK6, an Arabidopsis homologue of MAP kinase. Plant Cell Physiol. **42,** 1012–1016.

Zhang, S., and Klessig, D.F. (1997). Salicylic acid activates a 48-kD MAP kinase in tobacco. Plant Cell **9,** 809–824.

Zhang, S., and Klessig, D.F. (1998a). Resistance gene *N*-mediated *de novo* synthesis and activation of a tobacco mitogen-activated protein kinase by tobacco mosaic virus infection. Proc. Natl. Acad. Sci. USA **95,** 7433–7438.

Zhang, S., and Klessig, D.F. (1998b). The tobacco wounding-activated mitogen-activated protein kinase is encoded by SIPK. Proc. Natl. Acad. Sci. USA **95,** 7225–7230.

Zhang, S., and Liu, Y. (2001). Activation of salicylic acid-induced protein kinase, a mitogen-activated protein kinase, induces multiple defense responses in tobacco. Plant Cell **13,** 1877–1889.

Zhang, S., Liu, Y., and Klessig, D.F. (2000). Multiple levels of tobacco WIPK activation during the induction of cell death by fungal elicitins. Plant J. **23,** 339–347.

Exhibit 6

The Plant Cell, Vol. 16, 2614–2628, October 2004, www.plantcell.org © 2004 American Society of Plant Biologists

A Classical Arabinogalactan Protein Is Essential for the Initiation of Female Gametogenesis in Arabidopsis

Gerardo Acosta-García and Jean-Philippe Vielle-Calzada[1]

Laboratory of Reproductive Development and Apomixis, Department of Genetic Engineering, Centro de Investigación y Estudios Avanzados, Unidad Irapuato, Irapuato Guanajuato, Mexico

Classical arabinogalactan proteins (AGPs) are an abundant class of cell surface proteoglycans widely distributed in flowering plants. We have used a combination of enhancer detection tagging and RNA interference (RNAi)–induced posttrancriptional silencing to demonstrate that *AGP18*, a gene encoding a classical arabinogalactan protein, is essential for female gametogenesis in *Arabidopsis thaliana*. *AGP18* is expressed in cells that spatially and temporally define the sporophytic to gametophytic transition and during early stages of seed development. More than 75% of the T1 transformants resulted in T2 lines showing reduced seed set during at least three consecutive generations but no additional developmental defects. *AGP18*-silenced T2 lines showed reduced *AGP18* transcript levels in female reproductive organs, the presence of 21-bp RNA fragments specific to the *AGP18* gene, and the absence of in situ *AGP18* mRNA localization in developing ovules. Reciprocal crosses to wild-type plants indicate that the defect is female specific. The genetic and molecular analysis of *AGP18*-silenced plants containing a single T-DNA RNAi insertion suggests that posttranscriptional silencing of *AGP18* is acting both at the sporophytic and gametophytic levels. A cytological analysis of all defective *AGP18*-RNAi lines, combined with the analysis of molecular markers acting at key stages of female gametogenesis, showed that the functional megaspore fails to enlarge and mitotically divide, indicating that *AGP18* is essential to initiate female gametogenesis in Arabidopsis. Our results assign a specific function in plant development to a gene encoding a classical AGP.

INTRODUCTION

The life cycle of flowering plants consists of a diploid sporophytic phase and two morphologically different haploid gametophytic phases taking place in specialized reproductive organs. Distinct types of meiotically derived cells give rise to the male and female gametophytic phases. In the anther, many microsporocytes develop into pollen grains, which harbor the sperm cells and represent the male gametophyte. In the ovule, usually a single sporophytic cell (the megaspore mother cell [MMC]) undergoes meiosis and gives rise to four haploid products (the megaspores) during a process referred to as megasporogenesis. While three of the megaspores undergo programmed cell death, a single functional megaspore enlarges and gives rise to the female gametophyte (or megagametophyte). In *Arabidopsis thaliana*, female gametogenesis initiates when the single functional megaspore divides mitotically to form an eight-nucleate syncitium. Subsequent cellularization partitions the eight nuclei into seven cells: an egg cell and two synergids at the distal (or micropylar) pole of the female gametophyte, three antipodals at the proximal (or chalazal) pole, and a binucleated central cell whose nuclei fuse before fertilization. This type of development and organization of the female gametophyte defines the Polygonum type that prevails in >70% of the species examined (Maheshwari, 1950; Willemse and van Went, 1984; Reiser and Fischer, 1993; Drews and Yadegari, 2002). Whereas the fusion of a sperm with the egg cell forms a zygote that subsequently develops into an embryo, fertilization of the binucleated central cell eventually gives rise to the endosperm, a triploid tissue essential for seed viability.

Little is known about the genetic basis and molecular mechanisms that regulate the initiation of female gametogenesis in the ovule. A large collection of both sporophytic and gametophytic mutants defective in female gametophyte development has been identified in Arabidopsis (Schneitz et al., 1997; Christensen et al., 1998; Howden et al., 1998; Grini et al., 1999; Drews and Yadegari, 2002). Whereas sporophytic mutations act at the diploid level and are inherited in a Mendelian 3:1 ratio, gametophytic mutants are poorly transmitted through either one or both types of gametes and exhibit distorted segregation patterns. Many mutants that disrupt meiosis have been isolated (Klimyuk and Jones, 1997; Siddiqi et al., 2000; Yang and Sundaresan, 2000; Reddy et al., 2003), but little is known about other developmental aspects of megasporogenesis. To date, *SPOROCYTELESS* (*SPO*)/*NOZZLE* is the only gene shown to be required for the initiation of microsporogenesis and megasporogenesis (Schiefthaler et al., 1999; Yang et al., 1999). *SPO* encodes a nuclear protein related to MADS box transcription factors that is expressed during early anther and ovule development. In plants homozygous for *hadad* (*hdd*) and *prolifera* (*prl*), female gametophyte development is arrested at either the two-nucleate or the four-nucleate stage, respectively. Whereas the

[1] To whom correspondence should be addressed. E-mail vielle@ira.cinvestav.mx; fax 52-462-624-58-49.

The author responsible for distribution of materials integral to the findings presented in this article in accordance with the policy described in the Instructions for Authors (www.plantcell.org) is: Jean-Philippe Vielle-Calzada (vielle@ira.cinvestav.mx).

Article, publication date, and citation information can be found at www.plantcell.org/cgi/doi/10.1105/tpc.104.024588.

gene responsible for the mutation in *hdd* has yet to be identified (Moore et al., 1997), *PRL* encodes a Mcm7-like licensing factor essential for DNA replication (Springer et al., 1995). Two insertional alleles in *CYTOKININ-INDEPENDENT 1*, a gene encoding a putative Arabidopsis His kinase, were shown to cause nuclear degeneration in the female gametophyte as early as the four-nucleate stage (Christensen et al., 1998; Pischke et al., 2002). Recently, the *NOMEGA* gene was shown to be required for cell cycle progression beyond the two-nucleate stage; *NOMEGA* encodes a putative APC6/CDC16 component of the anaphase promoting complex in Arabidopsis (Kwee and Sundaresan, 2003). Several additional gametophytic mutants that fail to progress beyond the one-nucleate haploid stage have been identified (Christensen et al., 1998), but the corresponding genes have yet to be isolated and characterized.

Numerous studies showing that modifications of plant growth conditions can alter the sporophyte to gametophyte transition (Bell, 1989) or even the whole plant reproductive outcome (Knox, 1967) indicate that the presence of molecular signals that determine the fate of competent cells is fundamental for switching from a sporophytic into a gametophytic developmental pathway. Several regulatory proteins have been shown to have important functions in cell signaling and recognition during plant development. Arabinogalactan proteins (AGPs) are an abundant and heterogeneous class of highly glycosylated Hyp-rich glycoproteins widely distributed in the plant kingdom (Fincher et al., 1974; Clarke et al., 1979; Kreuger and van Holst, 1996; Sommer-Knudsen et al., 1998; Gaspar et al., 2001; Showalter, 2001). The recent characterization of genes encoding different AGP backbones in several species gave rise to the current distinction between classical and nonclassical AGPs (Chen et al., 1994; Du et al., 1994; Mau et al., 1995; Knox, 1999). Classical AGPs contain a domain responsible for attaching the protein backbone to a glycosylphosphotidylinositol (GPI) membrane anchor (Schultz et al., 1998; Youl et al., 1998; Sherrier et al., 1999; Schindelman et al., 2001; Borner et al., 2002; Sun et al., 2004). By contrast, nonclassical AGPs lack the GPI anchor signal and are soluble components of the extracellular matrix often containing Asn- or Hyp-rich domains (Majewska-Sawka and Nothnagel, 2000; Schultz et al., 2000; Gaspar et al., 2001). Molecular and biochemical evidence indicates that AGPs have specific functions during root formation (Willats and Knox, 1996; Casero et al., 1998; van Hengel and Roberts, 2002), the promotion of somatic embryogenesis (Serpe and Nothnagel, 1994; Kreuger and van Holst, 1993, 1996; van Hengel et al., 2001; van Hengel and Roberts, 2002), or the attraction of pollen tubes in the style (Du et al., 1994; Cheung et al., 1995; Wu et al., 1995; Jauh and Lord, 1996; Roy et al., 1998). The use of monoclonal antibodies directed against carbohydrate epitopes provided evidence suggesting that AGPs play an important role during the alternation between sporophytic and gametophytic transitions in the ovule (Pennell and Roberts, 1990; Pennell et al., 1991; McCabe et al., 1997). Although these studies elegantly showed that the establishment of a female reproductive lineage is associated with changes in the distribution of AGP epitopes (Pennell et al., 1992), they did not identify a specific AGP protein or the corresponding gene acting during ovule development or early embryo formation. A few mutations altering the activity of specific genes encoding AGPs in Arabidopsis have been described. Homozygous plants for *resistant to agrobacterium transformation 1* are resistant to root-dependent transformation via *Agrobacterium tumefaciens* (Nam et al., 1999); however, mutant plants are phenotypically indistinguishable from the wild type, and no developmental defects associated with the mutation have been described. The mutation is caused by a T-DNA insertion within the promoter region of the Arabidopsis *AGP17* gene (Gaspar et al., 2001). A second insertional mutant in a gene encoding a nonclassical AGP (*AGP30*) has recently been shown to be involved in root regeneration and seed germination (van Hengel and Roberts, 2003). Recently, hybrid-type proteoglycans having properties of both AGPs and lipid-transfer proteins have been shown to be essential for the differentiation of tracheary elements in *Zinnia elegans* and Arabidopsis (Motose et al., 2004).

In this study, we report the enhancer detection-based identification of *AGP18*, a classical *AGP* gene that specifically acts during female gametophyte development in Arabidopsis. To determine the function of *AGP18*, we introduced double-stranded RNA in wild-type plants and specifically degraded the endogenous *AGP18* transcript by RNA interference (RNAi). More than 75% of the primary transformants resulted in lines showing reduced seed set but no additional developmental abnormalities. Reciprocal crosses to wild-type plants suggested that the defect is female specific. The genetic and molecular analysis of a line containing a single T-DNA RNAi insertion suggests that posttranscriptional silencing of *AGP18* is acting both at the sporophytic and gametophytic levels. The cytological analysis of all defective *AGP18*-RNAi lines indicates that *AGP18* is essential to initiate female gametogenesis in Arabidopsis. Our results assign a specific function in plant development to a gene encoding a classical AGP.

RESULTS

Enhancer Detection Tagging of *AGP18*

Using the system established by Sundaresan et al. (1995), we have generated a *Ds* enhancer detector and a gene trap population to identify patterns of expression associated with genes acting during female gametophyte development in Arabidopsis. The enhancer detection vector relies on a maize (*Zea mays*) *Ds* transposon carrying a β-glucoronidase reporter gene (*uidA* or *GUS*) under the control of a minimal promoter. Such a reporter construct is not trapping genes but rather integrating into genomic sequences to serve as a detector of any given regulatory sequence that is acting as an enhancer of promoter activity at the specific location of the insertion (Bellen, 1999; Springer, 2000). The *Ds* enhancer detector element (DsE) also contains the neomycin phosphotransferase II (*NPTII*) gene (conferring resistance to kanamycin); *NPTII* acts as a selectable marker and facilitates the genetic analysis of segregating enhancer detector or gene trap lines.

Whole-mount staining and clearing procedures allow screening for reporter gene expression (GUS) at different developmental stages encompassing megasporogenesis and female gametogenesis, from the time when the ovule primordium has just started its elongation (before MMC differentiation) to stages

where the female gametophyte is fully differentiated (J.-P. Vielle-Calzada and U. Grossniklaus, unpublished results; Vielle-Calzada et al., 2000). Figure 1 shows the pattern of GUS expression identified in MET333. MET333 shows initial GUS expression in the chalazal region of the four-nucleate female gametophyte (Figure 1A). At the eight-nucleate stage, expression is restricted to the young antipodal cells and the cellularizing egg apparatus (Figure 1B). At maturity, the female gametophyte shows GUS expression in the synergids, the egg cell, and the antipodals but not in the central cell (Figure 1C). This pattern of expression persists after fertilization (Figure 1D); however, GUS is also expressed in the free nuclear endosperm after fertilization of the central cell (Figure 1D). During early seed development, GUS is expressed in the embryo proper, the suspensor, and the chalazal endosperm (Figure 1E). Interestingly, MET333 also shows GUS expression in cytoplasmic domains closely associated with the vegetative nucleus of mature pollen grains and in pollen tubes (Figure 1F) but not in microsporocytes at earlier stages of development. A detailed analysis of MET333 plants homozygous for kanamycin resistance did not reveal a mutant phenotype at any stage of plant reproductive development.

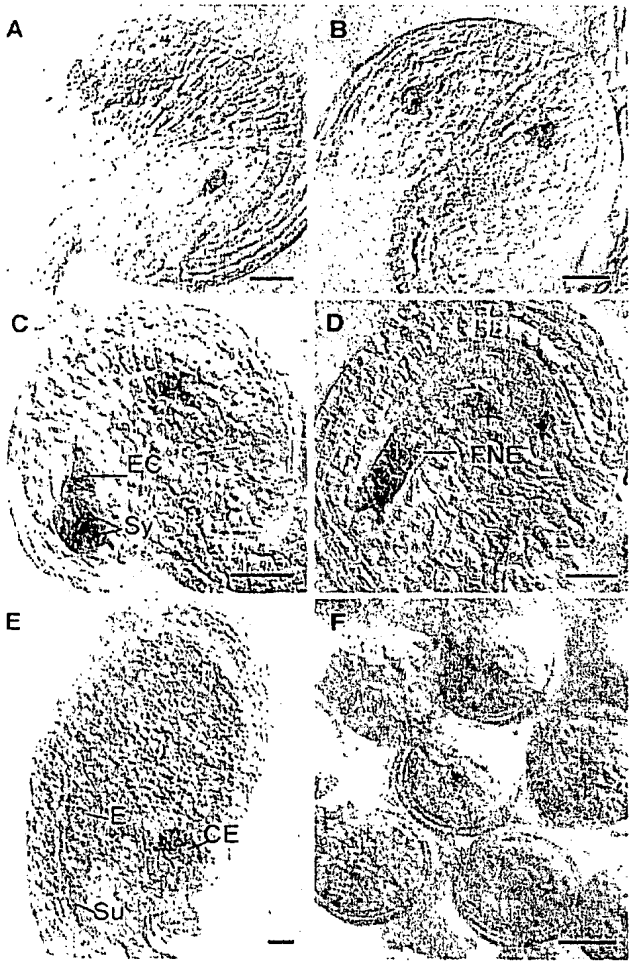

Figure 1. Pattern of GUS Expression in the Enhancer Detector Line MET333.

(A) Female gametophyte at four-nucleate stage.
(B) Cellularized female gametophyte.
(C) Mature female gametophyte before fertilization.
(D) Female gametophyte after fertilization.
(E) Embryo at four-cell stage.
(F) Mature pollen with GUS expression associated with the vegetative nucleus.
Sy, synergids; EC, egg cell; E, embryo; FNE, free nuclear endosperm; Su, suspensor; CE, chalazal endosperm. Bars in (A) to (E) = 20 μm; bar in (F) = 10 μm.

DNA gel blot analysis using a DsE-specific probe that includes a portion of *NPTII* showed that two copies of the DsE element were present in MET333 heterozygotes but were absent from wild-type siblings in which GUS expression was not detected (data not shown). Genomic sequences flanking both DsE elements were rescued using thermal asymmetric interlaced PCR (Liu et al., 1995). Sequence analysis of the PCR products showed that the DsE elements were inserted 254 and 995 bp upstream of the transcription initiation site of *AGP18* (At4g37450). Figure 2A illustrates the molecular structure of *AGP18* and the localization of both DsE insertion sites. *AGP18* encodes a classical AGP containing a C-terminal domain responsible for anchoring the protein to GPI. In animals, GPI anchors have been shown to provide an alternative to transmembrane proteins for anchoring proteins to components of the cell surface (Takos et al., 1997, 2000; Schultz et al., 1998; Svetek et al., 1999; Borner et al., 2002; Sharma et al., 2004). Additionally, AGP18 contains an N-terminal secretory signal predicted to direct the secretion of the protein via the endoplasmic reticulum, two Pro-rich domains that are possible targets of glycosylation (Tan et al., 2003), and a Lys-rich domain predicted to interact with negatively charged molecules (Figure 2B; Gilson et al., 2001; Schultz et al., 2002). The Lys-rich domain is present in only 3 of 15 classical AGPs found to be encoded in the genome of Arabidopsis (Schultz et al., 2002). RT-PCR analysis revealed that the levels of *AGP18* transcription in MET333 are similar to the wild type, confirming that *AGP18* expression is not diminished by the presence of the DsE insertions (Figure 2C).

AGP18 Is Expressed in Adjacent Sporophytic and Gametophytic Cells

To determine if the pattern of GUS expression identified in MET333 reflected the pattern of expression of *AGP18*, we determined the localization of *AGP18* mRNA by in situ hybridization. To avoid the detection of mRNA corresponding to other *AGP* transcripts structurally resembling *AGP18*, sense and antisense digoxygenin-labeled probes were generated using a specific portion of the first exon that shows no homology with other *AGP* genes. The results are summarized in Figure 3. Detailed analysis of all aerial parts of Arabidopsis demonstrated that *AGP18* mRNA could be localized only in developing anthers and ovules and transiently in clusters of companion cells closely associated with vascular elements of the stem. *AGP18* is initially

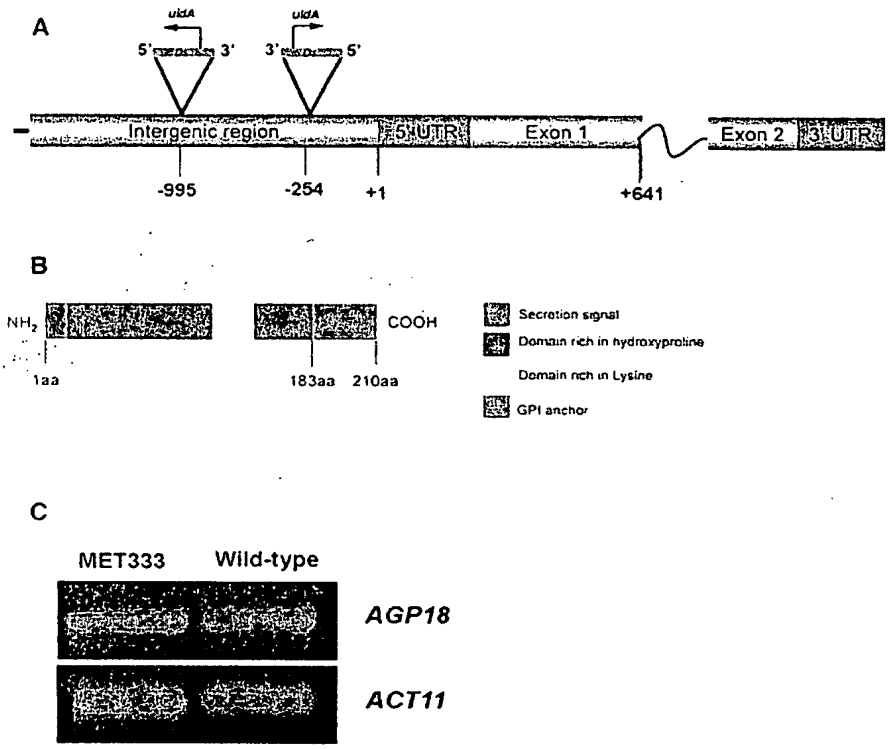

Figure 2. Genomic Structure and Protein Organization of AGP18.

The enhancer detector line MET333 has two DsE elements inserted in the 5′ regulatory region of *AGP18*.
(**A**) Genomic structure of *AGP18*. The arrows show the direction of transcription of *uidA* (GUS).
(**B**) Predicted protein structure of AGP18. aa, amino acids.
(**C**) RT-PCR analysis shows that the levels of transcription of *AGP18* are identical in MET333 and wild-type plants.

expressed in the MMC and the neighboring nucellar cells of the young ovule primordium (Figure 3A). *AGP18* expression persists in all four products of female meiosis (Figure 3B). At the end of megasporogenesis, when the three nonfunctional megaspores have already degenerated, AGP18 mRNA is abundant in the functional megaspore but also in the adjacent nucellar cells (Figure 3C). During female gametogenesis, *AGP18* is expressed in the developing female gametophyte (Figure 3D). At maturity, abundant *AGP18* mRNA can be detected in the synergids (Figure 3E), the egg cell, and the antipodals but not in the central cell. After fertilization, *AGP18* mRNA is present in the developing embryo as well as in the free nuclear endosperm (Figures 3F to 3H). Abundant levels of *AGP18* mRNA persist in the embryo until the late globular stage and subsequently start to decrease. No *AGP18* mRNA can be detected in seeds containing torpedo or cotyledonary embryos. In the anther, *AGP18* is expressed in the tapetum and the mature pollen grain (Figures 3K and 3L). These results indicate that GUS expression in MET333 overlaps with the localization of *AGP18* mRNA, confirming that DsE elements partially detect the expression of *AGP18*; however, the absence of GUS expression in MET333 sporophytic cells (the developing nucellus and the mature tapetum) suggests that additional regulatory elements driving the expression of *AGP18* are not detected by either DsE element.

Generation of *AGP18*-RNAi Plants and Analysis of RNA Levels

To determine the role of AGP18 in Arabidopsis, a 740-bp fragment of the *AGP18* cDNA was cloned into a pFGC5941 RNAi vector (Kerschen et al., 2004) in both sense and antisense orientations and used to transform wild-type Columbia plants. Figure 4A illustrates the RNAi construct that was used to conduct these experiments. pFGC5941 contains a 35S promoter of *Cauliflower mosaic virus* (CaMV35S) that drives the transcription of a partial *AGP18* sequence cloned in both sense and antisense orientations and separated by an intron of the chalcone synthase gene. After formation of hairpin RNA structures, the resulting double-stranded RNA transcripts can cause posttranscriptional silencing of endogenous gene activity (Waterhouse et al., 1998; Chuang and Meyerowitz, 2000; Smith et al., 2000). Although a detailed pattern of CaMV35S promoter activity during male and female gametogenesis has yet to be determined in Arabidopsis, we reasoned that *AGP18* transcripts localized in sporophytic

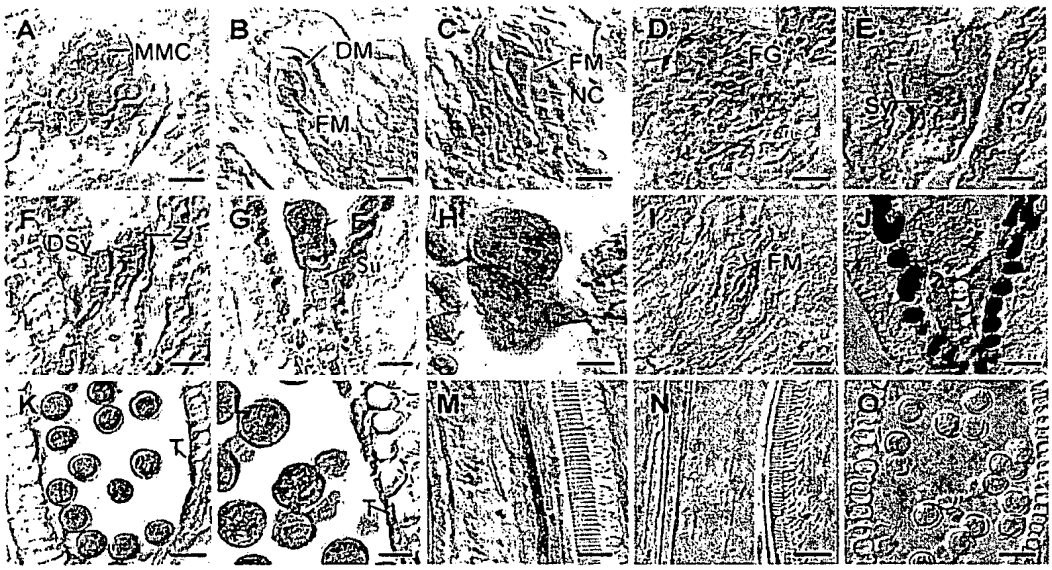

Figure 3. Localization of *AGP18* mRNA by in Situ Hybridization.

(A) MMC stage. Bar = 9 μm.
(B) Female meiosis stage. Bar = 8 μm.
(C) Functional megaspore stage with young nucellus. Bar = 8.5 μm.
(D) Two-nucleate stage female gametophyte. Bar = 14 μm.
(E) Mature female gametophyte. Bar = 8 μm.
(F) Zygote stage. Bar = 9μm.
(G) Embryo four-cell stage. Bar = 15 μm.
(H) Embryo at early globular stage. Bar = 11 μm.
(I) Functional megaspore and young nucellus, sense probe. Bar = 15 μm.
(J) Embryo at early globular stage, sense probe. Bar = 20 μm.
(K) Mature pollen. Bar = 24 μm.
(L) Anther showing the tapetum. Bar = 20 μm.
(M) Longitudinal section of a stem. Bar = 20 μm.
(N) Longitudinal section of a stem, sense probe. Bar = 20 μm.
(O) Mature pollen, sense probe. Bar = 20 μm.
(A) to **(H)** and **(K)** to **(M)** hybridizations with antisense probe; **(I)**, **(J)**, **(N)**, and **(O)** hybridizations with sense probe. NC, nucellar cells; FM, functional megaspore; DM, degenerating megaspores; Sy, synergids; DSy, degenerating synergid; FG, female gametophyte; Z, zygote; E, embryo; Su, suspensor; T, tapetum.

cells can be the target of RNAi-dependent silencing driven by CaMV35S. After floral-dipping transformation, 75 primary transformants were generated, none of which showed visible defects during vegetative growth, root development, or floral organogenesis; however, 58 out of 75 adult T1 transformants showed semisterility defects. All 58 transformants maintained a reduced fertility phenotype in the T2 generation. To determine a possible relationship between a decrease in *AGP18* transcript levels and the defective phenotype, RNA was extracted from developing gynoecia of *BASTA*-resistant *AGP18*-RNAi T2 lines and used for RNA gel blot analysis. The results are shown in Figure 4B, with actin as a constitutive control to show that equal amounts of RNA were used. Compared with wild-type plants, all 10 T2 lines tested showed a substantial decrease in the transcripts levels of *AGP18*. Among those lines, T2-12, T2-44, and T2-58 showed significantly >50% reduction in seed set, whereas T2-63 and T2-53 had a 27.4 and 49.8% reduction, respectively. No correlation was found between the level of *AGP18* expression determined by RNA gel blot analysis and the degree of sterility; this absence of correlation has been documented in previous studies showing that abnormal phenotypes induced by RNAi are not always associated with a detectable decrease in transcript levels (Kerschen et al., 2004; C. Napoly and R. Jorgensen, personal communication). The induction of posttrancriptional gene silencing has been shown to result in the production of 21- to 23-bp RNA fragments with a sequence identical to a portion of the silenced gene (Elbashir et al., 2000). To determine if the production of 21- to 23-bp RNA fragments could be associated with the degradation of the *AGP18* transcript, polyacrylamide gels were used to detect the presence of small RNA fragments corresponding to *AGP18*. As shown in Figure 4C, small RNAs corresponding to *AGP18* were detected in lines in which

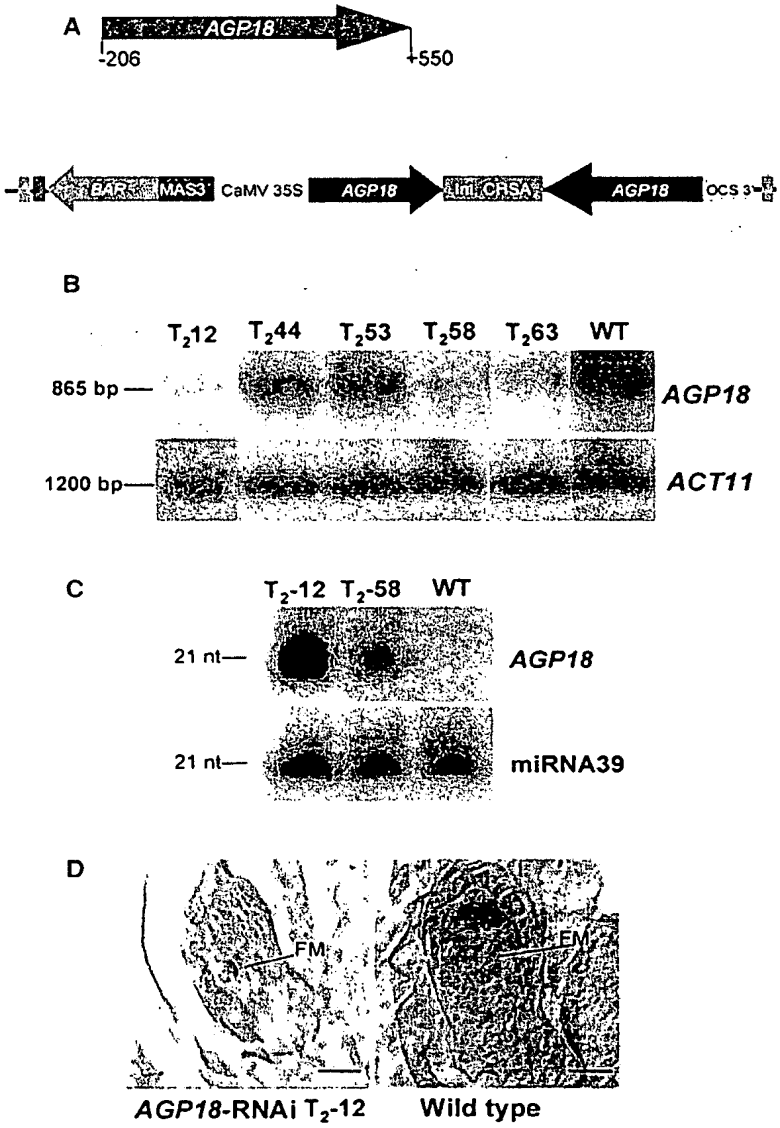

Figure 4. Accumulation of AGP18 Transcript, Presence of 21-bp Small RNAs, and Absence of *AGP18* Expression in the Gynoecium of *AGP18*-RNAi T2 Lines.

(A) Schematic diagram of the vector used to posttrancriptionally silence *AGP18*. The arrow indicates the sequence cloned in the RNAi silencing vector. Numbers indicate nucleotide positions with respect to initiation of the *AGP18* mRNA.

(B) Expression analysis of four *AGP18*-RNAi T2 lines and a wild-type control. RNA was isolated from mature gynoecia in both silenced and wild-type plants. A portion of the *AGP18* cDNA was used as a probe. RNA gel blots were subsequently rehybridized with a specific actin probe (*ACT11*) as a loading control.

(C) A polyacrylamide gel of 100 μg of low molecular weight RNA extracted from gynoecia of *AGP18*-RNAi T2 lines and wild-type plants was blotted and hybridized with a portion of the *AGP18* cDNA. The blot was rehybridized with a probe specific to the constitutively expressed microRNA 39 (miR39) as a control. nt, nucleotides.

(D) Localization of *AGP18* mRNA in developing ovules at the functional megaspore stage. In situ hybridization with specific *AGP18* digoxygenin-labeled antisense probes was performed on gynoecia of both silenced (*AGP18*-RNAi T2-12; bar = 8.5 μm) and wild-type plants (bar = 10 μm). FM, functional megaspore.

sufficient quantities of total RNA were available, including lines having strong fertility defects as T2-12 and T2-58 but not in wild-type plants. Finally, to determine if a decrease in transcript levels was associated with a decrease in *AGP18* expression within the ovule or the anther, we performed in situ hybridization in selected lines showing the lowest levels of *AGP18* transcript. As shown in Figure 4D, no *AGP18* mRNA could be detected in the young ovule at the functional megaspore stage of *AGP18*-RNAi transformants, indicating that the normal expression of *AGP18* during female gametogenesis is severely impaired in *AGP18*-RNAi lines.

Posttranscriptional Gene Silencing Is Specific to *AGP18*

Plant transformation with RNAi vectors targeting a conserved gene family has been shown to often result in simultaneous posttranscriptional gene silencing of several family members. In Arabidopsis, 16 genes are predicted to encode the protein backbones of classical AGPs (Schultz et al., 2000). *AGP17* and *AGP19* encode classical AGPs with 56 and 42% amino acid similarity to AGP18, respectively. All three proteins are the only Arabidopsis AGP members containing a Lys-rich domain. At the DNA level, *AGP17* and *AGP19* share 55 and 52% homology with *AGP18* in the 740-bp cDNA fragment that was used to generate the RNAi construct. To determine if the transcript levels of any of these two genes were also decreased in *AGP18*-RNAi lines, total RNA extracted from developing gynoecia of three T2 *AGP18*-RNAi lines showing decreased levels of *AGP18* mRNA accumulation were used to perform RT-PCR analysis. As shown in Figure 5, both *AGP17* and *AGP19* are expressed in the gynoecia of wild-type plants; however, none of the T2 *AGP18*-RNAi lines analyzed showed a significant decrease in either *AGP17* or *AGP19* expression. In lines T2-12 and T2-58, no amplification signal could be detected after blotting RT-PCR gels and hybridizing with the corresponding *AGP18* probe, confirming that in these lines *AGP18* expression is almost completely silenced. These results demonstrate that in *AGP18*-RNAi lines posttranscriptional gene silencing is specific to *AGP18*.

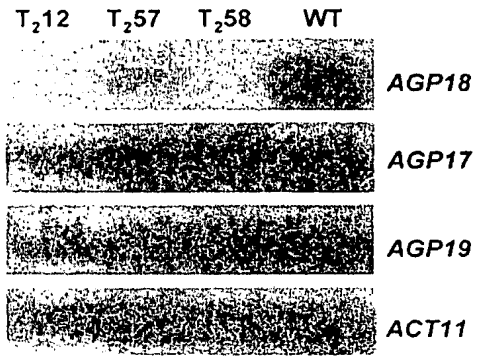

Figure 5. Posttranscriptional Gene Silencing Is Specific to *AGP18*.

RNA extracted from developing gynoecia of selected *AGP18*-RNAi T2 lines (T2-12, T2-57, and T2-58) was used for cDNA synthesis. PCR amplification was performed with primers specific to *AGP17*, *AGP18*, or *AGP19* (Schultz et al., 2002) using as a template samples corresponding to the same cDNA synthesis. Agarose gels were blotted on nitrocellulose membranes and probed with a corresponding *AGP* probe. Wild-type cDNA and amplification of *ACT11* were used as positive controls.

Ovule Abortion in *AGP18*-RNAi Lines Is Controlled at the Sporophytic and Gametophytic Levels

As shown in Figure 6A, the siliques of *AGP18*-RNAi T2 lines contain a variable number of aborted ovules that do not show signs of early seed formation. This defect can also be observed in the form of empty spaces within siliques of self-fertilized flowers from *AGP18*-RNAi plants. Gametophytic defects affecting the female gametophyte but not the male are expected to show a decrease in seed set of ~50%. As shown in Figure 6B, T2 lines showed a wide range of frequencies of ovule abortion, with >20% showing a frequency significantly >50% and four lines showing >70% of aborted ovules. To determine the nature of the reproductive defect found in RNAi lines, we conducted reciprocal crosses between lines showing >50% ovule abortion and wild-type plants. When T2 lines were used as female parents, the same percentage of ovule abortion was obtained for all lines tested (data not shown); however, in crosses where T2 lines were used as male parents, full fertility was recovered, suggesting that the sterility defect is female specific.

DNA gel blot analysis was used to determine that the number of RNAi T-DNA insertions present in the genome of T2 lines varied between 1 and 6 (data not shown). Because the T-DNA RNAi construct used is marked with a *BASTA* herbicide resistance marker, its segregation pattern can easily be followed in seedlings. We characterized the segregation of *BASTA* resistance in a group of *AGP18*-RNAi lines showing high levels of ovule abortion but different numbers of T-DNA insertions. A summary of these results are presented in Table 1. Interestingly, a single T-DNA RNAi insertion was present in the genome of T2-12, a line showing 74.9% of aborted ovules and the highest levels of *AGP18* silencing in female reproductive organs. As shown in Table 1, T2-12 segregated *BASTA*-resistant (*BASTA*^{r}) and *BASTA*-sensitive (*BASTA*^{s}) seedlings in a distorted ratio of 1:1 *BASTA*^{r}:*BASTA*^{s} ($\chi^2 = 2.41 < \chi^2_{0.05[1]} = 3.84$) as compared with 3:1 expected for normally transmitted insertions. In addition, no homozygous individuals have been identified in the T4 progeny resulting from self-pollination of 20 heterozygous T3-12 plants, suggesting that the transgene is poorly or not transmitted through the gametophytic phase of the Arabidopsis life cycle. The frequency of aborted ovules and the distorted segregation ratio in T2-12 suggests that posttranscriptional silencing of *AGP18* is affecting female reproductive development both at the sporophytic and gametophytic levels. In lines containing more than one T-DNA RNAi insertion, the number of *BASTA*^{r} seedlings is significantly increased, suggesting that not all insertions are abnormally transmitted through the gametophytic phase and that the degree of semisterility found in *AGP18*-RNAi lines is not directly proportional to the number of introduced T-DNA insertions. These results are in agreement with recent estimations of the efficiency of RNAi in transgenic plants (Kerschen et al., 2004).

To determine if fertility defects were consistently inherited, we quantified the sterility phenotype during the first three consecutive generations of four selected lines. As shown in

A

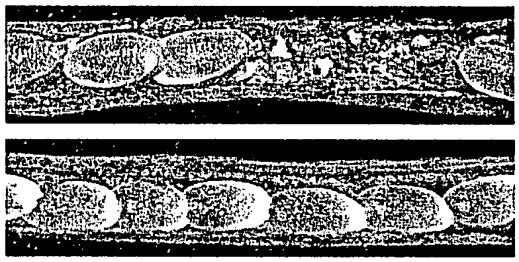

B

Frequency of ovule abortion in *AGP18* RNAi lines		
AGP18-RNAi lines analyzed	% aborted ovules	Selected lines
4 (5.33 %)	More than 70%	12, 58
12 (16 %)	40-69 %	44, 57
14 (18.6 %)	11-39%	63
27 (36 %)	6-11%	53
18 (24 %)	Less than 5 %	18

Figure 6. Siliques of *AGP18*-RNAi Lines Show Aborted Ovules.

(A) Micrographs of AGP18-RNAi and wild-type siliques. The asterisks indicate the aborted ovules observed in AGP18-RNAi lines.
(B) An average of 250 ovules was scored for each *AGP18*-RNAi line. A χ^2 statistical analysis showed that lines having >5% ovule abortion were significantly different from the wild type (2.5% ovule abortion).

Table 2, the percentage of aborted ovules is maintained in the T3 generation; however, a small decrease in the frequency of ovule abortion was observed in all lines evaluated. Statistical analysis of variance showed that this decrease is not statistically significant during the generations tested.

Female Gametophyte Development Is Defective in *AGP18*-RNAi Lines

To determine the cellular nature of the defect, whole-mounted cleared anthers and ovules were analyzed during male and female reproductive development. We initially determined the terminal phenotypes of all *AGP18*-RNAi lines by examining mature organs at developmental stages in which male and female gametogenesis have normally resumed and fully differentiated cellularized gametophytes are already formed. All 58 lines examined had a variable proportion of ovules showing a similar abnormal phenotype but no defects in pollen formation. Our observations are summarized in Figure 7. In the large majority of defective ovules, a single conspicuous cell with a centrally located nucleus was present in the nucellus. In all lines, the conspicuous cell did not show signs of degeneration, and the adjacent nucellar tissue was not reabsorbed; in rare cases, its nucleus was not observed. To determine the developmental stage at which female gametophyte development first departs from the wild type, we analyzed female gametogenesis at earlier developmental stages in ovules of line T2-12 (showing 74.9% of ovule abortion). All ovules of T2-12 undergo normal and synchronized megasporogenesis. Shortly after the differentiation of the functional megaspore (Figures 7A and 7E), a minority of ovules divide mitotically and give rise to two nuclei located at opposite ends of an enlarged cell showing a central vacuole. This type of ovule does not show differences with wild-type development (Figure 7B). By contrast, within the same gynoecium, the nucellus of the majority of ovules contains a single cell that closely resembles the differentiated functional megaspore but that shows no signs of subsequent enlargement or vacuolization (Figure 7F). At later stages of development, whereas some ovules undergo two additional divisions and form a normal female gametophyte identical to the wild type (Figure 7C), the majority contains a single cell that does not divide mitotically (Figures 7G and 7H). To determine if the frequency of aborted ovules scored in dissected siliques is similar to the frequency of ovules showing abnormal female gametophyte development, we quantified the number of ovules showing a single conspicuous cell in the nucellus of fully differentiated ovules. The results are shown in Table 3. For all lines examined, there is a close correlation between the two values, suggesting that defects in female gametophyte development are sufficient to explain the abnormal phenotype observed in *AGP18*-RNAi lines.

Table 1. Number of T-DNA Insertions, Segregation Analysis, and Percentage of Ovule Abortion in Selected T2 *AGP18*-RNAi Lines

Line	Number of Insertions	*BASTA*^{r}	*BASTA*^{s}	Ratio	Viable Ovules	Aborted Ovules	Percentage of Ovule Abortion
T2-12	1	127	153	1.0:1.2	62	185	74.90
T2-57	2	143	53	2.6:1.0	100	125	55.55
T2-58	2	186	15	12.4:1.0	67	167	71.36
T2-44	5	182	46	3.9:1.0	125	99	49.01

The Functional Megaspore Does Not Initiate Female Gametogenesis in *AGP18*-RNAi Ovules

To determine the identity of the cell that persists in the nucellus of defective ovules, we took advantage of additional enhancer detection and gene trap lines that show GUS expression in specific cells of the developing female gametophyte. Some of them represent ideal molecular markers to conduct crosses with *AGP18*-RNAi lines showing a high proportion of defective ovules. Figure 8 illustrates the pattern of GUS expression obtained in ovules of F1 plants resulting from crosses of line *AGP18*-RNAi T2-12 with individuals homozygous either for the ET499 or for the ET2209 enhancer detection element. In ET499, GUS is only expressed in the functional megaspore and not in the three dying megaspores or at earlier stages of megasporogenesis (Figures 8A to 8C; J.-P. Vielle-Calzada and U. Grossniklaus, unpublished results). This observation was confirmed in 100 whole-mounted and cleared ovules of homozygous ET499 plants. Other enhancer detection lines show GUS expression in the dying megaspores but not in the functional megaspore (Figure 8D), indicating that ET499 is an appropriate marker to characterize megaspores that have acquired a functional identity at the end of megasporogenesis. By constrast, ET2209 shows GUS expression at the onset of the second haploid mitotic division of the uncellularized female gametophyte and subsequently in all haploid differentiated cells: the synergids, the egg cell, the central cell, and the antipodals (Figure 8G; Vielle-Calzada et al., 2000). In defective *AGP18*-RNAi/+ ET499/+ F1 ovules, GUS expression is restricted to the conspicuous cell that persists in the nucellus after meiosis (Figures 8E and 8F), suggesting that in *AGP18*-RNAi lines female gametophyte development is arrested after the differentiation of the functional megaspore. By contrast, defective *AGP18*-RNAi/+ ET2209/+ F1 do not show GUS expression (Figure 8H), indicating that the arrested functional megaspore does not acquire the identity of a multinucleated female gametophyte or of any of the haploid gametophytic cells. These results indicate that defective *AGP18*-RNAi ovules fail to undergo haploid mitosis after differentiation of the functional megaspore.

Table 2. Inheritance of Ovule Abortion in *AGP18*-RNAi Lines

	Line			
Generation	12	44	57	58
T1	74.9% (247)	44.1% (224)	55.50% (225)	71.36% (234)
T2	73.2% (220)	45.2% (271)	54.90% (232)	74.00% (255)
T3	67.5% (234)	39.0% (230)	46.15% (244)	70.80% (222)

DISCUSSION

Here, we report the successful use of RNAi-induced posttranscriptional silencing to inactivate the *AGP18* gene and show that it plays an essential role during the initiation of female gametogenesis in Arabidopsis. *AGP18* encodes a classical AGP shown to be expressed in cells that spatially and temporally defines the sporophytic to gametophytic transition, but also during early stages of embryogenesis. More than 77% of independent transgenic Arabidopsis lines expressing the *AGP18*-RNAi construct showed moderate to severe fertility defects reminiscent of semisterile gametophytic mutants in Arabidopsis. Although in other experiments RNAi-dependent silencing is not always associated with mRNA turnover (Kerschen et al., 2004), all lines tested showed a decrease in *AGP18* transcript accumulation during female reproductive development in the T2 generation. In at least three lines, *AGP18* expression was almost completely suppressed. T2 lines with fertility defects showed ovules impaired in female gametogenesis but normal male gametophytic development and pollen formation. The use of molecular markers expressed at key stages of female gametogenesis determined that in defective ovules meiosis gives rise to a differentiated functional megaspore that is unable to give rise to a two-nucleate female gametophyte.

In plants developing a female gametophyte of the Polygonum type, megasporogenesis ends with the initiation of the haploid phase of the life cycle during the mitotic division of the functional megaspore nucleus (Huang and Russell, 1992). Although little is known about cellular communication during early ovule development, the interaction between sporophytic and gametophytic tissues has been suggested to be essential for female gametogenesis. For example, the isolation of the meiotic precursors and young tetrads by the accumulation of callosic walls has been interpreted as an interfacial reaction leading to the necessary separation of the two generations and the consequent protection of the haploid phase in ferns, mosses, and flowering plants (Dickinson, 1994; Bell, 1995). In Arabidopsis, the deposition of callose in dying meiotic products separates these cells from the functional megaspore (Webb and Gunning, 1990); however, the frequent formation of plasmodesmata connecting the functional megaspore to its adjacent nucellar cells indicates that cell-to-cell communication at the sporophytic–gametophytic transition is important during female gametophyte development (Bajon et al., 1999). In wild-type plants of Arabidopsis, several changes occur during the cytoplasmic maturation of the functional megaspore, including the polarized enlargement of the cell after the micropylar chalazal axis, the formation of a central vacuole, and the concomitant division of the nucleus (Webb and Gunning, 1990;

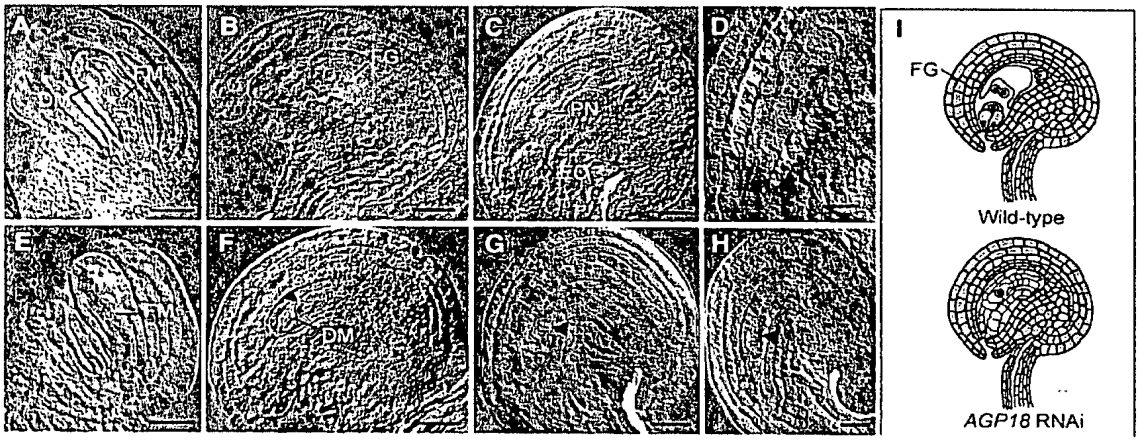

Figure 7. Female Gametophyte Development Is Defective in Ovules of *AGP18*-RNAi Lines.

Wild-type and *AGP18*-RNAi T2 gynoecia were fixed, cleared, whole mounted, and viewed under Nomarsky optics.
(A) to **(D)** Development of wild-type ovules.
(A) Functional megaspore in a developing ovule.
(B) Female gametophyte at the two-nucleate stage.
(C) Mature female gametophyte.
(D) Young embryo at the two-cellular stage.
(E) to **(H)** Development of *AGP18*-RNAi T2-12 defective ovules.
(E) Functional megaspore in the developing T2-12 ovule.
(F) Arrested cell in defective T2-12 mature ovule (arrowhead); normal ovules in the same gynoecium are at the two-nucleate stage.
(G) Arrested cell in defective T2-12 mature ovule (arrowhead); normal ovules in the same gynoecium contain a mature female gametophyte.
(H) Arrested cell in T2-12 mature ovule; normal ovules in the same gynoecium contain seeds undergoing early stages of embryogenesis.
(I) Schematic representation compares a mature wild-type ovule to a mature *AGP18*-RNAi T2-12 defective ovule.
FM, functional megaspore; DM, degenerating megaspore cells; EC, egg cell; AC, antipodal cells; FG, female gametophyte; PN, polar nuclei. Arrowheads indicate the presence of an arrested cell at the one-nucleate stage. Bars = 20 μm.

Grossniklaus and Schneitz, 1998; Schneitz, 1999). No signs of cell enlargement or initial vacuolization were detected in arrested functional megaspores of AGP18-RNAi plants. In combination with results from expression analysis of molecular markers acting at specific stages of development, these observations indicate that the function of *AGP18* is required after differentiation of the functional megaspore for the initiation of female gametogenesis.

Several interpretations of the functional activity of *AGP18* during ovule development can be proposed based on the analysis of heterozygous *AGP18*-RNAi lines containing a single T-DNA insertion. Although T2-12 shows a 1:1 segregation ratio of *BASTA*^{r} to *BASTA*^{s} seedlings expected for defective traits causing gametophytic lethality, it also shows >70% of arrested female gametophytes, indicating that the gametophytic activity of RNAi-mediated silencing of *AGP18* is not sufficient to explain the defective phenotype. As shown by in situ hybridization, *AGP18* is expressed in the MMC and the adjacent nucellar cells; therefore, it is possible that, to ensure the initiation of female gametogenesis, the activity of *AGP18* is required in both sporophytic as well as gametophytic cells. Differences on the degree of penetrance of the RNAi effect at the diploid and haploid levels could explain the variable but incomplete sterility shown by all *AGP18*-RNAi lines. Recent studies suggest that the maximal reduction of target transcript levels is obtained in RNAi lines containing a single T-DNA insertion (Kerschen et al., 2004). Although each target sequence is characterized by an inherent degree of susceptibility to RNAi-dependent silencing, a systematic study to assess the efficiency of posttranscriptional gene silencing in the gametophytic phase has not been conducted. Therefore, it is currently not possible to assess the effectiveness of *AGP18* silencing in the female gametophyte. A second possibility is that key RNA factors generated by RNAi-mediated *AGP18* silencing are produced at the diploid level and meiotically transmitted to a variable number of functional megaspores not carrying a T-DNA RNAi insertion; alternatively, these factors could be transported from adjacent nucellar cells to the functional megaspore via plasmodesmata. Although the transport of mRNA or proteins has not been reported in female meiotic products, detailed ultrastructural studies of megasporogenesis in Arabidopsis have shown that multiple plasmodesmata form between the functional megaspore and its adjacent nucellar cells (Bajon et al., 1999). Under this hypothesis, the function of *AGP18* could be strictly gametophytic; however, the non-fully penetrant effect of RNAi-mediated silencing factors generated at the diploid level would be responsible for the abortion of female gametophytes at a frequency significantly higher than 50%. A third alternative includes the possibility that gametophytic lethality in T2-12 results from differences in the degree of RNAi silencing mediated by the CaMV35S promoter. A potential lack

Table 3. Frequency of Ovules Showing an Arrested Cell Phenotype

AGP18-RNAi Line	Viable Ovules	Aborted Ovules	Ovules with Arrested Cells
T2-12	138 (27.7%)	185 (74.9%)	359 (72.23%)
T2-57	196 (43.3%)	125 (55.5%)	257 (56.73%)
Wild type	443 (99.4%)	6 (2.4%)	3 (0.60%)

of CaMV35S activity during microsporogenesis could partially explain the absence of pollen abnormalities associated with the expression of *AGP18* during anther development. To date, a detailed pattern of the CaMV35S promoter activity during male and female gametogenesis has yet to be reported in Arabidopsis. Although it is generally believed that this promoter is not active during the gametophytic phase (Bechtold et al., 2000), it is not clear at which developmental stage of the sporophytic to gametophytic transition its activity is no longer detected in either male or female gametes. Although this lack of quantitative information on the pattern of CaMV35S complicates the elucidation of the role played by *AGP18* during the alternation of diploid and haploid phases, experiments showing that RNAi factors transmitted during meiosis can trigger posttranscriptional silencing in the female gametophyte support the hypoythesis that the CaMV35S promoter can be used to successfully target gametophytically expressed genes (our unpublished results). The use of specific promoters to drive RNAi-mediated silencing exclusively in the gametophyte or in the nucellus should lead to the elucidation of the specific role of gametophytic and sporophytic *AGP18* activity during the initiation of female gametogenesis.

Classical AGPs play a role in mechanisms as distinct as cell division, cell expansion, or cell determination (Nothnagel, 1997; Schultz et al., 1998; van Hengel and Roberts, 2003). Monoclonal antibodies (MAbs) raised against AGP epitopes have been extensively used to investigate the cellular localization of AGPs (VandenBosch et al., 1989; Knox, 1992); however, these probes do not easily allow the elucidation of single AGP distribution patterns because they can recognize many different AGPs containing a conserved sugar epitope but different protein backbones. Elegant immunolocalization studies have shown that the establishment of a reproductive lineage in certain

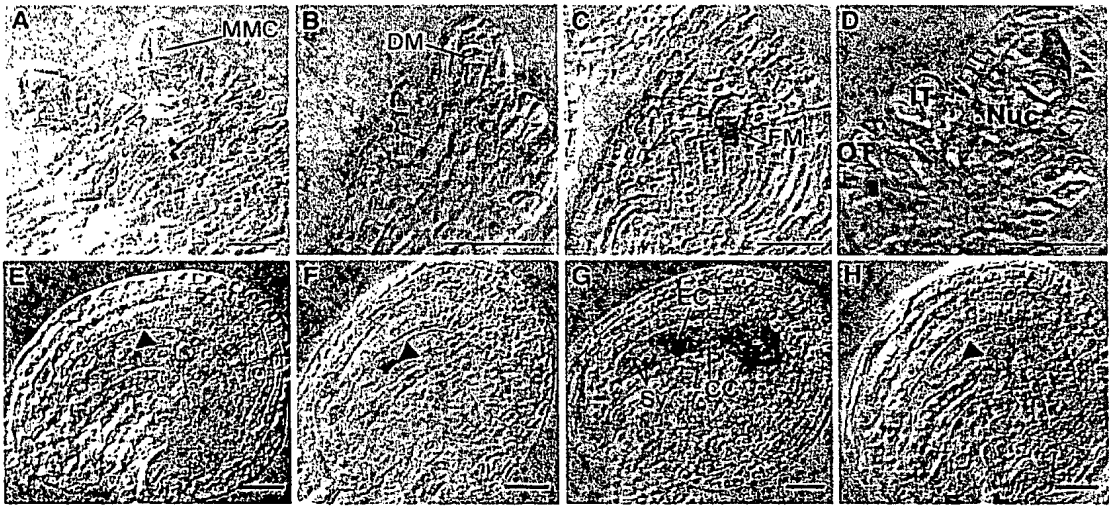

Figure 8. The Functional Megaspore Does Not Initiate Female Gametogenesis in *AGP18*-RNAi Ovules.

Ovules of F1 plants resulting from crosses of line *AGP18*-RNAi T2-12 with individuals homozygous either for the ET499 or for ET2209 were either fixed and whole-mount cleared or processed for histochemical localization of GUS activity. Shown are patterns of GUS expression in ET499 (**[A]** to **[C]**), ET4127 (**D**), F1 plants resulting from the cross of *AGP18*-RNAi T2-12 and homozygous ET499 plants (**[E]** and **[F]**), ET2209 (**G**), and F1 plants resulting from the cross of *AGP18*-RNAi T2-12 and homozygous ET2209 plants (**H**).

(A) Ovules of ET499 at MMC not showing GUS expression.

(B) Ovules of ET499 showing absence of expression in all three dying megaspores.

(C) Functional megaspore showing GUS expression in ET499.

(D) Ovule of ET4127 showing GUS expression in a dying megaspore.

(E) Whole-mounted cleared ovule showing the phenotype observed in defective *ET499;AGP18-RNAi T2-12* F1 ovules.

(F) GUS expression in the arrested functional megaspore of defective *ET499;AGP18-RNAi T2-12* F1 ovules. The arrowhead shows the position of the arrested functional megaspore.

(G) Pattern of GUS expression in the mature female gametophyte of ET2209.

(H) Absence of GUS expression in defective *ET2209;AGP18-RNAi T2-12* F1 ovules.

FM, functional megaspore; IT, inner integument; OT, outer integument; Nuc, nucellus; DM, dying megaspore; EC, egg cell; Sy, synergid cells; CC, central cell. The arrowheads indicate the arrested cells. Bars = 20 μm.

species was associated with changes in the distribution of AGP epitopes (Knox et al., 1989; Pennell et al., 1992). In *Pisum sativum*, the determination of reproductive cells in male and female gametes is associated with the loss of a cell surface arabinose-containing epitope recognized by the Mab MAC207 (Pennell and Roberts, 1990). Interestingly, a second AGP epitope recognized by MAb JIM8 became detectable only during differentiation of anthers and ovules in *Brassica napus* (Pennell et al., 1991). During ovule development, this epitope was initially detected in the wall of the two- to four-nucleate female gametophyte, in nucellar cells adjacent to the developing female gametophyte, and later in the plasma membrane of all cells forming the egg apparatus, but not the central cell. The presence of this epitope was also detected in the tapetum, in developing pollen grains, and in the stem vasculature (Pennell et al., 1991). Our results show that *AGP18* is expressed in reproductive tissues, particularly in cell types that are involved in establishing the sporophytic to gametophytic transitions. During female gametophyte development, *AGP18* is initially expressed in the MMC, in all four meiotically derived megaspores, the functional megaspore, and the adjacent nucellar cells. *AGP18* expression persists in all female gametophyte cells except the central cell. During male gametophytic development, *AGP18* is expressed in pollen grains and the cells of the tapetum. Developing seeds also express AGP18 during the first stages of embryogenesis; interestingly, abundant *AGP18* mRNA is detected at early stages of endosperm development, indicating that transcription in the central cell occurs only after double fertilization. We only detected additional *AGP18* expression in restricted clusters of companion cells present in the vasculature of the stem. The pattern of *AGP18* mRNA localization is almost identical to the pattern of localization of the epitope recognized by JIM8, strongly suggesting that an AGP encoded by a gene homologous to *AGP18* is detected by JIM8 in *B. napus*. The generation of AGP18-RNAi lines opens new possibilities for immunolocalization analysis with JIM8 and new antibodies raised against AGP18 to further elucidate the function and distribution of AGPs during reproductive development.

Our results indicate that *AGP18* plays a crucial role during interactions between sporophytic and gametophytic cells in the young ovule and that these interactions are essential for the establishment of the female gametophytic phase in Arabidopsis. Although the nature of this communication has yet to be characterized at the genetic and molecular levels, the elucidation of the developmental function of a gene encoding a classical AGP creates new perspectives for the understanding of cell surface signaling and the molecular mechanisms that regulate sexual reproduction in flowering plants.

METHODS

Plant Material and Growth Conditions

The transposant line MET333 (*Arabidopsis thaliana* Heynh. var Landsberg *erecta*) was identified in a collection of enhancer detector lines generated in our laboratory, using the system implemented by Sundaresan et al. (1995), looking for expression patterns during female gametophyte development. To select plants carrying the *Ds* transposon, 50 mg/L of kanamycin and 0.66 μg/mL of 1-naphtalenacetamide were added to MS solid medium (Sigma, St. Louis, MO). Resistant seedlings were transferred to soil and grown in a greenhouse under long-day conditions.

Generation of RNAi Lines

A 740-bp fragment containing the first exon and a region of 5′ untranslated region of *AGP18* was amplified by RT-PCR using RNA extracted from wild-type developing gynoecia using the following primers containing restriction sites as indicated in boldface: 5′-**AATCTAGAGGCGCGCC**ACGGCTACATCTGTCTGT-3′ (*Xba*I and *Asc*I; sense primer) and 5′-AA**GGATCCATTTAAAT**AATGTACCTGATCGTCGG-3′ (*Bam*HI and *Swa*I; antisense primer). The PCR fragment generated with the sense/antisense primer combination was cloned in pCRII TOPO (Invitrogen, Carlsbad, CA) and subsequently digested with *Swa*I and *Asc*I restriction enzymes. The resulting DNA fragment was cloned using appropriate restriction sites in the silencing vector pFGC5941 (kindly donated by Carolyn Napoli and Rich Jorgensen, www.chromdb.org). The PCR fragment cloned in pCRII TOPO was digested with *Xba*I and *Bam*HI (to obtain the antisense fragment) and cloned in appropriate restriction sites of pFGC5941. The resulting pFGC5941 vector contained *AGP18* in both sense and antisense orientations separated by a chalcone synthase intron and under the control of the CaMV35S promoter. Four-week-old Arabidopsis plants (Columbia-0) were transformed by floral dipping as previously described (Clough and Bent, 1998). Seeds from *Agrobacterium tumefaciens*–treated plants were selected and directly grown under greenhouse long-day conditions (16 h light). Resistant seedlings were selected by spraying the herbicide *BASTA* (50 mg/L; Finale; AgrRvo, Montvale, NJ) three times each week for 2 weeks. Presence of *AGP18*-RNAi insertions was confirmed by PCR amplification on DNA extracted from seedlings. Seeds from mature plants were collected and plated onto MS medium supplemented with glufosinate ammonium (10 μg/mL; Crescent Chemical, Augsburg, Germany).

RNA Analysis

For RNA gel blots, total RNA was extracted from developing gynoecia from selected *AGP18*-RNAi transformants and wild-type plants using Trizol (Invitrogen) and following the manufacturer's instructions. Fifty micrograms of RNA were separated in a 1.3% agarose gel containing 17% formaldehyde and blotted onto hybond N^+ membranes. Blots were hybridized with random-primed (Amersham Biosciences, Buckinghamshire, UK) ^{32}P-labeled 810-bp probe corresponding to the complete *AGP18* cDNA (At4g37450) and an *ACT11* (At3g12110) probe generated by PCR using the following primers: ACT11-S (5′-TTCAACACTCCTGCCATG-3′) and ACT11-AS (5′-TGCAAGGTCCAAACGCAG-3′). The temperature of hybridization was 65°C in Church's buffer.

For small RNA analysis, total RNA from developing gynoecia was enriched for low molecular weight RNAs using Hamilton's homogenization solution (Hamilton and Baulcombe, 1999) as described in Mette et al. (2000). Low molecular weight RNA was normalized by spectrophotometry to 100 μg/lane, separated by electrophoresis through 15% polyacrylamide, 7 M urea, 0.5× Tris-borate EDTA gel, and transferred to Zeta-Probe GT membranes (Bio-Rad, Hercules, CA). After transfer, membranes were cross-linked with 200 mJ of UV and baked at 80°C for 1 h. To detect small RNAs in *AGP18*-RNAi lines, an *AGP18* cDNA probe as described above was randomly labeled and hybridized at 62°C in Church's buffer. An oligonucleotide probe corresponding to the sequence of miR39 (5′- GATATTGGCGCGGCTCAAGCA-3′; Llave et al., 2002) was 5′-end labeled with [γ ^{32}P]ATP and hybridized as a loading control. For RT-PCR analysis, total RNA was isolated from developing gynoecia of wild-type and *AGP18*-RNAi lines using Trizol following the manufacturer's instructions. First-strand cDNA was synthesized using

2 μg of total RNA and Superscript II reverse transcriptase (Invitrogen). For semiquantitative RT-PCR, 3 μL of the first-strand cDNA reaction served as a template in a PCR reaction that used specific primers for *AGP18* (At4g37450), *AGP17* (At2g23130), *AGP19* (At1g68725), and *ACT11*. After estimating the amount of amplified DNA produced at different rounds of PCR cycles, we determined that 20 cycles ensured that the amplified product was proportional to the initial concentration of template present in the reaction. After electrophoresis on a 1% agarose gel and blotting into hybond N· membranes, hybridization was performed with ^{32}P cDNA probes specific to each *AGP* gene tested and labeled with the random primer method (Amersham Biosciences). Hybridization was performed at 62°C as described (Maniatis et al., 1989). *AGP17* primers were as follows: sense (5′-GCTTTTAAGCCCGCCTGCTCC-3′) and antisense (5′-CTGAATACAAAATGTGAGCTG-3′). *AGP19* primers were as follows: sense (5′-AAGTTGCACCAGTAATCAGCC-3′) and antisense (5′-TCCTTTAAGCTGATTTAAGGC-3′). *AGP18* primers were as follows: sense (5′-CACGCTTGGTTAAACTCC-3′) and antisense (5′-TTTTTTCATCACTGACAG-3′).

Whole-Mount Preparations and Histological Analysis

Wild-type and *AGP18*-RNAi siliques were dissected longitudinally with hypodermic needles (1-mL insulin syringes) and fixed with FAA buffer (50% ethanol, 5% acetic acid, and 10% formaldehyde), dehydrated in increasing ethanol concentration, cleared in Herr's solution (phenol: chloral hydrate:85% lactic acid:xylene:oil of clove [1:1:1:0.5:1]), and observed on a Leica microscope (Wetzlar, Germany) under Nomarski optics. GUS staining assays for stages before fertilization were conducted as described by Vielle-Calzada et al. (2000). For developmental stages after fertilization, we used the protocol described by Köhler et al. (2003) with slight modifications. Longitudinally dissected siliques were fixed for 2 h at −20°C in 90% acetone and subsequently immersed in GUS staining buffer (10 mM EDTA, 0.1% Triton, 0.5 mM $Fe^{2+}CN$, 0.5 mM $Fe^{3+}CN$, 100 μg m^{-1} chloranphenicol, and 1 mg mL^{-1} 5-bromo-4-chloro-3-indolyl-β-D-galactoside in 50 mM sodium phosphate buffer, pH 7.0) for 1 to 3 d at 37°C. The tissue was cleared in Hoyer's solution and observed under Nomarski optics.

In Situ Hybridization

Developing flower buds, developing flowers, isolated gynoecia, and siliques of wild-type and *AGP18*-RNAi T2-12 plants were fixed in 4% paraformaldehyde and embedded in Paraplast (Fisher Scientific, Fair Lawn, NJ). Sections of 12-μm thickness were cut using a Leica microtome and mounted on ProbeOnPlus slides (Fischer Biotech, Pittsburgh, PA). A fragment of 180 bp that included a portion of the first exon of *AGP18* was amplified using sense (5′-CGACGATCAGGTACATTAG-3′) and the antisense (5′-CATCACTGACAGATATGAA-3′) primers and subsequently cloned in the pCRII TOPO vector (Invitrogen). The resulting construct was digested with *Not*I and *Bam*HI to synthesize sense and antisense digoxygenin-labeled probes, respectively, and hybridization was conducted as described by Vielle-Calzada et al. (1999).

Sequence data from this article have been deposited with the EMBL/GenBank data libraries under accession number NM119909 (At4g37450).

ACKNOWLEDGMENTS

We thank Carolyn Napoli, Richard Jorgensen, and Ueli Grossniklaus for sharing materials before publication. We also thank Plinio Guzmán, Luis Herrera-Estrella, and Daphné Autran for critically reading the manuscript. We are grateful to past and current members of our laboratory for their help generating the Mexican MET/MGT transposon collection. Marcelina García-Aguilar and Andrés Estrada-Luna provided assistance with histological analysis; Santos García-Aguilar helped with plant handling. This work was supported by the Consejo Nacional de Ciencia y Tecnología (B-34324 and Z-029) and the Howard Hughes Medical Institute. G.A.G. is the recipient of a graduate scholarship from the Consejo Nacional de Ciencia y Tecnología. J.-P.V.C. is an International Scholar of the Howard Hughes Medical Institute.

Received May 27, 2004; accepted August 3, 2004.

REFERENCES

Bajon, C., Horlow, C., Motamayor, J.C., Sauvanet, A., and Robert, D. (1999). Megasporogenesis in *Arabidopsis thaliana* L.: An ultrastructural study. Sex. Plant Reprod. **12,** 99–109.

Bechtold, N., Jaudeau, B., Jolivet, S., Maba, B., Vezon, D., Voisin, R., and Pelletier, G. (2000). The maternal chromosome set is the target of the T-DNA in the in planta transformation of *Arabidopsis thaliana*. Genetics **155,** 1875–1887.

Bell, P.R. (1989). The alternation of generations. Adv. Bot. Res. **16,** 55–93.

Bell, P.R. (1995). Incompatibility in flowering plants: Adaptation of an ancient response. Plant Cell **7,** 5–16.

Bellen, H.J. (1999). Ten years of enhancer detection: Lessons from the fly. Plant Cell **11,** 2271–2282.

Borner, G.H.H., Sherrier, D.J., Stevens, T.J., Arkin, I.T., and Dupree, P. (2002). Prediction of glycosylphophatidylinositol-anchored proteins in Arabidopsis. A genomic analysis. Plant Physiol. **129,** 486–499.

Casero, P.J., Casimiro, I., and Knox, J.P. (1998). Occurrence of cell surface arabinogalactan-protein and extensin epitopes in relation to pericycle and vascular tissue development in the root apex of four species. Planta **204,** 252–259.

Chen, C.G., Pu, Z.Y., Moritz, R.L., Simpson, R.J., Bacic, A., Clarke, A.E., and Mau, S.L. (1994). Molecular cloning of a gene encoding for an arabinogalactan-protein from pear (*Pyrus communis*) cell suspension culture. Proc. Natl. Acad. Sci. USA **91,** 305–309.

Cheung, A.Y., Wang, H., and Wu, H.M. (1995). A floral transmitting tissue-specific glycoprotein attracts pollen tubes and stimulates their growth. Cell **82,** 383–393.

Christensen, C.A., Subramanian, S., and Drews, G.N. (1998). Identification of gametophytic mutations affecting female gametophyte development in Arabidopsis. Dev. Biol. **202,** 136–151.

Chuang, C.F., and Meyerowitz, E. (2000). Specific and heritable genetic interference by double-stranded RNA in *Arabidopsis thaliana*. Proc. Natl. Acad. Sci. USA **97,** 4985–4990.

Clarke, A.E., Anderson, R.L., and Stone, B.A. (1979). Form and function of arabinogalactans and arabinogalactan proteins. Phytochemistry **18,** 521–540.

Clough, S.J., and Bent, A.F. (1998). Floral dip: A simplified method for Agrobacterium-mediated transformation of *Arabidopsis thaliana*. Plant J. **16,** 735–743.

Dickinson, H.G. (1994). The regulation of alternation of generation in flowering plants. Biol. Rev. **69,** 419–422.

Drews, G.N., and Yadegari, R. (2002). Development and function of the angiosperm female gametophyte. Annu. Rev. Genet. **36,** 99–124.

Du, H., Simpson, R.J., Moritz, R.L., Clarke, A.E., and Bacic, A. (1994). Isolation of the protein backbone of an arabinogalactan-protein from the styles of *Nicotiana alata* and characterization of a corresponding cDNA. Plant Cell **6,** 1643–1653.

Elbashir, S.M., Lendeckel, W., and Tuschl, T. (2000). RNA interference is mediated by 21- and 22-nucleotide RNAs. Genes Dev. **15,** 188–200.

Fincher, G.B., Sawyer, W.H., and Stone, B.A. (1974). Chemical and physical properties of an arabinogalactan-peptide from wheat endosperm. Biochem. J. **139,** 535–545.

Gaspar, Y., Johnson, K., McKenna, J.A., Bacic, A., and Schultz, C. (2001). The complex structures of arabinogalactan-proteins and the journey towards understanding function. Plant Mol. Biol. **47,** 161–176.

Gilson, P., Gaspar, Y., Oxley, D., Youl, J.J., and Bacic, A. (2001). NaAGP4 is an arabinogalactan protein whose expression is suppressed by wounding and fungal infection in *Nicotiana alata*. Protoplasma **215,** 128–139.

Grini, P.E., Schnittger, A., Schwarz, H., Zimmermann, I., Schwab, B., Jurgens, G., and Hulskamp, M. (1999). Isolation of ethyl methanesulfonate-induced gametophytic mutants in *Arabidopsis thaliana* by a segregation distortion assay using the multimarker chromosome 1. Genetics **151,** 849–863.

Grossniklaus, U., and Schneitz, K. (1998). The molecular and genetic basis of ovule and megagametophyte development. Semin. Cell Dev. Biol. **9,** 227–238.

Hamilton, A.J., and Baulcombe, D.C. (1999). A species of small antisense RNA in posttranscriptional gene silencing in plants. Science **286,** 950–952.

Howden, R., Park, S.K., Moore, J.M., Orme, J., Grossniklaus, U., and Twell, D. (1998). Selection of T-DNA-tagged male and female gametophytic mutants by segregation distortion in Arabidopsis. Genetics **149,** 621–631.

Huang, B.Q., and Russell, S.D. (1992). Female germ unit: Organization, isolation and function. Int. Rev. Cytol. **140,** 233–293.

Jauh, G.Y., and Lord, E.M. (1996). Localization of pectins and arabinogalactan-proteins in lily (*Lilium longiflorum L.*) pollen tube and style, and their possible roles in pollination. Planta **199,** 251–261.

Kerschen, A., Napoli, C.A., Jorgensen, R.A., and Müller, A.E. (2004). Effectiveness of RNA interference in transgenic plants. FEBS Lett. **566,** 223–228.

Klimyuk, V.I., and Jones, J.D.G. (1997). *AtDMC1*, the Arabidopsis homologue of the yeast *DMC1* gene: Characterization, transposon-induced allelic variation and meiosis-associated expression. Plant J. **11,** 1–14.

Knox, J.P. (1992). Cell adhesion, cell separation and plant morphogenesis. Plant J. **2,** 137–141.

Knox, J.P. (1999). Intriguing, complex and everywhere: Getting to grips with arabinogalactan-proteins. Trends Plant Sci. **4,** 123–125.

Knox, J.P., Day, S., and Roberts, K. (1989). A set of cell surface glycoproteins forms an early marker of cell position, but not cell type, in the root apical meristem of *Daucus carota L.* Development **106,** 47–56.

Knox, R.B. (1967). Apomixis. Seasonal and population differences in a grass. Science **157,** 325–326.

Köhler, C., Hennig, L., Spillane, C., Pien, S., Gruissem, W., and Grossniklaus, U. (2003). The Polycomb-group protein MEDEA regulates seed development by controlling expression of the MADS-box gene *PHERES1*. Genes Dev. **17,** 1540–1553.

Kreuger, M., and van Holst, G.J. (1993). Arabinogalactan proteins are essential in somatic embryogenesis of *Daucus carota L.* Planta **189,** 243–248.

Kreuger, M., and van Holst, G.J. (1996). Arabinogalactan proteins and plant differentiation. Plant Mol. Biol. **30,** 1077–1086.

Kwee, H.S., and Sundaresan, V. (2003). The *NOMEGA* gene required for female gametophyte development encodes the putative APC6/CDC16 component of the Anaphase Promoting Complex in Arabidopsis. Plant J. **36,** 853–866.

Llave, C., Xie, Z., Kasschau, D.K., and Carrington, J.C. (2002). Cleavage of Scarecrow-like mRNA target directed by a class of Arabidopsis miRNA. Science **297,** 2053–2056.

Liu, Y.G., Mitsukawa, N., Oosumi, T., and Whittier, R.F. (1995). Efficient isolation and mapping of Arabidopsis thaliana T-DNA insert junctions by thermal asymmetric interlaced PCR. Plant J. **8,** 457–463.

Maheshwari, P. (1950). An Introduction to the Embryology of Angiosperms. (New York: McGraw-Hill).

Majewska-Sawka, A., and Nothnagel, E.A. (2000). The multiple roles of Arabinogalactan proteins in plant development. Plant Physiol. **122,** 3–9.

Maniatis, T., Fritsch, T., and Sambrook, J. (1989). Molecular Cloning: A Laboratory Manual. (Cold Spring Harbor, NY: Cold Spring Harbor Laboratory Press), pp. 7.37–7.39.

Mau, S.L., Chen, C.G., Pu, Z.Y., Moritz, R.L., Simpson, R.J., Bacic, A., and Clarke, A.E. (1995). Molecular cloning of cDNAs encoding the protein backbones of arabinogalactan proteins from the filtrate of suspension-cultured cells of *Pyrus communis* and *Nicotiana alata*. Plant J. **8,** 269–281.

McCabe, P.F., Valentine, T.A., Forsberg, L.S., and Pennell, R.I. (1997). Soluble signals from cells identified at the cell wall establish a developmental pathway in carrot. Plant Cell **9,** 2225–2241.

Mette, M.F., Aufsatz, W., van der Winden, J., Matzke, M.A., and Matzke, A.J.M. (2000). Transcriptional silencing and promoter methylation triggered by double-stranded RNA. EMBO J. **19,** 5194–5201.

Moore, J.M., Vielle-Calzada, J.P., Gagliano, W., and Grossniklaus, U. (1997). Genetic characterization of *hadad*, a mutant disrupting female gametogenesis in *Arabidopsis thaliana*. Cold Spring Harb. Symp. Quant. Biol. **62,** 35–47.

Motose, H., Suriyama, M., and Fukuda, H. (2004). A proteoglycan mediates inductive interaction during plant vascular development. Nature **429,** 873–878.

Nam, J., Mysore, K.S., Zheng, C., Knue, M.K., Matthysse, A.G., and Gelvin, S.B. (1999). Identification of T-DNA tagged Arabidopsis mutants that are resistant to transformation by *Agrobacterium*. Mol. Gen. Genet. **261,** 429–438.

Nothnagel, E.A. (1997). Proteoglycans and related components in the plant cells. Int. Rev. Cytol. **174,** 195–291.

Pennell, R.I., Janniche, L., Kjellbom, P., Scofield, G.N., Peart, J.M., and Roberts, K. (1991). Developmental regulation of a plasma membrane arabinogalactan protein epitope in oilseed rape flowers. Plant Cell **3,** 1317–1326.

Pennell, R.I., Janniche, L., Scofield, G.N., Booij, H., de Vries, S.C., and Roberts, K. (1992). Identification of a transitional cell state in the developmental pathway to carrot somatic embryogenesis. J. Cell Biol. **119,** 1371–1380.

Pennell, R.I., and Roberts, K. (1990). Sexual development in the pea is presaged by altered expression of arabinogalactan protein. Nature **344,** 547–549.

Pischke, M.S., Jones, L.G., Otsuga, D., Fernandez, D.E., Drews, G.N., and Sussman, M.R. (2002). An Arabidopsis histidine kinase is essential for megagametogenesis. Proc. Natl. Acad. Sci. USA **26,** 15800–15805.

Reddy, T.V., Kaur, J., Agashe, B., Sundaresan, V., and Siddiqi, I. (2003). The DUET gene is necessary for chromosome organization and progression during male meiosis in Arabidopsis and encodes a PHD finger protein. Development **130,** 5975–5987.

Reiser, L., and Fischer, R.L. (1993). The ovule and the embryo sac. Plant Cell **5,** 1291–1301.

Roy, S., Jauh, G.Y., Hepler, P.K., and Lord, E.M. (1998). Effects of Yariv phenylglycoside on cell wall assembly in the lily pollen tube. Planta **204,** 450–458.

Schiefthaler, U., Balasubramanian, S., Sieber, P., Chevalier, D., Wisman, E., and Schneitz, K. (1999). Molecular analysis of *NOZZLE*, a gene involved in pattern formation and early sporogenesis during

sex organ development in Arabidopsis thaliana. Proc. Natl. Acad. Sci. USA **96**, 11664–11669.

Schindelman, G., Morikami, A., Jung, J., Baskin, T.I., Carpita, N.C., Derbyshire, P., McCann, M.C., and Benfey, P.N. (2001). COBRA encodes a putative GPI-anchored protein, which is polarly localized and necessary for oriented cell expansion in Arabidopsis. Genes Dev. **15**, 1115–1127.

Schneitz, K. (1999). The molecular and genetic control of ovule development. Curr. Opin. Plant Biol. **2**, 13–17.

Schneitz, K., Hülskamp, M., Kopczak, S.D., and Pruitt, R.E. (1997). Dissection of sexual organ ontogenesis: A genetic analysis of ovule development in *Arabidopsis thaliana*. Development **124**, 1367–1376.

Schultz, C., Gilson, P., Oxley, D., Youl, J., and Bacic, A. (1998). GPI-anchors on arabinogalactan-proteins: Implications for signaling in plants. Trends Plant Sci. **3**, 426–431.

Schultz, C., Johnson, K.L., Currie, G., and Bacic, A. (2000). The classical arabinogalactan protein gene family of Arabidopsis. Plant Cell **12**, 1751–1767.

Schultz, C.J., Rumsewicz, M.P., Johnson, K.L., Jones, B.J., Gaspar, Y.M., and Bacic, A. (2002). Using genomic resources to guide research directions. The arabinogalactan protein gene family as a test case. Plant Physiol. **129**, 1448–1463.

Serpe, M.D., and Nothnagel, E.A. (1994). Effects of Yariv phenylglycosides on *Rosa* cell suspensions: Evidence for the involvement of arabinogalactan-proteins in cell proliferation. Planta **193**, 542–550.

Sharma, P., Varma, R., Sarasij, R.C., Gousset, K., Khrihnamoorthy, G., Rao, M., and Mayor, S. (2004). Nanoscale organization of multiple GPI-anchored proteins in living cell membranes. Cell **116**, 577–589.

Sherrier, D.J., Prime, T.A., and Dupree, P. (1999). Glycosylphosphatidylinositol-anchored cell-surface proteins from Arabidopsis. Electrophoresis **20**, 2027–2035.

Showalter, A.M. (2001). Arabinogalactan-proteins: Structure, expression, and function. Cell. Mol. Life Sci. **58**, 1399–1417.

Siddiqi, I., Ganesh, G., Grossniklaus, U., and Subbiah, V. (2000). The *dyad* gene is required for progression through female meiosis in Arabidopsis. Development **127**, 197–207.

Smith, N.A., Singh, S.P., Wang, M.B., Stoutjesdijk, P.A., Green, A.G., and Waterhouse, P.M. (2000). Total silencing by intron-spliced hairpin RNAs. Nature **407**, 319–320.

Sommer-Knudsen, J., Bacic, A., and Clarke, A.E. (1998). Hidroxyproline-rich plant glycoproteins. Phytochemistry **47**, 483–497.

Springer, P.S. (2000). Gene traps: Tools for plant development and genomics. Plant Cell **12**, 1007–1020.

Springer, P.S., McCombie, W.R., Sundaresan, V., and Martienssen, R.A. (1995). Gene trap tagging of *PROLIFERA*, an essential MCM2-3-5-like gene in Arabidopsis. Science **268**, 877–880.

Sun, W., Zhao, Z.D., Hare, M.C., Kieliszewski, M.J., and Showalter, A.M. (2004). Tomato LeAGP-1 is a plasma membrane-bound, glycosylphosphatidylinositol-anchored arabinogalactan-protein. Physiol. Plant. **120**, 319–327.

Sundaresan, V., Springer, P., Volpe, T., Haward, S., Jones, J.D., Dean, C., Ma, H., and Martienssen, R. (1995). Patterns of the gene action in plant development is revealed by enhancer trap and gene trap transposable elements. Genes Dev. **9**, 1797–1810.

Svetek, J., Yadav, M.P., and Nothnagel, E.A. (1999). Presence of a glycosylphosphatidylinositol lipid anchor on rose arabinogalactan proteins. J. Biol. Chem. **274**, 14724–14733.

Takos, A.D., Dry, I.B., and Soole, K.L. (1997). Detection of glycosylphosphatidylinositol-anchored proteins on the surface of *Nicotiana tabacum* protoplasts. FEBS Lett. **405**, 1–4.

Takos, A.M., Dry, I.B., and Soole, K.L. (2000). Glycosyl-phosphatidylinositol-anchor addition signals are processed in *Nicotiana tabacum*. Plant J. **21**, 43–52.

Tan, L., Leykam, J.F., and Kieliszewski, M.J. (2003). Glycosylation motifs that direct arabinogalactan addition to arabinogalactan-proteins. Plant Physiol. **3**, 1362–1369.

VandenBosch, K.A., Bradley, D.J., Perotto, S., Butcher, G.W., and Brewin, J.J. (1989). Common components of the infection thread matrix and the intercellular space identified by immunocytochemical analysis of pea nodules and uninfected roots. EMBO J. **8**, 335–342.

van Hengel, A.J., and Roberts, K. (2002). Fucosylated arabinogalactan-proteins are required for full root cell elongation in Arabidopsis. Plant J. **32**, 105–113.

van Hengel, A.J., and Roberts, K. (2003). AtAGP30, an arabinogalactan-protein in the cell walls of the primary root, plays a role in the root generation and seed germination. Plant J. **36**, 256–270.

van Hengel, A.J., Tadesse, Z., Immerzeel, P., Schols, H., van Kammen, A., and de Vries, S.C. (2001). N-acetylglusamine and glucosamine-containing arabinogalactan proteins control somatic embryogenesis. Plant Physiol. **125**, 1880–1890.

Vielle-Calzada, J.P., Baskar, R., and Grossniklaus, U. (2000). Delayed activation of the paternal genome during seed development. Nature **404**, 91–94.

Vielle-Calzada, J.P., Thomas, J., Spillane, C., Coluccio, A., Hoeppner, M.A., and Grossniklaus, U. (1999). Maintenance of genomic imprinting at the Arabidopsis medea locus requires zygotic *DDM1* activity. Genes Dev. **13**, 2971–2982.

Waterhouse, P.M., Graham, M.W., and Wang, M.B. (1998). Virus resistance and gene silencing in plants can be induced by simultaneous expression of sense and antisense RNA. Proc. Natl. Acad. Sci. USA **95**, 13959–13964.

Webb, M.C., and Gunning, E.S. (1990). Embryo sac development in *Arabidopsis thaliana*. I. Megasporogenesis, including the microtubular cytoskeleton. Sex. Plant Reprod. **3**, 244–256.

Willats, W.G.T., and Knox, J.P. (1996). A role for arabinogalactan-proteins in plant cell expansion: Evidence from studies on the interaction of β-glucosyl Yariv reagent with seedlings of *Arabidopsis thaliana*. Plant J. **9**, 919–925.

Willemse, M.T.M., and van Went, J.L. (1984). The female gametophyte. In Embryology of Angiosperms, B.H. Johri, ed (New York: Springer-Verlag), pp. 159–196.

Wu, H., Wang, H., and Cheung, A.Y. (1995). A pollen tube growth simulator glycoprotein is deglycosylated by pollen tubes and displays a glycosylation gradient in the flower. Cell **82**, 395–403.

Yang, W.C., and Sundaresan, V. (2000). Genetics of gametophyte biogenesis in Arabidopsis. Curr. Opin. Plant Biol. **3**, 53–57.

Yang, W.C., Ye, D., Xu, J., and Sundaresan, V. (1999). The *SPOROCYTELESS* gene of Arabidopsis is required for initiation of sporogenesis and encodes a novel nuclear protein. Genes Dev. **15**, 2108–2117.

Youl, J.J., Bacic, A., and Oxley, O. (1998). Arabinogalactan-proteins from *Nicotiana alata* and *Pyrus communis* contain glycosylphophatidylinositol membrane anchors. Proc. Natl. Acad. Sci. USA **95**, 7921–7926.

Exhibit 7

The Plant Journal (2003) **34**, 383–392

TECHNICAL ADVANCE

A chemical-regulated inducible RNAi system in plants

Hui-Shan Guo[1], Ji-Feng Fei[1], Qi Xie[1] and Nam-Hai Chua[2,*]
[1]*Laboratory of Molecular Cell Biology, Temasek Life Sciences Laboratory, National University of Singapore, 1 Research Link, 117604 Singapore, and*
[2]*Laboratory of Plant Molecular Biology, Rockefeller University, 1230 York Avenue, New York, NY 10021, USA*

Received 15 November 2002; revised 21 January 2003; accepted 28 January 2003.
*For correspondence (fax +1 212 327 8327; e-mail chua@mail.rockefeller.edu).

Summary

Constitutive expression of an intron-containing self-complementary 'hairpin' RNA (ihpRNA) has recently been shown to efficiently silence target genes in transgenic plants. However, this technique cannot be applied to genes whose silencing may block plant regeneration or result in embryo lethality. To obviate these potential problems, we have used a chemical-inducible Cre/*loxP* (CLX) recombination system to trigger the expression of an intron-containing inverted-repeat RNA (RNAi) in plants. A detailed characterization of the inducible RNAi system in transgenic *Arabidopsis thaliana* and *Nicotiana benthamiana* plants demonstrated that this system is stringently controlled. Moreover, it can be used to induce silencing of both transgenes and endogenous genes at different developmental stages and at high efficiency and without any detectable secondary affects. In addition to inducing complete silencing, the RNAi can be produced at various times after germination to initiate and obtain different degrees of gene silencing. Upon induction, transgenic plants with genetic chimera were obtained as demonstrated by PCR analysis. Such chimeric plants may provide a useful system to study signaling mechanisms of gene silencing in *Arabidopsis* as well as other cases of long-distance signaling without grafting. The merits of using the inducible CLX system for RNAi expression are discussed.

Keywords: inducible, constitutive, RNAi, dsRNA, DNA excision, Cre/*loxP*.

Introduction

RNA-mediated gene silencing is a conserved mechanism that recognizes double-stranded RNA (dsRNA) as a signal to trigger sequence-specific degradation of homologous mRNA. dsRNA has been used as a powerful tool for the investigation of RNA silencing in a variety of organisms, such as RNA interference (RNAi) in *Caenorhabditis elegans* (Fire *et al.*, 1998) and mammalian cells (Paddison *et al.*, 2002; Sui *et al.*, 2002) and post-transcriptional gene silencing (PTGS) in plants (Chuang and Meyerowitz, 2000; Waterhouse *et al.*, 1998). In plants and *C. elegans*, RNA silencing involves two steps: (i) a local induced silencing, including an initial processing of the triggering dsRNA into short interfering RNA (siRNA) of 21–25 nt (Elbashir *et al.*, 2001; Hamilton and Baulcombe, 1999) and (ii) a systemic spread of the silencing signal throughout the entire organism (Voinnet *et al.*, 2000; Winston *et al.*, 2002). The presence of a spliceable intron in the transgene encoding the dsRNA appears to enhance the silencing efficiency (Smith *et al.*, 2000; Wesley *et al.*, 2001). Constitutive expression of intron-containing self-complementary 'hairpin' RNA (ihpRNA) constructs can induce PTGS with almost 100% efficiency when directed against viruses or endogenous genes (Smith *et al.*, 2000).

The completion of the sequencing of the *Arabidopsis* genome has uncovered a large number of genes with unknown functions. Potentially, the dsRNA-mediated gene silencing technique can be used to investigate the functions of these genes. The most effective silencing, brought about by intron-containing dsRNA, would produce phenotypes resembling those of the null alleles of the target genes. If the target gene is required for basic cell function or development, constitutive dsRNA-mediated silencing of the gene may produce detrimental effects or even cause plant lethality resulting in no recovery of transgenic plants for investigation. This problem can be circumvented somewhat by inducing gene silencing, using either *Agrobacterium*

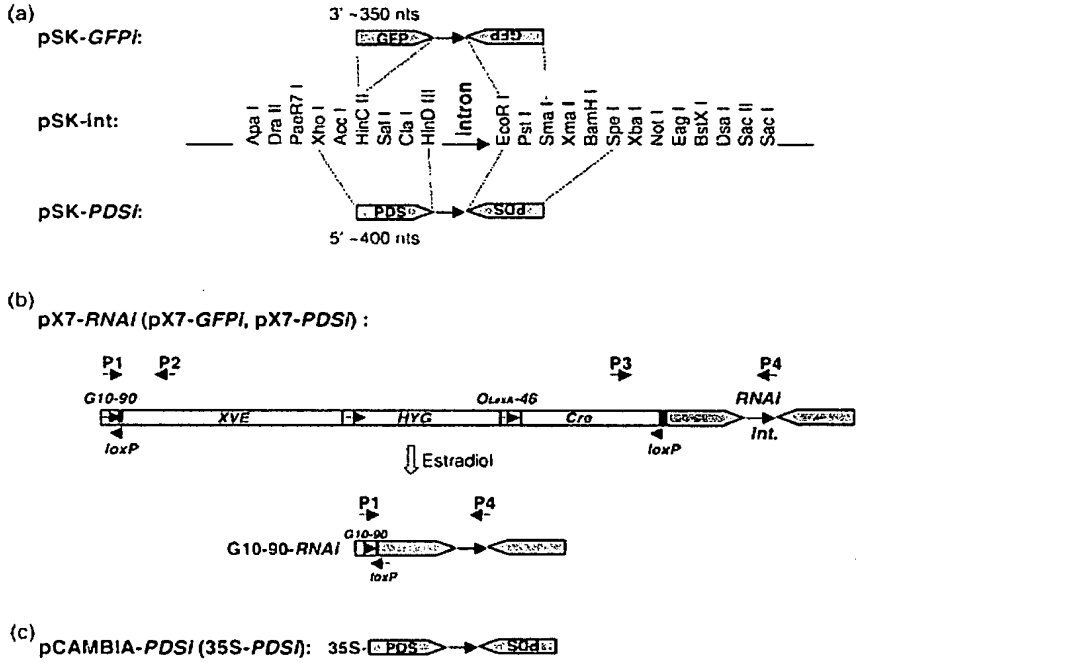

Figure 1. Schematic diagrams of the inducible and constitutive RNAi constructs.
(a) A schematic diagram of an intron-containing intermediate vector pSK-int with multiple restriction sites on both arms of the intron. DNA fragments encoding sense and antisense RNA (approximately 350 nt of 3′ *GFP* or approximately 400 nt of 5′ *PDS*, respectively) were cloned into pSK-int at 5′ and 3′ arms of the intron in appropriate restriction sites indicated by dotted lines, resulting in pSK-GFPi and pSK-PDSi.
(b) A schematic diagram showing structural features of the inducible pX7-RNAi construct and Cre/*loxP*-mediated DNA recombination (see Zuo *et al.*, 2001 for details). *XVE*, a chimeric transactivator containing the regulator domain of an estrogen receptor (Zuo *et al.*, 2000); *HYG*, a hygromycin-resistance marker; *Cre*, the bacteriophage P1 Cre recombinase with an intron (Zuo *et al.*, 2001); *loxP*, specific recognition sites of Cre; *OlexA-46*, eight copies of the *LexA* DNA binding site fused to the −46 CaMV 35S promoter; *G10-90*, a strong, synthetic, constitutive promoter; *int*, actin 11 intron (ATU27981, nt 1957–2111); *RNAi*, DNA sequences encoding the intron-containing inverted-repeat RNAs; G10-90-*RNAi*, the reconstituted transcription unit derived from Cre/*loxP*-mediated DNA recombination after inducer treatment. Arrows inside transcription units indicate the direction of transcription. P1–4 denote primers used for PCR analysis shown in Figure 5(c).
(c) A fragment of PDS-int-PDS was cloned between the 35S promoter and the terminator in the binary plasmid pCAMBIA 1300 (AF234296) to give 35S-*PDSi*, a constitutive RNAi construct.

infiltration (Voinnet and Baulcombe, 1997) or virus-derived vectors (Dalmay *et al.*, 2000; Peele *et al.*, 2001; Ratcliff *et al.*, 2001; Turnage *et al.*, 2002). However, these two methods have limited application in functional genomics because of their transient nature, and their silencing effects are not heritable.

In this paper, we describe the development of an inducible gene silencing system using intron-containing, inverted-repeat RNA (referred to as inducible RNAi). The chemical-inducible system we use here is the CLX system, an XVE-based (XVE for LexA-VP16-ER) (Zuo *et al.*, 2000), site-specific DNA recombination mediated by Cre/*loxP* (Zuo *et al.*, 2001). The Cre expression is placed under the control of the chimeric transcription factor XVE, whose activity is strictly regulated by estrogens. Upon induction by 17β-estradiol, Cre/*loxP*-mediated recombination leads to activation of the RNAi transcription cassette by bringing it immediately downstream of the constitutive G10-90 promoter (Zuo *et al.*, 2001; Figure 1). Compared to other inducible systems, the most significant feature of the CLX system is that it is strigently controlled, and upon induction, it produces DNA recombination with high efficiency (for a review, see Hare and Chua, 2002; Ow, 2001).

Here, we show that the inducible RNAi system can be used to silence, with high efficiency, the expression of a *GFP* transgene and an endogenous phytoene desaturase (*PDS*) gene in *Nicotiana benthamiana* as well as in *Arabidopsis thaliana*. Upon induction at seed germination or post-germination stages, the efficiency and effectiveness of *PDS* silencing are comparable to those obtained with a 35S-RNAi construct. A stable and reproducible inducible RNAi phenotype was obtained in subsequent transgenic generations. The merits of the inducible RNAi system for silencing of endogenous genes are discussed.

Results

Silencing of a GFP transgene

To evaluate the function of the inducible RNAi system, the construct pX7-*GFPi* (Figure 1b) was introduced into a

transgenic *N. benthamiana* line carrying a 35S-*GFP* transgene (GFP-16c) (Ruiz *et al.*, 1998) by *Agrobacterium*-mediated transformation. T_1 seeds from 12 transgenic lines (GFP-16c/pX7-*GFPi*, named as 16c-GFPi) were germinated on the inductive medium (MS + 2 μM 17β-estradiol) containing hygromycin (hyg). After 2 weeks, eight lines showed uniform red fluorescence under UV light, which was caused by chlorophyll autofluorescence in the absence of GFP accumulation. Some red seedlings stopped growing upon continued incubation on the selective medium, presumably because of the complete Cre/*loxP*-mediated excision of the hygromycin-resistance gene upon induction. The remaining four lines initially displayed a mixture of red/green fluorescence after 2 weeks of treatment with the inducer, but propagation of the red color to the entire plant was observed in these lines 2 weeks after they were transferred from the inductive medium to the soil (Figure 2a, left). No difference was observed between 16c-GFPi seedlings germinated on the selective medium in the absence of the inducer (MS + hygromycin) and GFP-16c control plants, as judged by the degree of green fluorescence (Figure 2b, right).

Northern blots were analyzed with total RNA from treated red fluorescent 16c-GFPi seedlings, untreated green fluorescent 16c-GFPi seedlings and GFP-16c control seedlings. *GFP* mRNA was almost undetectable in red 16c-GFPi seedlings (Figure 2b, upper panel, +), as compared with GFP-16c control (0) or untreated 16c-GFPi seedlings (–). GFP-related siRNA, which is a key component of RNA silencing, was detected in red seedlings using a radiolabeled *GFP*-specific probe (Figure 2b, lower panel, +), whereas no GFP-related siRNA could be detected in GFP-16c control or untreated 16c-GFPi green seedlings (0 and –). Both fluorescence and RNA analyses indicated silencing of the *GFP* transgene in 16c-GFPi plants upon treatment with 17β-estradiol.

A transgenic line of *A. thaliana* (ecotype C24), which showed constitutive expression of a 35S-*GFP* transgene (Dalmay *et al.*, 2000) was transformed with the pX7-*GFPi* construct to test the inducible RNAi system. Twenty-nine T_1 independent lines (named as At-GFPi) were obtained by floral dip transformation. Upon germination on the inductive medium, all 29 At-GFPi lines displayed red fluorescence, indicating silencing of the *GFP* transgene. By contrast, all seedlings germinated on the medium without the inducer showed uniform green fluorescence, indicating GFP expression (data not shown). Northern blots were analyzed with total RNA (Figure 2c, upper panel) and GFP-related siRNA (Figure 2c, lower panel) from treated, red fluorescent At-GFPi seedlings (Figure 2c, +) and untreated, green fluorescent At-GFPi seedlings (Figure 2c, –). Similar results were obtained as with the *N. benthamiana* 16c-GFPi plants, providing molecular evidence for silencing of the *GFP* transgene in At-GFPi plants upon 17β-estradiol treatment.

We used 15 At-GFPi lines for further investigation of 17β-estradiol-induced silencing at post-germination stage. Two-week-old T_1 seedlings germinated on the selective medium in the absence of the inducer were transferred to fresh MS medium. All seedlings at this stage continued to display green fluorescence. However, when seedlings were transferred to the inductive medium, 10 lines displayed strong inducible *GFP* silencing as indicated by their uniform red fluorescence after 1-week induction (data not shown). The remaining five lines showed varying initiation of *GFP* silencing after 1-week induction. Further incubation with the inducer up to 2 weeks resulted in complete *GFP* silencing as reflected by the uniform red fluorescence in all these plants.

Efficient inducible silencing of an endogenous PDS gene in Arabidopsis thaliana

We chose the phytoene desaturase (*PDS*) gene of *A. thaliana* and *N. benthamiana* to test the ability of the inducible RNAi system to silence endogenous genes. The *PDS* gene was selected because loss of the phytoene desaturase enzyme blocks carotenoid synthesis culminating in a photobleaching phenotype because of photo-oxidation of chlorophylls (Ruiz *et al.*, 1998). This visible phenotype facilitated visual monitoring of the induction process of *PDS* silencing. The constructs pX7-*PDSi(At)* and pX7-*PDSi(Nb)* (Figure 1b) were transformed into *A. thaliana* (ecotype Columbia) and *N. benthamiana*, respectively. In addition, pCAMBIA-*PDSi(At)* (Figure 1c) containing a 35S-*PDSi(At)* was also transformed into *A. thaliana* (ecotype Columbia).

We tested 35 lines of putative transgenic *A. thaliana* carrying the 35S-*PDSi(At)* transgene by virtue of their ability to grow on the selective medium. Thirty-two lines (35S-PDSi(At)) displayed the photobleaching phenotype. Most lines appeared near-white and stopped growing (data not shown) after 4–6 weeks on the culture medium. Only two lines that displayed varying green patches in their bleached leaves survived. Seedlings of these two lines exhibited abnormal development and poor fertility, and produced only a small amount of seeds.

Eighty-one independent *A. thaliana* transgenic lines transformed with pX7-*PDSi(At)* were obtained. In the absence of the inducer, all transgenic T_1 lines (At-PDSi) displayed normal development and fertility. T_2 seeds from 12 independent T_1 lines were germinated on the selective medium in the absence or presence of the inducer. All T_2 seedlings grew with normal phenotype on the medium in the absence of the inducer (Figure 3a). However, in the presence of the inducer, seedlings of all the 12 T_2 At-PDSi lines showed uniform photobleaching phenotype in the cotyledons at 6–9 days post-induction (Figure 3b,c). Similar to the 35S-PDSi(At) lines, most of these seedlings

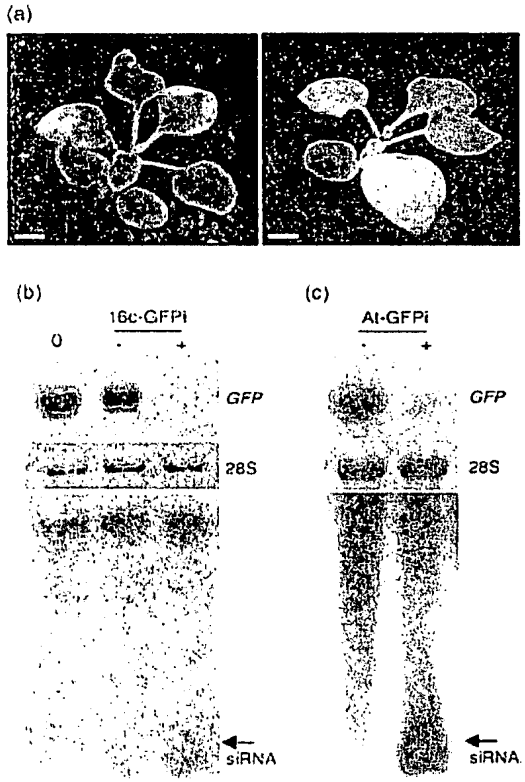

Figure 2. 17β-estradiol-inducible *GFP* silencing in *Nicotiana benthamiana* transgenic line 16c-GFPi and *Arabidopsis thaliana* line At-GFPi.
(a) 16c-GFPi plants were first germinated on an inductive (left) or selective (right) medium for 2 weeks, before being transferred to soil, and photographed under UV light at 2 weeks after transfer. Left, an induced 16c-GFPi plant exhibited uniform red fluorescence in the whole plant. Note that in this plant initiation of *GFP* silencing was indicated by a mixture of red/green fluorescence. Right, an untreated 16c-GFPi plant showing green fluorescence. Scale bar = 0.5 cm.
(b, c) Northern blot analysis of induced silencing in 16c-GFPi plants (b) and At-GFPi plants (c). Total high (top and middle panels) and low (lower panel) molecular weight RNAs were extracted from 2-week-old red fluorescent seedlings after 17β-estradiol induction (+), untreated green fluorescent seedlings (−), and GFP-16c control plants (0). Equal RNA loading (5 μg per leaf) was monitored by methylene blue staining of the 28S RNA (middle panel), and the blot was probed with a *GFP*-specific sequence (top panels). Bottom panels show the blot for siRNA, which was hybridized with a ^{32}P-labeled transcript corresponding to the 3′-terminal region (350 nt) of *GFP*. Each lane contained 50 μg RNA. Arrow indicates the position of a 25-base DNA oligonucleotide.

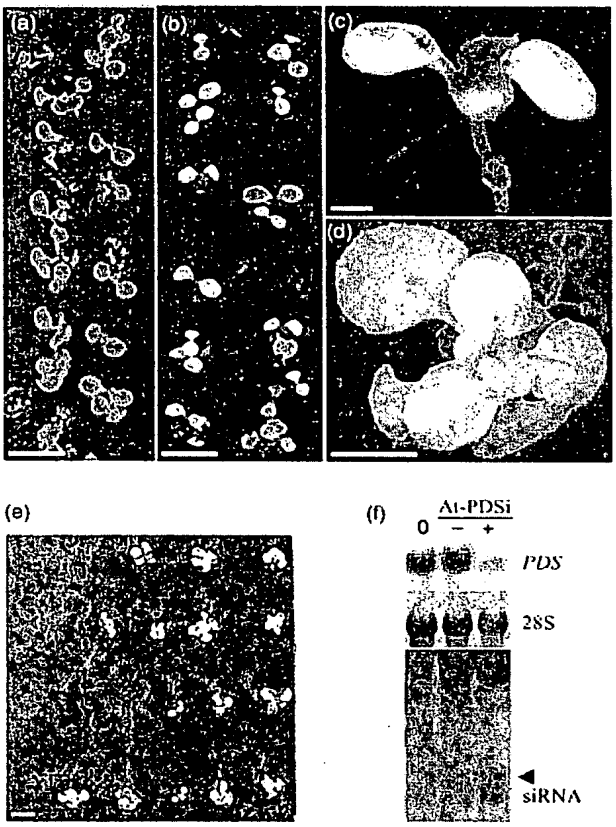

Figure 3. Inducible *PDS* silencing in transgenic *Arabidopsis thaliana* plants (At-PDSi) at seed germination stage.
(a–d) At-PDSi seeds of line 2 were germinated on selective media in the absence (a) or presence of an inducer (b, c, d).
(b) Seedlings with induced *PDS* silencing showed a uniform photobleaching phenotype in the cotyledons at 6 days.
(c,d) *PDS* silencing was seen in the first pair of true leaves as well as the leaves that developed later (c, 9 days, d, 28 days). Scale bars = 0.5 cm in (a, b, d) and 0.1 cm in (c).
(e) Seeds of At-PDSi line 1 (a single transgenic locus) were germinated on MS in the presence of 17β-estradiol without the selective antibiotic hygromycin. Fifteen out of 19 plants showed induced *PDS* silencing. The photograph was taken at 29 days post-induction. Scale bar = 0.5 cm.
(f) Northern analysis of inducible *PDS* silencing in At-PDSi plants. Total high (top and middle panels) and low (lower panel) molecular weight RNAs were extracted from WT Columbia seedlings (0), uninduced At-PDSi control seedlings (−), and a mixture of induced At-PDSi seedlings, which showed a photobleaching phenotype (+). The blot (top panel) was probed with a *PDS*-specific sequence corresponding to the 3′ region for detection of the endogenous *PDS* mRNA. Each lane contained 5 μg RNA, and 28S RNA visualized by methylene blue staining was used as a loading control. Bottom panel shows the blot for siRNA, which was hybridized with a ^{32}P-labeled transcript corresponding to the 5′-terminal region (400 nt) of *PDS*. Each lane contained 50 μg RNA. The arrow indicates the position of a 25-base DNA oligonucleotide.

stopped growing within 4–6 weeks (Figure 3d). Northern analysis showed that endogenous *PDS* mRNA levels were significantly reduced in bleached leaves of treated At-PDSi lines (Figure 3f, upper panel, +), but readily detected in untreated lines (Figure 3f, upper panel, −) and WT control seedlings (Figure 3f, upper panel, 0), indicating that the photobleaching phenotype resulted from silencing of the endogenous *PDS* gene. PDS-related siRNA was detected in treated, bleached At-PSDi seedlings (Figure 3f, lower panel, +) using a *PDS*-specific probe, whereas no PDS-related siRNA could be detected in either WT control seedlings (Figure 3f, lower panel, 0) or untreated At-PDSi seedlings (Figure 3f, lower panel, −).

To rule out any toxic or non-specific secondary physiologic effects because of 17β-estradiol-induced *PDS* silencing, T_2 seeds of At-PDSi line 1, which showed a 3 : 1 segregation ratio for Hyg^R:Hyg^S, were germinated on an inducer-containing medium without hygromycin, the selective antibiotic. After 3 weeks of incubation, 15 out of 19 T_2 seedlings showed the photobleaching phenotype and ceased to grow (Figure 3e), whereas the remaining four seedlings were normal. These four seedlings were sensitive to hygromycin as they ceased to grow after being transferred to a hygromycin-containing medium. The approximately 3 : 1 segregation pattern of both the selection marker and the photobleaching phenotype suggested that the four hygromycin-sensitive plants were WT, in agreement with the Mendelian segregation ratio for a single transgenic locus. These four plants showed no response to 17β-estradiol and did not exhibit any morphological alteration, indicating that the inducer had no secondary non-specific physiological effect on WT plants. Our results suggest that the inducible RNAi system is able to silence the endogenous *PDS* of *Arabidopsis* at the seed germination stage with comparable efficiency and effectiveness as the constitutive 35S-*PDSi* transgene.

We also examined post-germination induction of *PDS* silencing. Two- or four-week-old T_2 At-PDSi seedlings on the culture medium in the absence of the inducer were transferred to the inductive medium, and similar results were obtained from the seedlings of both age groups. We observed two photobleaching phenotypes. In the first group which includes At-PDSi lines 2, 5, 7, and 8, a strong *PDS* silencing was seen, 1 week after induction, with newly emerged leaves showing uniform bleaching surrounding the central area of the leaves. The bleaching was subsequently propagated to the entire leaf. Figure 4(a–d) shows results from one representative line 2. Most of these plants with a strong photobleaching phenotype stopped growing. The second group includes At-PDSi lines 1, 3, 4, 6, and 9–12, and these lines showed varying photobleaching phenotypes. After 2 weeks of induction, photobleaching was limited to the areas near the veins (Figure 4e, a plant of line 12) or to the white/green patchy regions in the entire leaf (Figure 4f, a plant of line 1); however, the leaves became near-white over the next 2 weeks (Figure 4g,h, a plant of line 1). Although the *PDS* silencing extended to most rosette leaves and some cauline leaves (Figure 4h), these plants with varying degree of *PDS* silencing could still develop normally and were fertile after transfer to the soil.

We collected seeds from six T_2 plants of At-PDSi line 1 with induced silencing. When germinated on the selective medium (MS + Hyg), none of the T_3 progeny showed *PDS* silencing. When the seeds were germinated on MS medium with neither the selective antibiotic nor the inducer, four T_2 lines showed no *PDS* silencing. On the other hand, more than 10% of the progeny seedlings of the other two T_2 lines showed a constitutive photobleaching phenotype. The constitutive bleached plants presumably derived from some

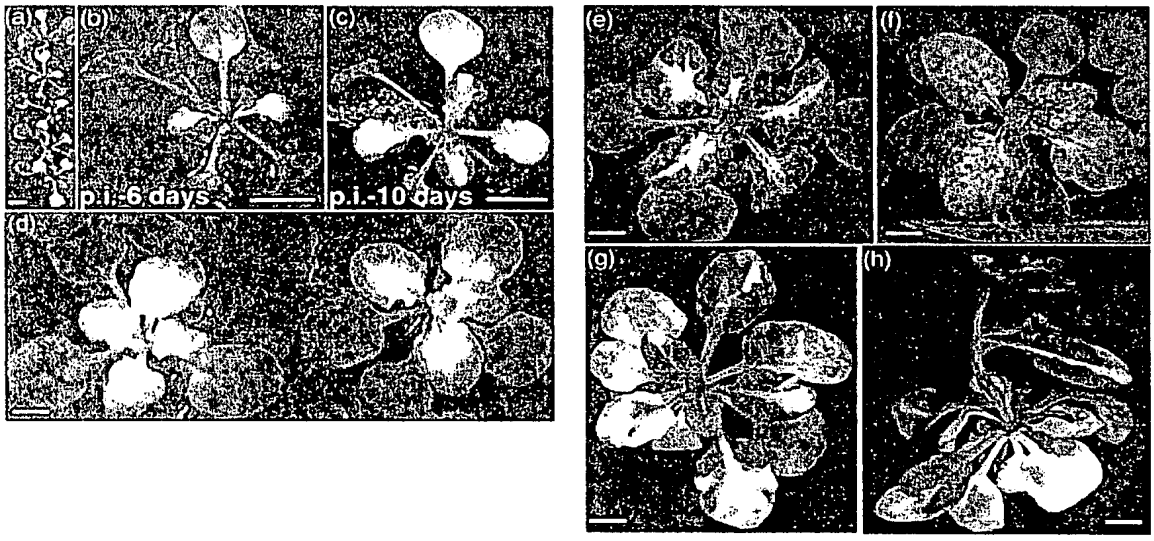

Figure 4. Post-germination induction of *PDS* silencing in At-PDSi *Arabidopsis thaliana* transgenic plants.
(a–d) Strong induction of *PDS* silencing was seen in 2-week-old seedlings of line 2 after transfer to the inductive medium for 6 days (a, b) or 10 days (c). Note that (b) and (c) are from the same plant. Four-week-old seedlings of line 2 were transferred to the inductive medium and the picture was taken at 2 weeks post-induction (d).
(e–h) Delayed onset of *PDS* silencing. Four-week-old seedlings from different At-PDSi transgenic lines 12 (e) and 1 (f–h) were transferred to the inductive medium. Photobleaching was limited to the perivascular regions (e) or white/green patchy regions (f). The plants were photographed at 2 weeks after induction. Photobleaching progressed with time in the old leaves and extended to new rosette and cauline leaves when plants were photographed at 3 weeks (g) or 4 weeks (h) after induction. All scale bars represent 0.5 cm.

converted germ line cells in the L2 layers of T_2 plants that have undergone 17β-estradiol-induced Cre/*loxP* DNA recombination (Zuo *et al.*, 2001), and therefore expressed G10-90-*PDSi* constitutively (Figure 1b).

Molecular analyses of inducible PDS silencing in At-PDSi plants

The delayed onset of *PDS* silencing in the second group prompted us to analyze the relationship between the photobleaching phenotype, endogenous *PDS* mRNA levels, and dsRNA induction upon 17β-estradiol-induced Cre/*loxP* DNA excision. T_2 progenies of At-PDSi line 1 were analyzed in detail. First, dsRNA corresponding to the *PDSi* transcript region (Figure 1) was analyzed. Two-week-old seedlings of line 1-1 (heterozygous) and line 1-2 (homozygous) were transferred to the inductive medium. RNA was extracted from a portion of the seedlings at 42 h post-induction. Total RNA was digested with Rnase1™ (Promega, USA), and dsRNA was analyzed by hybridization with a *PDS* 5′-terminal probe containing sequences corresponding to the *PDSi* region (Figure 1). Figure 5(b) shows that signals of the expected size were detected in the treated seedlings of both lines 1-1 and 1-2 (lanes 2 and 3), but not in the untreated seedlings of line 1-1 (lane 1).

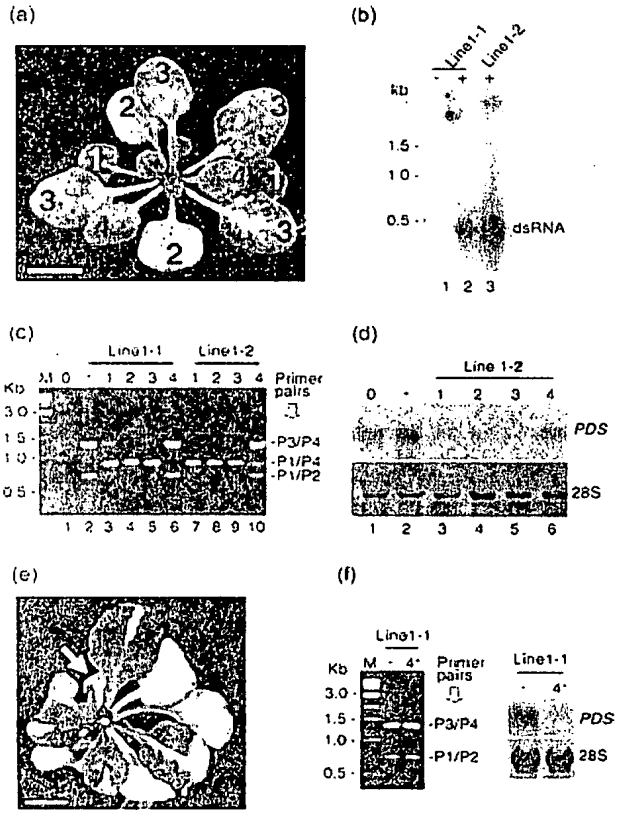

Figure 6. Inducible *PDS* silencing with uniform photobleaching phenotype in one *Nicotiana benthamiana* transgenic (Nb-PDSi) line.
(a) Seeds were germinated on the selective medium in the presence of the inducer (MS + Hyg + 17β-estradiol), and seedlings were photographed at 2 weeks post-germination.
(b) Two-week-old seedlings were transferred to the inductive medium without hygromycin, and seedlings were photographed at 2 weeks post-induction. The green plant is presumably a WT plant that exhibited no secondary effect upon 17β-estradiol treatment. Scale bar = 0.5 cm.

Figure 5. Molecular characterization of delayed onset of *PDS* silencing in *A. thaliana* transgenic plants.
(a) Two-week-old seedlings of At-PDSi line 1-1 were transferred to the inductive medium, and the plant was photographed at 18 days post-induction. Scale bar represents 0.5 cm. Leaves with increasing degrees of photobleaching were labeled with numbers 1–4, and those with a similar phenotype were labeled with the same number. Leaves designated 1 were formed before seedlings were transferred to the inductive medium.
(b) Seedlings of At-PDSi line 1-1 and 1-2 were either untreated (–) or treated (+) for 42 h with 17β-estradiol, RNA was analyzed for the presence of pre-silencing dsRNA. Lane 1, line 1-1, untreated, 100 μg RNA; lane 2, treated line 1-1, 50 μg RNA; lane 3, treated lane 1-2, 100 μg RNA. RNAs were digested with Rnase1™ before being loaded onto formaldehyde-containing gels. The filter was hybridized with a *PDS*-specific 5′ sequence corresponding to the *PDSi* region (Figure 1a). Molecular weight standards are shown on the left.
(c) PCR analysis of genomic DNA prepared from WT Columbia (lane 1), untreated line 1-1 (lane 2), 18-day 17β-estradiol-treated line 1-1 (lanes 3–6) or line 1-2 (lanes 7–10). Leaves with similar phenotype (panel a) were pooled from several plants, and the group numbers indicated on top of the blot. Primers P1–4 were used as illustrated in Figure 1(b). The expected PCR products from different combinations of primer pairs were indicated on the right, M, DNA molecular markers.
(d) Northern analysis of endogenous *PDS* mRNA levels. RNAs were extracted from the same samples as for DNA preparation (panel c), and the corresponding group numbers are indicated on the top. Each lane contained 5 μg RNA.
(e) Showing one plant of At-PDSi line 1-1 treated with 17β-estradiol for 18 days as described in (a) one week after been transferred to high light intensity. Note that the silenced leaves including the old ones (one indicated by arrow) became strongly bleached. Compare this plant to those shown in Figure 4(g,h). Scale bar = 0.5 cm.
(f) Molecular analysis of inducer-treated transgenic plants 1 week after inducer withdrawal and transfer to the soil. Some seedlings of At-PDSi line 1-1 treated with 17β-estradiol for 18 days as described in (a) were transferred to the soil. After 1 week, leaves belonging to group 4 as well as two younger leaves that displayed photobleaching phenotype were pooled for PCR (left panel) and Northern blot analysis (right panel). Untreated line 1-1 was used as controls (–). For right panel, each leaf contained 5 μg RNA.

For the remaining seedlings on the inductive medium, new leaves that emerged after 1-week induction also became patchy in appearance, and photobleaching progressed with time in both the heterozygous T_2 line 1-1 and the homozygous T_2 line 1-2, similar to that in the parental T_1 line 1. To facilitate further analysis, leaves with varying degrees of photobleaching were numbered as shown in Figure 5(a).

PCR analysis was performed using primers specific for the excised sequences and flanking non-excised sequences (see Figure 1b). Based on a previous study (Zuo *et al.*, 2001), the P1/P2 and P3/P4 primer pairs were expected to yield PCR fragments of 696 and 1331 bp, respectively, from a non-recombinant T-DNA. By contrast, following Cre/*loxP*-mediated recombination and reconstitution of the G10-90-*PDSi* transcription unit, the P1/P4 primer pair produced a PCR product of 992 bp (Figure 1b). Leaves with similar phenotype were pooled from several plants for DNA preparation at 18 days post-induction. No fragment was amplified from WT Columbia (Figure 5c, lane 1), whereas P1/P2 and P3/P4 fragments were detected in untreated line 1-1 (Figure 5c, lane 2), indicating no DNA recombination. The P1/P4 fragment was detected in bleached (group 2 leaves) and patchy leaves (group 3 leaves) of both line 1-1 (Figure 5c, lanes 4 and 5) and line 1-2 (Figure 5c, lanes 8 and 9), indicating complete DNA excision in these leaves after 2 weeks of inducer treatment. In the near-green young leaves (group 4 leaves), however, varying amounts of the DNA excision were found (Figure 5c, lanes 6 and 10). There was no DNA excision in the sample collected from group 4 leaves of line 1-1 because only P1/P2 and P3/P4 fragments were amplified (Figure 5c, lane 6). By contrast, P1/P2, P3/P4, and P1/P4 fragments were detected in the samples collected from group 4 leaves of line 1-2 (Figure 5c, lane 10), indicating that DNA recombination occurred in some of the leaves.

We also found that DNA excision occurred in the old leaves (group 1 leaves) that were already developed before plants were transferred to the inductive medium. P1/P4 fragment was amplified from both line 1-1 (incomplete excision; Figure 5c, lane 3) and line 1-2 (complete excision; Figure 5c, lane 7), consistent with the highly effective inducer-dependent DNA recombination, probably as a result of penetration of 17β-estradiol to almost all cells in the lower leaves.

Endogenous *PDS* mRNA levels of T_2 line 1-2 were assessed by Northern analysis 18 days after induction. Consistent with the photobleaching phenotype and DNA excision, *PDS* mRNA levels were significantly decreased in groups 2 and 3 leaves (Figure 5d, lanes 4 and 5), and slightly decreased in group 4 leaves compared to that in untreated line 1-1 control seedlings (lane 2) and WT Columbia control seedlings (lane 1). As expected, *PDS* mRNA was also degraded in group 1 old leaves (Figure 5d, lane 3), consistent with the DNA excision assay. Although *PDS* silencing in old leaves was indeed induced after treatment, the persistence of the green color presumably resulted from the continued presence of carotenoids that were synthesized before the T_2 seedlings were transferred to the inductive medium. This residual amount of pre-formed carotenoids was able to protect chlorophylls from photooxidation under low light intensity (our assay condition: 35 μmol sec^{-1} m^{-2}). However, when these plants were transferred to high light intensity (70 μmol sec^{-1} m^{-2}), all leaves including the old ones became strongly bleached (Figure 5e).

Some line 1-1 seedlings treated with the inducer for 18 days were transferred to the soil, and the phenotype of group 4 leaves as well as that of the newly emerged rosette leaves was followed. Group 4 leaves became patchy in appearance, and they became progressively bleached until near-white in appearance in 1 week. Similar results were observed in another two newly grown rosette leaves, which displayed limited areas of photobleaching. DNA and RNA were extracted from new photobleached leaves (including group 4 leaves), and PCR analysis showed that only P1/P2 and P3/P4 fragments were amplified (Figure 5f), indicating no DNA excision in these leaves. However, RNA analysis demonstrated a severe reduction in *PDS* mRNA levels, indicating that the *PDS* gene was silenced presumably via signals generated by the lower leaves.

Inducible silencing of endogenous PDS gene in transgenic Nicotiana benthamiana

Similar results were obtained in *N. benthamiana* transformed with the p*X7-PDSi(Nb)* construct. Inducible *PDS* silencing was observed when the inducer was given at germination (Figure 6a) or post-germination stages (Figure 6b). Northern analysis of endogenous *PDS* mRNA levels (data not shown) confirmed the visual photobleaching phenotype, suggesting that the inducible RNAi system is capable of inducing endogenous gene silencing in *N. benthamiana* and probably other plant species as well.

Discussion

In this work, we report the development of an inducible dsRNA-mediated silencing (inducible RNAi) system for conditional gene silencing in transgenic plants. This system contains two steps: (i) the inducible expression of dsRNA resulting from 17β-estradiol-induced DNA recombination and (ii) induction of target gene silencing by the dsRNA. A detailed characterization of the 17β-estradiol-inducible silencing system in transgenic *A. thaliana* and *N. benthamiana* plants demonstrated that this system is stringently controlled and can produce, at high efficiency, conditional silencing of both a *GFP* transgene and an

endogenous *PDS* gene and without any detectable secondary affect. At seed germination stage, all tested At-PDSi lines showed a uniform photobleaching phenotype similar to that obtained with constitutively silenced 35S-PDSi lines. This suggests that the efficiency and effectiveness of the inducible RNAi system against endogenous genes are comparable to those obtained with constitutive expression of dsRNA (constitutive RNAi).

The highly efficient gene silencing obtained by intron-containing dsRNA expressed from a constitutive promoter would produce loss-of-function transgenic plants similar to null mutants. If the target gene is essential for basic cell function and development, constitutive RNAi would probably prevent shoot regeneration, cause plant lethality or embryogenesis defect, and block the ability of the transformed plants to produce subsequent generations. These problems can be avoided by using the inducible RNAi system described here. Moreover, the inducible RNAi system provides the possibility to induce gene silencing at different stages of plant development post-germination. This is demonstrated by the At-PDSi lines described here, in which a portion of the tested 2- or 4-week-old seedlings showed strong photobleaching after induction similar to that shown by transgenic plants with 35S-PDSi phenotypes. Moreover, the varying initiation and degrees of inducible gene silencing generate plants with a range of loss-of-function phenotype much like an allelic series, facilitating functional analysis.

Both heterozygous (line 1-1) and homozygous (line 1-2) progeny of At-PDSi line 1 retain the ability to reproduce inducible *PDS* silencing as the parental line, indicating that the inducible RNAi can be transmitted to the next generation. Having stable and reproducible RNAi transgenic lines would allow genetic crosses to be made and investigations of gene functions to be carried out with subsequent generations. Other silencing induction systems, such as *Agrobacterium* infiltration (Voinnet and Baulcombe, 1997) and infection with vectors derived from RNA viruses (Dalmay *et al.*, 2000; Ratcliff *et al.*, 2001) or DNA viruses (Peele *et al.*, 2001; Turnage *et al.*, 2002), have limited utility for functional genomics because of their transient nature, and the silencing effects are not heritable. Moreover, *Agrobacterium* infiltration cannot be applied to *Arabidopsis* because of its small plant size and clumpy rosette leaves. In the case of virus-induced gene silencing, some infected plants display stunted growth and they often do not produce inflorescences, flowers, or seeds (Turnage *et al.*, 2002). Moreover, disease symptoms caused by viral infection could confound the interpretation of the phenotype as a result of silencing of the target gene. By contrast, the inducible RNAi system described here can be triggered by simply treating plants with the inducer for a certain period of time. Treated plants display a specific silencing phenotype without any non-specific effects (see Figures 2a, 4e–h and 6b).

We have chosen the inducible Cre/loxP DNA excision system (CLX) rather than the XVE transient inducible system (Zuo *et al.*, 2000) to produce the inducible RNAi for several reasons. The mechanism for RNA silencing involves an initial induction process followed by a systemic spread of the silencing signal (for review, see Mlotshwa *et al.*, 2002). The local initiation of gene silencing by dsRNA is equally effective for both transgene and endogenous genes (Smith *et al.*, 2000; Wesley *et al.*, 2001). However, unlike the widespread, persistent silencing observed for a *GFP* transgene, systemic silencing of endogenous genes was transient and limited (Palauqui and Vaucheret, 1998; Voinnet *et al.*, 2000). Amplification of the signal is necessary for efficient systemic silencing (Palauqui and Vaucheret, 1998; Voinnet *et al.*, 1998). It has been proposed that the silencing signal is perpetuated by transgenes, but not by endogenous genes (Fagard and Vaucheret, 2000; Mlotshwa *et al.*, 2002). The CLX system can rescue the weak amplification of the silencing signal by endogenous genes. Once the Cre/*loxP*-mediated DNA excision occurred upon inducer treatment, expression of the downstream intron-containing dsRNA would be permanently activated. This situation mimics the expression of an RNAi using a constitutive promoter, which is the most efficient, effective, and high-throughput system for gene silencing, and the systemic spread of silencing signal is therefore not required. Expression of dsRNA from the inducible XVE system (Zuo *et al.*, 2000) without DNA recombination would require repeated applications of 17β-estradiol to the transgenic plants for sustained expression, and this may not be practical for plants growing in the soil.

The strong photobleaching induction in At-PDSi lines (lines 2, 5, 7, and 8) at post-germination stages is believed to be a result of complete DNA excision, which would reconstitute the G10-90-*PDSi* transcription unit to produce *PDSi* transcripts constitutively throughout the entire plant. In this case, no silencing signal amplification was required. This interpretation is consistent with our PCR analysis of At-PDSi lines (second group), displaying a delayed onset of gene silencing. In both line 1-1 and line 1-2 leaves, complete excision of DNA within the loxP sites showed strong photobleaching or patchy *PDS*-silencing phenotype. In near-green leaves where incomplete or no DNA excision was detected, only a weak systemic spread (weak signal amplification) of *PDS* silencing to upper rosette leaves was seen during the 18-day incubation with the inducer (Figure 5a–d). However, upon an additional week of growth after inducer withdrawal, strong *PDS* gene silencing was also detected in group 4 leaves and in the next two younger leaves (Figure 5f). These results suggest a limited systemic translocation of the silencing signal to two to three upper leaves.

Because of 17β-estradiol instability (Zuo *et al.*, 2000), a second or even multiple treatment with fresh inducer may

be needed to fully reactivate this RNAi system in some transgenic lines. With appropriate improvement of the induction conditions, a higher DNA excision efficiency, and therefore a higher proportion of lines showing strong induction, may be obtained. Nevertheless, the incomplete Cre/*loxP* DNA excision, which results in genetic chimera in transgenic plants, may provide a useful system to study mechanisms of long-distance signal transduction in gene silencing in *Arabidopsis*, which is difficult to graft (Turnbull *et al.*, 2002). The mechanisms involved in systemic RNA silencing in plant systems are being actively investigated using grafting and transient expression approaches with *N. benthamiana* or *N. tabacum* (Guo and Ding, 2002; Mallory *et al.*, 2001; Voinnet *et al.*, 2000). No mutations specific to systemic silencing have yet been reported in plant systems. Because of the small plant size and the clumpy rosette leaves, it is impossible to carry out localized infiltration of *Arabidopsis* with *Agrobacterium*, and grafting manipulation in *Arabidopsis* is also a challenging task. For these reasons, the ability to generate genetic chimera in transgenic *Arabidopsis* producing RNAi only from treated tissues would be very useful for future investigations. As shown by PCR analysis in At-PDSi line 1-1 and line 1-2, DNA excision occurred in lower rosette leaves, but not in upper rosette leaves. Gene silencing resulting from local RNAi induction (complete excision, Figure 5c,d) or signal-mediated long-distance (no excision) induction (Figure 5f) can be predicted by simple PCR analysis. The ability to generate genetic chimera in *Arabidopsis* may also find useful applications in research on other types of long-distance signaling (e.g. flowering time) in plants.

Experimental procedures

Plasmid construction

DNA manipulations and cloning were carried out using standard procedures (Sambrook *et al.*, 1989). The third intron of *Arabidopsis* actin gene 11 (ATU27981, nt 1957–2111) was selected for the intron-containing intermediate construct (pSK-int). This intron was amplified by PCR using two primers: Pint5′, 5′-TAC**GTAAGT**A-GATCTTCAACACC-3′; and Pint3′, 5′-GGAATT**CTGCA**AACACACA-AGACAAT-3′. The primers were designed such that their border sequences contained the consensus sequence (bold letters) for plant introns: AG//GTAAGT...TGCAG//G (Shapiro and Senapathy, 1987). Two restriction sites *Sna*BI and *Eco*RI (underlined) were added for cloning purposes. A PCR fragment of 155 bp was digested with *Sna*BI/*Eco*RI and cloned into *Eco*RV/*Eco*RI-digested pBluscript II SK+ to yield the intermediate construct pSK-int (Figure 1a).

To clone sequences encoding the inverted-repeat RNA into the pSK-int intermediate vector, a 357 bp fragment corresponding to nucleotides (nt) 360–716 of the *GFP* 3′-terminal sequence (Voinnet and Baulcombe, 1997) was cloned into the 5′ and 3′ arms of the intron (Figure 1a), and the resulting plasmid was named as pSK-*GFPi*. The 5′-terminal sequences of *PDS* of *A. thaliana* and *N. benthamiana* were obtained by RT-PCR amplification with specific primers. For *A. thaliana PDS*, the primers were: Pat5′, 5′-GACTAGTATGGTTGTGTTTGGGAATG-3′; and Pat3′, 5′-GATATCCTTCCATGCAGCTATC-3′. These primers were used to obtain a fragment of 405 bp corresponding to nt 128–532 of the *A. thaliana PDS* cDNA (L16237), and *Spe*I and *Eco*RV restriction sites (underlined) were added to the cDNA fragment. For PCR amplification of the *N. banthamiana PDS* sequence, the primers were: Pnb5′, 5′-GACTAGTATGCCTCAAATTGGACTTGT-3′; and Pnb3′, 5′-CAGCTG- TAGACAAACCACCCAAAC-3′ homologous to regions of the tomato *PDS* cDNA (M88683) nt 318–337 and nt 676–696, respectively. These primers were designed with the addition of *Spe*I and *Pvu*II restriction sites (underlined). Using *N. benthamiana* RNA as templates, a 386 bp fragment was obtained with RT-PCR, whose sequence exhibited high homology with the tomato *PDS* cDNA. RT-PCR fragments derived from *A. thaliana* (At) and *N. benthamiana* (Nb) were cloned into the pCR-Blunt vector (Invitrogen, USA) to give pCR-*PDS(At)* and pCR-*PDS(Nb)*, respectively. Fragments of *Spe*I–*Eco*RI and *Hin*dIII–*Xho*I were inserted into both arms of the intron of pSK-int digested with the appropriate restriction enzymes as shown in Figure 1(a) to obtain pSK-*PDSi(At)* and pSK-*PDSi(Nb)*, respectively.

For inducible dsRNA transformation constructs, the kanamycin-resistance gene in pX6-GFP (Zuo *et al.*, 2001) was replaced with a hygromycin-resistance gene, and the derivative called pX7-GFP. To create an inducible expression of intron-containing dsRNA, fragments of *Xho*I–*Xba*I from pSK-*GFPi*, pSK-*PDSi(At)*, and pSK-*PDSi(Nb)* were subcloned into pX7-GFP digested with *Xho*I/*Spe*I (*Xba*I and *Spe*I are compatible), resulting in pX7-*GFPi*, pX7-*PDSi(At)*, and pX7-*PDSi(Nb)*, respectively (Figure 1b).

In addition, the *Pst*I–*Sac*I fragment from pSK-*PDSi(At)* was cloned into a modified binary vector pCAMBIA-1300 (AF234296), which contained a 35S promoter and a 35S terminator, to give pCAMBIA-*PDSi(At)*, which is a constitutive RNAi construct (Figure 1c).

Upon request, vectors described in this paper are available to academic researchers for non-commercial projects.

Plant materials, transformation, and growth conditions

A transgenic *N. benthamiana* line (GFP-16c) carrying a 35S-*GFP* transgene with a kanamycin-selectable marker at a single locus in homozygous condition (Ruiz *et al.*, 1998) and a transgenic *A. thaliana* ecotype C24 line (Dalmay *et al.*, 2000) carrying a similar transgene were used for pX7-*GFPi* transformation. *A. thaliana* ecotype Columbia was used for pX7-*PDSi(At)* and pCAMBIA-*PDSi(At)* transformation. WT *N. benthamiana* was used for pX7-*PDSi(Nb)* transformation. *N. benthamiana* transformation was carried out by co-culture with *Agrobacterium*, whereas *A. thaliana* was transformed by the floral dip method (Clough and Bent, 1998). The selective medium contained MS medium plus hygromycin (20 mg l^{-1} for *A. thaliana* and 40 mg l^{-1} for *N. benthamiana*), whereas the inductive medium contained, in addition, 17β-estradiol (2 μM). GFP fluorescence was examined using a 100 W hand-held long-wavelength UV lamp.

Analyses of RNA and DNA

Total RNA was isolated from plant tissues by LiCl precipitation (Verwoerd *et al.*, 1989). The LiCl supernatant fraction was precipitated with 3 volumes of ethanol to obtain genomic DNA and low molecular weight RNA (siRNA). dsRNA was obtained by digesting total RNA with Rnase1™ (Promega, USA) (0.5 U Rnase μg^{-1} total RNA) at 37°C for 3 h. For Northern analysis, total RNA or dsRNA was separated on 1.2% agarose formaldehyde gels, transferred to

Hybond-N+ membranes, and hybridized with ^{32}P-labeled cDNA probes specific for the respective RNA. Low molecular weight RNA analysis was done as described (Hamilton and Baulcombe, 1999; Llave *et al.*, 2000). The probes for GFP and PDS siRNA were ^{32}P-labeled 3′-terminal 356 nt of GFP or 5′-terminal 400 nt of PDS antisense RNA, respectively, transcribed by T7 RNA polymerase. The PCR analysis with approximately 200 ng of genomic DNA was subjected to 94°C for 20 sec, 50°C for 20 sec, and 72°C for 2 min for 30 cycles. Primers for PCR analysis were: P1, 5′-GCCGCCACG-TGCCGCCACGTGCCGCC-3′; P2, 5′-CTCGTCAATTCCAAGGGCAT-CGGT-3′; P3, 5′-CTGGACACAGTGCCCGTGTCGGA-3′; P4, identical to Pint3′ for intron amplification (see Results).

Acknowledgements

We thank Dr David Baulcombe for seeds of transgenic *N. benthamiana* (line 16c) and transgenic *A. thaliana* carrying a 35S-*GFP* transgene.

References

Chuang, C.F. and Meyerowitz, E.M. (2000) Specific and heritable genetic interference by double-stranded RNA in *Arabidopsis thaliana*. *Proc. Natl. Acad. Sci. USA*, **97**, 4985–4990.

Clough, S.J. and Bent, A.F. (1998) Floral dip: a simplified method for *Agrobacterium*-mediated transformation of *Arabidopsis thaliana*. *Plant J.* **16**, 735–743.

Dalmay, T., Hamilton, A., Mueller, E. and Baulcombe, D.C. (2000) Potato virus X amplicons in *Arabidopsis* mediate genetic and epigenetic gene silencing. *Plant Cell*, **12**, 369–379.

Elbashir, S.M., Martinez, J., Patkaniowska, A., Lendeckel, W. and Tuschl, T. (2001) Functional anatomy of siRNAs for mediating efficient RNAi in *Drosophila melanogaster* embryo lysate. *EMBO J.* **20**, 6877–6888.

Fagard, M. and Vaucheret, H. (2000) Systemic silencing signal (s). *Plant Mol. Biol.* **43**, 285–293.

Fire, A., Xu, S., Montgomery, M.K., Kostas, S.A., Driver, S.E. and Mello, C.C. (1998) Potent and specific genetic interference by double-stranded RNA in *Caenorhabditis elegans*. *Nature*, **391**, 806–811.

Guo, H.S. and Ding, S.W. (2002) A viral protein inhibits the long range signaling activity of the gene silencing signal. *EMBO J.* **21**, 398–407.

Hamilton, A.J. and Baulcombe, D.C. (1999) A species of small antisense RNA in post-transcriptional gene silencing in plants. *Science*, **286**, 950–952.

Hare, P.D. and Chua, N.H. (2002) Excision of selectable marker genes from transgenic plants. *Nat. Biotechnol.* **20**, 575–580.

Llave, C., Kasschau, K.D. and Carrington, J.C. (2000) Virus-encoded suppressor of post-transcriptional gene silencing targets a maintenance step in the silencing pathway. *Proc. Natl. Acad. Sci. USA*, **97**, 13401–13406.

Mallory, A.C., Ely, L., Smith, T.H., Marathe, R., Anandalakshmi, R., Fagard, M., Vaucheret, H., Pruss, G., Bowman, L. and Vance, V.B. (2001) HC-Pro suppression of transgene silencing eliminates the small RNAs but not transgene methylation or the mobile signal. *Plant Cell*, **13**, 571–583.

Mlotshwa, S., Voinnet, O., Mette, M.F., Matzke, M., Vaucheret, H., Ding, S.W., Pruss, G. and Vance, V.B. (2002) RNA silencing and the mobile silencing signal. *Plant Cell*, **14** (Suppl.), S289–S301.

Ow, D.W. (2001) The right chemistry for marker gene removal? *Nat. Biotechnol.* **19**, 115–116.

Paddison, P.J., Caudy, A.A. and Hannon, G.J. (2002) Stable suppression of gene expression by RNAi in mammalian cells. *Proc. Natl. Acad. Sci. USA*, **99**, 1443–1448.

Palauqui, J.C. and Vaucheret, H. (1998) Transgenes are dispensable for the RNA degradation step of cosuppression. *Proc. Natl. Acad. Sci. USA*, **95**, 9675–9680.

Peele, C., Jordan, C.V., Muangsan, N., Turnage, M., Egelkrout, E., Eagle, P., Hanley-Bowdoin, L. and Robertson, D. (2001) Silencing of a meristematic gene using geminivirus-derived vectors. *Plant J.* **27**, 357–366.

Ratcliff, F., Martin-Hernandez, A.M. and Baulcombe, D.C. (2001) Technical advance. Tobacco rattle virus as a vector for analysis of gene function by silencing. *Plant J.* **25**, 237–245.

Ruiz, M.T., Voinnet, O. and Baulcombe, D.C. (1998) Initiation and maintenance of virus-induced gene silencing. *Plant Cell*, **10**, 937–946.

Sambrook, J., Fritsch, E.F. and Maniatis, T. (1989) *Molecular Cloning: a Laboratory Manual*. Cold Spring Harbor, NY: Cold Spring Harbor Laboratory Press.

Shapiro, M.B. and Senapathy, P. (1987) RNA splice junctions of different classes of eucaryotes: sequence statistics and functional implcations in gene expression. *Nucl. Acids Res.* **15**, 7155–7174.

Smith, N.A., Singh, S.P., Wang, M.B., Stoutjesdijk, P.A., Green, A.G. and Waterhouse, P.M. (2000) Total silencing by intron-spliced hairpin RNAs. *Nature*, **407**, 319–320.

Sui, G., Soohoo, C., Affar, el, B., Gay, F., Shi, Y., Forrester, W.C. and Shi, Y. (2002) A DNA vector-based RNAi technology to suppress gene expression in mammalian cells. *Proc. Natl. Acad. Sci. USA*, **99**, 5515–5520.

Turnage, M.A., Muangsan, N., Peele, C.G. and Robertson, D. (2002) Geminivirus-based vectors for gene silencing in *Arabidopsis*. *Plant J.* **30**, 107–114.

Turnbull, C.G., Booker, J.P. and Leyser, H.M. (2002) Micrografting techniques for testing long-distance signalling in *Arabidopsis*. *Plant J.* **32**, 255–262.

Verwoerd, T.C., Dekker, B.M. and Hoekema, A. (1989) A small-scale procedure for the rapid isolation of plant RNAs. *Nucl. Acids Res.* **17**, 2362.

Voinnet, O. and Baulcombe, D.C. (1997) Systemic signalling in gene silencing. *Nature*, **389**, 553.

Voinnet, O., Lederer, C. and Baulcombe, D.C. (2000) A viral movement protein prevents spread of the gene silencing signal in *Nicotiana benthamiana*. *Cell*, **103**, 157–167.

Voinnet, O., Vain, P., Angell, S. and Baulcombe, D.C. (1998) Systemic spread of sequence-specific transgene RNA degradation in plants is initiated by localized introduction of ectopic promoterless DNA. *Cell*, **95**, 177–187.

Waterhouse, P.M., Graham, M.W. and Wang, M.B. (1998) Virus resistance and gene silencing in plants can be induced by simultaneous expression of sense and antisense RNA. *Proc. Natl. Acad. Sci. USA*, **95**, 13959–13964.

Wesley, S.V., Helliwell, C.A., Smith, N.A. *et al.* (2001) Construct design for efficient, effective and high-throughput gene silencing in plants. *Plant J.* **27**, 581–590.

Winston, W.M., Molodowitch, C. and Hunter, C.P. (2002) Systemic RNAi in *C. elegans* requires the putative transmembrane protein SID-1. *Science*, **295**, 2456–2459.

Zuo, J., Niu, Q.W. and Chua, N.H. (2000) Technical advance: an estrogen receptor-based transactivator XVE mediates highly inducible gene expression in transgenic plants. *Plant J.* **24**, 265–273.

Zuo, J., Niu, Q.W., Moller, S.G. and Chua, N.H. (2001) Chemical-regulated, site-specific DNA excision in transgenic plants. *Nat. Biotechnol.* **19**, 157–161.

Exhibit 8

The Plant Journal (2003) **36**, 731–740 doi: 10.1046/j.1365-313X.2003.01914.x

TECHNICAL ADVANCE

Temporal and spatial control of gene silencing in transgenic plants by inducible expression of double-stranded RNA

Shuai Chen, Daniel Hofius, Uwe Sonnewald and Frederik Börnke*
Institut für Pflanzengenetik und Kulturpflanzenforschung (IPK), Corrensstrasse 3, 06466 Gatersleben, Germany

Received 3 June 2003; revised 31 July 2003; accepted 4 September 2003.
*For correspondence (fax +49 39482 5515; e-mail boernke@ipk-gatersleben.de).

Summary

Downregulation of endogenous genes via post-transcriptional gene silencing (PTGS) is a key to the characterization of gene function in plants. The recent discovery that double-stranded RNA (dsRNA) is an extremely effective trigger of gene silencing greatly enhanced the predictability of this approach. However, strong constitutive silencing often leads to pleiotropic effects, which make it difficult to directly relate phenotype to gene function, or even interferes with the recovery of viable transgenic plants. Here, we show that strong genetic interference can be achieved in a chemically inducible fashion, allowing for temporal and spatial control of gene silencing in transgenic plants. To this end, transgenic tobacco plants were established expressing dsRNA in the form of intron-spliced hairpin structures under the control of the ethanol-inducible *alc* gene expression system. Targeting magnesium (Mg)-chelatase subunit I (*Chl I*) and glutamate 1-semialdehyde aminotransferase (*GSA*), both involved in chlorophyll (chl) biosynthesis, resulted in rapid and specific mRNA degradation upon induction with ethanol. Ethanol-inducible silencing of the target genes caused strong but transient phenotypical alterations featured by a progressive loss of chl in young leaves, which persisted for about 7–9 days before newly growing leaves completely recovered. About 10–30% of the primary transformants showed phenotype development upon induction. Local silencing of *Chl I* could be achieved by confined ethanol treatment of a single leaf without affecting any other part of the plant. Inducible gene silencing using the *alc* system promises to obviate the problems associated with constitutive RNA silencing and enables to dissect primary and secondary effects of PTGS at temporal and spatial resolution.

Keywords: chemically inducible expression, ethanol, double-stranded RNA, gene silencing, functional genomics, *Nicotiana tabacum*.

Introduction

The recent completion of the *Arabidopsis thaliana* genome sequence (The Arabidopsis Genome Initiative, 2000) and the accumulation of sequence data from a number of other model plants and important crop species, such as rice (Goff *et al.*, 2002; Yu *et al.*, 2002), have provided a vast new resource to define gene function at the morphological, biochemical, or physiological level. A critical step in exploiting these genomic resources, however, depends on the development of novel tools and approaches for the functional analysis of a given gene. In the past, the use of loss-of-function or reduced-expression mutants has proven to be a powerful tool to relate a mutant phenotype to the function of a particular gene. Traditionally, these reverse genetic approaches rely on transposon insertions or classic genetic screens (for review, see Page and Grossniklaus, 2002). However, their use is limited by the untargeted nature of the mutagenesis and their restriction to a few genetically tractable plant species. The discovery of the antisense phenomenon of plant gene silencing (van der Krol *et al.*, 1988; Smith *et al.*, 1988), and subsequently co-suppression (van der Krol *et al.*, 1990; Napoli *et al.*, 1990), provided an alternative means for investigating the role of specific gene products in plant growth and metabolism and has been particularly versatile in studying plant primary metabolism (Frommer and Sonnewald, 1995; Stitt and Sonnewald, 1995). The antisense and co-suppression

phenomena are collectively referred to as post-transcriptional gene silencing (PTGS), which describes a nucleotide sequence-specific RNA degradation process naturally providing a defense mechanism against invasive nucleic acids such as viruses, transposons, and transgenes (Baulcombe, 2002; Matzke *et al.*, 2001; Vance and Vaucheret, 2001; Voinnet *et al.*, 1998). A set of mechanistically related pathways were also found in fungi (quelling) and in animals (RNA interference (RNAi)) and requires a conserved set of gene products (for recent reviews, see Carthew, 2001; Cogoni and Macino, 2000; Plasterk, 2002). According to current models of PTGS, an endogenous RNA-dependent RNA polymerase initially synthesizes a double-stranded RNA (dsRNA) molecule using the target transcript as template (Dalmay *et al.*, 2000; Mourrain *et al.*, 2000), which is subsequently processed into 21–25 ntRNA fragments of both polarities (Hamilton and Baulcombe, 1999). These short interfering RNAs (siRNAs) are then incorporated into a dsRNA-induced silencing complex (RISC) to guide cycles of specific RNA degradation (Hammond *et al.*, 2000; Tang *et al.*, 2003; Zamore *et al.*, 2000). In some experiments, however, when conventional antisense and co-suppression constructs are used to trigger PTGS, RNA-silencing occurs only in a portion of the transformants or their progenies or the constructs even fail to induce silencing, rendering these approaches largely ineffective. Recently, considerable progress in effectively triggering PTGS has been made by using constructs designed to express dsRNA fragments, usually in the form of self-complementary hairpin RNA, consistently yielding a high degree and frequency of PTGS. This often gives rise to phenotypes that resemble those of the null alleles of the target genes (Chuang and Meyerowitz, 2000; Levin *et al.*, 2000; Smith *et al.*, 2000). However, because of the high degree of silencing, which is achieved by this method, functional analysis of a particular gene product required during plant transformation and regeneration from culture is limited, as viable plants might not be recovered. Moreover, constitutive gene silencing consistently entails pleiotropic effects, which might superimpose the primary impact of reduced gene expression and thus mask true gene function. This is especially true, if metabolic processes are under scrutiny, as the observed phenotype could rather reflect a physiological adaptation to the loss of a metabolic function than a primary response to the latter. To overcome these problems a system for inducible gene silencing of candidate genes would be highly desirable.

The problems have partially been solved by the introduction of virus-induced gene silencing (VIGS) systems where a recombinant virus carrying a partial sequence of a host gene is used to infect the plant. When the virus spreads systemically, the endogenous transcripts, which are homologous to the insert in the viral vector, are degraded by PTGS (Baulcombe, 1999). Although several VIGS vectors have been described (Gosselé *et al.*, 2002; Holzberg *et al.*, 2002; Liu *et al.*, 2002; Ratcliff *et al.*, 2001; Turnage *et al.*, 2002), these approaches suffer from a number of shortcomings. First, the use of each system is restricted by the host range of the virus it is derived from and thus no such system is broadly applicable to a wide range of plant species. Second, the VIGS phenotype is superimposed, and sometimes complicated, by at least mild disease symptoms of virus infection, which cause significant biochemical perturbations not directly linked to the suppression of the target gene. This causes problems especially in physiological investigations. Most of these limitations should be overcome by the use of a chemically inducible promoter to drive expression of the silencing construct, allowing the investigator to control when a specific gene will be inactivated. The optimal system would employ a non-toxic inducer with high specificity and minimal potential to elicit physiological responses. Moreover, the system should have the capacity to achieve high level of expression but with a concomitant negligible activity in the absence of the inducer. One such system is the *alc* gene switch based on a regulon derived from the filamentous fungus *Aspergillus nidulans* (Caddick *et al.*, 1998; Roslan *et al.*, 2001; Salter *et al.*, 1998). In plants, the system basically consists of two modules: the AlcR transcriptional regulator expressed from the cauliflower mosaic virus (CaMV) 35S promoter and a modified *alc*A promoter in front of the gene of interest. In the presence of ethanol, AlcR binds to the modified *alc*A promoter and drives expression of the target gene. Several studies demonstrated the efficiency of the *alc* system in a wide range of plant hosts, including *Arabidopsis, Brassica napus, Nicotiana tabacum,* and potato tubers (Caddick *et al.*, 1998; Junker *et al.*, 2003; Roslan *et al.*, 2001; Salter *et al.*, 1998; Sweetman *et al.*, 2002). Induction of the system can be achieved by either root drenching of the plants with ethanol solution (Caddick *et al.*, 1998; Roslan *et al.*, 2001; Salter *et al.*, 1998) or exposing the plants to ethanol vapor (Sweetman *et al.*, 2002). Alternatively, the *alc* gene switch can also be activated by other related chemicals. A recent study demonstrated a more rapid induction of the system upon the application of acetaldehyde, the physiological inducer of the *alc* regulon in *A. nidulans*, than that of ethanol (Junker *et al.*, 2003).

We initiated the study described herein to determine whether the *alc* system can be used to achieve inducible gene silencing in transgenic tobacco. To this end, nuclear genes involved in the chlorophyll (chl) biosynthetic pathway were targeted, because it was assumed that the host gene silencing would be easy to visualize and quantify as loss of chl. Our data demonstrate that transgenic tobacco plants designed to express double-stranded hairpin constructs under the control of the ethanol responsive promoter exhibit a rapid but transient development of the characteristic phenotype upon induction. Using repeated application of ethanol, extended periods of gene silencing

could be maintained. We further show that spatial silencing of a target gene could be achieved by ethanol treatment of a single tobacco leaf. With these attributes, inducible PTGS using the *alc* system promises to extend the kind of silencing studies that can be carried out in transgenic plants, in particular, with respect to temporal and spatial resolution of silencing effects, rendering the system extremely useful for metabolic studies.

Results

Construction of silencing vectors and plant transformation

To evaluate the suitability of the *alc* system for inducible gene silencing, two nuclear target genes were selected, which have previously been described to yield a readily discernable phenotype in conventional antisense experiments. Magnesium (Mg)-chelatase is a heteromeric enzyme complex composed of three-subunits (designated CHL I, CHL H, and CHL D) that catalyzes the incorporation of Mg^{2+} into protophorphyrin IX, which represents the first committed step in chl biosynthesis. Antisense suppression of *Chl I* in transgenic tobacco led to a strongly reduced green pigmentation as a result of the decreased chl biosynthetic capacity (Papenbrock *et al.*, 2000). A key regulatory step in tetrapyrrole biosynthesis in higher plants, providing the precursors for chl and heme synthesis, is the formation of 5-aminolevulinate catalyzed by the activity of glutamate 1-semialdehyde aminotransferase (GSA). Expression of GSA antisense RNA in tobacco plants results in a decline in chl content apparently leading to pale leaves (Höfgen *et al.*, 1994).

Constructs for inducible expression of dsRNA in transgenic plants were assembled in the appropriate plant transformation vector (Caddick *et al.*, 1998), which contained the *AlcR* gene driven by the constitutive CaMV 35S promoter and gene-specific fragments in sense and antisense orientation interspersed by a short intron under control of the modified *alcA* promoter (alc-*dsRNA* gene cassette, Figure 1). In parallel, inducible antisense constructs were made to target *Chl I* and *GSA*, respectively, by putting the corresponding antisense fragment under the control of the ethanol-inducible promoter (alc-*anti* gene cassette, Figure 1). After *Agrobacterium*-mediated gene transfer (Rosahl *et al.*, 1987), 80 primary transformants for each construct were transferred to the greenhouse. Prior to the application of ethanol, all transgenic plants were indistinguishable from wild-type plants, indicating that the promoter was not leaky. Northern analysis of transgene-specific dsRNA further confirmed tight control of the promoter under un-induced conditions in that no detectable levels of dsRNA were present prior to the application of the

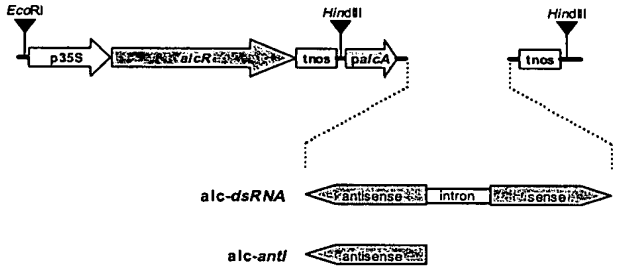

Figure 1. Diagrammatic representation (not to scale) of *alc*-system-derived silencing constructs.
The *alcR* cDNA is under control of the *CaMV 35S* (*p35S*) promoter and positioned upstream of the *nos* terminator (*tnos*). The alc-*dsRNA* construct contains either a *Chl I* or *GSA* fragment in antisense and sense orientation separated by intron 1 of potato GA20 oxidase (200 bp) in spliceable orientation. The alc-*antisense* construct comprises simply the respective antisense fragment. In both constructs, all fragments were inserted downstream of the chimeric *palcA* promoter, which consists of the *CaMV 35S* minimal promoter (−31 to +5) fused at the TATA-box to upstream promoter sequences of *alcA* (Caddick *et al.*, 1998).

inducer (data not shown). However, after ethanol induction, 26 (33% efficiency) of the alc-*dsChl I* transgenics and 10 (13% efficiency) of the alc-*dsGSA* plants displayed the characteristic phenotype previously described from constitutively silenced plants. Phenotypes of individual transformants varied from heavily bleached leaves with only small green areas remaining (11 alc-*dsChl I* and 4 alc-*dsGSA* plants, respectively) to variegation patterns of likewise green and yellow to white patches (six alc-*dsChl I* and three alc-*dsGSA* plants, respectively) and pale areas along the major leaf veins (nine alc-*dsChl I* and three alc-*dsGSA* plants, respectively). The overall efficiency using the *alc* system for inducible gene silencing was much lower than that of the recently published inducible RNAi system based on estradiol induction (Guo *et al.*, 2003). Whether this was because of differences in constructs or vectors or because of a species difference is currently unknown.

Specific silencing of the target gene in phenotypically affected plants was further confirmed by Northern blotting using gene-specific probes (data not shown). Reduction in *Chl I* and *GSA* mRNA steady state level correlated with the strength of the observed phenotype. Contrastingly, none of the plants solely expressing the antisense fragment targeted against *Chl I* and *GSA* displayed any visible phenotype upon induction (data not shown). Northern blotting was applied to screen for individuals expressing the respective antisense transgenes. Several plants expressing considerable amounts of the antisense transcript could be identified for each construct (data not shown). From these data, we conclude that ethanol-inducible expression of dsRNA causes silencing of endogenous genes comparable to that in constitutively silenced plants. Selected primary transformants for each construct were selfed and the T1 generation was subject to a detailed analysis.

*Rapid and reversible phenotypical changes in plants containing alc-*dsRNA *expression cassettes*

Three alc-*dsChl I* lines (14, 16, and 45), and two alc-*dsGSA* lines (60 and 70) were chosen for a detailed analysis according to their strong inducible phenotype observed in the T_0 generation. Seeds were germinated on kanamycin-containing medium and resistant seedlings were analyzed 4 weeks after transfer to soil. Application of 1% ethanol by root drenching led to the development of the characteristic phenotype featured by the loss of chl. The phenotype started to develop approximately 36 h post-induction (hpi) for alc-*dsChl I* lines and approximately 48 hpi for alc-*dsGSA* lines, and was first visible in the top leaves (Figure 2). The bleached patches expanded as the leaves grew, and also appeared in nascent leaves over a period of

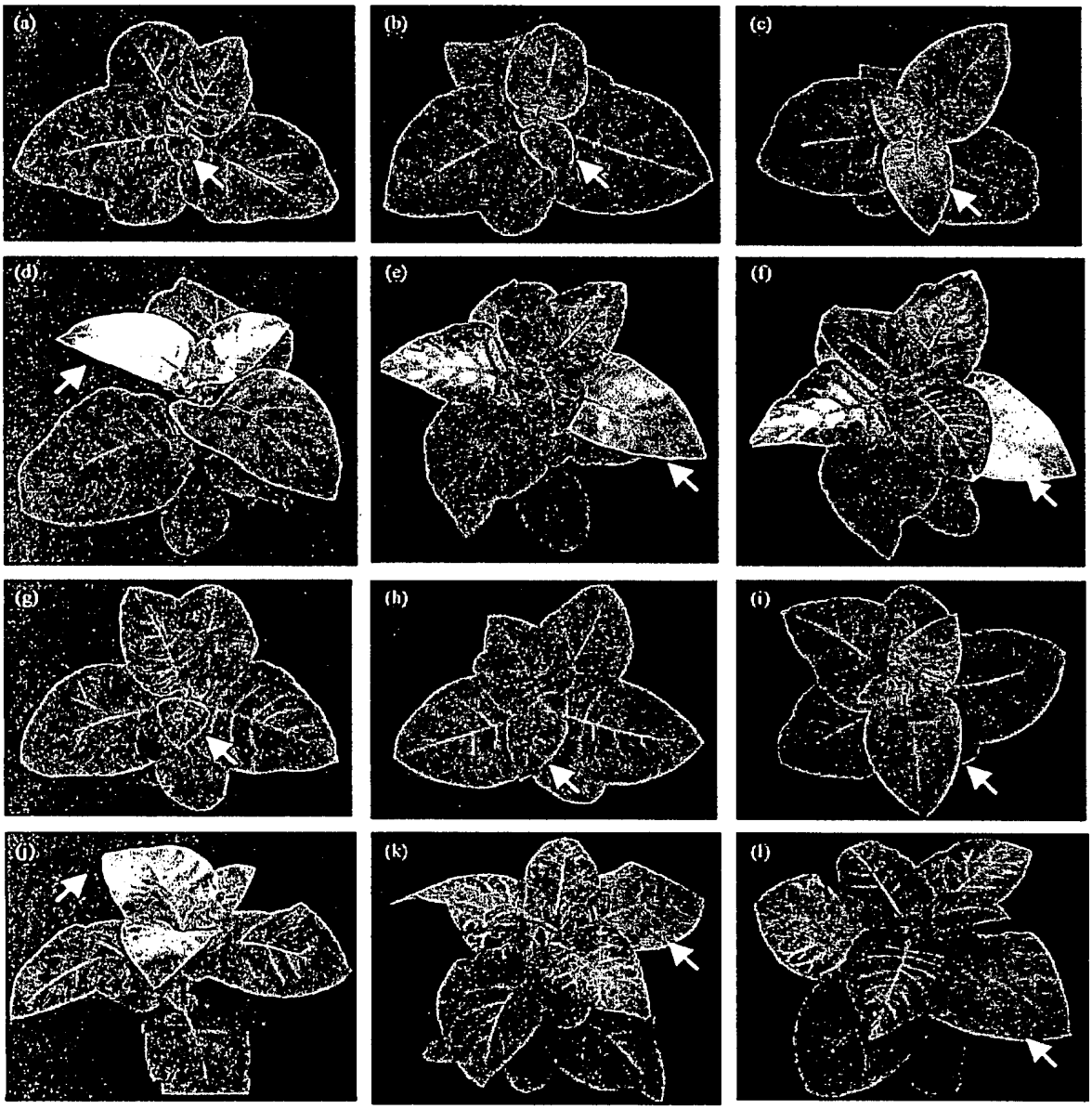

Figure 2. Time course of phenotype development in alc-*dsRNA* lines after application of ethanol.
(a–f) alc-*dsChl I* line 16 before, and 2, 4, 5, 9, and 12 dpi, respectively.
(g–l) alc-*dsGSA* line 60, before, and 2, 4, 5, 7, and 9 dpi. The arrow indicates the type of leaf that has been followed for molecular analyses.
Plants (42 days old) were induced via root drenching with 100 ml 1% (v/v) ethanol and photographs were taken at different time points.

7–9 days. After that, newly emerging leaves looked like the wild type again while those initially affected never recovered. Whether this was because of the developmental control of chl-synthesizing enzymes (Härtel *et al.*, 1997; He *et al.*, 1994) or because of stable silencing is currently unknown. Leaves that were mature prior to induction always remained green. Upon a second induction, the silencing phenotype could be re-established in the newly grown leaves of transgenic plants (data not shown).

In some cases, the silencing effect caused by a single induction might be too transient to reveal the full sequence of consequences of reduced gene expression. In order to investigate whether extended periods of gene silencing could be achieved by repeated ethanol treatments, alc-*dsChl I* plants were root-drenched with 1% ethanol every 2 days for 15 days in total. Phenotypic changes became apparent 2 days post-induction (dpi) but, in contrast to the single-induction experiments, they were maintained over the entire period of ethanol treatment (Figure 6b). Therefore, using re-iterated treatments, extended periods of gene silencing can be maintained.

Kinetics of inducible gene silencing

In order to follow the kinetics of target transcript reduction in alc-*dsRNA* lines, samples were taken from leaves expected to become phenotypically affected at different time points after application of ethanol. To compensate for plant-to-plant variation, at least three plants were probed at each time point and samples were pooled after preparation of total RNA. Northern analysis revealed that the *Chl I* mRNA was significantly reduced as early as 8 h after ethanol induction. Transcript levels further declined to undetectable levels at 48 hpi so as to rise again from 72 hpi onwards. The initial amount was reached again at approximately 9 dpi in newly emerging leaves, which were phenotypically normal (Figure 3a). *Chl I* transcript levels in ethanol-treated wild-type plants remained stable over the time course of the experiment (data not shown). Similar kinetics of target transcript decay and duration of mRNA downregulation was observed in the alc-*dsGSA* plants (Figure 3b). In the line under investigation (line 60), an additional band migrating above the endogenous *GSA* transcript appeared upon induction and was detectable upto 48 hpi. As PTGS has been shown to affect RNA processing (Mishra and Hanada, 1998), we used RT-PCR to investigate whether splicing of the endogenous *GSA* messenger was impaired in these plants. No PCR product that could possibly represent an incompletely spliced RNA was detected. However, if primers specific for the intron included in the transgene construct were used, a weak but specific band was amplified (data not shown). Therefore, the additional band on the *GSA* Northern blot was tentatively assigned to the unspliced intron-containing inverted-repeat fragment. This band was never observed in any other alc-*dsGSA* line; however, line 60 had the strongest phenotype and high expression of the transgene might interfere with its correct splicing because of sub-optimal splice sites.

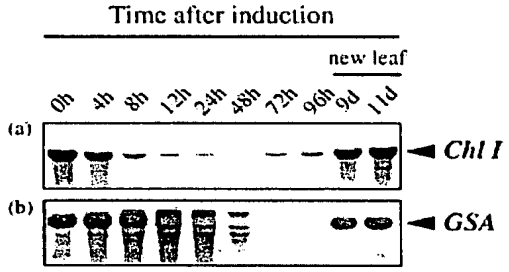

Figure 3. Efficient downregulation of target mRNA following ethanol-inducible expression of dsRNA constructs.
(a) Time course of *Chl I* transcript degradation in alc-*dsChl I* plants (line 16).
(b) Time course of *GSA* mRNA degradation in alc-*dsGSA* plants (line 60).
Transgenic tobacco plants (42 days old) were induced with 100 ml 1% (v/v) ethanol via root drenching. Leaves were followed being *c.* 5 cm in size at the time point of induction. After the indicated periods of time, total RNA was isolated and Northern blot hybridization was performed with the respective cDNA probe. At 9 and at 11 dpi, newly grown leaves were taken for the analysis.

In order to follow the silencing process in alc-*dsGSA* lines on the protein level, samples were taken from the same leaves as before and subjected to a Western analysis using GSA-specific antibodies (kindly provided by Dr B. Grimm, Humboldt University, Berlin, Germany). Within 48 hpi, a considerable reduction of the GSA amount occurred in the transgenics (Figure 4), which is in good accordance with phenotype development in these plants. No detectable protein was observed 72–96 hpi. When newly developing leaves were probed for GSA 9 dpi, the amounts were comparable to those before induction.

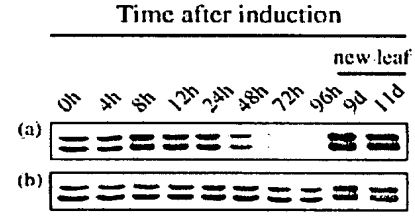

Figure 4. Time course of GSA protein degradation in alc-*dsGSA* plants after ethanol treatment.
(a) Level of GSA protein in alc-*dsGSA* plants (line 60) after induction.
(b) Ethanol-treated control plants.
Plants (42 days old) were induced with 100 ml 1% (v/v) ethanol via root drenching. Leaves were followed being *c.* 5 cm in size at the time point of induction. After the indicated periods of time, total protein was prepared and Western blot analysis was performed using an anti-GSA antibody. At 9 and at 11 dpi, newly grown leaves were taken for the analysis.

Changes in chlorophyll contents upon induction of gene silencing

In order to investigate the degree of gene silencing, which could be achieved with the ethanol-inducible system compared to plants constitutively silenced for *GSA* and *Chl I* (Höfgen *et al.*, 1994; Papenbrock *et al.*, 2000), the decrease in chl content in phenotypically affected leaves over time was taken as an indirect measure for chl biosynthetic capacity. Therefore, leaves were followed that were approximately 5 cm in length at the time point of induction. Samples were taken at different time points and analyzed for their chl content. To compensate for local variations within a plant, two samples were taken from each leaf. To compensate for plant-to-plant variation, at least five plants were harvested at each time point for each construct tested. After application of ethanol, a gradual decline in chl content was observed in lines expressing dsRNA constructs (Figure 5), whereas chl content in ethanol-treated control plants increased over the time course of the experiment as a result of the developmental control of chl biosynthesis. In case of alc-*dsChl I* plants, the progressive loss of chl became apparent as early as 24 hpi, while ethanol-treated alc-*dsGSA* plants lost their chl more slowly. This is in good accordance with the temporal differences in phenotype development of the two mutants. Seven days post-induction, chl content in alc-*dsChl I* plants was only approximately 3% of that before treatment, whereas chl content in phenotypically affected leaves of alc-*dsGSA* was reduced to levels of about 20% of those before treatment.

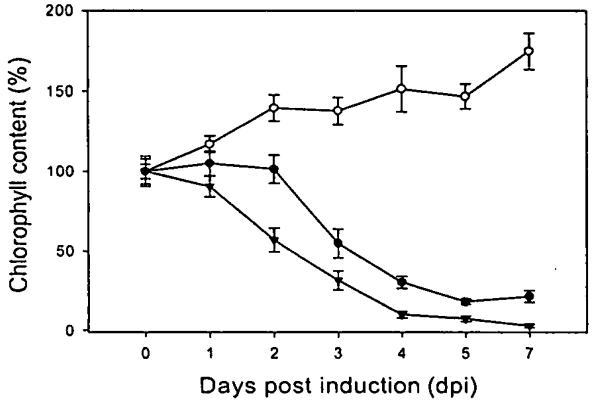

Figure 5. Changes in chl content in alc-*dsRNA* transgenic plants after ethanol induction.
Control plants (○), alc-*dsGSA* line 60 (●), and alc-*dsChl I* line 16 (▼) were induced with 100 ml 1% (v/v) ethanol via root drenching, and chl content was measured at the times indicated. Samples were taken from leaves being c. 5 cm in size at the time of induction until 7 dpi. The chl content is expressed as a value relative to that at day 0. Bars show the SD of five replicates.

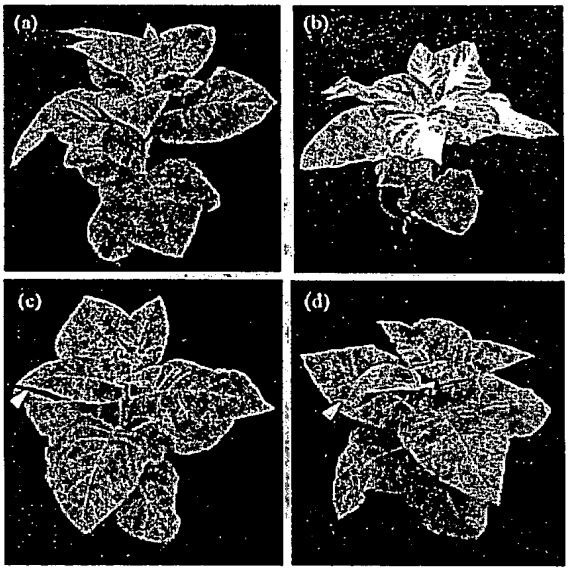

Figure 6. Temporal and spatial control of *Chl I* gene silencing.
(a, b) Wild-type (a) and alc-*dsChl I* (b) plants (line 16) were root-drenched with 1% ethanol solution every 2 days. The pictures were taken at 15 dpi.
(c, d) Local *Chl I* silencing. The leaf indicated by an arrow was enclosed with 3 ml of 4% (v/v) ethanol for 48 h. (c), wild-type control plant; (d), alc-*dsChl I* plant from line 16.

Spatial control of gene silencing using the alc *system*

Previous studies demonstrated that spatial induction of *alc*-reporter gene constructs could be achieved by exposing single leaf to ethanol vapor (Sweetman *et al.*, 2002). In order to test whether this was also possible for inducible gene silencing, an individual leaf of an alc-*dsChl I* plant was exposed to ethanol vapor using a similar 'bagging' experiment as described before by Sweetman *et al.*, (2002). As shown in Figure 6(d), the respective leaf displayed the typical symptoms of *Chl I* downregulation observed in whole plant induction experiments. The phenotype was restricted to the treated leaf only, indicating that neither transport of ethanol into adjacent parts of the plant nor spread of silencing occurred. Thus, our data demonstrate that confined vapor treatment allows for spatial control of gene silencing using the *alc* system.

Discussion

Downregulation of endogenous genes via PTGS using sense or antisense constructs is a crucial tool to assess gene function in transgenic plants. Recent findings indicate that expression of self-complementary hairpin RNAs greatly enhances the efficacy of such experiments (Chuang and Meyerowitz, 2000; Levin *et al.*, 2000; Smith *et al.*, 2000; Stoutjesdijk *et al.*, 2002; Waterhouse *et al.*, 1998). Although

these approaches have been proven to be extremely useful, they are not without problems. One drawback of these studies is that constitutive gene silencing often entails pleiotropic effects on growth and development of the transgenic plants, which complicate the interpretation of the phenotype and might mask true gene function. Furthermore, if expression of the target gene is essential for early growth or regeneration during tissue culture, vital plants might not be recovered. Here, we show that temporal and spatial control of gene silencing in transgenic plants can be achieved by ethanol-inducible expression of dsRNA constructs using the *alc* system.

We used two genes involved in chl biosynthesis, namely *Chl I* and *GSA*, to test downregulation by ethanol-inducible expression of antisense fragments and dsRNA constructs, respectively. Suppression of either of the two target genes was assumed to result in a loss of pigmentation because of reduced chl biosynthesis (Höfgen *et al.*, 1994; Papenbrock *et al.*, 2000). However, only constructs giving rise to dsRNA were effective in triggering gene silencing, as revealed by rapid development of the characteristic phenotype after induction with ethanol. Constructs designed to express conventional antisense fragments failed to interfere with expression of the target gene, which was further confirmed by Northern blotting. This is consistent with the assumption that dsRNA is a much stronger trigger of PTGS than ssRNA, possibly by circumventing the initial conversion of ssRNA into dsRNA by an RNA-dependent RNA polymerase (Béclin *et al.*, 2002; Dalmay *et al.*, 2000). First signs of phenotype development occurred at 36 hpi for alc-*dsChl I* to 48 hpi for alc-*dsGSA*, most likely reflecting differences in mRNA and protein turnover rates of the respective endogene. The time point of phenotype development was highly reproducible in several independent induction experiments (data not shown) and is much more rapid than the 10 days to 3 weeks, which have been reported to be necessary for phenotype induction using various virus-based gene silencing systems (Gosselé *et al.*, 2002; Hiriart *et al.*, 2002; Ratcliff *et al.*, 2001; Turnage *et al.*, 2002). Using a single induction, the phenotype persisted for approximately 9 days, which is considerably shorter than what has been shown for VIGS (Gosselé *et al.*, 2002; Ratcliff *et al.*, 2001; Turnage *et al.*, 2002). However, re-iterated ethanol treatment permits to maintain stable silencing for extended periods, which should enable to follow the full sequence of consequences of reduced gene expression whenever desirable.

One of the most interesting features of gene silencing is that it can act non-cell-autonomously, meaning that it can be induced locally and subsequently spread throughout the organism, implying the existence of a mobile silencing signal (Klahre *et al.*, 2002; Palauqui *et al.*, 1997; Voinnet *et al.*, 1998). Little is known about the nature of the signal, but it seems likely that the sequence-specific component is an RNA (Boutla *et al.*, 2002; Mlotshwa *et al.*, 2002). However, evidence suggests that highly expressed transgenes are much better for systemic silencing than are endogenous genes, suggesting that the amount of target RNA is important in establishing systemic silencing in response to the mobile signal (Palauqui and Vaucheret, 1998; Palauqui *et al.*, 1997; Voinnet *et al.*, 1998). This is consistent with the finding that using the *alc* system, local silencing of *Chl I* could be achieved by confined ethanol treatment of a single leaf. In this case, no other parts of the plant but the treated leaf displayed any visible signs of *Chl I* silencing, indicating that no systemic spread of PTGS occured. Spatial control of gene silencing is desirable in some situations, for instance to study the function of widely expressed genes on an organ or tissue basis without affecting the entire plant. On the other hand, the system allows for the investigation of physiological perturbations on the whole plant level, which were caused by local silencing of a particular gene.

To determine the degree of silencing, which could be achieved by inducible expression of dsRNA constructs on the biochemical level, the decline in chl content in phenotypically affected leaves was taken as an indirect measure for chl biosynthetic capacity. A reduction in chl of approximately 80% was achieved in alc-*dsGSA* plants, which is in the range of what has been reported for transgenic tobacco plants constitutively expressing *GSA* antisense RNA (Höfgen *et al.*, 1994). Transgenic tobacco plants constitutively silenced for *Chl I* were shown to have approximately 40% of the chl content as compared to the control (Papenbrock *et al.*, 2000). Inducible silencing of *Chl I* using the *alc* system reduced the chl content in phenotypically affected leaves to approximately 3% of that before induction, indicating a much stronger effect on *Chl I* expression than that in constitutively silenced plants. It is reasonable to assume that in case of constitutive silencing, there is a considerable selection against the reduction of Mg-chelatase activity below a certain threshold level, which does not support plant growth under autotrophic conditions. Thus, in some cases, inducible PTGS using the *alc* system is likely to provide a valid strategy to obtain a degree of silencing, which otherwise prevents the regeneration of viable transgenics.

Recently, an alternative system to achieve chemical-regulated inducible gene silencing has been described, which takes advantage of 17β-estradiol-inducible recombination to trigger the expression of an intron-containing inverted-repeat RNA (CLX system; Guo *et al.*, 2003). In this case, induction of the system leads to permanent activation of PTGS mimicking expression from a constitutive promoter. However, because of the nature of the inducer, the CLX system might not be readily applicable to soil-grown plants, and thus its use in physiological studies is limited.

In summary, the data presented here demonstrate the utility of the *alc* gene system to achieve transient gene

silencing by inducible expression of dsRNA constructs. The *alc* system offers an enormous flexibility with respect to time point of induction, expression level, spatial control, and duration of expression, and is applicable to a variety of plant species. In contrast to other chemically regulated systems, ethanol, or alternatively acetaldehyde, is comparatively a benign inducer and exerts only minimal physiological side-effects in concentrations necessary for induction (Junker *et al.*, 2003). These attributes greatly enhance the reproducibility of silencing experiments, which is of particular importance in metabolic studies requiring a large population of uniformly silenced individuals. The system provides a powerful tool to investigate molecular and physiological alterations associated with repression of a target gene at temporal and spatial resolution. Thus, dissection of primary and secondary effects of gene silencing should be greatly facilitated, allowing more precise predictions of gene function.

Experimental procedures

Transgenic plants, growth, and maintenance

Tobacco plants (*N. tabacum* cv. Samsun NN) were obtained from Vereinigte Saatzuchten eG (Ebsdorf, Germany) and grown in tissue culture under a 16-h light/8-h dark regime (irradiance 150 μmol quanta m^{-2} sec^{-1}) at 50% humidity on Murashige and Skoog medium (Sigma, St Louis, MO, USA) containing 2% (w/v) sucrose. Plants in the greenhouse were kept in soil under a light/dark regime of 16 h light (25°C) and 8 h (20°C) dark.

Plasmid construction and plant transformation

All constructs for plant transformation were cloned into p35S:*alcR*, a derivative of pBin19 (Bevan, 1984), carrying the *alcR* gene from *A. nidulans* between the CaMV 35S promoter and the *nos* terminator (Caddick *et al.*, 1998) using standard procedures (Sambrook *et al.*, 1989). Fragments containing portions of the respective target gene in sense and antisense orientation separated by an intron were initially assembled into a pUC-based vector. To this end, the first intron of the gibberellin 20 (GA20) oxidase gene from *Solanum tuberosum* (kindly provided by S. Biemelt, IPK Gatersleben, Germany) was PCR amplified using the primers 5′-cctgcaggctcgagactagtagatctggtacggaccgtactactcta-3′ and 5′-cctgcagggtcgactctagaggatcccctatataatttaagtggaaaa-3′. The oligonucleotides were designed to introduce *Pst*I/*Xho*I/*Spe*I/*Bgl*II sites at the 5′ end and *Bam*HI/*Xba*I/*Sal*I/*Pst*I sites at the 3′ end, into the resulting PCR product. The 200-bp intron fragment was inserted into a pUC18 vector devoid of the polylinker site via blunt-end ligation resulting in the plasmid pUC-RNAi. A 655-bp fragment of the *N. tabacum Chl I* gene (GenBank Accession number U67064) comprising nucleotides 454–1108 was amplified by PCR from tobacco cDNA and inserted as a *Bam*HI/*Sal*I fragment in sense orientation downstream of the GA20 intron into pUC-RNAi using the before-mentioned restriction sites. The same fragment was inserted in antisense orientation into the *Bgl*II/*Xho*I sites of pUC-RNAi already carrying the *Chl I* sense fragment. Subsequently, the entire fragment comprising sense and antisense fragments of *Chl I* interspersed by the potato GA20 oxidase intron was excised from pUC-RNAi using the flanking *Pst*I restriction sites and inserted into a pUC-based plasmid between a chimeric *alcA* promoter and a *nos* terminator sequence (Caddick *et al.*, 1998). The resulting *alcA* expression cassette was subsequently inserted into the *Hin*dIII site of p35S:*alcR* yielding the construct alc-*dsChl I*. An 804-bp fragment of *N. tabacum GSA* (Höfgen *et al.*, 1994; GenBank Accession number X65974) comprising nucleotides 298–1101 of the respective cDNA clone, was amplified by PCR and manipulated as described above to form plasmid alc-*dsGSA*.

To obtain constructs for ethanol-inducible antisense RNA expression, the same fragments as used before were linked in reverse orientation to the chimeric *alcA* promoter, and the entire cassette was subsequently ligated into p35S:*alcR* as above.

Transformation of tobacco plants by *Agrobacterium*-mediated gene transfer using *A. tumefaciens* strain C58C1:pGV2260 was carried out as described previously by Rosahl *et al.*, (1987).

Constructs and biomaterials concerning the ethanol-inducible system are available for academic research purposes subject to satisfactory completion of a material transfer agreement with Syngenta. For further information, contact the Licensing Manager, Syngenta; Jealotts Hill International Research Center, Bracknell, Berkeshire RG42 6EY, UK.

Ethanol induction

Plants (42 days old) cultivated in the greenhouse in 2.5-l pots were induced with 100 ml of 1% (v/v) ethanol solution via root drenching. Normal watering was resumed after application. Samples for RNA, chl, and protein analysis were taken at various time points indicated in the section under Results. If not otherwise stated, young leaves, being approximately 5 cm at the time point of induction, were followed over the time course of the experiment. For spatial induction, an individual leaf was enclosed in a 15 cm × 10 cm transparent plastic bag with 3 ml of 4% (v/v) ethanol as described previously by Sweetman *et al.*, (2002). The bag was removed after 48 h and phenotype development was monitored by eye.

RNA analysis

Total RNA was extracted from tobacco leaf material as described by Logemann *et al.*, (1987), and 30 μg per sample was separated on a 1.5% (w/v) formaldehyde-agarose gel using conditions described by Sambrook *et al.*, (1989). After electrophoresis, RNA was transferred to a nitrocellulose membrane (GeneScreen, NEN Life Science Products, Boston, USA) and fixed by UV cross-linking. Filters were pre-hybridized, hybridized, and washed essentially as described by Sweetman *et al.*, (2002). *GSA* and *Chl I* transcripts were detected using a random-primed [^{32}P]-labeled cDNA fragment.

Protein analysis

Protein extracts were prepared by homogenization of leaf material in a buffer containing 25 mM HEPES, pH 7.0, 12 mM $MgCl_2$, 0.5 mM EDTA, 8 mM DTT, 10 μM PMSF, 0.1% Triton, and 10% glycerol. Protein content was determined according to Bradford (1976), After heat denaturation, 30 μg of total protein was subjected to electrophoresis on a 10% (w/v) SDS-polyacrylamide gel and subsequently transferred onto nitrocellulose membrane (Porablot, Macherey und Nagel, Düren, Germany). Immunodetection was carried out using the ECL kit (Amersham Pharmacia Biotech, Freiburg, Germany) according to the manufacturer, using a rabbit

anti-GSA primary antibody (kindly provided by Dr Bernhard Grimm, Humboldt University, Berlin, Germany) and peroxidase-conjugated secondary antibody (Pierce, Rockford, IL, USA).

Chlorophyll determination

Chlorophyll was measured in ethanol extracts and concentrations were determined as described by Lichtenthaler (1987).

Acknowledgements

We thank Syngenta Limited for kindly providing the plasmids containing the *alc* system. We are grateful to Prof. Dr Bernhard Grimm (Humboldt University, Berlin, Germany) for providing the anti-GSA serum. We particularly wish to express our gratitude to Dr Chengcai Chu (Chinese Academy of Sciences, Beijing, China) for skilfull cloning work during the initial phase of the project and to Andrea Knospe for plant transformation.

References

Baulcombe, D.C. (1999) Fast forward genetics based on virus-induced gene silencing. *Curr. Opin. Plant Biol.* **2**, 109–113.

Baulcombe, D. (2002) RNA silencing. *Curr. Biol.* **12**, R82–R84.

Béclin, C., Boutet, S., Waterhouse, P. and Vaucheret, H. (2002) A branched pathway for transgene-induced RNA silencing in plants. *Curr. Biol.* **12**, 684–688.

Bevan, M. (1984) Binary *Agrobacterium* vectors for plant transformation. *Nucl. Acids Res.* **12**, 8711–8721.

Boutla, A., Kalantidis, K., Tavernarakis, N., Tsagris, M. and Tabler, M. (2002) Induction of RNA interference in *Caenorhabditis elegans* by RNAs derived from plants exhibiting post-transcriptional gene silencing. *Nucl. Acid Res.* **30**, 1688–1694.

Bradford, M.M. (1976) A rapid and sensitive method for the quantification of microgram quantities of protein utilizing the principle of protein-dye binding. *Anal. Biochem.* **72**, 248–254.

Caddick, M.X., Greenland, A.J., Jepson, I., Krause, K.P., Qu, N., Riddell, K.V., Salter, M.G., Schuch, W., Sonnewald, U. and Tomsett, A.B. (1998) An ethanol inducible gene switch for plants used to manipulate carbon metabolism. *Nat. Biotechnol.* **16**, 177–180.

Carthew, R.W. (2001) Gene silencing by double stranded RNA. *Curr. Opin. Cell Biol.* **13**, 244–248.

Chuang, C.H. and Meyerowitz, E.M. (2000) Specific and heritable genetic interference by double-stranded RNA in *Arabidopsis thaliana*. *Proc. Natl. Acad. Sci. USA*, **97**, 4985–4990.

Cogoni, C. and Macino, G. (2000) Post-transcriptional gene silencing across kingdoms. *Curr. Opin. Genet. Dev.* **10**, 638–643.

Dalmay, T., Hamilton, A., Mueller, E. and Baulcombe, D. (2000) An RNA-dependent RNA polymerase gene in *Arabidopsis* is required for posttranscriptional gene silencing mediated by a transgene but not by a virus. *Cell*, **101**, 543–553.

Frommer, W.B. and Sonnewald, U. (1995) Molecular analysis of carbon partitioning in solanaceous species. *J. Exp. Bot.* **46**, 587–607.

Goff, S.A., Ricke, D., Lan, T.H. *et al.* (2002) A draft sequence of the rice genome (*Oryza sativa* L. ssp. *japonica*). *Science*, **296**, 92–100.

Gosselé, V., Faché, I., Meulewataeter, F., Cornelissen, M. and Metzlaff, M. (2002) SVISS – a novel transient gene silencing system for gene function discovery and validation in tobacco plants. *Plant J.* **32**, 859–866.

Guo, H.S., Fei, J.F., Xie, Q. and Chua, N.H. (2003) A chemical-regulated inducible RNAi system in plants. *Plant J.* **34**, 383–392.

Hamilton, A.J. and Baulcombe, D. (1999) A species of small antisense RNA in posttranscriptional gene silencing in plants. *Science*, **286**, 950–952.

Hammond, S.M., Bernstein, E., Beach, D. and Hannon, G.J. (2000) An RNA-directed nuclease mediates post-transcriptional gene silencing in *Drosophila* cells. *Nature*, **404**, 293–296.

Härtel, H., Kruse, E. and Grimm, B. (1997) Restriction of chlorophyll synthesis due to expression of glutamate 1-semialdehyde aminotransferase antisense RNA does not reduce the light-harvesting antenna size in tobacco. *Plant Physiol.* **113**, 1113–1124.

He, Z.-H., Li, J., Sundqvist, C. and Timko, M.P. (1994) Leaf developmental age controls expression of genes encoding enzymes of chlorophyll and heme biosynthesis in pea (*Pisum sativum* L.). *Plant Physiol.* **106**, 537–546.

Hiriart, J.-B., Lehto, K., Tyystjärvi, E., Junttila, T. and Aro, E.-M. (2002) Suppression of a key gene involved in chlorophyll biosynthesis by means of virus induced gene silencing. *Plant. Mol. Biol.* **50**, 213–224.

Höfgen, R., Axelsen, K.A., Kannangara, C.G., Schüttke, I., Pohlenz, H.-D., Willmitzer, L., Grimm, B. and von Wettstein, D. (1994) A visible marker for antisense mRNA expression in plants: inhibition of chlorophyll synthesis with a glutamate 1-semialdehyde aminotransferase antisense gene. *Proc. Natl. Acad. Sci. USA*, **91**, 1726–1730.

Holzberg, S., Brosio, P., Gross, C. and Pogue, G.P. (2002) Barley stripe mosaic virus-induced gene silencing in a monocot plant. *Plant J.* **30**, 315–327.

Junker, B.H., Chu, C., Sonnewald, U., Willmitzer, L. and Fernie, A.R. (2003) In plants the alc gene expression system responds more rapidly following induction with acetaldehyde than with ethanol. *FEBS Lett.* **535**, 136–140.

Klahre, U., Crété, P., Leuenberger, S.A., Iglesias, V.A. and Meins, F. (2002) High molecular weight RNAs and small interfering RNAs induce systemic posttranscriptional gene silencing in plants. *Proc. Natl. Acad. Sci. USA*, **99**, 11981–11986.

van der Krol, A., Lenting, P.E., Veenstra, J., van der Meer, I.M., Koes, R.E., Gerats, A.G.M., Mol, J.N.M. and Stuitje, A.R. (1988) An antisense chalcone synthase gene in transgenic plants inhibits flower pigmentation. *Nature*, **333**, 866–869.

van der Krol, A.R., Mur, L.A., Beld, M., Mol, J.N. and Stuitje, A.R. (1990) Flavonoid genes in petunia: addition of a limited number of gene copies may lead to a suppression of gene expression. *Plant Cell*, **2**, 291–299.

Levin, J.Z., de Framond, A.J., Tuttle, A., Bauer, M.W. and Heifetz, P.B. (2000) Methods of double-stranded RNA-mediated gene inactivation in *Arabidopsis* and their use to define an essential gene methionine biosynthesis. *Plant Mol. Biol.* **44**, 759–775.

Lichtenthaler, H.K. (1987) Chlorophylls and caroteinoides: pigments of photosynthetic biomembranes. *Meth. Enzymol.* **148**, 350–382.

Liu, Y., Schiff, M. and Dinesh-Kumar, S.P. (2002) Virus-induced gene silencing in tomato. *Plant J.* **31**, 777–786.

Logemann, J., Schell, J. and Willmitzer, L. (1987) Improved method for the isolation of RNA from plant tissues. *Anal. Biochem.* **163**, 16–20.

Matzke, M., Matzke, A.J. and Kooter, J.M. (2001) RNA: guiding gene silencing. *Science*, **293**, 1080–1083.

Mishra, K.K. and Hanada, A.K. (1998) Post-transcriptional silencing of pectin methylesterase gene in transgenic tomatos fruits results from impaired pre-mRNA processing. *Plant J.* **14**, 583–592.

Mlotshwa, S., Voinnet, O., Mette, M.F., Matzke, M., Vaucheret, H., Ding, S.W., Pruss, G. and Vance, V.B. (2002) RNA silencing and the mobile silencing signal. *Plant Cell*, **14**, S289–S301.

Mourrain, P., Béclin, C., Elmayan, T. *et al.* (2000) Arabidopsis SGS2 and SGS3 are required for posttranscriptional gene silencing and natural virus resistance. *Cell*, **101**, 533–542.

Napoli, C., Lemieux, C. and Jorgensen, R. (1990) Introduction of chimeric chalcone synthase gene into petunia results in reversible co-suppression of homologous genes *in trans*. *Plant Cell*, **2**, 279–289.

Page, D.R. and Grossniklaus, U. (2002) The art and design of genetic screens: *Arabidopsis thaliana*. *Nat. Rev. Genet.* **3**, 124–136.

Palauqui, J.C. and Vaucheret, H. (1998) Transgenes are dispensable for the RNA degradation step of cosuppression. *Proc. Natl Acad. Sci. USA*, **95**, 9675–9680.

Palauqui, J.C., Elmayan, T., Pollien, J.M. and Vaucheret, H. (1997) Systemic acquired silencing: transgene-specific posttranscriptional gene silencing is transmitted by grafting from stocks to non-silenced scions. *EMBO J.* **16**, 4738–4745.

Papenbrock, J., Pfündel, E., Mock, H.-P. and Grimm, B. (2000) Decreased and increased expression of the subunit CHL I diminishes Mg chelatase activity and reduces chlorophyll synthesis in transgenic tobacco plants. *Plant J.* **22**, 155–164.

Plasterk, R.H. (2002) RNA silencing: the genome's immune system. *Science*, **296**, 1263–1265.

Ratcliff, F., Martin-Hernandez, A.M. and Baulcombe, D.C. (2001) Tobacco rattle virus as a vector for analysis of gene function by silencing. *Plant J.* **25**, 237–245.

Rosahl, S., Schell, J. and Willmitzer, L. (1987) Expression of a tuber-specific storage protein in transgenic tobacco plants: demonstration of an esterase activity. *EMBO J.* **6**, 1155–1159.

Roslan, H.A., Salter, M.G., Wood, C.D. *et al.* (2001) Characterisation of the ethanol-inducible alc gene expression system in *Arabidopsis thaliana*. *Plant J.* **28**, 225–235.

Salter, M.G., Paine, J.A., Riddel, K.V., Jepson, I., Greenland, A.J., Caddick, M.X. and Tomsett, B.A. (1998) Characterisation of the ethanol-inducible alc gene expression system for transgenic plants. *Plant J.* **16**, 127–132.

Sambrook, J., Fritsch, E.F. and Maniatis, T. (1989) *Molecular Cloning: a Laboratory Manual*, 2nd edn. Cold Spring Harbor: Cold Spring Harbor Laboratory Press.

Smith, N.A., Singh, S.P., Wang, N.B., Stoutjesdijk, P.A., Green, A.G. and Waterhouse, P.M. (2000) Total silencing by intron-spliced hairpin RNAs. *Nature*, **407**, 319–320.

Smith, C.J., Watson, C.F., Ray, J., Bird, C.R., Morris, P.C., Schuch, W. and Grierson, D. (1988) Antisense RNA inhibition of polygalacturonase genes in transgenic tomatos. *Nature*, **334**, 724–726.

Stitt, M. and Sonnewald, U. (1995) Regulation of metabolism transgenic plants. *Annu. Rev. Plant Physiol. Plant Mol. Biol.* **46**, 341–368.

Stoutjesdijk, P.A., Singh, S.P., Liu, Q., Hurlstone, C.J., Waterhouse, P.M. and Green, A.G. (2002) hpRNA-mediated targeting of the *Arabidopsis FAD2* gene gives highly efficient and stable silencing. *Plant Physiol.* **129**, 1723–1731.

Sweetman, J.P., Chu, C., Qu, N., Greenland, A.J., Sonnewald, U. and Jepson, I. (2002) Ethanol vapor is an efficient inducer of the alc gene expression system in model and crop plant species. *Plant Physiol.* **129**, 943–948.

Tang, G., Reinhart, B.J., Bartel, D.P. and Zamore, P.D. (2003) A biochemical framework for RNA silencing in plants. *Genes Dev.* **17**, 49–63.

The Arabidopsis Genome Initiative (2000) Analysis of the genome sequence of the flowering plant *Arabidopsis thaliana*. *Nature*, **408**, 796–815.

Turnage, M.A., Muangsan, N., Peele, C.G. and Robertson, D. (2002) Geminivirus-based vectors for gene silencing in *Arabidopsis*. *Plant J.* **30**, 107–114.

Vance, V. and Vaucheret, H. (2001) RNA silencing in plants – defense and counterdefense. *Science*, **292**, 2277–2280.

Voinnet, O., Vain, P., Angell, S. and Baulcombe, D. (1998) Systemic spread of sequence-specific transgene RNA degradation in plants is initiated by localized introduction of ectopic promoterless DNA. *Cell*, **95**, 177–187.

Waterhouse, P.M., Graham, H.W. and Wang, M.B. (1998) Virus resistance and gene silencing in plants can be induced by simultaneous expression of sense and antisense RNA. *Proc. Natl. Acad. Sci. USA*, **95**, 13959–13964.

Yu, J., Hu, S., Wang, J. *et al.* (2002) A draft sequence of the rice genome (*Oryza sativa* L. ssp. *indica*). *Science*, **296**, 79–91.

Zamore, P.D., Tuschl, T., Sharp, P.A. and Bartel, D.P. (2000) RNAi: double-stranded RNA directs the ATP-dependent cleavage of mRNA at 21–23 nucleotide intervals. *Cell*, **101**, 25–33.

Planta (2004) 218: 379–387
DOI 10.1007/s00425-003-1117-1

Exhibit 9

ORIGINAL ARTICLE

Marina Byzova · Christoph Verduyn · Dirk De Brouwer
Marc De Block

Transforming petals into sepaloid organs in *Arabidopsis* and oilseed rape: implementation of the hairpin RNA-mediated gene silencing technology in an organ-specific manner

Received: 21 May 2003 / Accepted: 25 August 2003 / Published online: 8 October 2003

Abstract Oilseed rape (*Brassica napus* L.) genotypes with no or small petals are thought to have advantages in photosynthetic activity. The flowers of field-grown oilseed rape form a bright-yellow canopy that reflects and absorbs nearly 60% of the photosynthetically active radiation (PAR), causing a severe yield penalty. Reducing the size of the petals and/or removing the reflecting colour will improve the transmission of PAR to the leaves and is expected to increase the crop productivity. In this study the 'hairpin' RNA-mediated (hpRNA) gene silencing technology was implemented in *Arabidopsis thaliana* (L.) Heynh. and *B. napus* to silence B-type MADS-box floral organ identity genes in a second-whorl-specific manner. In *Arabidopsis*, silencing of B-type MADS-box genes was obtained by expressing *B. napus APETALA3* (*BAP3*) or *PISTILLATA* (*BPI*) homologous self-complementary hpRNA constructs under control of the *Arabidopsis* A-type MADS-box gene *APETALA1* (*API*) promoter. In *B. napus*, silencing of the *BPI* gene family was achieved by expressing a similar hpRNA construct as used in *Arabidopsis* under the control of a chimeric promoter consisting of a modified petal-specific *Arabidopsis AP3* promoter fragment fused to the *API* promoter. In this way, transgenic plants were generated producing male fertile flowers in which the petals were converted into sepals (*Arabidopsis*) or into sepaloid petals (*B. napus*). These novel flower phenotypes were stable and heritable in both species.

Keywords Apetalous · *Arabidopsis* · *Brassica* · Double sepaloid · MADS-box · Petal

M. Byzova · C. Verduyn · D. De Brouwer
M. De Block (✉)
Bayer BioScience N.V., Jozef Plateaustraat 22,
9000 Gent, Belgium
E-mail: marc.deblock@bayercropscience.com
Fax: + 32-9-2240694

Abbreviations *PAR*: photosynthetically active radiation · *ST-LS1*: potato light-inducible tissue-specific ST-LS1 gene · *GUS*: β-glucuronidase

Introduction

Flowers of oilseed rape (*Brassica napus*) have four well-developed bright-yellow petals. During flowering time, flowers form a very bright-yellow layer that reflects and absorbs solar radiation. As consequence, only 24% of the photosynthetically active radiation (PAR) reaches the leaf canopy (Chapman et al. 1984). This accelerates leaf and bract senescence, reduces dry matter accumulation, and lowers seed set (Daniels et al. 1986).

A few strategies to improve the photosynthetic efficiency of oilseed rape by utilising different apetalous variants (Buzza 1983; Jiang and Becker 2003) or the *stamenoid petal* (stap) variant with flowers bearing staminoid petals (Fray et al. 1997) have been proposed. Physiological analyses have revealed the potential benefit of such a petalless flower phenotype on *B. napus* yield (Rao et al. 1991; Fray et al. 1995).

The currently used apetalous genotypes are controlled either by two recessive genes (Fray et al. 1996) or by an interaction of cytoplasmic genes and two pairs of nuclear genes (Jiang and Becker 2003). This genetic complexity makes it difficult to fully implement the apetalous trait into commercial rapeseed varieties. Additionally, the apetalous character appears to be unstable under field conditions at high temperatures and in long days (Rao et al. 1991). The *B. napus stap* variant also possesses poor agronomic attributes, such as deformed leaves and poor vigour (Fray et al. 1997).

A more promising strategy to improve PAR transmission in oilseed rape would be the use of a single dominant gene that converts the bright-yellow petals into small non-light reflecting structures such as sepals. Such an organ conversion is preferable over the removal of the petals to avoid interfering with insect pollination. Pierre et al. (1996) have shown that honeybees, the main

pollinators on oilseed rape, do not crawl over the anthers and stigma of apetalous flowers as they do in petalous ones but often insert their tongues between the sepals to collect the nectar. In this way pollination might be reduced, resulting in a lower seed set.

The molecular mechanisms governing floral organ identity are well understood. According to the "A–E" model, the organ identity of each floral whorl is determined by a unique combination of four organ identity activities, called A, B, C and E (Weigel and Meyerowitz 1994; Pelaz et al. 2000; Jack 2001; Theißen 2001; Fig. 1). Expression of the (A)-type genes specifies sepal formation. The combination of (A + B + E) activities specifies the formation of petals, while combined (B + C + E) functions specify stamen formation. Expression of the (C + E)-type genes determines the development of carpels (Fig. 1). All types of organ identity genes have been cloned from *Arabidopsis*. An example of the A-type gene is *API* (Mandel et al. 1992). The B-type genes are *AP3* (Jack et al. 1992) and *PI* (Goto and Meyerowitz 1994), and the C-type gene is *AGAMOUS* (*AG*) (Yanofsky et al. 1990). The E-function is provided by three *SEPALLATA* genes (Pelaz et al. 2000). All these genes are transcription factors belonging to the MADS-box gene family.

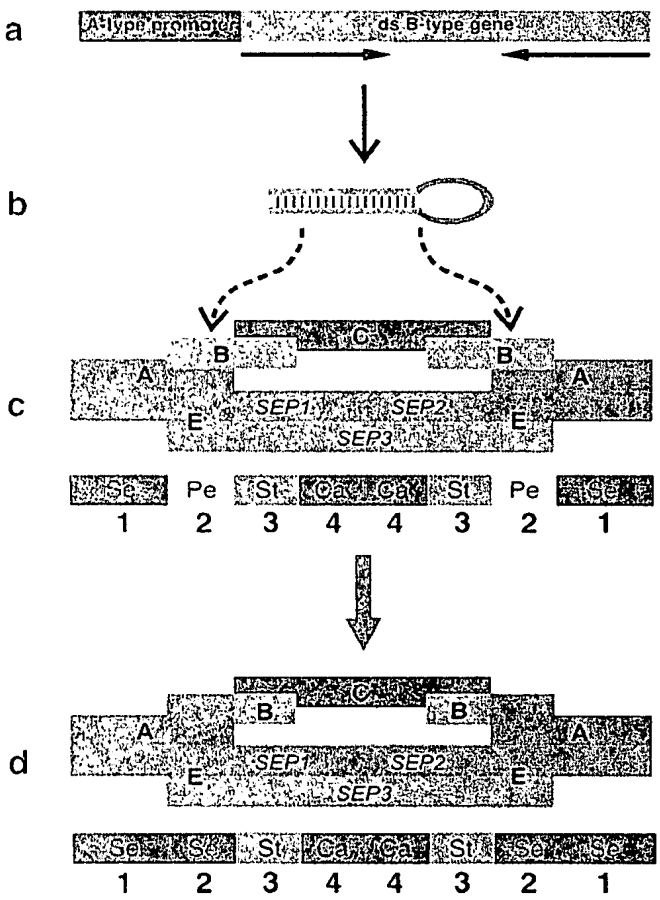

Fig. 1a–d Experimental strategy. **a** Representation of the basic construct used in this study. A DNA fragment of a 3'-coding region of a B-type MADS-box gene (*yellow box*) was sub-cloned as an inverted repeat (directions are indicated by *arrows*) with a part of the GUS gene or the intron IV2 from gene ST-LS1 (Vancanneyt et al. 1990) as a spacer (*blue box*). The constructs were driven by an A-type MADS-box gene promoter (*green box*). **b** Transcripts produced by the construct are predicted to form a hairpin structure. **c** Domains of the A, B, C and E functions and the corresponding organ identities in floral whorls in wild-type plants. **d** Domains of the A, B, C and E functions and the corresponding organ identities in floral whorls in transgenic plants. In transgenic plants, down-regulation of the B-type function in the second whorl only leads to development of sepals instead of petals. Numbers indicate whorls. *Se* sepals, *Pe* petals, *St* stamens, *Ca* carpels

In this paper, silencing of the B-type MADS-box genes in a second-whorl-specific manner was obtained in both *Arabidopsis* and *B. napus* flowers by expressing a *B. napus* B-type gene hpRNA construct under control of an *Arabidopsis* A-type MADS-box gene promoter (Fig. 1). In this way, *Arabidopsis* lines with double sepaloid flowers and *B. napus* lines with flowers in which petals are converted into sepaloid petals were generated. The novel flower phenotypes were stable and heritable in both species.

Materials and methods

Plant material

Arabidopsis thaliana (L.) Heynh. ecotype C24, kindly provided by Dr. M. Van Lijsebettens (VIB, Gent, Belgium), and the double haploid *Brassica napus* L. line cv. Simon (Bayer BioScience N.V., Gent, Belgium) were used in this study.

Plasmid construction

The 3'- coding regions of the *BAP3* and *BPI* genes were cloned by means of RT–PCR performed on total RNA isolated from *B. napus* flower buds. RT–PCR was performed according to the protocol of the SuperScript First-Strand Synthesis System for RT–PCR (Invitrogen). *AP3* cDNA-specific primers:

- 5'-CGCACTCAGATTAAGCAGAGGC-3' and
- 5'-GGAAGGTAATGATGTCAGAGGC-3'

and *PI* cDNA-specific primers:

- 5'-GGGAGAAGATATACAGTCTCTCAAC-3' and
- 5'-GAATCGGTTGCACTCTATATCC-3'

were chosen based on the published sequences (Jack et al. 1992, GenBank Accession D30807; Goto and Meyerowitz 1994, GenBank Accession M86337). In the pAP1::hpBAP3 construct, one of the *BAP3*-specific DNA fragments, 380-bp in length, was cloned as a inverted repeat with the β-glucuronidase (GUS) fragment containing nucleotides 744–975 as a spacer. In the pAP1::hpBPI construct, one of the *BPI*-specific fragments, 255-bp in length, was cloned as an inverted repeat with the intron IV2 from the potato light-inducible tissue-specific gene ST-LS1, 251-bp in length, as a spacer (Vancanneyt et al. 1990). In the pAP1::hpBAP3 and pAP1::hpBPI constructs, gene-specific structures were driven by a 1,182-bp fragment of the *API* promoter. The fragment of the *API* promoter (−1182 to +1) was cloned by means of PCR from pKY65 plasmid kindly provided by Martin Yanofsky. In pΔAP3-AP1::hpBPI fragments of the *AP3* promoter, containing nucleotides −727 to −556 and −224 to −1 were cloned by PCR based on

the published sequence (Irish and Yamamoto 1995, GenBank Accession U30729) and linked to the 5'-end of the *API* promoter. Plasmid constructs were introduced into *Agrobacterium tumefaciens* strain C58C1rif by electroporation.

Plant transformation

The transformations of *A. thaliana* and *B. napus* were essentially done as described by Valvekens et al. (1992) and De Block et al. (1989), respectively.

Cytology

The embedding was done in Historesin as advised by the manufacturer (Leica, Heidelberg, Germany). Sections 5 μm thick were stained with 0.05% toluidine blue.

In situ hybridization

Embedding in methacrylate, sectioning, and the removal of the plastic were essentially done as described by Baskin et al. (1992). The in situ hybridizations on 7-μm sections were essentially done as described by De Block and De Brouwer (1993).

Microscopy

Sections were examined with an Axioplan (Zeiss, Jena, Germany) microscope equipped with Normaski differential interference contrast.

Spectrophotometric determination of chlorophyll

The total chlorophyll (a + b) content was measured as described by Bruisma (1963).

Results

General strategy: silencing the B-type MADS-box genes in a second floral whorl-specific manner

To convert petals into sepals without interfering with anther development, the strategy outlined in Fig. 1 was used. Following the A–E flower development model it is expected that silencing of a B-type MADS-box gene, *AP3* or *PI*, in the second whorl will redirect the development of petals into sepals. This could be obtained by expressing in the second, but not in the third whorl self-complementary 'hairpin' RNA (hpRNA) constructs containing *AP3*- and/or *PI*-specific sequences. Down-regulation of the B-type MADS-box genes in the third whorl has to be avoided to maintain normal male fertility. For this purpose an A-type promoter driving the expression of the hpRNA construct could be used.

Starting from the *PI* and *AP3* sequences (Jack et al. 1992; Goto and Meyerowitz 1994), we identified in the amphidiploid *B. napus* five *AP3*-like (*BAP3*) and three *PI*-like (*BPI*) genes that were actively expressed during flower development (data not shown). Fragments of the 3'-coding region of the *BAP3* and *BPI* genes were isolated. The nucleotide sequence similarity between members of the same B-type MADS-box gene subfamily turned out to be on average 95%. Each *B. napus* gene subfamily shared with its unique *Arabidopsis* counterpart about 91% sequence similarity, containing multiple blocks of more than 20 bases of perfect homology. This high sequence similarity should be sufficient to silence the target genes in both *Arabidopsis* and *B. napus* by using the same hpRNA constructs (Helliwell and Waterhouse 2003). The feasibility of the strategy to convert petals into sepals by silencing the B-type MADS-box genes only in the second floral whorl was first evaluated in the model plant *Arabidopsis thaliana*.

Generation of *Arabidopsis* transgenic lines with male fertile double sepaloid flowers

To make constructs that produce hpRNA B-type MADS-box gene transcript, the 3'-coding regions of one *BAP3* and one *BPI* gene, were subcloned as an inverted repeat (see Materials and methods). Both hpBAP3 and hpBPI gene-specific sequences were driven by a 1.1-kb promoter fragment of the *Arabidopsis API* gene. The resulting pAP1::hpBAP3 and pAP1::hpBPI constructs were introduced separately into *Arabidopsis*.

A total of 125 pAP1::hpBAP3 and 56 pAP1::hpBPI transgenic lines was generated. All the plants were normal in terms of vegetative growth while they had morphological changes in flower organs. 16.9% of the pAP1::hpBPI and 5.6% of the pAP1::hpBAP3 lines exhibited the desirable double sepaloid phenotype (Fig. 2b). Instead of petals, sepals developed in the second floral whorl, indistinguishable from those of the first whorl except for their slightly smaller size. Despite their transformation, these organs developed in the positions and on a time course characteristics of petals. Some other pAP1::hpBAP3 T_0 plants had a range of phenotypes related to the severity of homeotic transformations observed in petal and stamen development. 10.4% of the pAP1::hpBAP3 lines produced flowers with short white petals and 20% of the lines had homeotic aberrations in stamens ranging from weak carpelloidy to complete transformation of stamens into carpels (Table 1). In contrast to the pAP1::hpBAP3 lines, no aberrations in the third floral whorl were observed in the pAP1::hpBPI transgenic plants (Table 1).

Microscopic analysis of cross-sections of mature pAP1::hpBPI double sepaloid flowers revealed that the mesophyll cells of the second-whorl organs were sepaloid in nature, as indicated by the presence of chloroplasts and their larger size than those normally found in wild-type petals. The abaxial epidermis was like that of sepals, consisting of stomata and irregularly shaped cells (Fig. 2d). The same results were obtained for pAP1::hpBAP3 double sepaloid flowers (data not shown).

To confirm that the double sepaloid phenotype of *Arabidopsis* transgenic plants was caused by depletion of expression of endogenous B-type homeotic genes in the

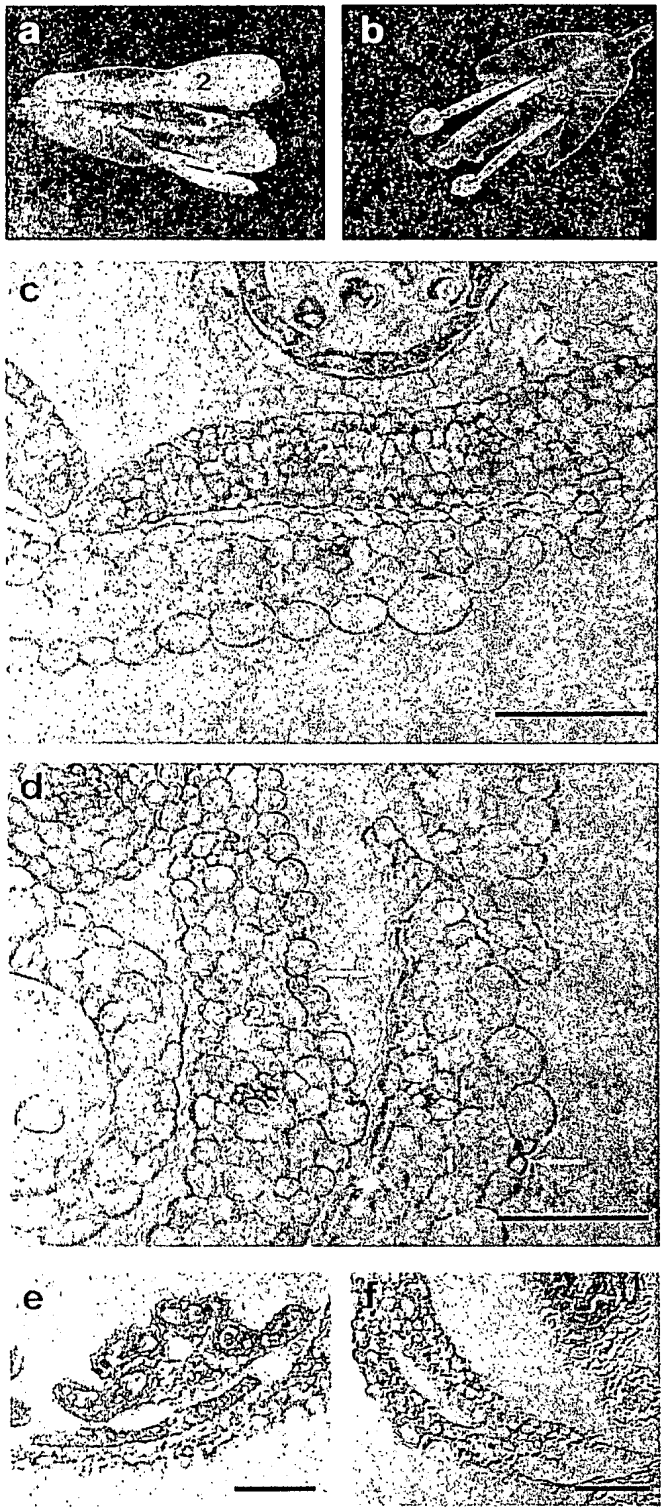

Fig. 2a–f Analysis of the double sepaloid pAP1::hpBPI *Arabidopsis thaliana* flowers. **a** C24 *Arabidopsis* wild-type mature flower. **b** Mature transgenic flower. Second-whorl organs are sepals (*arrow*) that are slightly smaller than the true sepals. **c, d** Cytological transverse sections taken approximately in the middle of anthers of flower buds at stage 12. **c** Cellular morphology of first- and second-whorl organs of a wild-type flower. Mesophyll cells of the second-whorl petals are smaller than those of sepals developed in the first whorl. Abaxial epidermal cells of petals are regular in shape. **d** Cellular morphology of first- and second-whorl organs of a transgenic flower. Mesophyll and epidermal cells of the second-whorl organs are slightly smaller in size than cells of the first-whorl sepals. The shape of the cells of the second-whorl sepals is similar to those of the first-whorl sepals. Stomata (*arrows*) are present in the abaxial epidermis of the second-whorl organs as in normal first-whorl sepals. **e, f** In situ analysis of *PI* expression in transverse sections of wild-type and transgenic flowers. The hybridisation signal is confined to the second- and the third-whorl organs in wild-type flowers (e). In transgenic flowers (f) *PI* expression is detected in the third-whorl organs only. Numbers indicate whorls. Bars = 50 μm (c, d, f), 100 μm (e)

second whorl, the *PI* mRNA expression pattern in pAP1::hpBPI was examined by in situ hybridization. In wild-type *Arabidopsis* flowers, *PI* mRNA is detected from stage 3 (Smyth et al. 1990) in second- third- and fourth-whorl primordia. In the second and third whorls it persists until anthesis (Goto and Meyerowitz 1994). In pAP1::hpBPI double sepaloid flowers the *PI* transcript was not detectable in the second-whorl primordia at any of the stages examined (Fig. 2f). Expression of *PI* in developing stamens was similar to that observed in the wild type.

As it has been shown that expression of both *PI* and *AP3* genes is reduced when either the *PI* or *AP3* gene is mutated (Jack et al. 1992; Goto and Meyerowitz 1994), we anticipated that inhibition of expression of one of the B-type MADS-box genes in a tissue where both genes are active would lead to reduction of expression of the counterpart gene in the same manner. To verify this hypothesis, in situ hybridization of the pAP1::hpBPI flowers using the *BAP3*-specific fragment as a probe was performed. As was predicted, *AP3* RNA was not detected in the second whorl of developing organs. However, no reduction in the level of the *AP3* mRNA was observed in stamens (data not shown).

Heritability and stability of the double sepaloid trait was tested by self-pollination. The trait was heritable and in the case of pAP1::hpBPI stable through the T_1 and T_2 generations. In the case of pAP1::hpBAP3 some T_1 and T_2 lines produced flowers with homeotic aberrations in stamens, as previously observed in the T_0 plants.

In *B. napus*, silencing of B-type MADS-box genes in the second whorl results in the transformation of petals into sepaloid petals

To evaluate whether the expression of the pAP1::hpBAP3 and pAP1::hpBPI genes would also result in a double sepaloid phenotype in *B. napus*, 48 and 53 transgenic lines, respectively, were generated.

All the pAP1::hpBAP3 lines had wild-type flowers. Among the pAP1::hpBPI transgenic lines, 22.6%

Table 1 Phenotypic analysis of T_0 *Arabidopsis thaliana* plants

[a]Range of aberrations in stamens from mild to complete conversion of stamens into carpels

Transformed constructs	Total number of transgenic lines	Plants with mutant phenotype (%)		
		Double sepaloid Fertile	Double sepaloid Partially male sterile[a]	Short petals Fertile
pAP1::hpBPI	56	16.9	< 2	18.9
pAP1::hpBAP3	125	5.6	20	10.4

exhibited an apetalous or partially apetalous phenotype characterised by the appearance of flowers without petals or bearing 1, 2 or 3 petals only (Table 2). Frequently, the petals were significantly smaller and narrower than those from wild type (data not shown). However, this phenotype was unstable and not heritable.

The absence of the double sepaloid phenotype in transgenic *B. napus* lines with the same constructs used in *Arabidopsis* could be due to an inability of the *Arabidopsis AP1* promoter to direct transcription of adequate amounts of double-stranded transcripts necessary to trigger silencing of all target *BAP3* or *BPI* genes expressed in rapeseed flowers. Starting from this hypothesis, a new construct was generated that could produce higher amounts of hpRNA. Because the pAP1::hpBAP3 *B. napus* transgenic plants did not exhibit any phenotypes different from those of wild-type plants, and in *Arabidopsis* the most stable double sepaloid flower phenotype was obtained with the hpBPI construct, we continued only with the hpRNA *BPI* gene.

To enhance the level of expression of hpBPI specifically in the second whorl, an *Arabidopsis* modified *AP3* regulatory fragment was added to the *AP1* promoter.

Discrete *cis*-acting elements regulating spatial and temporal expression of the *Arabidopsis AP3* gene have been identified (Hill et al. 1998; Tilly et al. 1998). Based on these data the positive regulator of the *AP3* expression during the early stages of flower development was combined with the petal-specific regulatory region (see Materials and methods). The modified *AP3* promoter was introduced in the pAP1::hpBPI construct directly upstream of the *AP1* sequence. This pΔAP3-AP1::hpBPI construct was transformed into *B. napus*.

Of the 125 primary transformants, 11.2% produced flowers with aberrant second-whorl organs. Of these 11.2% lines, half (5.6%) produced flowers in which petals were converted into sepaloid petals (Fig. 3a, Table 2). These organs were yellowish-green, indicating the presence of chloroplasts in their cells that is characteristic of wild-type sepals. The size of the sepaloid petals was comparable to the size of true sepals. These organs were narrow and almost strap-like in shape, like sepals, but had a small lamina and base, characteristic of a petal. In addition the lamina portion was wrinkled (Fig. 3a).

The aberrant *B. napus* flowers with sepaloid petals were analysed microscopically to verify the identity of tissues in the second-whorl organs. As shown in Fig. 3c the size and the shape of epidermal and mesophyll cells of these organs were indistinguishable from the first-whorl sepals. Moreover, the mesophyll cells of the sepaloid petals contained a large number of chloroplasts (Fig. 3d).

In addition, spectrophotometric analysis of chlorophyll fluorescence, which was done on the first and the second floral organs of transgenic plants, revealed that chlorophyll content in the sepaloid petals is only 30% less than in the true wild-type sepals (data not shown).

In situ hybridization of flower sections with a *BPI*-specific probe confirmed the absence of a detectable level of *BPI* gene expression in the second whorl of the transgenic flowers, indicating that the complete *BPI* gene family was down-regulated (Fig. 3e).

The other half of the 11.2% transgenic pΔAP3-AP1::hpBPI lines exhibited partial apetalous and apetalous phenotypes similar to those observed in pAP1::hpBPI transgenic plants (Table 2).

The flower phenotype with sepaloid petals is a stable trait in *B. napus* transgenic plants

The stability of transformation of petals to sepaloid petals in *B. napus* was tested for six lines, of which the original T_0 plants had flowers with sepaloid petals and contained only one copy the pΔAP3-AP1::hpBPI transgene. The T_0 plants were first maintained by selfing. The transgenic plants of these T_1 generations had flowers with sepaloid petals while the azygous segregants had normal wild-type flowers. For each line ten transgenic plants of the T_1 generation were backcrossed with the original non-transgenic double haploid *B. napus* line cv.

Table 2 Phenotypic analysis of T_0 *Brasssica napus* plants

Transformed constructs	Total number of transgenic lines	Plants with mutant phenotype (%)	
		Sepaloid petals	Apetalous/partially apetalous
pAP1::hpBAP3	48	0	0
pAP1::hpBPI	53	0	22.6
pΔAP3-AP1::hpBPI	125	5.6	5.6

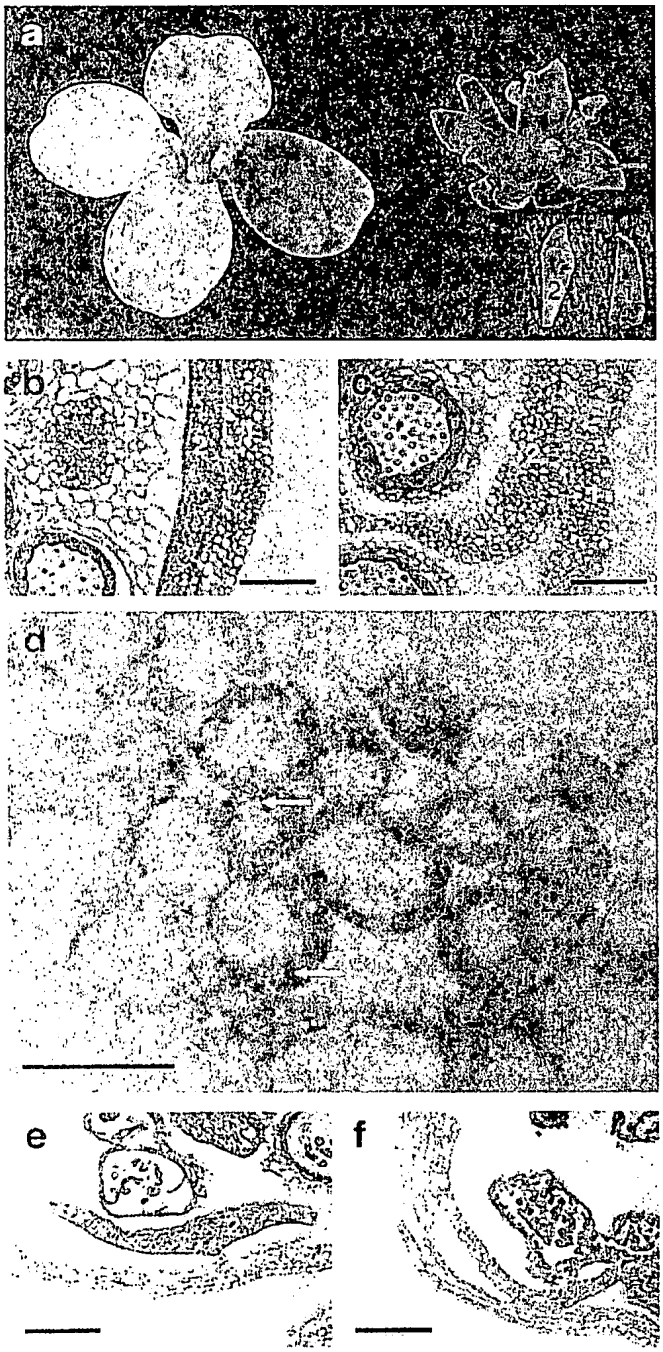

◀

Fig. 3a–e Analysis of the pΔAP3-AP1::hpBPI *B. napus* flowers. **a** Morphological features of *Brassica napus* flowers: mature wild-type flower (*left*), mature flower of a transgenic plant (*right*). The second-whorl organs of a transgenic flower are yellowish-green sepaloid petals (*arrow*). The size of these organs is similar to sepals developed in the first whorl, but the lamina-base structure can still be distinguished (for comparison see the detached organs in the *bottom right corner*: the second-whorl organ (*left*), the first-whorl organ (*right*) of a transgenic flower). **b–d** Cytological transverse sections taken approximately in the middle of anthers at the early yellow bud stage (Smith and Scarisbrick 1990). **b** Cellular morphology of first- and second-whorl organs of a wild-type flower. Mesophyll cells of petals are smaller than those of sepals. Epidermal cells of petals are regular in shape. **c** Cellular morphology of the first- and second-whorl organs of a transgenic plant. The shape and the size of mesophyll and epidermal cells of the second-whorl organs are similar to those of the first-whorl sepals. **d** Cytology of a sepaloid petal showing the presence of chloroplasts (two examples indicated by *arrows*) in the mesophyll cells. **e, f** In situ analysis of *BPI* expression on transverse sections of wild-type and transgenic flowers. The hybridization signal is confined to the second- and the third-whorl organs in wild-type flowers (**e**). In transgenic flowers (**f**) *BPI* expression is detected in the third-whorl organs only. Numbers indicate whorls. Bars = 20 μm (**d**), 100 μm (**b, c**), 200 μm (**e, f**)

Simon. Depending on whether the T_1 plant used was homo- or heterozygous for the transgene, all or 50% of the F_1 plants, respectively, had sepaloid petals in their flowers. A second backcross was done with 15 plants of each line. As expected, in the F_2 generations there was a 1:1 segregation of wild-type plants and plants with sepaloid petals. The flower phenotype of the transgenic F_2 plants was identical to those of the T_0, T_1 and F_1 transgenic plants.

Discussion

The hpRNA-mediated gene silencing technology has been proven to be a very efficient tool for gene discovery and functional genomics in diverse organisms such as fungi (Pickford et al. 2002), nematodes (Bargmann 2001), and animals (Harborth et al. 2001). In plants this technology has been used successfully to generate virus resistance (Waterhouse et al. 1998) as well as to obtain consistent and profound inhibition of the expression of transgenes and endogenous genes (Levin et al. 2000; Smith at al. 2000; Wesley et al. 2001; Liu et al. 2002).

Chuang and Meyerowitz (2000) demonstrated that the hpRNA-mediated silencing technology could be used to interfere with flower development. A range of aberrant flower phenotypes was obtained by down-regulating the floral organ genes *AGAMOUS*, *CLAVATA3*, *APETALA1*, and *PERIANTHIA* using hpRNA constructs driven by the constitutive 35S and nopaline synthase promoters. Recently, it has been shown that the hpRNA-mediated silencing technique can be used to silence genes in an organ-specific way. The fatty acid composition of *Arabidopsis* and cotton seeds was modified by down-regulating the seed expression of two fatty acid desaturase genes using hpRNA constructs driven by seed-specific promoters (Liu et al. 2002; Stoutjesdijk et al. 2002).

In this article we present for the first time to our knowledge implementation of the hpRNA-mediated technology to silence a multigene family in a floral whorl-specific manner. Silencing of the B-type MADS-box genes that are present in single copy in *Arabidopsis* but are present in multiple copies in *B. napus* causes complete transformation of petals to sepals in *Arabidopsis* and partial transformation in *B. napus*. This flower phenotype is stable and heritable in both species.

In *Arabidopsis*, unlike the silencing of the *PI* gene, silencing of the *AP3* gene results in homeotic aberrations in anthers in 20% of the cases. This implies that in these lines partial silencing of the *AP3* gene also occurs in developing stamens. These results can be attributed to two possibilities. First, in wild-type *Arabidopsis* flowers *API* is expressed during early floral stages throughout all four whorls and is down-regulated in whorls 3 and 4 by the *AG* gene during stage 3, persisting in whorls 1 and 2 only (Mandel et al. 1992; Bowman at al. 1993). However, in contrast to the endogenous promoter, the smaller *API* promoter fragment we used might have some activity in the central whorls after stage 3 as proposed by Yun et al. (2002). The activity of the pAP1::hpBAP3 gene might have led to down-regulation of *AP3* in the third floral whorl. Alternatively, an aberrant stamen development in the pAP1::hpBAP3 transgenic plants might be the result of the spreading of a silencing signal between floral whorls.

Both hypotheses imply that a certain amount of dsRNA of the *AP3* gene present in the third whorl of transgenic flowers is sufficient to trigger silencing of *AP3*. This is not the case for the *PI* gene, for which the down-regulation did not result in aberrant anther phenotype. *PI* and *AP3* are both expressed in developing petals and stamens. However *PI* expression levels are similar in both whorls, whereas *AP3* expression is lower in developing stamens than in petals (Zhou et al. 2002). It may be that for this reason a lower threshold concentration of hpRNA is required in stamens to provoke a partial inhibition of the *AP3* gene expression.

Although systemic spreading of silencing may be a concern for implementation of the hpRNA-mediated silencing technology in tissue-specific applications in plants (Wang and Waterhouse 2002), the stability of the aberrant flower phenotype throughout development of our transgenic plants indicates that at least in the case of the B-type MADS-box genes there is no significant spreading of silencing between the meristems of adjacent floral organs.

Another phenomenon that might limit application of the hpRNA gene silencing technique is spreading of RNA targeting. During this process spreading of the RNA silencing signal occurs from the initial target sequence into the adjacent 5′ and 3′ regions (Jones at al. 1999; Vaistij at al. 2002). This may result in the participation of the entire transcribed region of the target gene in the RNA silencing process. As a consequence, expression of other homologous genes can be inhibited. Based on this hypothesis and the fact that different types of MADS-box genes share a high percentage of homology at the MADS-box regions (Purugganan et al. 1995), target-site spreading along the *AP3* or *PI* transcribed sequences would led to silencing of not only *AP3* and *PI* but also of other MADS-box genes that are expressed in the developing second-whorl organs. In this case petals will be converted not only into sepals but also into organs with staminoid and/or carpeloid and/or other aberrant structures. The absence of such phenotypes in our transgenic plants suggests that silencing of B-type MADS-box genes was not associated with the spreading of RNA targeting. The absence of the target-site spreading process was also observed by Vaistij et al. (2002) for the ribulose-1,5-bisphosphate carboxylase/oxygenase and phytoene desaturase genes. These results demonstrate that the hpRNA-mediated gene silencing technology can be applied not only to silence all genes of a multigene family but also to silence specifically a single member of a subfamily or even of a multigene family.

B. napus plants transformed with the improved pΔAP3-AP1::hpBPI construct have small yellowish-green sepaloid petals in the second whorl. Although mesophyll and epidermal cells of these sepaloid petals are sepaloid in morphology, the light-yellow colour suggests that some petal-specific biochemical pathways are still active in the cells of these organs. In addition, the small lamina and base of these organs are petal characteristics. It might be that undetectable levels of *BPI* transcripts are still sufficient for maintenance of some petaloid features.

Recently, in *Arabidopsis* an alternative approach was used to interfere with the expression of *AP3* in a second-whorl-specific manner (Guan et al. 2002). A zinc finger protein designed to bind to a region upstream of *AP3* was fused to the human transcriptional repression domain of mSIN3. When the *API* promoter was used to drive the expression of this artificial zinc finger transcription factor, flowers were obtained that were partially apetalous or that contained some sepaloid petals. Although the use of synthetic transcription factors is a promising approach to interfere with gene regulation, high expression levels of these transcription factors are probably needed to obtain a full phenotype by gene repression. Due to technical limitations the use of such artificial transcription factors is less feasible when multiple genes with redundant function, like the B-type MADS-box genes in *B. napus*, have to be repressed.

Theoretically, in *Arabidopsis* a double sepaloid flower phenotype may also be obtained by silencing the *SEPALLATA* genes in the second whorl (Fig. 1). However, due to the redundant function of the *SEPALLATA* genes, all three genes would have to be silenced together (Pelaz et al. 2000).

In conclusion, *Arabidopsis* and *B. napus* lines with a flower phenotype that is, respectively, double sepaloid or has sepaloid petals, and that is male fertile and stable in subsequent generations can be obtained by a hpRNA-mediated gene silencing of the *PISTILLATA* gene exclusively in the second floral whorl. Further physiological studies of *B. napus* transgenic lines will allow quantification of the effect of the flower architecture with sepaloid petals on the distribution of PAR and on other important agronomic features such as pollination and overall seed yield.

Acknowledgements We thank Dr. Peter Waterhouse (CSIRO Plant Industry, Canberra, Australian Capital Territory, Australia), Dr.

Bart Den Boer and Dr. Jean Broadhvest (Bayer BioScience N.V., Gent, Belgium) for their helpful advice in writing the manuscript.

References

Bargmann CI (2001) High-throughput reverse genetics: RNAi screens in *Caenorhabditis elegans*. Genome Biol 2: REVIEWS1005.1–1005.3

Baskin TI, Bushy CH, Fowke LC, Sammut M, Gubler F (1992) Improvements in immunostaining samples embedded in methacrylate: localization of microtubules and other antigens throughout developing organs in plants of diverse taxa. Planta 187:405–413

Bowman JL, Alvarez J, Weigel D, Meyerowitz EM, Smyth DR (1993) Control of flower development in *Arabidopsis thaliana* by *APETALA1* and interacting genes. Development 119:721–743

Bruisma J (1963) The quantitative analysis of chlorophyll *a* and *b* in plant extracts. Phytochem Phytobiol 2:241–249

Buzza GC (1983) The inheritance of an apetalous flower character in canola (*Brassica napus* L.). Cruciferae Newslett 8:11–12

Chapman JF, Scarisbrick DH, Daniels RW (1984) Field studies on C^{14} assimilate fixation and movement in oil-seed rape (*Brassica napus* L.). J Agric Sci 102:23–31

Chuang C-F, Meyerowitz EM (2000) Specific and heritable genetic interference by double-stranded RNA in *Arabidopsis thaliana*. Proc Natl Acad Sci USA 97:4985–4990

Daniels RW, Scarisbrick DH, Smith LJ (1986) Oilseed rape physiology. In: Scarisbrick DH, Daniels RW (eds) Oilseed rape. Collins, London, pp 83–126

De Block M, De Brouwer D (1993) RNA–RNA in situ hybridization usingdigoxigenin-labeledprobes:theuseofhigh-molecular-weight polyvinyl alcohol in the alkaline phosphatase indoxyl-nitroblue tetrazolium reaction. Anal Biochem 215:86–89

De Block M, De Brouwer D, Tenning P (1989) Transformation of *Brassica napus* and *Brassica oleracea* using *Agrobacterium tumefaciens* and the expression of the *bar* and *neo* genes in the transgenic plants. Plant Physiol 91:694–701

Fray MJ, Evans EJ, Kelly A, Arthur AE, Lydiate DJ (1995) Evaluation of the effects of apetalous flowers and upright pods on seed yield using double haploid lines. Proceedings of the 9th international rapeseed congress, July 1995, Cambridge, UK. The Dorset Press, Dorchester, UK, pp 497–499

Fray MJ, Evans EJ, Lydiate DJ, Arthur AE (1996) Physiological assessment of apetalous flowers and erectophile pod in oilseed rape (*Brassica napus*). J Agric Sci 127:193–200

Fray MJ, Puangsomlee P, Goodrich J, Coupland G, Evans EJ, Arthur AE, Lydiate DJ (1997) The genetics of stamenoid petal production in oilseed rape (*Brassica napus*) and equivalent variant in *Arabidopsis thaliana*. Theor Appl Genet 94:731–736

Goto K, Meyerowitz EM (1994) Function and regulation of the *Arabidopsis* floral homeotic gene *PISTILLATA*. Genes Dev 8:1548–1560

Guan X, Stege J, Kim M, Dahmani Z, Fan N, Heifetz P, Barbas III CF, Briggs SP (2002) Heritable endogenous gene regulation in plants with designed polydactyl zinc finger transcription factors. Proc Natl Acad Sci USA 99:13296–13301

Harborth J, Elbashir SM, Bechert K, Tuschl T, Weber K (2001) Identification of essential genes in cultured mammalian cells using small interfering RNAs. J Cell Sci 114:4557–4565

Helliwell C, Waterhouse P (2003) Constructs and methods for high-throughput gene silencing in plants. Methods 30:289–295

Hill TA, Day CD, Zondlo SC, Thackeray AG, Irish VF (1998) Discrete spatial and temporal cis-acting elements regulate transcription of the *Arabidopsis* floral homeotic gene *APETALA3*. Development 125:1711–1721

Irish VF, Yamamoto YT (1995) Conservation of floral homeotic gene function between *Arabidopsis* and *Antirrhinum*. Plant Cell 7:1635–1644

Jack T (2001) Relearning our ABCs: new twists on an old model. Trends Plant Sci 6:310–316

Jack T, Brockman LL, Meyerowitz EM (1992) The homeotic gene *APETALA3* of *Arabidopsis thaliana* encodes a MADS-box and is expressed in petals and stamens. Cell 68:683–697

Jiang L, Becker HC (2003) Inheritance of apetalous flowers in a mutant of oilseed rape. Crop Sci 43:508–510

Jones L, Hamilton AJ, Voinnet O, Thomas CL, Maule AJ, Baulcombe DC (1999) RNA–DNA interactions and DNA methylation in post-transcriptional gene silencing. Plant Cell 11:2291–2302

Levin JZ, De Framond AJ, Tuttle A, Bauer MW, Heifetz PB (2000) Methods of double-stranded RNA-mediated gene inactivation in *Arabidopsis* and their use to define an essential gene in methionine biosynthesis. Plant Mol Biol 44:759–775

Liu Q, Singh S, Green A (2002) High-oleic and high-stearic cottonseed oils: nutritionally improved cooking oils developed using gene silencing. J Am Coll Nutr 21:205S-211S

Mandel MA, Gustafson-Brown C, Savidge B, Yanofsky MF (1992) Molecular characterization of the *Arabidopsis* floral homeotic gene *APETALA1*. Nature 360:273–277

Pelaz S, Ditta GS, Baumann E, Wisman E Yanofsky M (2000) B and C floral organ identity functions require *SEPALLATA* MADS-box genes. Nature 406:200–203

Pickford AS, Catalanotto C, Cogoni C, Macino G (2002) Quelling in *Neurospora crassa*. Adv Genet 46:277–303

Pierre J, Pierre LS, Marilleau R, Pham-Delegue MH, Tanguy X, Renard M (1996) Influence of the apetalous character in rape (*Brassica napus*) on the foraging behavior of honeybees (*Apis mellifera*). Plant Breeding 115:484–487

Purugganan MD, Rounsley SD, Schmidt RJ, Yanofsky MF (1995) Molecular evolution of flower development: diversification of the plant MADS-box regulatory gene family. Genetics 140:345–356

Rao MSS, Mendham NJ, Buzza GC (1991) Effect of the apetalous flower character on radiation distribution in the crop canopy, yield and its components in oilseed rape (*Brassica napus*). J Agric Sci 117:189–196

Smith LJ, Scarisbrick DH (1990) Reproductive development in oilseed rape (*Brassica napus* cv. Bienvenu). Ann Bot 65:205–212

Smith NA, Singh SP, Wang MB, Stoutjesdijk PA, Green AG, Waterhouse PM (2000) Total silencing by intron-spliced hairpin RNAs. Nature 407:319–20

Smyth DR, Bowman JL, Meyerowitz EM (1990) Early flower development in *Arabidopsis*. Plant Cell 2:755–767

Stoutjesdijk PA, Singh SP, Liu Q, Hurlstone CJ, Waterhouse PA, Green AG (2002) hpRNA-mediated targeting of the *Arabidopsis* FAD2 gene gives highly efficient and stable silencing. Plant Physiol 129:1723–1731

Theißen G (2001) Development of floral organ identity: stories from the MADS house. Curr Opin Plant Biol 4:75–85

Tilly JJ, Allen DW, Jack T (1998) The CArG boxes in the promoter of the *Arabidopsis* floral organ identity gene *APETALA3* mediate diverse regulatory effects. Development 125:1647–1657

Vaistij FE, Jones L, Baulcombe DC (2002) Spreading of RNA targeting and DNA methylation in RNA silencing requires transcription of the target gene and a putative RNA-dependent RNA polymerase. Plant Cell 14:857–867

Valvekens D, Van Lijsebettens M, Van Montagu M (1992) *Arabidopsis* regeneration and transformation (root explant system). In: Lindsey K (ed) Plant tissue culture manual, vol A8. Kluwer, Dordrecht, pp 1–17

Vancanneyt G, Schmidt R, O'Connor-Sanchez A, Willmitzer L, Rocha-Sosa M (1990) Construction of an intron-containing marker gene: splicing of the intron in transgenic plants and its use in monitoring early events in *Agrobacterium*-mediated plant transformation. Mol Gen Genet 220:245–250

Wang MB, Waterhouse PM (2002) Application of gene silencing in plants. Curr Opin Plant Biol 5:146–150

Waterhouse PM, Graham MW, Wang MB (1998) Virus resistance and gene silencing in plants can be induced by simultaneous expression of sense and antisense RNA. Proc Natl Acad Sci USA 95:13959–13964

Weigel D, Meyerowitz EM (1994) The ABCs of floral homeotic genes. Cell 78:203–209

Wesley SV, Helliwell CA, Smith NA, Wang MB, Rouse DT, Liu Q, Gooding PS, Singh SP, Abbott D, Stoutjesdijk PA, Robinson SP, Gleave AP, Green AG, Waterhouse PM (2001) Construct design for efficient, effective and high-throughput gene silencing in plants. Plant J 27: 581–590

Yanofsky MF, Ma H, Bowman JL, Drews GN, Feldmann KA, Meyerowitz EM (1990) The protein encoded by the *Arabidopsis* homeotic gene *agamous* resembles transcription factors. Nature 346:35–39

Yun JY, Weigel D, Lee I (2002) Ectopic expression of *SUPERMAN* suppresses development of petals and stamens. Plant Cell Physiol 43:52–57

Zhou Y, Wang H, Gilmer S, Whitwill S, Keller W, Fowke LC (2002) Control of petal and pollen development by the plant cyclin-dependent kinase inhibitor *ICK1* in transgenic *Brassica* plants. Planta 215:248–257

ACADEMIC PRESS

Available online at www.sciencedirect.com

SCIENCE DIRECT®

Methods 30 (2003) 322–329

METHODS

www.elsevier.com/locate/ymeth

Making a better RNAi vector for *Drosophila*: use of intron spacers

Young Sik Lee and Richard W. Carthew*

Department of Biochemistry, Molecular Biology, and Cell Biology, Northwestern University, 2153 North Campus Drive, Evanston, Illinois 60208, USA

Accepted 7 February 2003

Abstract

Double-stranded RNA induces sequence-specific inhibition of gene expression at a posttranscriptional level in eukaryotes (RNAi). This natural phenomenon has been developed into a tool for studying gene function in several model organisms, including *Drosophila melanogaster*. Transgenes bearing inverted repeats are able to exert an RNAi effect in *Drosophila*, but cloning difficulties and inconsistent silencing complicate the method. We have constructed a transgene containing inverted repeats separated by a functional intron such that mRNA produced by the transgene is predicted to form loopless hairpin RNA following splicing. A single copy of the transgene effectively and uniformly silences expression of a target gene (*white*) in transgenic flies. We have developed a vector that is designed to produce intron-spliced hairpin RNA corresponding to any *Drosophila* gene. The vector is under control of the upstream activating sequence (UAS) of the yeast transcriptional activator GAL4. The UAS/GAL4 system allows hairpin RNA to conditionally silence gene expression in *Drosophila* in a tissue-specific manner. Moreover, the presence of the intron spacer greatly enhances the stability of inverted-repeat sequences in bacteria, facilitating the cloning procedure.

1. Introduction

The sequencing of the *Drosophila melanogaster* genome provides an exceptional opportunity to analyze the different functions governed by its genes [1]. Traditionally, genes are characterized by loss-of-function phenotypes caused by mutations that are induced randomly by chemical, physical, or insertional mutagenesis. The annotated sequence of the *Drosophila* genome enables reverse-genetic approaches to be used on a genome-wide scale to generate loss-of-function phenotypes. Targeted gene knockouts have recently been described in *Drosophila* [2,3], but this approach is laborious and does not allow for conditional silencing of gene expression.

Recently, RNA interference (RNAi) has been demonstrated to be an effective reverse-genetic approach to generating loss-of-function phenotypes. The presence of double-stranded RNA (dsRNA) causes the sequence-specific posttranscriptional silencing of a corresponding gene in a variety of organisms [4]. Thus, RNAi is used to inactivate genes of interest and provides a powerful tool to study gene function. Injection of dsRNA into *Drosophila* embryos silences gene activity effectively, but its effect is transient and is not inherited in the next generation [5,6]. To overcome this problem, methods have been developed to express dsRNA stably in transgenic *Drosophila*. Most of these methods employ transgenes having an inverted-repeat (IR) configuration, which are able to produce dsRNA as extended hairpin RNA [7–10]. An alternative method has used a transgene that is symmetrically transcribed from opposing promoters [11]. A general problem with these methods is that transgenic lines often induce a variable RNAi silencing effect that exhibits incomplete penetrance and expressivity. Consequently, the copy number of silencing transgenes usually needs to be increased to observe uniform and complete gene silencing. Moreover, it is often difficult to make stable recombinant plasmids containing IRs in *Escherichia coli*. Introduction of a spacer sequence between the repeats helps stabilize some recombinant plasmids, but there are still significant reported stability problems.

In this paper, we describe an IR-based transgene designed such that the repeats are separated by a functional intron and thus are defined exons. We report that,

* Corresponding author. Fax: 1-847-467-1380.
E-mail address: r-carthew@northwestern.edu (R.W. Carthew).

1046-2023/03/$ - see front matter © 2003 Elsevier Science (USA). All rights reserved.
doi:10.1016/S1046-2023(03)00051-3

in *Drosophila*, the transgene is a powerful repressor of gene activity in vivo, with one copy of the transgene exerting uniformly strong silencing. We further describe a modular system combining GAL4-regulated gene expression with conditional production of the silencing dsRNA to allow systematic RNAi in *Drosophila* using IR exons. With this system, inhibition of gene activity is flexibly induced in any spatial or temporal pattern, allowing for precise disruption of gene function. This technique could potentially be a powerful and economical approach to studying gene function in *Drosophila* and to manipulating gene function in specific tissues of postembryonic individuals.

2. First-generation transgenic RNAi in *Drosophila*

We initially developed a method to express dsRNA as extended hairpin-loop RNA [10]. Its design was modeled on the successful application of hairpin RNAs in generating RNAi in plants and the nematode *Caenorhabditis elegans* by expression of transgenes with IR sequences. To facilitate cloning of IRs into recombinant plasmids, we placed a 5-base nonpalindromic sequence centered at the axis of dyad symmetry that was a *Sfi*I site, GGCCATCTAGGCC (Fig. 1). This allowed us to easily ligate gene fragments together in inverted orientation, and it increased the stability of the IR DNA during plasmid replication. Sequence repeats are often deleted in *E. coli* because cruciform intermediates form during replication of plasmid DNA and are excised by the *sbcBC* gene products. Insertion of nonrepetitive sequence greater than 4 bp in length between IRs inhibits cruciform excision during replication [12]. Recombinant plasmids were replicated in a recombination-deficient strain. No strain is guaranteed to propagate all recombinant clones, but the SURE strain (Stratagene) is deficient in *recBC sbcBC* and eliminates all known restriction systems. Other strains we used were JM103 and JM105, which are also mutant for *sbcBC*.

To construct an IR transgene, the IR fragment is first cloned into a generic high-copy plasmid vector such as pBluescript (Stratagene) by directional *Eco*RI–*Xho*I two-way ligation. Stable recombinants are selected, and then the IR fragment is shuttled from pBluescript into the *Drosophila* transformation plasmid vector pUAST [13]. We found it more difficult to directly clone IR fragments made in vitro into pUAST, which we circumvented by shuttling the fragment first through pBluescript. On the 5′ side of the multicloning site, pUAST contains a *Drosophila* promoter linked to GAL4-responsive upstream activating sequence (UAS) enhancer repeats and on the 3′ side of the multicloning site, pUAST contains a polyadenylation signal sequence. Recombinant plasmids are then injected with helper plasmid into *Drosophila* embryos and transformant flies are generated by standard P element transformation [14]. Cloning the IR into a UAS vector allowed us to use the modular design of the GAL4/UAS system in *Drosophila* for misexpressing transgenes. Many useful lines of *Drosophila* express the yeast GAL4 protein in a variety of cells/tissues at various stages of the fly life cycle [13]. GAL4 acts as a sequence-specific transcription activator in *Drosophila*. The GAL4 line is

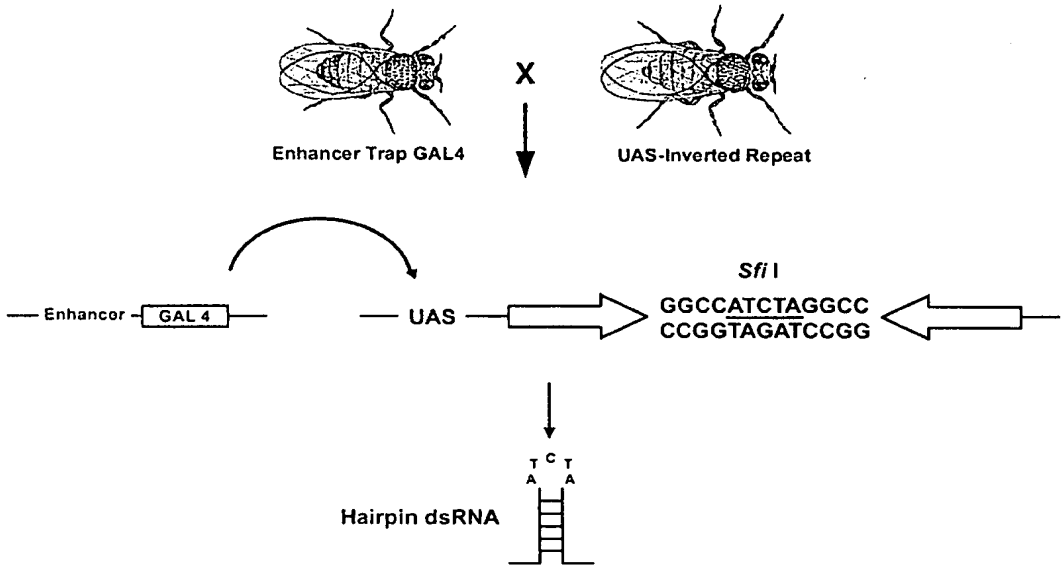

Fig. 1. First-generation transgenic RNAi. Inverted repeats are made by head–head or tail–tail ligation through a *Sfi*I site, which is introduced at one end of each repeat. The inverted repeat is placed downstream of the upstream activating sequence (UAS) promoter, and transgenic lines are made. When these UAS lines are crossed to GAL4 driver lines, the F1 heterozygotes contain both GAL4 and UAS genes [13]. Tissue-specific expression of the inverted repeats by GAL4 protein produces hairpin-loop RNA that is competent to induce RNAi in *Drosophila*.

crossed to a target UAS line carrying a single target P element inserted at a unique and random position in the genome. The target element carries a GAL4-responsive UAS enhancer, and progeny that contain both GAL4 and UAS elements express the IR sequence in cells expressing GAL4. Phenotypes due to the presence of hairpin-loop RNA in these cells can then be scored directly in flies. The RNAi system takes advantage of two very useful techniques in *Drosophila:* P element transformation and the modular GAL4/UAS system. The modular design makes analysis by RNAi flexible since hairpin-loop RNA can be produced in any spatial or temporal pattern. Moreover, RNAi is conditional, dependent on the presence of both UAS and GAL4 elements in the same individual. Thus, RNAi that might induce lethal or sterile phenotypes is conditionally generated in selected flies, and stably inherited *Drosophila* lines carrying the UAS element alone can be propagated without deleterious RNAi effect.

One feature of the target element that was critical for the success of this method was that the IR was stable in the *Drosophila* genome. This appears to be the case since UAS lines have been maintained in our lab stocks for 2 years without loss of RNAi potency when crossed with GAL4 driver lines. However, two other features of the method have proved to be more problematic. First, RNAi silencing is frequently variable, with only a fraction of treated animals exhibiting complete silencing. This partial effect is also observed at the level of target mRNA abundance in that a pooled population of treated animals might exhibit at most a fourfold reduction in mRNA levels. Thus, treated individuals have a spectrum of RNAi-induced phenotypes, which makes interpretation of gene function somewhat difficult. Moreover, there is frequently a variation in the strength of RNAi effects between different transformant lines carrying the same IR transgene. This is likely due to influence of nearby chromosomal modulation of transgene expression that depends on the point of transgene insertion. Since RNAi silencing is not complete, weak or strong IR expression translates to a corresponding weak or strong silencing effect. A second problem with this first-generation RNAi vector has been the variable success in cloning IRs from different genes. Some IRs are easily cloned even into *sbcBC*$^+$ bacterial strains. However, some IRs have proved recalcitrant to cloning in any strain or any plasmid. To date, we have been unable to predict which sequences will produce problems when cloned as IRs. This makes transgene production a somewhat empirical trial-by-error process.

3. Transgenic RNAi with inverted exon repeats

The problems with the first-generation vector inspired us to devise a new approach to produce hairpin RNA in vivo. It was reported that intron-spliced hairpin RNA can induce gene silencing in plants more efficiently than standard hairpin-loop RNA [15]. In a sense, the inverted repeats are structural and functional exons. The nonpalindromic intron sequence may also provide stability to the DNA construct with inverted repeats in bacteria. This led us to test an RNAi construct containing inverted repeats separated by an intron sequence, from which loopless hairpin dsRNA is predicted to be produced following splicing in *Drosophila* (Fig. 2). As a proof-of-principle demonstration of its effectiveness, we decided to test the approach on silencing the *white* gene.

The *Drosophila white* gene encodes an ABC transporter involved in localizing pigments to eye pigment granules [16]. The *white* gene was chosen because expression can be easily monitored phenotypically by changes in eye color. A *white*$^+$ eye is dark red in color while the eye of a null *white* mutant is completely white in color (Fig. 3). Since cloned variants of *white* are routinely used in *Drosophila* transformation vectors as the selectable marker for transformation of *white* mutant flies, we adopted an opposing transformation strategy. That is, we constructed a transformation vector with a *white* IR but no independent marker gene for selecting transformants. We then transformed *white*$^+$ flies with the vector and selected transformants that had a *white* loss-of-function phenotype. If an inserted *white* IR transgene successfully silenced its endogenous target gene, the transformant would be white-eyed.

The 74-nucleotide second intron of the *white* gene bears all features of a consensus *Drosophila* intron, and it was found to efficiently splice in *Drosophila* embryonic extracts in vitro [17,18]. Since *white* is normally not expressed in embryos, this result indicates that the intron can be spliced in heterologous tissues. Thus, we chose the second intron to separate inverted repeats of *white* coding sequence in our model transgene.

The 629-bp third exon of *white* was chosen to be the inverted sequence in the transgene that would mediate the RNAi effect. The third exon was amplified by PCR with unique *Pst*I and *Eco*RI sites, and it was ligated in inverted orientation upstream of a 703-bp fragment containing the *white* second intron and third exon (Fig. 2). The tail-to-tail repeat was placed into the pGMR transformation vector plasmid [19]. pGMR drives expression of transgenes specifically in the developing and adult compound eye by virtue of the eye-specific GMR promoter. This ensured that the *white* IR transgene would be expressed only in the same cells that normally express the endogenous target *white* gene. The *Drosophila* consensus sequence for a 5′ splice site is AG|GTRAGT, where | designates the splice site and R indicates A or G [17]. It is noteworthy that the ligation between the two DNA fragments through the *Pst*I site does not change the consensus sequence required for

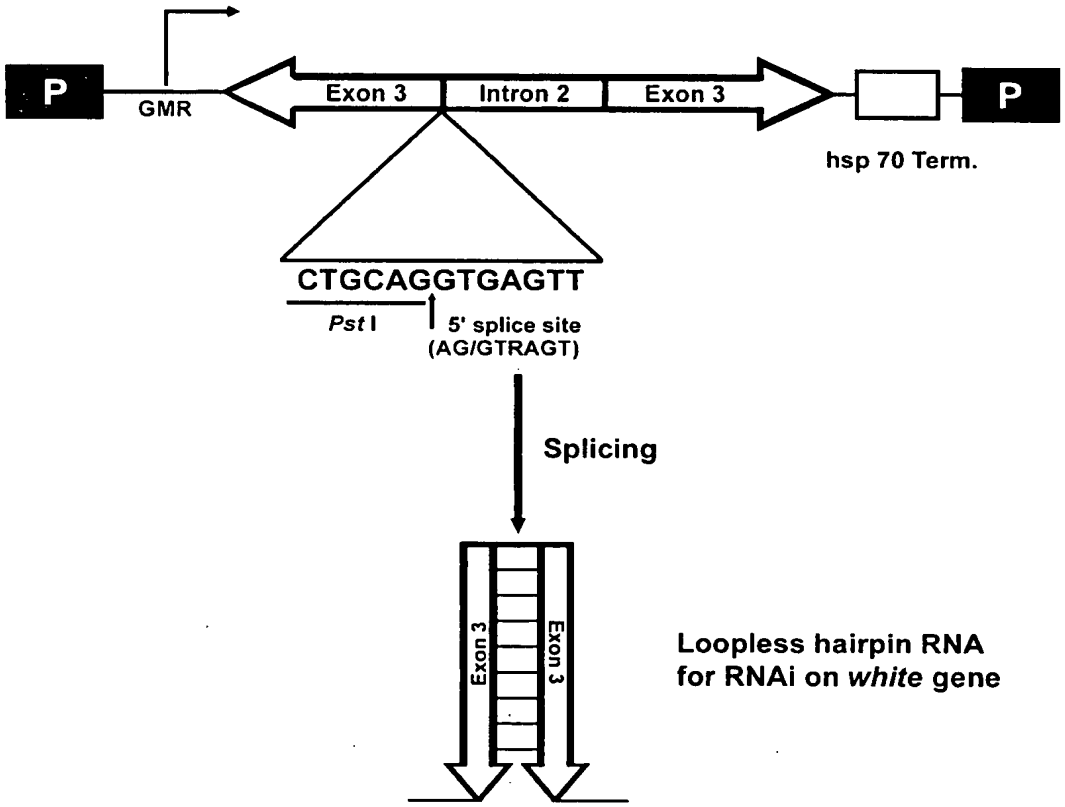

Fig. 2. Scheme for the generation of transgenic RNAi against the *Drosophila white* gene by intron-spliced hairpin RNA. Inverted repeats corresponding to the third exon of the *white* gene and separated by the second intron of the same gene were placed into the pGMR transformation vector. A fragment containing the *white* second intron and third exon was ligated to a fragment containing the inverted *white* third exon to generate a *PstI* site at the point of ligation. Note that the *PstI* site is coincident with the 5′ splice site but does not disrupt sequences necessary for 5′ splice site function. The *Drosophila* consensus sequence for a 5′ splice site is shown in parentheses, in which / designates the splice site and R indicates A or G. The transgene is under transcriptional control of the GMR enhancer, which is exclusively active in the developing and adult retinal tissue that also expresses the endogenous *white* gene.

5′ splice site recognition (Fig. 2). Since we intended to induce RNAi on the endogenous *Drosophila white* gene, an *XhoI–NsiI* fragment corresponding to the pGMR *white* marker gene was deleted from pGMR.

Although we transformed ligation products including inverted repeats into the SURE strain (Stratagene) of *E. coli* to maximize the stability of the DNA, the repeats were also stable in a DH5α strain, possibly as a result of the short *white* second intron sequence contributing to the stability of the inverted-repeat sequences. In contrast, attempts at cloning an IR of the *white* third exon separated by a *SfiI* spacer into plasmids was repeatedly unsuccessful in a variety of host bacterial strains.

The pGMR-derived plasmid containing the DNA fragment for intron-spliced *white* hairpin RNA was introduced into the germ line of CantonS flies by P element transformation [14]. From approximately 1500 injected animals, eight independent transformant lines that exhibited a *white* loss-of-function phenotype were established. This transformation frequency is within an order of magnitude of the average transformation frequency using a standard P element vector [14], which suggests that *white* RNAi from the IR transgene acts as a reliable marker for transformation. All eight transformant lines exhibited a yellow to pale-yellow eye color phenotype with one copy of the transgene (Fig. 3). Moreover, all individual flies from each line exhibited a uniform eye color phenotype, indicating strong penetrance and expressivity of the RNAi effect. Only females were compared to avoid any effect related to dosage compensation of the transgene. No additional or abnormal phenotypes were observed in silenced individuals, indicating that silencing was specific. The effect was stably maintained over each adult's lifetime, and silencing has been maintained over the many generations that these lines have so far been kept. Transformant adults bearing two copies of the transgene had an eye color indistinguishable from that of *white* null mutants (Fig. 3). Levels of *white* mRNA on a Northern blot were reduced in two transformant lines tested compared to wild type, to a degree consistent with their eye color phenotypes (data not shown). In conclusion, the

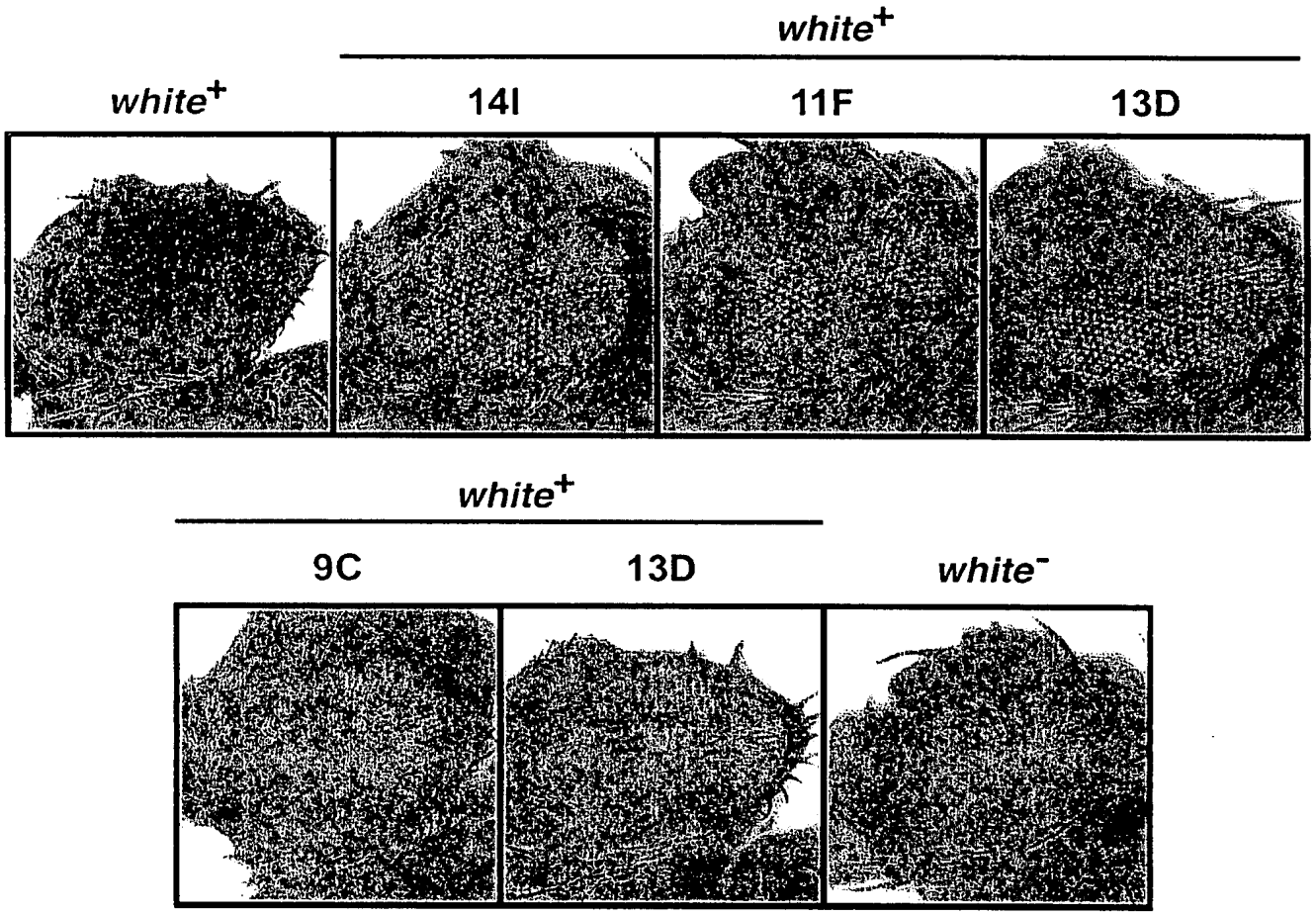

Fig. 3. Eye color phenotypes of female adults (3–5 days of age) that carry the *white* intron–hairpin GMR transgene. The top left shows a parental CantonS (wild-type *white*) fly. The lower right shows a w^{1118} null mutant for the *white* gene. A P[*GMR-whiteIR*] transformant line designated 13D has the transgene on the X chromosome of the parental CantonS strain, whereas the 9C, 11F, and 14I lines have the transgene on the third chromosome of CantonS. The eye colors of transformants bearing a single copy of the transgene is shown in the top. The bottom shows eye colors of transformants bearing two copies of the transgene.

inverted exon repeat of *white* effectively silences the expression of the endogenous *white* gene in vivo.

4. A modular and multipurpose transgenic RNAi vector

Since the RNAi construct bearing an intron strongly inhibited *white* gene expression, we adapted this method to create an all-purpose RNAi vector that employs spliced hairpin RNA. The vector is derived from the pUAST transformation plasmid. This then offers the advantages of the GAL4/UAS modular expression system, as outlined earlier. We constructed the vector (pWIZ, for white intron zipper) into which gene fragments can be subcloned upstream and downstream of the 74-nucleotide *white* intron (Fig. 4). The intron is flanked by *Eco*RI, *Bgl*II, *Not*I, *Xho*I, *Spe*I, and *Avr*II sites on the 5′ side and by *Nhe*I, *Mlu*I, and *Xba*I sites on the 3′ side. The entire cassette is downstream of the UAS enhancer–promoter and upstream of the SV40 transcription termination site. The *Avr*II and *Nhe*I sites in pWIZ conform to the consensus sequences for 5′ and 3′ splice sites, respectively. Thus, any DNA fragment inserted into the *Avr*II or *Nhe*I site is fully competent to be spliced as an exon. Moreover, the *Spe*I, *Avr*II, *Nhe*I, and *Xba*I sites are unique in pWIZ, providing convenient cloning sites for gene fragments.

To construct an IR transgene using pWIZ, a DNA fragment corresponding to the gene of interest is inserted twice into pWIZ, with inserts in opposite orientations on each side of the intron (Fig. 5). The simplest means to insert the DNA is as a PCR fragment. The system is designed so that a single PCR fragment derived from only two PCR primers can be inserted on each side of the intron. This is because *Spe*I, *Avr*II, *Nhe*I, and *Xba*I sites are all ligation-compatible with each other. Consequently, restriction sites compatible with *Avr*II and *Nhe*I sites should be placed in the PCR

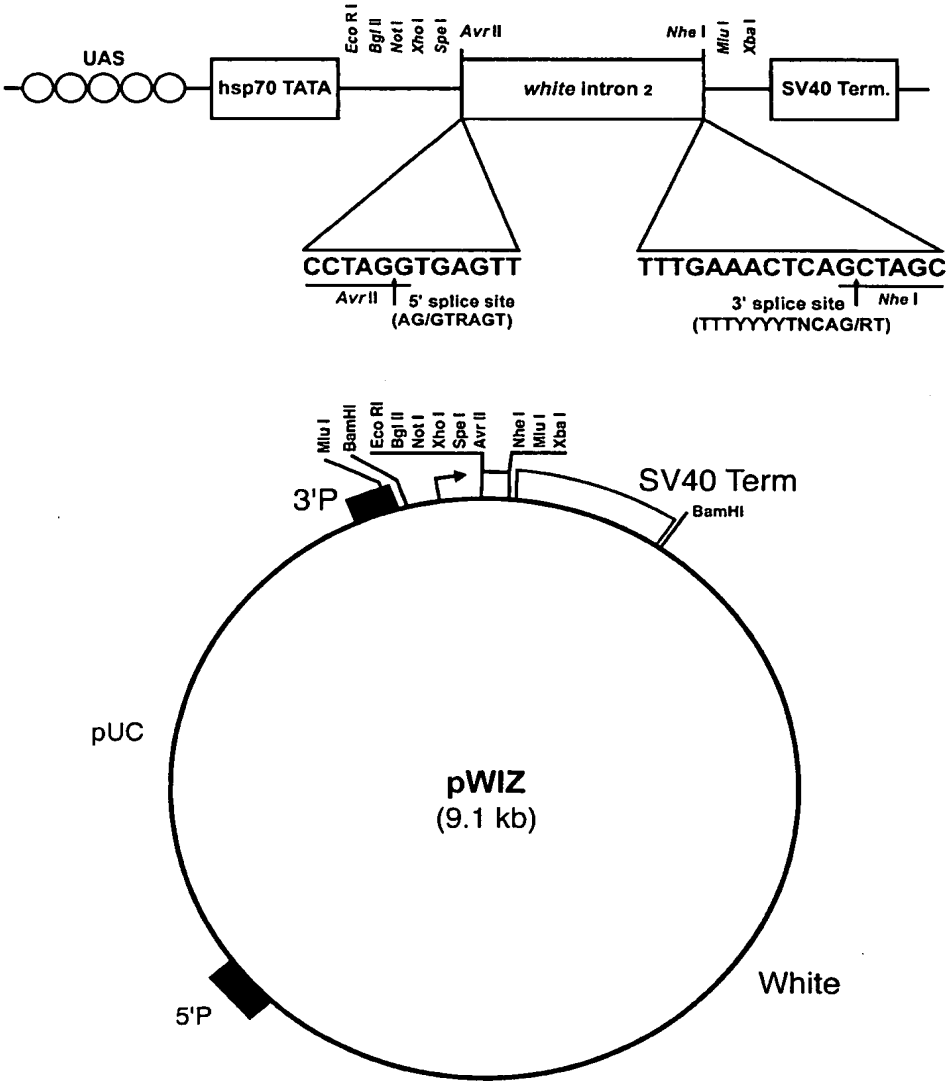

Fig. 4. Schematic representation of the pWIZ vector. The pWIZ vector was constructed by placing the 74-bp second intron of the *white* gene into the pUAST transformation vector [13]. The intron is flanked by unique *Eco*RI, *Bgl*II, *Not*I, *Xho*I, *Spe*I, and *Avr*II sites on the 5′ side and *Nhe*I and *Xba*I sites on the 3′ side to facilitate cloning. The sequences at the junction of the 5′ and 3′ splice sites in the vector are highlighted, and arrows indicate the 5′ and 3′ splice sites. The consensus sequences for 5′ and 3′ splicing are shown in parentheses: /, the splice site; R, purine; Y, pyrimidine; N, any base. Below is shown a restriction map of the pWIZ plasmid.

primers at their 5′ ends. The resulting PCR product will then have *Avr*II- and *Nhe*I-compatible ends after appropriate restriction digestion. The RNAi construct is made by two sequential insertions of the same PCR product into the *Avr*II and *Nhe*I sites of pWIZ (Fig. 5). For efficient digestion, we add an extra 4 nucleotides to the 5′ side of each primer restriction site. The size of amplified DNA ranges from 500 to 700 bp. Most important, we ensure that the sequence does not contain any internal restriction sites used in the PCR primers, nor should the fragment have sequences in either sense or antisense orientation that match either 5′ or 3′ consensus splice sites. This latter aspect is important to prevent cryptic splicing from disrupting hairpin RNA formation. The PCR product is digested with the appropriate enzyme and ligated into the *Avr*II site of pWIZ. After a clone with the desired orientation of the insert is selected by restriction mapping, the same PCR product is ligated into the *Nhe*I site of the pWIZ derivative, and recombinants with the insert in opposite orientation to the first are screened and selected.

We have made five transgenic RNAi constructs for genes under study in our laboratory using the pWIZ vector. All of these constructs are stable as inverted repeats in *E. coli* strains such as SURE cells. Moreover, they have been introduced into the *Drosophila* genome

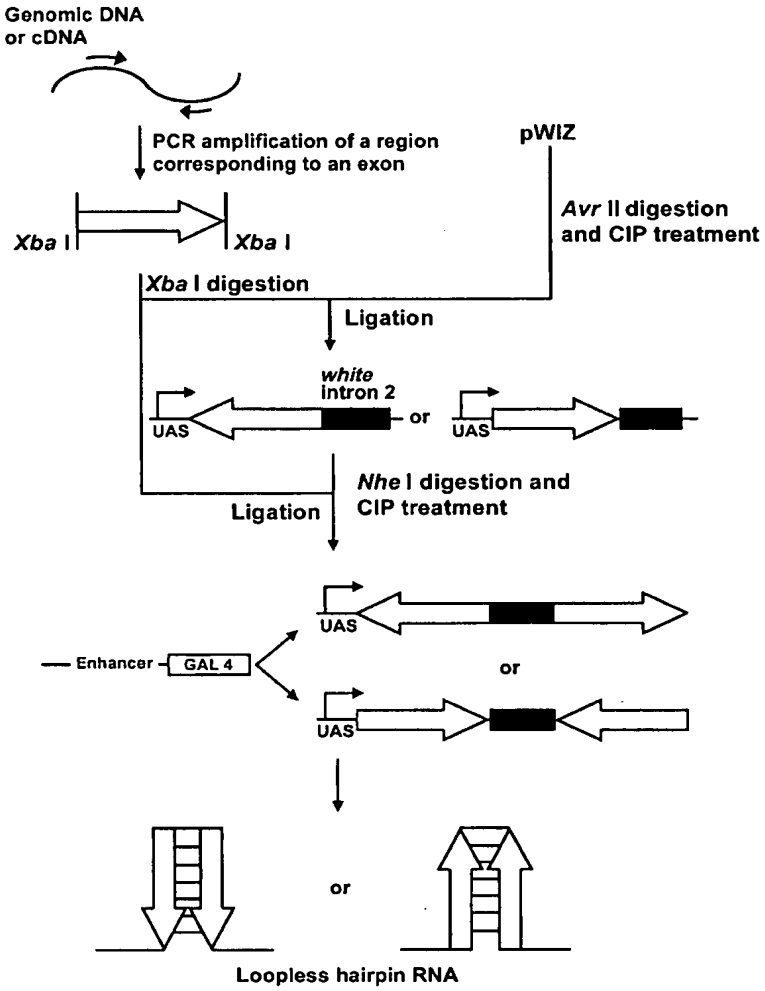

Fig. 5. A typical procedure for making a RNAi construct using the pWIZ vector. A DNA fragment corresponding to a *Drosophila* target gene is amplified by PCR. A restriction site (*Spe*I, *Avr*II, *Nhe*I, or *Xba*I) compatible with *Avr*II and *Nhe*I should be present at the 5′ end of each PCR primer. The fragment can correspond to part of an exon, a complete exon, or several contiguous exons. Several criteria should be used in choosing the fragment: it should be 500 to 700 bp in length, it should not have internal restriction sites corresponding to the PCR primer sites, and it should not have sequences in either sence or antisense orientation that match a 5′ or 3′ consensus splice site. This latter aspect is critical to prevent cryptic splice sites from disrupting proper splicing of the hairpin RNA. As shown, an *Xba*I site is generated at each end of a PCR-amplified exon for cloning the PCR product. The PCR product is inserted twice by two ligation steps into the *Avr*II and *Nhe*I sites of pWIZ. CIP, calf intestinal phosphatase used to dephosphorylate the 5′ ends of vector DNA prior to ligation. Recombinants are selected in the desired orientation, such that after the second ligation step, inserts are in opposite orientation on either side of the *white* intron. IRs that are head–head or tail–tail repeats might be used depending upon whether cryptic splice sites are present in the constructs. Transformation follows to generate stable transgenic lines carrying the WIZ gene. Upon mating of transgenic animals harboring the WIZ gene with animals carrying tissue- or cell-specific GAL4 drivers, the F1 progeny produce loopless hairpin RNA. This induces RNAi against target genes in tissue- and cell-specific patterns.

by P element transformation, and all constructs transformed efficiently to give stable lines.

5. Concluding remarks

In conclusion, we have developed transgenic RNAi in *Drosophila* that can be applied to many developmental and physiological processes. Hairpin RNA produced from a transgene composed of inverted repeats can specifically silence gene expression in *Drosophila*. The presence of a spacer between the inverted repeats makes for easier cloning but is offset by a weaker silencing activity in vivo [8,20]. In plants, using a functional intron as the spacer between inverted repeats strongly enhanced silencing activity of the RNAi transgene [15]. We have shown that using a functional intron as a spacer between inverted repeats produces strong and uniform RNAi silencing in *Drosophila*. A similar observation has been recently noted in *Drosophila* when inverted repeats

composed of cDNA–genomic DNA hybrids are separated by functional introns [21]. We have also described a multifunctional RNAi transformation vector (pWIZ) containing an intron spacer that makes RNAi simple to perform for the following reasons. A single PCR fragment of a gene is sufficient to construct a targeting vector; the inverted repeat sequence need not have splice sites present since they are provided by pWIZ; splice sites are preserved when the repeat fragments are inserted; the intron spacer provides stability to the inverted repeats when the plasmid is replicated in *E. coli*. Once the vector is transformed into *Drosophila*, it is conditionally quiescent until crossed with GAL4-expressing lines. Many useful GAL4-expressing lines are available, making the RNAi approach adaptable for most studies of *Drosophila*. This method is likely to be very useful for analyzing the function of the many *Drosophila* genes for which no loss-of-function mutations are available. Finally, the method provides a powerful tool to create loss-of-function phenotypes in a manner conditional for particular tissues and developmental times.

References

[1] M.D. Adams, S.E. Celniker, R.A. Holt, C.A. Evans, J.D. Gocayne, P.G. Amanatides, S.E. Scherer, P.W. Li, R.A. Hoskins, R.F. Galle, et al., Science 287 (2000) 2185–2195.
[2] Y.S. Rong, K.G. Golic, Science 288 (2000) 2013–2018.
[3] Y.S. Rong, K.G. Golic, Genetics 157 (2001) 1307–1312.
[4] S.M. Hammond, A.A. Caudy, G.J. Hannon, Nat. Rev. Genet. 2 (2001) 110–119.
[5] J.R. Kennerdell, R.W. Carthew, Cell 95 (1998) 1017–1026.
[6] L. Misquitta, B.M. Paterson, Proc. Natl. Acad. Sci. USA 96 (1999) 1451–1456.
[7] G. Lam, C.S. Thummel, Curr. Biol. 10 (2000) 957–963.
[8] E. Fortier, J.M. Belote, Genesis 26 (2000) 240–244.
[9] S. Martinek, M.W. Young, Genetics 156 (2000) 1717–1725.
[10] J.R. Kennerdell, R.W. Carthew, Nat. Biotechnol. 18 (2000) 896–898.
[11] E. Giordano, R. Rendina, I. Peluso, M. Furia, Genetics 160 (2002) 637–648.
[12] A. Davison, D.R. Leach, Genetics 137 (1994) 361–368.
[13] A.H. Brand, N. Perrimon, Development 118 (1993) 401–415.
[14] A.C. Spradling, G.M. Rubin, Science 218 (1982) 341–347.
[15] N.A. Smith, S.P. Singh, M.-B. Wang, P.A. Stoutjesdijk, A.G. Green, P.M. Waterhouse, Nature 407 (2000) 319–320.
[16] S.M. Mackenzie, A.J. Howells, G.B. Cox, G.D. Ewart, Genetica 108 (2000) 239–252.
[17] S.M. Mount, C. Burks, G. Hertz, G.D. Stormo, O. White, C. Fields, Nucleic Acids Res. 20 (1992) 4255–4262.
[18] M. Guo, P.C.H. Lo, S.M. Mount, Mol. Cell. Biol. 13 (1993) 1104–1118.
[19] B.A. Hay, T. Wolff, G.M. Rubin, Development 120 (1994) 2121–2129.
[20] A. Piccin, A. Salameh, C. Benna, F. Sandrelli, G. Mazzotta, M. Zordan, E. Rosato, C.P. Kyriacou, R. Costa, Nucleic Acids Res. 29 (2001) E55.
[21] S. Kalidas, D.P. Smith, Neuron 33 (2002) 177–184.

Exhibit 11

The Plant Cell, Vol. 17, 859–875, March 2005, www.plantcell.org © 2005 American Society of Plant Biologists

The Cotton *ACTIN1* Gene Is Functionally Expressed in Fibers and Participates in Fiber Elongation

Xue-Bao Li,[a,b] Xiao-Ping Fan,[b] Xiu-Lan Wang,[a] Lin Cai,[b] and Wei-Cai Yang[b,c,1]

[a] College of Life Sciences, Central China Normal University, Wuhan 430079, China
[b] Temasek Life Sciences Laboratory, National University of Singapore, Singapore 117604
[c] Institute of Genetics and Developmental Biology, Chinese Academy of Sciences, Beijing 100080, China

Single-celled cotton fiber (*Gossypium hirsutum*) provides a unique experimental system to study cell elongation. To investigate the role of the actin cytoskeleton during fiber development, 15 *G. hirsutum ACTIN* (*GhACT*) cDNA clones were characterized. RNA gel blot and real-time RT-PCR analysis revealed that *GhACT* genes are differentially expressed in different tissues and can be classified into four groups. One group, represented by *GhACT1*, is expressed predominantly in fiber cells and was studied in detail. A 0.8-kb *GhACT1* promoter sufficient to confirm its fiber-specific expression was identified. RNA interference of *GhACT1* caused significant reduction of its mRNA and protein levels and disrupted the actin cytoskeleton network in fibers. No defined actin network was observed in these fibers and, consequently, fiber elongation was inhibited. Our results suggested that *GhACT1* plays an important role in fiber elongation but not fiber initiation.

INTRODUCTION

Actin cytoskeleton plays an important role in cell morphogenesis in plants as demonstrated by pharmacological, biochemical, and genetic studies (Kost and Chua, 2002; Mathur and Hülskamp, 2002). The actin cytoskeleton may be involved in the transportation of organelles and vesicles carrying membranes and cell wall components to the site of cell growth as in root hairs, trichome cells, and pollen tubes. Therefore, the actin cytoskeleton is essential for cell elongation and tip growth. Disruption of the actin cytoskeleton during trichome development by actin-interacting drugs resulted in randomly distorted trichomes with unextended branches (Mathur et al., 1999; Szymanski et al., 1999). Similarly, inhibition of F-actin elongation blocked the initiation of polar growth and elongation of root hairs (Miller et al., 1999). Furthermore, reduction in actin arrays resulted in dramatic reduction of root hair length and caused severe bulges in the *actin2* (*act2*) mutant and serious retardation of root growth in the *act7* mutant in *Arabidopsis thaliana* (Gilliland et al., 2002, 2003). Misexpression of the reproductive *ACT11* gene in vegetative tissues of Arabidopsis altered morphology of most organs in plants because of its effects on the proportion of different actin isovariants (Kandasamy et al., 2002). In polarized elongating cell types, such as root hairs and trichomes, it is believed that long F-actin cables oriented longitudinally throughout the shank and subapical, and net-axially aligned fine F-actins are essential for the intracellular trafficking of organelles and secretory vesicles to the growing apical region to deliver new membranous and cell wall materials (Mathur et al., 1999; Miller et al., 1999; Szymanski et al., 1999; Baluska et al., 2000; Hepler et al., 2001; Chueng et al., 2002). The unstable dynamic F-actin cytoskeleton also plays a role in localized expansion of root hairs and trichome cells (Ketelaar et al., 2003; Mathur, et al., 2003a).

The actin cytoskeleton controls polar cell growth through its interaction with several actin binding proteins, such as actin depolarizing factor (Dong et al., 2001; Chen et al., 2002), profilin (Clarke et al., 1998), Rho family GTPase (Yang, 1998; Chueng et al., 2002; Fu et al., 2002), and the calcium signaling pathway (Malhó, 1998; Franklin-Tong, 1999; Li et al., 1999). The effective regulation of actin turnover by actin regulators may be critical for pollen tube growth (Chen et al., 2002, 2003) and for polar cell expansion in cell types other than root hair and trichome (Fu et al., 2002). Recent studies showed genetically that the actin cytoskeleton by interacting with the ARP2/ARP3 complex plays a pivotal role in controlling cell shape of trichome cells and several other cell types in Arabidopsis (Mathur et al., 2003a, 2003b). In cotton (*Gossypium hirsutum*), F-actin has been implicated in regulating microtubule orientation during fiber development shown by in vitro drug studies (Seagull, 1990). However, the role of the actin cytoskeleton in cotton fiber cell development remains largely unknown.

Actins in plants are encoded by a multigene family that comprises dozens or even hundreds of actin genes. In Arabidopsis, the actin gene family contains 10 distinct members, of which eight are functional genes and two are pseudogenes (McDowell et al., 1996). In other plant species, the actin gene family also appears to have dozens of members (Baird and Meagher, 1987; Thangavelu et al., 1993; Meagher and Williamson, 1994). Studies on actin sequences revealed that structural and

[1] To whom correspondence should be addressed. E-mail wcyang@genetics.ac.cn; fax 86-10-62551272.
The authors responsible for distribution of materials integral to the findings presented in this article in accordance with the policy described in the Instructions for Authors (www.plantcell.org) are: Xue-Bao Li (xbli@mail.ccnu.edu.cn) and Wei-Cai Yang (wcyang@genetics.sc.cn).
Article, publication date, and citation information can be found at www.plantcell.org/cgi/doi/10.1105/tpc.104.029629.

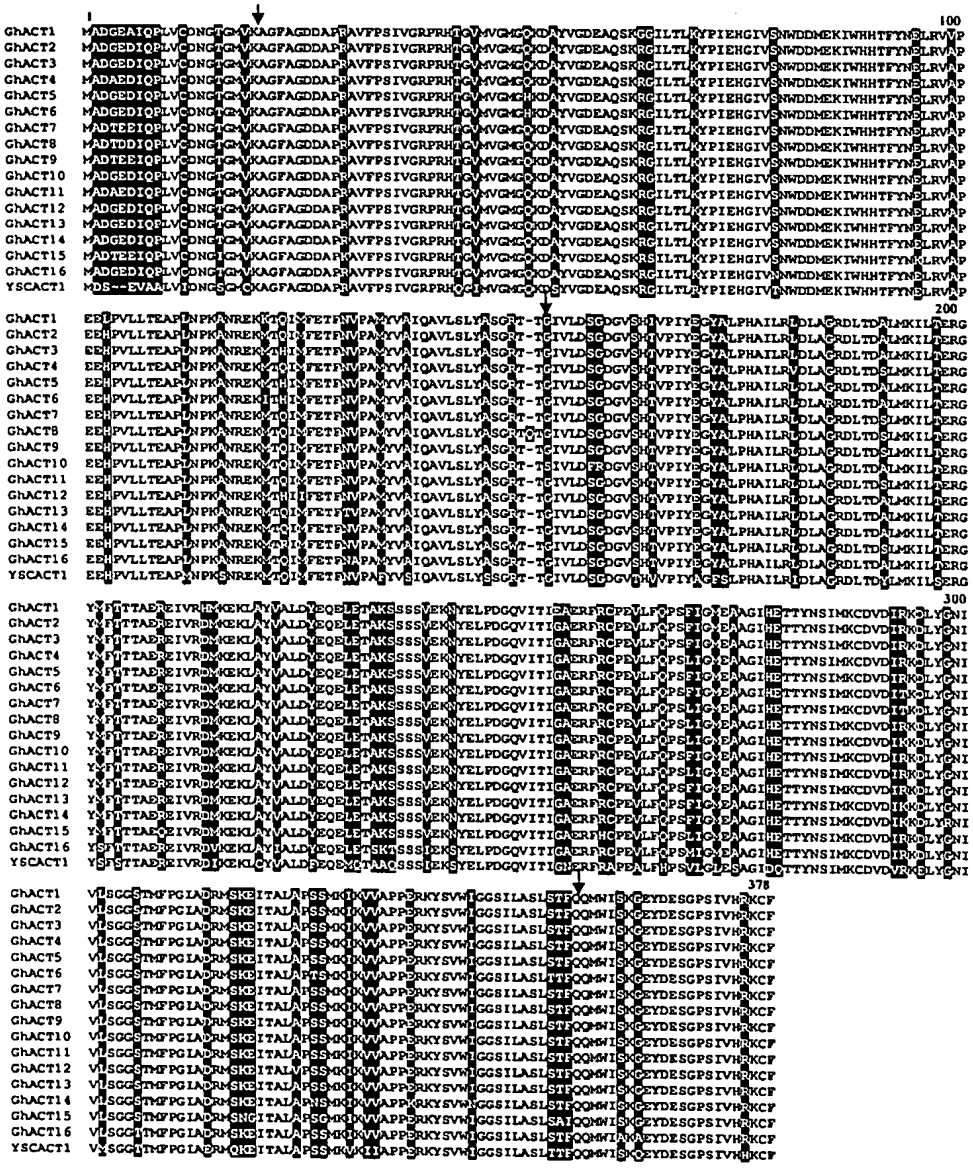

Figure 1. Comparison of the Predicted Amino Acid Sequences of Cotton *GhACT* Genes.

Multiple alignment of amino acid sequences of 16 cotton *GhACT* genes and yeast *YSCACT1*. Amino acid substitutions are highlighted in black. Arrows indicate the positions of the three introns in cotton *GhACT* genes. *GhACT1* to *GhACT15* were from this work; *GhACT16* is a putative actin derived from a genomic sequence in GenBank (accession number AF059484).

functional divergence occurred within the gene family during evolution (McDowell et al., 1996; Meagher et al., 1999a). Members of the actin gene family are divergent and differentially expressed during plant development. Arabidopsis contains two major actin gene classes: a vegetative class that is expressed predominantly in leaves, stems, roots, petals, and sepals and a reproductive class that is strongly expressed in pollens, ovules, and embryonic tissues (McDowell et al., 1996; Kandasamy et al., 1999). The soybean (*Glycine max*) actin gene family includes at least three divergent classes: μ-, κ-, and λ-actin. The μ-actin transcripts are differentially accumulated in leaves, roots, and hypocotyls. The κ- and λ-actin proteins are preferentially localized

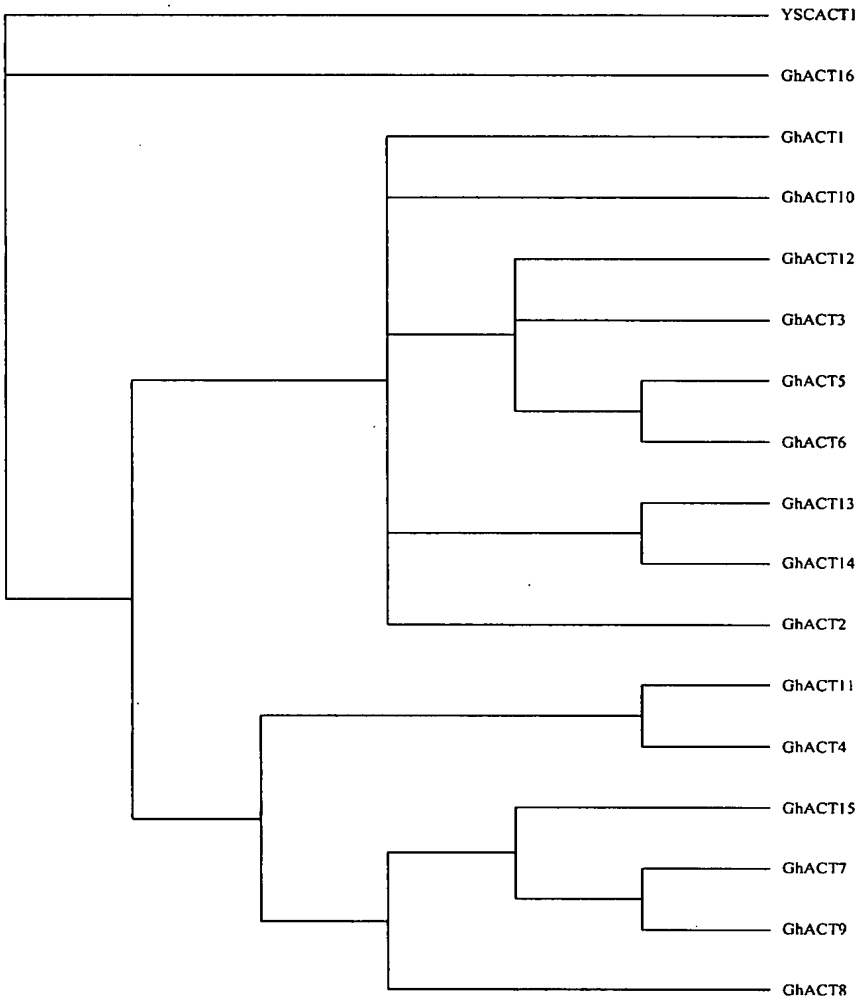

Figure 2. Phylogenetic Relationships of Cotton Actins.

The rooted gene tree shown is based on majority-rule consensus from 500 bootstrap replicates and resulted from heuristic searching in PAUP 4.0, based on amino acid sequences of the *GhACT* genes. Cotton GhACT1 to GhACT15 actins were from this work; *GhACT16* is a putative actin derived from a genomic sequence in GenBank (accession number AF059484); YSCACT1 is a yeast actin (accession number L00026) used as an outgroup.

in roots (McLean et al., 1990). In other plant species, such as rice (*Oryza sativa*) and tobacco (*Nicotiana tabacum*), actin genes also appear to be expressed in a tissue-specific manner (McElroy et al., 1990; Thangavelu et al., 1993). Although actin genes in a few plant species such as Arabidopsis have been well characterized, our knowledge of cotton actin genes, especially its role in fiber development, needs to be explored.

Cotton fibers, as a premier natural fiber and extensively used in the textile industry, are derived from epidermal cells of the reproductive organ, the ovule. Approximately 30% of the ovule epidermal cells elongate and develop into single-celled fibers at anthesis. Each fiber is perhaps the longest single cell in higher plants. Its elongation rate and the final length attained are far above that of common plant cells (Cosgrove, 1997). Fiber development is a highly regulated process involving four sequential stages: fiber initiation, primary cell wall formation, secondary cell wall formation, and maturation (Basra and Malik, 1984). Thus, the cotton fiber represents a unique experimental system for studying the control of cell elongation without the complication of cell division and multicellular development (Ruan et al., 2001). The study on fiber development not only provides the basic understanding of cell differentiation and elongation, but also identifies potential target genes for genetic manipulation of cotton fiber. Here, we reported the identification and characterization of the actin gene family in cotton and explored its role in fiber development using RNA interference (RNAi) technology.

Table 1. Primers Used in Gene-Specific RT-PCR of *GhACT* Genes

Genes	Primers
GhACT1	5′-CCCTTGAATATTAAATAAATAAAAAAATA-3′
	5′-TTGTGCTCAGTGGGGGTTCAACC-3′
GhACT2	5′-TGCCCGGAAGTCCTCTTCCAG-3′
	5′-ATTTTCCCAGAAGTTTGACCGCGC-3′
GhACT3	5′-CCCTTGAATATTAAATAATAATAAGCAC-3′
	5′-TTGTGCTCAGTGGGGGTTCAACT-3′
GhACT4	5′-GGGGGAGCCTTGAATATGAAATTG-3′
	5′-TTGTGCTCAGTGGGGGTTCAACC-3′
GhACT5	5′-ATTTTCCCAGAAGTTTGACCGCGC-3′
	5′-TGCCCGGAAGTCCTCTTCCAA-3′
GhACT7	5′-TTAAAGAAAATATAAGAAATAAGCATCA-3′
	5′-GTATGCCAGTGGTCGGACGACA-3′
GhACT8	5′-TTAAAGAAAATATAAGAAATAAGCATCA-3′
	5′-GTATGCCAGTGGTCGGACGCAG-3′
GhACT9	5′-ATCTTCAACATAAAAGATCATCCCACT-3′
	5′-GATCTATCTTGGCATCACTCAGCA-3′
GhACT10	5′-AACCAGATATTAAATATAATTTCCGTAG-3′
	5′-GGGAAATTGTCCGTGACATGAAG-3′
GhACT11	5′-ACAATAGCTATTGACATTAATGTTTGC-3′
	5′-TTGTGCTCAGTGGGGGTTCAACT-3′
GhACT12	5′-AACCAGATATTAAATATAATTTCCGTAG-3′
	5′-GGGAAATTGTCCGTGACATGAAA-3′
GhACT13	5′-CCCTTGAATATTAAATAATAATAAGCAC-3′
	5′-TTGTGCTCAGTGGGGGTTCAACC-3′
GhACT14	5′-AACCAGATATTAAATATAATTTCCGTAA-3′
	5′-ATTGGAGCTGAGAGATTCCGTTG-3′
GhACT15	5′-ATCTTCAACATAAAAGATCATCCCACT-3′
	5′-GATCTATCTTGGCATCACTCAGCG-3′
GhUBI	5′-CTGAATCTTCGCTTTCACGTTATC-3′
	5′-GGGATGCAAATCTTCGTGAAAAC-3′

The efficiency of each primer pair was detected using *GhACT* cDNA clones as standard templates, and the RT-PCR data were normalized with the relative efficiency of each primer pair.

RESULTS

Isolation and Characterization of *GhACT* cDNAs

To isolate genes involved in cotton fiber development, we have randomly sequenced >300 cDNA clones from a fiber cDNA library (Li et al., 2002). Clones, including an actin cDNA, likely involved in cell elongation were chosen for further study. Using the actin cDNA clone as probe, we further isolated 15 unique actin cDNAs (designated *GhACT* genes; accession numbers in GenBank, AY305723 to AY305737) from a cotton cDNA library. Sequence analysis predicted that all *GhACT* genes, except *GhACT8*, encode a 377–amino acid polypeptide. The *GhACT8* encodes an actin containing 378 amino acid residues with a Gln insertion at position 151 (Figure 1). The *GhACT* genes share high sequence homology at nucleotide level (70 to 97% identity) in the coding region and at the amino acid level (93 to 99% identity). There is only 1 to 7% substitution rate at amino acid level compared with each other (Figure 1). In total, 21 charged substitutions occurring at 14 charged positions were present in GhACTs. Among them, charged amino acids were exclusively substituted with uncharged residues at six locations (Arg/Gly, Thr or Gln, Asp/Ala, Glu/Gly, His/Leu, or Lys/Trp) and were only substituted by a synonymous charged amino acid at other positions. The charged amino acids at residues 6 and 292 were substituted by either a charged amino acid or an uncharged residue (Figure 1), suggesting that these positions may not be important for actin structure. While at residue 123, both charged and polar uncharged amino acids were present in GhACTs. In addition, 11 uncharged amino acids at six positions were substituted by a charged residue. Often in this case, Gln was substituted by a His and Gly replaced by an Arg. Intriguingly, most nonsynonymous substitutions occur only in GhACT1 protein. For example, positively charged amino acids were substituted by a nonpolar, uncharged amino acid at positions 64 and 103. On the other hand, nonpolar amino acids were replaced by positively charged and negatively charged polar residues at positions 121 and 253, respectively. At position 213, the negatively charged Asp was substituted by a positively charged His, suggesting that GhACT1 may have a different structure and function than other GhACT variants.

Phylogenetic analysis on amino acid sequences showed that the 16 GhACTs available could be divided into nine subgroups (Figure 2). Among them, five subgroups contain only a single member, and the remaining four subgroups have two to four members. Each of GhACT1, GhACT2, GhACT8, GhACT10, and GhACT16 forms an independent clade, suggesting that these GhACTs diverged early during evolution, whereas GhACT3, GhACT5, GhACT6, and GhACT12 together form a single branch, indicating that divergence of these genes occurred relatively late.

GhACT Genes Are Differentially Expressed in Different Organs

To identify *GhACT* genes that are preferentially expressed in cotton fibers, the expression patterns of 15 *GhACT* cDNA clones were analyzed by real-time quantitative SYBR-Green RT-PCR using gene-specific primers (Table 1) as described in Methods. The cotton polyubiquitin gene (*GhUBI*; X.B. Li and W.C. Yang, unpublished data) expressed equally in all tissue types with cycle threshold (Ct) values at 17.52 ± 0.35 and was chosen as a standard control to normalize differences in RNA template concentrations. Five out of the fifteen *GhACT* genes are expressed at relatively high levels in fiber cells (Figure 3A). *GhACT2* is expressed at high levels in all tissues compared with other *GhACTs*, and its expression level reaches a relative value of 17 in fibers as compared with ~5 in other tissue types. For example, *GhACT2* expression in fibers is ~370-fold higher than *GhACT14*. *GhACT1* and *GhACT5* are strongly expressed in fiber and very low in leaf, stem, root, and anther, indicating that they are preferentially expressed in fiber cells. *GhACT4* and *GhACT11* also showed similar expression patterns as *GhACT1* and *GhACT5* in fiber and were moderately expressed in other tissues, whereas the transcripts of other *GhACT* genes are very low, as shown in the small values in the *y* axis. Overall, *GhACT3*, *GhACT9*, *GhACT10*, and *GhACT12* are expressed at least five-fold less in fibers compared with *GhACT1*, *GhACT2*, *GhACT4*, *GhACT5*, and *GhACT11*. By contrast, the expression of *GhACT7*,

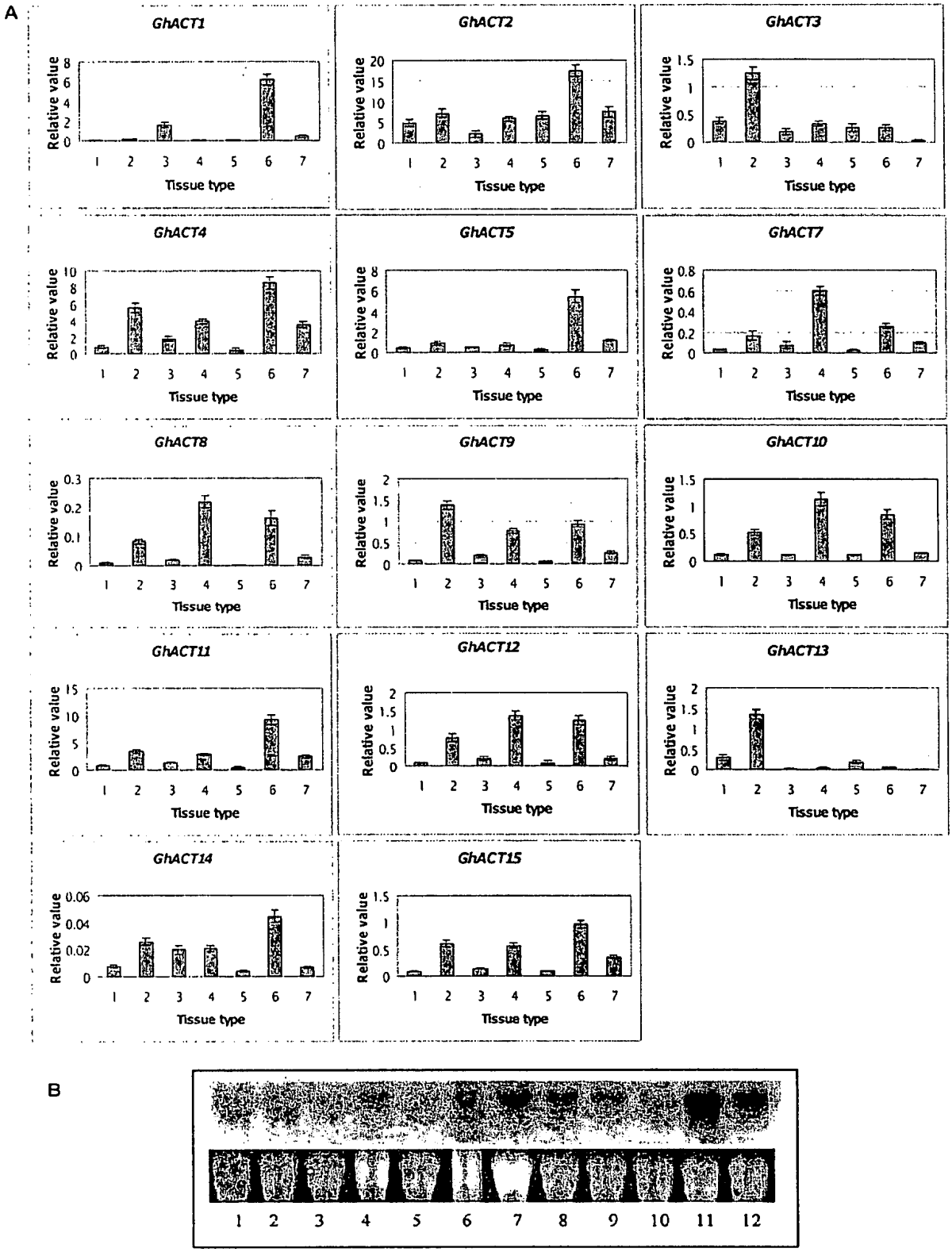

Figure 3. Analyses of Expression of *GhACT* Genes in Cotton Tissues.

GhACT8, *GhACT14*, and *GhACT15* is extremely low if compared with *GhACT1*, *GhACT2*, *GhACT4*, *GhACT5*, and *GhACT11*. Moreover, *GhACT6* expression is not detectable in all the tissues examined. The results of the real-time RT-PCR revealed that the actin genes in cotton were differentially expressed, with *GhACT1*, *GhACT2*, *GhACT4*, *GhACT5*, and *GhACT11* being the predominant forms in fiber cells (Figure 3A).

RNA gel blot analysis, using the 3′-untranslated region (UTR) of *GhACT1* as a probe, further demonstrated that *GhACT1* accumulated at high level in fibers and at a relatively lower level in ovules. The level of *GhACT1* transcripts reached the highest level during 8 to 14 d postanthesis (DPA) and decreased gradually as the ovule developed. At 28 DPA, hardly any transcript was detected. No or very little transcripts were detected in anthers, petals, leaves, and roots (Figure 3B). A moderate level of *GhACT1* was detected in cotyledons. This result further confirmed that the *GhACT1* gene is preferentially expressed, especially in elongation phase in cotton fiber cells.

Isolation and Characterization of *GhACT* Genes

Five genomic DNA clones, representing *GhACT1*, *GhACT2*, and *GhACT15* (Figure 4A), were isolated from a cotton genomic library using *GhACT1* cDNA as probe. The isolated *GhACT1* gene is ~3.9 kb in length, including 1.6 kb of the 5′ promoter region, 1.8 kb transcribed region, and 0.5 kb 3′ downstream sequence. Sequence comparison between cDNA and genomic clones revealed that the three *GhACT* genes all contain four exons and three introns (Figure 4A). The three introns are located exactly at the same positions in all three genes: between amino acid residues 20 and 21, within residue 152, and between residues 355 and 356, respectively. The size and position of introns in *GhACT1* and *GhACT2* are almost identical (Figure 4A). Intron 1 is 545 and 565 bp in length in *GhACT1* and *GhACT2*, respectively, much longer than intron 2 and intron 3. By contrast, intron 1 in *GhACT15* is relatively short, with only 109 bp. The lengths of introns 2 and 3 are similar in all three genes. These data indicate that *GhACT* gene structure is quite conserved in cotton.

To determine the actin gene family copy numbers, cotton genomic DNA was digested with *Bam*HI, *Eco*RI, *Eco*RV, *Hin*dIII, *Sac*I, and *Xal*I and subjected to DNA gel blot analysis. There was one major band and one to two weak bands when the 0.8-kb 5′ noncoding region of *GhACT1* was used as a probe. The major band represents *GhACT1*, and the weaker bands most likely are due to cross-hybridization with other members of the actin gene family, though the 5′ noncoding region was used as probe (Figure 5A). Furthermore, several bands were detected when using the more conserved exon 3 of *GhACT1* as a probe under highly stringent conditions (Figure 5B). This suggested that there are at least four to eight members of the actin family that share a highly conserved coding region with *GhACT1*, and the remains may diverge earlier during the evolution of the cotton actin gene family.

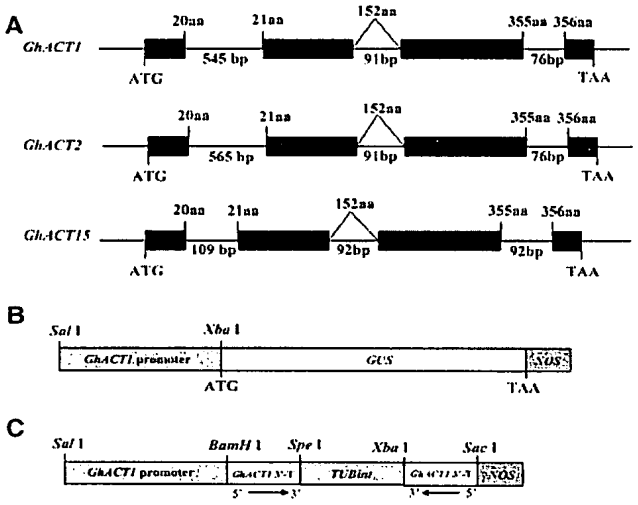

Figure 4. *GhACT* Gene Structure, *GhACT1*::*GUS*, and *GhACT1* RNAi Construction.

(A) Exons are denoted by black boxes. Introns, 5′-flanking region, and 3′- UTR are denoted by lines. The lengths of the introns in base pairs are indicated. The number at the boundaries of each exon indicates the codon at which the intron is located. The translation initiation and termination codons are shown. aa, amino acids.
(B) The length of the *GhACT1* promoter and cloning sites used for *GhACT1*::*GUS* fusion are shown.
(C) *GhACT1* RNAi construction.

The *GhACT1*::β-*Glucuronidase* Fusion Gene Is Predominantly Expressed in Cotton Fibers

To characterize the precise expression pattern of *GhACT* genes in cotton fibers, we chose *GhACT1* for further study because it represents *GhACTs* that are expressed preferentially in fibers (Figure 3A) among the three available genomic sequences. A 0.8-kb promoter region of *GhACT1* was subcloned upstream of the β-*glucuronidase* (*GUS*) reporter gene in pBI101 vector, giving rise to the *GhACT1*::*GUS* gene (Figure 4B). The *GhACT1*::*GUS* construct was introduced into cotton cultivar Coker312

Figure 3. (continued).

(A) Real-time RT-PCR analysis of expression of *GhACT* genes in cotton tissues. Relative value of *GhACT* gene expression in cotton tissues, including leaf (1), stem (2), cotyledon (3), root (4), anther (5), fiber (6), and petal (7), was shown as percentage of GhUBI expression activity (see Methods).
(B) RNA gel blot analysis of *GhACT1* transcripts in cotton. Total RNA (20 μg/lane) from petal (1), anther (2), leaves (3), cotyledon (4), root (5), ovule (6 to 10) at 4, 8, 14, 21, and 28 DPA, and fiber (11 and 12) at 8 and 14 DPA was fractionated on a 1.2% denaturing agarose gel and transferred onto a nylon membrane (see Methods). Top panel, autoradiograph of RNA hybridization; bottom panel, RNA gel before transfer to membrane showing equal loading of RNAs.

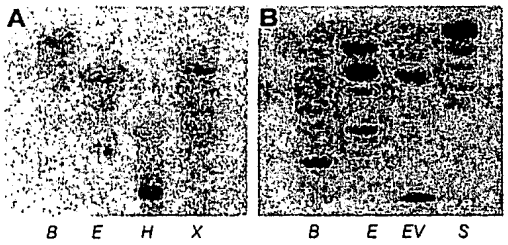

Figure 5. Genomic DNA Gel Blot Analysis of the *GhACT1* Gene.

Thirty micrograms of genomic DNA was digested with restriction enzymes as indicated and fractionated on a 0.8% agarose gel. DNA gel blots were hybridized with ^{32}P-labeled *GhACT1* 5′-region gene-specific probe (0.8 kb) **(A)** and ^{32}P-labeled *GhACT1* exon 3 probe (0.6 kb) (B). *B*, *Bam*HI; *E*, *Eco*RI; *H*, *Hin*dIII; *X*, *Xba*I; *EV*, *Eco*RV; *S*, *Sac*I.

via *Agrobacterium tumefaciens*–mediated DNA transformation. A total of 230 transformed T0 plants from 21 independent calli were obtained and transplanted to soil for seeds. A total of 52 of 230 T0 transgenic plants were examined in detail for *GUS* expression patterns. In all of the 52 transgenic plants examined, strong *GUS* activity was detected only in young fibers (Figures 6A to 6E), whereas no or weak *GUS* staining was observed in ovules, anthers, petals, sepals, leaves, and roots, including their trichomes (Figures 6F and 6J). In comparison, plants transformed with the positive control pBI121 (35S::*GUS*) exhibited strong *GUS* activity in all tissues, and the nontransformed plants showed no *GUS* activity in fibers as well as in other tissues under the same staining conditions (data not shown). The same pattern of *GhACT1*::*GUS* expression was further confirmed in T1 and T2 transgenic plants. In addition, the *GhACT1*::*GUS* expression was observed at a moderate level in cotyledons of the germinating embryos at the first 1 to 2 d, when the root had just emerged from the embryo and the two cotyledons had not yet unfolded. In 3- to 4-d-old seedlings, moderate *GUS* activity was still observed in the cotyledon tissues (Figure 6G). Hypocotyls showed a low level of *GUS* activity in only one of the 21 independent transgenic lines examined. *GhACT1*::*GUS* expression was not detected in the roots of 3- to 8-d-old seedlings. Occasionally, weak expression was detected in the root tip in one transgenic line. As the seedling grew, *GUS* activity gradually decreased and finally disappeared in the cotyledons (Figures 6H and 6I). In 2-week-old seedlings, no significant *GUS* activity in the transgenic plants was detected. These results indicated that the 0.8-kb *GhACT1* promoter was sufficient to direct its fiber-specific expression and regulate its dynamic expression during cotton plant development.

Suppression of *GhACT1* Expression Dramatically Reduces Fiber Elongation

To study the role of actin cytoskeleton in fiber elongation, we chose a *GhACT1* gene that is expressed preferentially in fibers and less expressed in other tissues or organs (Figure 3A). Therefore, it was expected that knockdown of this gene would have no or less effect on other tissues. Knockdown approaches using RNAi technology were employed. The 150-bp 3′-terminal fragment of *GhACT1* was constructed in the opposite direction with an intron from a cotton tubulin gene as a spacer (Li et al., 2002), then subcloned into pBI101 downstream of its own promoter (Figure 4C) and introduced into cotton cultivar Coker312 via Agrobacterium-mediated DNA transfer. Fourteen independent transgenic lines were regenerated. RNA gel blot analysis showed that the level of *GhACT1* mRNAs was reduced significantly down to very low level in fibers of the transgenic plants, using *GhACT1* 3′-UTR fragment as a probe (Figure 7A). To understand whether the reduced actin mRNAs also include other *GhACT* gene products, we further analyzed the expression levels of all the *GhACT* genes in fibers from RNAi transgenic plants by real-time quantitative SYBR-Green RT-PCR using gene-specific primers (Table 1). The results revealed that the expression of the *GhACT1* RNAi resulted in complete *GhACT1* silence in line T1 and ~10-fold reduction in lines T2, T3, and T4 (Figure 8). On the contrary, its impact on the expression of other *GhACT* genes was minor, with ~10% reduction (Figure 8). To confirm that the reduction in *GhACT1* mRNA also led to reduction at the actin protein level, protein gel blot analysis using actin antibody was performed. A strong band was detected in nontransgenic control fibers, whereas no or weak signals were detected in the transgenic lines (Figure 7B). This indicated that there was significant reduction in the actin proteins (mostly GhACT1) as a result of the reduction in *GhACT1* expression, and the remaining signals in the transgenic lines (Figure 7B, lanes 2 to 5) likely represented the other GhACT proteins expressed in fibers or residual GhACT1. These data suggest that GhACT1 is one of the dominant and functional actin isoforms in fibers.

All *GhACT1* RNAi transgenic plants showed a short-fiber phenotype (Figure 9) that cosegregated with the kanamycin selection marker (data not shown) and the reduction of actin protein levels, indicating that the phenotype was a result of the actin reduction caused by *GhACT1* silence. Fiber cells differentiate and rapidly emerge from the surface of the ovule at 0 to 1 DPA in wild-type plants (Figure 9A), whereas fibers in transgenic plants (Figure 9D) were much shorter. At 2 DPA, fiber cells in wild-type plants reached ~500 μm long (Figure 9B), whereas transgenic fibers were only ~150 to 380 μm in length (Figure 9E). Fiber length at 3 DPA in most transgenic plants (Figure 9F) was equal to fibers at 2 DPA in wild-type cotton (Figure 9B) and much shorter than fibers at 3 DPA in wild-type plants (Figure 9C). Measurement of fiber length showed that fiber elongation in transgenic plants was ~1.5- to 3-fold slower than that in wild-type plants (Figure 10), which correlated with the reduction of actin protein level (see Figure 7B). The results suggest that the reduction in total actins, including GhACT1, slowed down fiber elongation. Moreover, a portion of the ovules was sterile, and bolls in transgenic plants were smaller than those in the wild type after maturation, indicating that *GhACT1* RNAi also slightly affected pollination or seed development. However, all the transgenic lines were unaffected in vegetative growth and flower development. No inhibition on fiber initiation was observed in the *GhACT1* transgenic lines, suggesting the *GhACT1* gene is most likely not involved in fiber initiation but plays a role in fiber elongation.

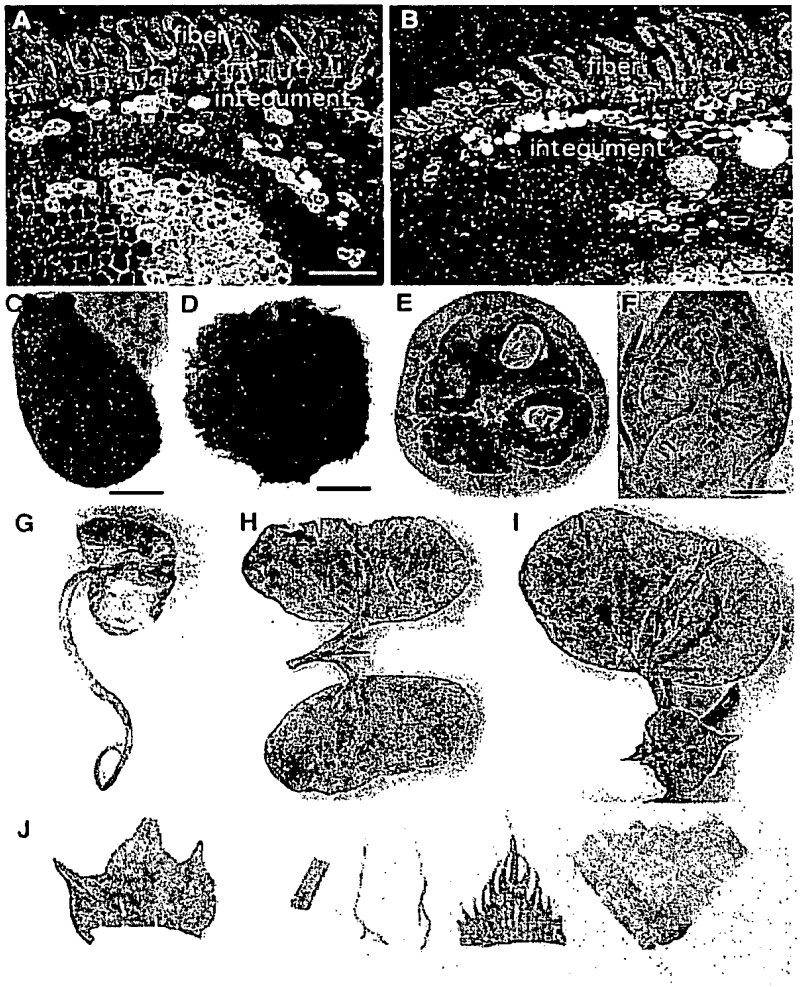

Figure 6. Histochemical Localization of *GUS* Activity in Transgenic Cotton Plants Containing the *GhACT1*::*GUS* Fusion Genes.

(A) and **(B)** Dark-field micrographs of 5-μm-thick cross sections of 1- to 2-DPA ovules. A high level of *GUS* activity (represented by pink dots) was only found in the fiber, and very weak *GUS* staining was seen in the inner cell layers. No *GUS* staining was detected in the epidermal atrichoblast and integument.

(C) to **(J)** Bright field of micrographs or photographs of ovules and other tissues/organs.

(C) and **(D)** *GUS* staining in ovules at 1 **(C)** and 2 **(D)** DPA. Strong *GUS* activity was observed in the fibers.

(E) A cross section of a transgenic cotton boll at 14 DPA. Strong *GUS* activity was detected in the developing fibers, and very weak *GUS* staining was seen in embryos.

(F) A longitudinal section of a transgenic flower bud before anthesis. Weak *GUS* staining was found in some pollen grains.

(G) to **(I)** *GUS* staining in transgenic seedlings.

(G) Three-day-old seedling. *GUS* gene was expressed moderately in the cotyledons.

(H) Parts of a 7-d-old seedling. Weak *GUS* expression was found only in cotyledons.

(I) Parts of a 10-d-old seedling. *GUS* activity was very low in cotyledons, and no *GUS* expression was detected in other tissues, such as leaf and shoot apex.

(J) No *GUS* activity was detected in leaf, stem, root, sepal, and petal (from left to right) of transgenic cotton.

Bars = 80 μm in **(A)** and **(B)**, 1 mm in **(C)** and **(D)**, and 2 mm in **(F)**.

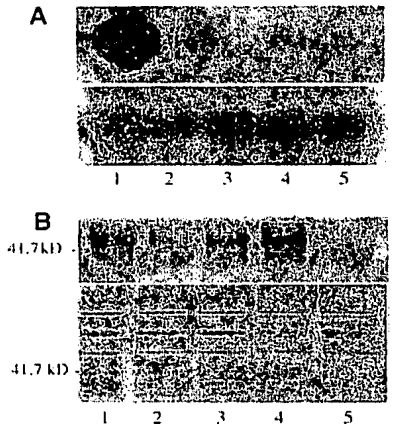

Figure 7. RNA Gel Blot and Protein Gel Blot Analyses of *GhACT1* Expression in RNAi Transgenic Fibers of Cotton.

(A) RNA gel blot analysis. Total RNAs from fibers at 10 DPA from a wild-type plant (1) and *GhACT1* RNAi transgenic lines (2 to 5) were fractionated on 1.2% denaturing agarose gel and transferred to a nylon membrane (see Methods). Top panel, autoradiograph of RNA gel blot hybridized with ^{32}P-dCTP–labeled *GhACT1* probe; bottom panel, autoradiograph of the same RNA gel blot hybridized with ^{32}P-dCTP–labeled 18S RNA probe (control) showing equal loading of RNAs.

(B) Protein gel blot analysis. Total soluble proteins of fibers at 10 DPA from a wild-type plant (1) and *GhACT1* RNAi transgenic lines (2 to 5) were separated by electrophoresis in a 12% SDS-PAGE gel. The protein gel blot was stained with anti-actin antibody (top panel) and Coomassie blue (bottom panel).

Impact of *GhACT1* Suppression on the Actin Cytoskeleton in Fiber Cells

To investigate if changes in the actin cytoskeleton in *GhACT1* RNAi transgenic fibers occurred, we studied actin cytoskeleton in fiber cells using rhodamine-phalloidin staining for F-actin. During fiber cell elongation in wild-type plants, F-actin exhibited a complicated net-like structure from thin filaments to thick and longitudinally extending cables. At the early stage of fiber elongation, actin filaments were organized into arrays parallel to the growing axis and extended into the tip of the fiber cells (Figure 9G). With further elongation of fiber cells, the actin cytoskeleton was comprised of relatively thin arrays and thick cables along the long axis of the fiber (Figure 9H). The F-actin cytoskeleton displayed an increasingly complicated network consisting predominantly of thick and longitudinally long cables (Figure 9I). By contrast, actin filaments in transgenic fibers were obviously reduced in the number of filaments, and a more random array was observed (Figure 9J). During further development of the fibers, they were less bundled into arrays and cables (Figure 9K, compare with Figure 9H) and exhibited a defective F-actin organization (Figures 9K and 9L). As a result of RNAi of *GhACT1* expression in transgenic fibers, the devoid of the well-organized actin cytoskeleton consequently resulted in the reduction in fiber cell elongation, leading to the short-fiber phenotype. These data suggested that downregulation of the *GhACT1* gene has an impact on actin cytoskeleton network in fiber cells.

DISCUSSION

Divergence of the Protein Structure of the GhACTs

Although plant actins are quite conserved, the divergence on protein structures occurred during evolution. In this study, the 16 cotton actins deduced from the isolated *GhACT* genes have diverged into nine subclasses compared with six subclasses in Arabidopsis (McDowell et al., 1996). Variation among GhACTs occurs more significantly than that found among the Arabidopsis actins. Figure 11 shows GhACT1 protein structure, indicating that those significant substitutions on amino acids among the cotton actins may have an impact on their surface properties. The 14 positions where charged substitutions took place are found among the GhACTs, whereas only nine such positions appear among Arabidopsis actins (McDowell et al., 1996). At these positions, unlike Arabidopsis actins, only six positions were conservative substitutions, and the other positions showed nonconservative interchanges, whereas human actins contain only conservative substitutions. The nonconservative replacements of charged residues located on several surfaces of the actin molecule (Figure 11) may be involved in functional non-equivalency of actin isovariants as actin monomers polymerize from G-actin to F-actin and alter actin–actin or actin–actin binding protein interaction. For example, the uncharged polar Gln51 just adjacent to the DNase I binding loop involved in intermonomer interactions within the filament (Holmes et al., 1990) is replaced by a positively charged His in GhACT5 and GhACT6. Because actin subdomain 2, in particular the DNase I binding loop, is directly involved in conformational changes (Otterbein et al., 2001), it is likely that this nonsynonymous substitution will have an impact on GhACT5 and GhACT6 structure and function. Recent genetic studies in Arabidopsis clearly showed that substitutions in AtACT2 have dramatic impact on its functions in root hair development (Gilliland et al., 2002; Ringli et al., 2002; Diet et al., 2004). Missense mutation in *der1* mutants (Ala183Val in *der1-1*, Arg97His in *der1-2*, and Arg97Cys in *der1-3*) all caused deformed root hairs. Furthermore, Glu356Stop in *enl2* enhances *der1* phenotypically (Diet et al., 2004), indicating that C-terminal residues are not absolutely required for its function. On the contrary, the conservative substitutions in the N-terminal peptide of Arabidopsis actins may affect polymerization and myosin binding (McDowell et al., 1996). Either a charged (His or Arg) or an uncharged polar amino acid (Gln) at position 123 of cotton actins may suggest that Gln and His are functionally interchangeable. Besides the charged substitutions, there were four positions where a noncharged Gly was substituted by a charged Glu or Arg seen in GhACT1 (Gly_{253} to Glu), GhACT6 (Gly_{184} to Arg), GhACT8 (Gly_{158} to Arg), and GhACT14 (Gly_{297} to Glu), respectively. These substitutions are not found in Arabidopsis actin genes (McDowell et al., 1996). It would be interesting to know whether these nonsynonymous substitutions have structural and functional impacts on transition from G-actin to F-actin.

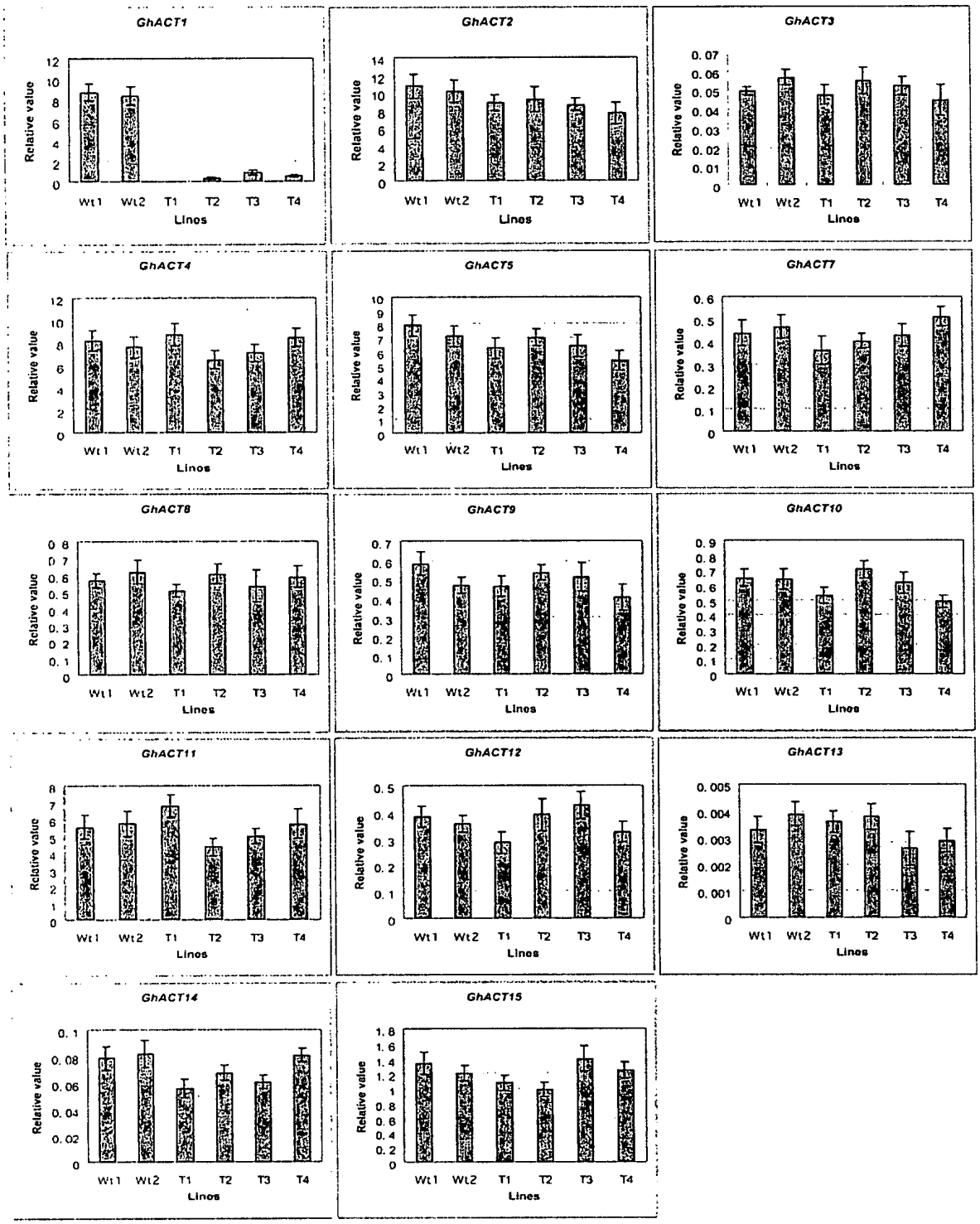

Figure 8. Real-Time RT-PCR Analysis of *GhACT1* RNAi Expression in Transgenic Fibers.

Relative value of *GhACT* gene expression in 8-DPA fibers is shown as a percentage of *GhUBI* expression activity (see Methods). The *GhACT1* expression was significantly silenced by RNAi in the transgenic fibers, whereas the activities of the other *GhACT* genes were little affected in fibers of all the transgenic lines. Wt1 and Wt2, wild-type plants; T1 to T4, transgenic *GhACT1* RNAi lines.

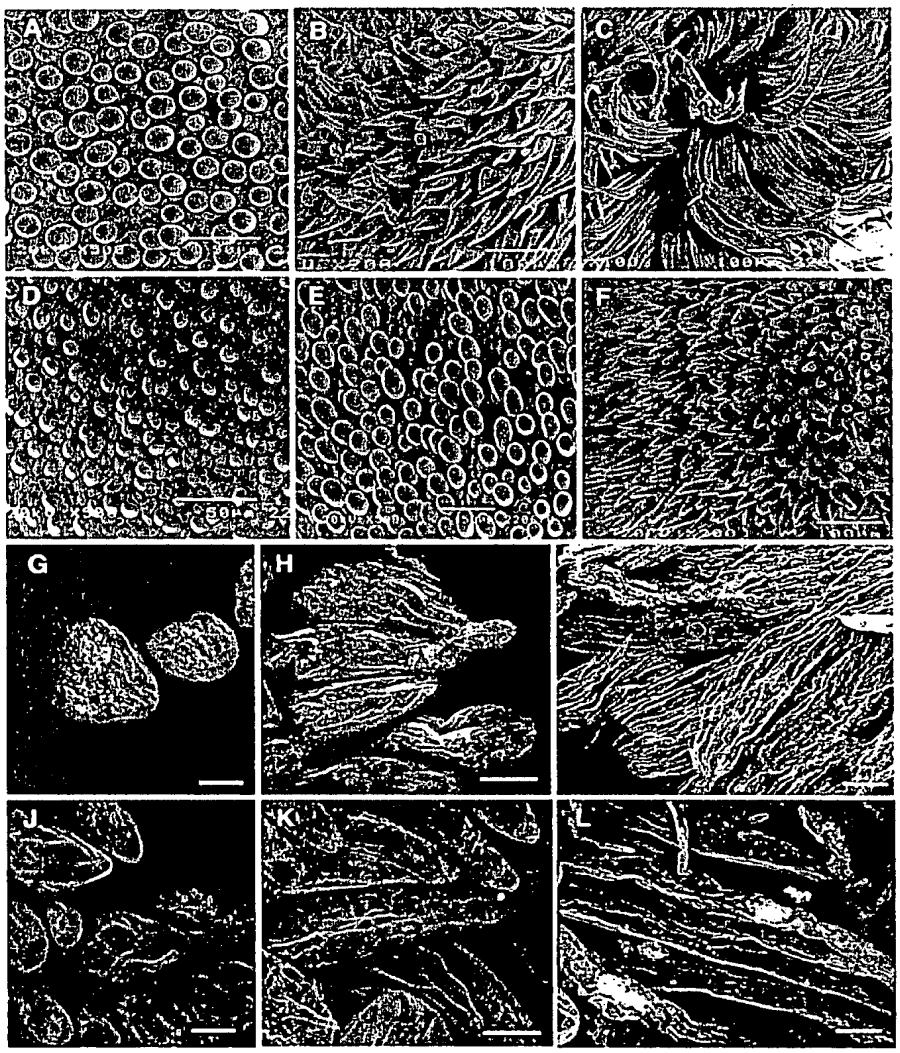

Figure 9. Comparison of Fiber Growth Rate and F-Actin Organization in Fiber Cells between Transgenic *GhACT1* RNAi and Wild-Type Plants.

(A) to **(F)** Scanning electron micrographs of the ovule surface of transgenic *GhACT1* RNAi and wild-type plants.

(A) to **(C)** Ovules of wild-type plants at 1 **(A)**, 2 **(B)**, and 3 **(C)** DPA. Note the length of fibers increases with time.

(D) to **(H)** Ovules of transgenic plants at 1 **(D)**, 2 **(E)**, and 3 **(F)** DPA. Note the length of fibers is much shorter than that in wild-type plants at the same stages.

(G) to **(L)** Organization of actin filaments in fiber cells of wild-type and transgenic *GhACT1* RNAi cotton.

(G) to **(I)** Fiber cells of wild-type cotton at 1 **(G)**, 2 **(H)**, and 3 **(I)** DPA. Actin filaments were organized into arrays parallel to the growing axis and extended into the tip of the fiber cells at 1 DPA **(G)**. Actin filaments were arranged into thin arrays and thick cables along the shank in fiber cells at 2 DPA **(H)** and assumed a more complicated net structure of thick and longitudinally extending cables in >3-DPA fiber cells **(I)**.

(J) to **(L)** Fiber cells of transgenic cotton at 1 **(J)**, 2 **(K)**, and 5 **(L)** DPA. Fewer F-actin cables were present.

Bars = 5 μm in **(G)** and **(J)** and 10 μm in **(H)**, **(I)**, **(K)**, and **(L)**.

A unique feature of the actin gene family is the position of introns that are conserved among actin genes in cotton and other plant species (Shah et al., 1983; Baird and Meagher, 1987; Nairn et al., 1988; Stranathan et al., 1989; McElroy et al., 1990; Meagher and Williamson, 1994; Cox et al., 1995; An et al., 1996). In Arabidopsis, actin genes have three small introns at identical locations as in *GhACT* genes except *ACT2*, in which the first intron between codons 20 and 21 is missing (McDowell et al., 1996). In *GhACT1* and *GhACT2*, the first intron is rather large (545 and 565 bp, respectively) compared with the second and third

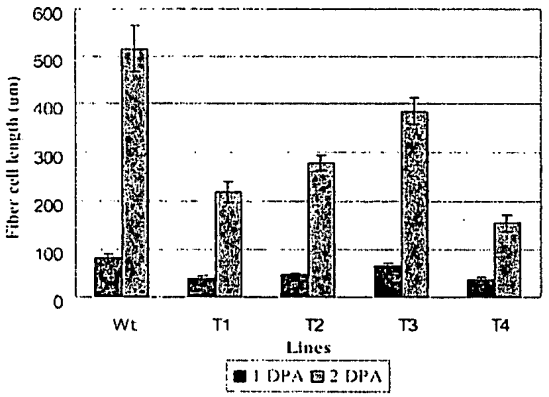

Figure 10. Fiber Length of Transgenic *GhACT1* RNAi and Wild-Type Cotton Seeds at 1 and 2 DPA.

Ovules were sectioned and the length of 30 fiber cells was measured under a microscope for each transgenic line and wild type. Data was processed with Microsoft Excel. Compared with the wild type, fiber cells of transgenic plants are much shorter and are approximately one-half to one-third of wild-type fibers.

introns (91 and 76 bp, respectively) that are more conserved, indicating that the first intron is more divergent than intron 2 and intron 3. Furthermore, unlike the other known plant actin genes studied, *GhACT1* and *GhACT2* share high similarity in the sequences of all three introns, suggesting that both genes may have very close evolutionary relationship.

Nevertheless, the triplet CAG insertion 4 bp upstream the second exon–intron junction in *GhACT8* challenged the conserved intron organization paradigm that the three introns are located at the same positions in all actin genes in the plant kingdom (McDowell et al., 1996). In actin genes examined so far, the second intron is always located at amino acid residue 152. However, in *GhACT8*, the second intron was located at amino acid residue 153 instead of residue 152 because of the insertion. The functional and evolutionary implications of this insertion remain unknown, although *GhACT8* is expressed at high levels in fiber and root.

GhACT1 Is Preferentially Expressed during Fiber Development

In this study, we demonstrated that differential expression of the *GhACT* gene occurs in cotton, as did the members of this actin family in several other plant species, such as Arabidopsis (McDowell et al., 1996; Meagher et al., 1999b), soybean (McLean et al., 1990), tobacco (Thangavelu et al., 1993), and rice (McElroy et al., 1990). The differential expression data may imply that the specialized functional expressions of actin genes are required for proper development of the respective cell and tissue types and may reflect the divergent evolution of actin gene regulatory elements for expression in plant development.

The data presented here provide evidence for strong expression of some *GhACT* genes in cotton fibers. The high level of *GhACT* gene expression coincides with the rapid elongation of the fiber cell, suggesting that actin cytoskeleton plays an essential role in fiber elongation. It seems that specialized *GhACT* genes had been evolved to meet the requirement of the actin cytoskeleton for rapid fiber elongation. This is manifested by the fiber-specific expression of *GhACT1*, as well as *GhACT2* and *GhACT5*. Real-time RT-PCR and RNA gel blot analysis showed that the *GhACT1* transcripts accumulated preferentially in developing fibers, whereas only low or undetectable levels of RNAs were found elsewhere. The transcripts of *GhACT1* reach the highest level in young fibers during 8 to 14 DPA, and then there is a gradual and visible decrease of mRNA as the fiber cells developed further. Similarly, genes involved in osmoregulation and cell expansion during fiber development are also expressed at a high level (Orford and Timmis, 1998; Smart et al., 1998; Ruan et al. 2001). Consistently, *GhTua2/3* and *GhTua4* genes increased in abundance from 10 to 20 DPA, whereas *GhTua1* and *GhTua5* transcripts were abundant only through to 14 DPA and dropped significantly at 16 DPA with the onset of secondary wall synthesis (Whittaker and Triplett, 1999). Our previous study indicated that the *GhTUB1* gene was preferentially expressed in the early stage of fiber development (Li et al., 2002). This suggests that strict developmental control on genes, such as *GhACT1*, involved in cell elongation during cotton fiber and ovule development had evolved.

To study the developmental control mechanisms, we isolated the *GhACT1* gene and its promoter. The 0.8-kb 5′ upstream sequence was cloned upstream the *GUS* reporter and transferred to cotton plants. GUS assay showed that the promoter is very active in developing fibers, whereas no or very little activity is present in leaf, stem, root, petal, and sepal. It should be emphasized that *GhACT1* was not expressed in leaf, stem, root, petal, and sepal trichomes, suggesting that the actin isotype encoded by *GhACT1* may be specific for fiber growth, rather than that of other trichomes. This is consistent with the *GhACT1* expression pattern revealed by real-time RT-PCR and RNA gel blot analysis, indicating that the 0.8-kb *GhACT1* promoter is sufficient to drive its tissue-specific expression and contains all the *cis* regulatory elements for its developmental regulation, as for actin genes in Arabidopsis (An et al., 1996; Huang et al., 1996; McDowell et al., 1996; Meagher et al., 1999b; Vitale et al., 2003). Thus, the 0.8-kb *GhACT1* promoter can be useful for isolating transcriptional factors that recognize the promoter sequence and for directing target gene expression in fiber cells. By comparing other fiber-specific promoter sequences such as *E6*, *H6*, and *FbL2A* (John and Crow, 1992; John and Keller, 1995, 1996; Rinehart et al., 1996), we hope to be able to identify fiber-specific *cis* elements and *trans* regulatory factors in the future.

GhACT1 Plays a Major Role in Fiber Elongation

Fiber cell development, similar to trichome morphogenesis in leaf and stem (Mathur et al., 1999), requires the actin cytoskeleton for elaborating and maintaining the spatial patterning. During the early stage of fiber elongation, a rapid rate of actin turnover must keep pace with the equally rapid rates of fiber growth. The downregulation of *GhACT1* via RNAi technology in the transgenic fibers greatly reduces actin level that consequently affects

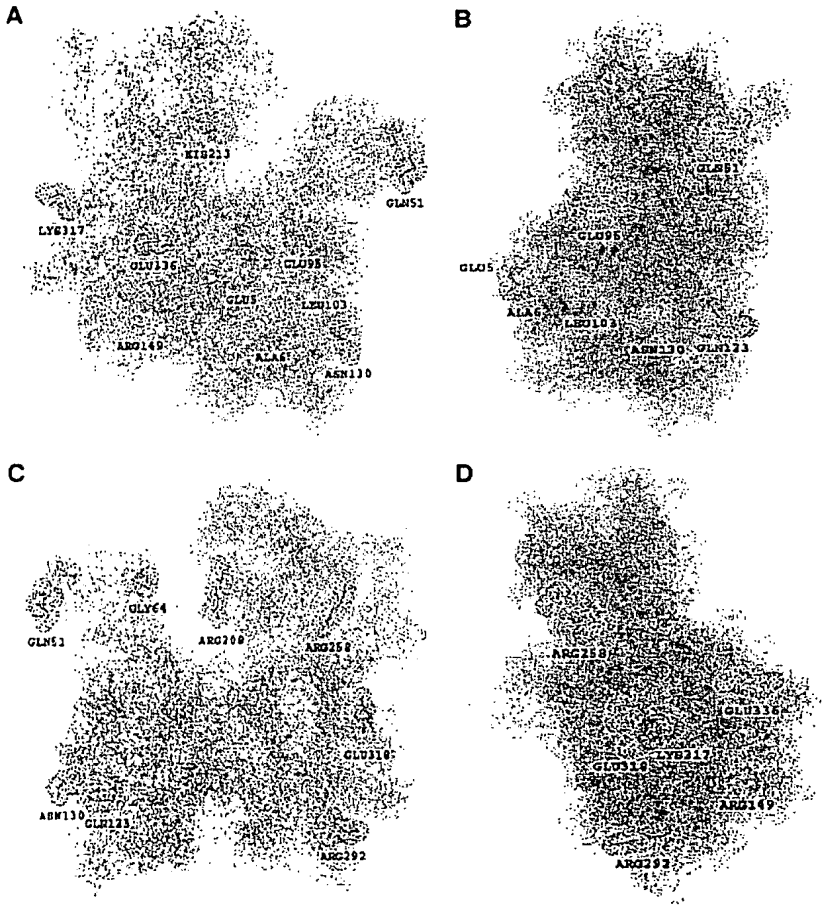

Figure 11. Significant Amino Acid Substitutions within Cotton GhACT Proteins.

The model was constructed using the spdbv37sp5 protein structure program (SwissModel first approach mode) from the Web site http://swissmodel.expasy.org/ of the Swiss Institute of Bioinformatics. Front **(A)**, right side **(B)**, back **(C)**, and left side **(D)** views, respectively, of the space-filling model for cotton GhACT1. The GhACT1 structure was built based on the known actin three-dimensional structure. Substitutions involving charged or strongly polar amino acid interchanges among the 15 cotton actin isoforms (GhACT1 to GhACT15) are shown in the labeled amino acid residues.

actin cytoskeleton organization, and as a result, fiber elongation is inhibited (Figure 9). This demonstrated that *GhACT1* plays a major role in fiber elongation, although we could not completely rule out the contribution of *GhACT* genes (such as *GhACT2* and *GhACT5*). The growth of cotton fiber cells is different from that of most other plant cells because of its rapid and synchronous tip elongation. It has been reported that F-actin plays an important role in pollen tube growth (Mascarenhas, 1993; Chen et al., 2002), in trichome morphogenesis (Mathur et al., 1999), in root hair tip growth (Miller et al., 1999), and in cell elongation of other cell types (Baluska et al., 2000; Waller et al., 2002; Yamamoto and Kiss, 2002). In the tip-growing pollen tube, F-actin arrays are very dynamic, changing from large spherical bodies to F-actin bundles oriented predominantly parallel to the growth axis (Tiwari and Polito, 1988). Similar F-actin arrays were also found for root hair growth (Miller et al., 1999) as well as root tip growth (Blancaflor and Hasenstein, 1997). However, Arabidopsis *act7* mutants showed remarkably reduced F-actin in the cells of the root elongation zone. As a result, mutants displayed a series of abnormal phenotypes, such as delayed and less efficient germination, increased root twisting and waving, and retarded and slowed root growth (Gilliland et al., 2003). The *act2-1* insertion fully disrupted *ACT2* gene expression and significantly decreased the level of total actin protein, resulting in much shorter root hairs (Gilliland et al., 2002; Ringli et al., 2002). Immunocytochemical analysis revealed only several thin actin bundles in the short mutant root hairs, and in the very apex of these stunted root hairs, the actin bundles were often looping through the tip or showing dense but diffuse fluorescence labeling (Gilliland et al., 2002). It was believed that actin isovariants of Arabidopsis have

evolved distinct reproductive and vegetative functions and have showed functional nonequavalency among each other. Misexpression of the pollen-specific reproductive ACT1 isovariant in vegetative tissues altered actin polymerization and F-actin organization and thereby dramatically affects plant development and morphogenesis (Kandasamy et al., 2002). In cotton fiber, we found that the F-actin was organized into short and thin arrays in tip orientation at the early stage of fiber development, and with further development, F-actin cytoskeleton displayed an increasingly complicated net-like structure consisting predominantly of thick and longitudinally extending cables in fiber cells. On the other hand, when GhACT1 isovariant level was reduced significantly in the transgenic fiber cells, F-actin bundles were reduced with only a few filaments (Figure 9), similar to *act7* and *act2* mutants. The reduced and defective actin cytoskeleton was unable to meet rapid fiber elongation. This suggested that F-actin arrays maintained by a significant amount of actins (mostly GhACT1) is critical for fiber cell elongation, like in root hair and trichome cell types.

F-actin might transport vesicles toward the cell periphery, especially near the polar region during tip growth. When the movement of F-actins was blocked, the vesicles could not be released in the cell periphery (polar region), resulting in the inhibition of the coleoptile cell elongation (Waller and Nick, 1997; Waller et al., 2002). In root hair development of *Vicia sativa*, the elongating net-axial fine bundles of actin filaments (FB-actin) function in polar growth by targeting and releasing Golgi vesicles to the vesicle-rich region of the hair cells. When the elongation of FB-actin was blocked by cytochalasin D, the tip growth of root hair cells was stopped (Miller et al., 1999). In our study, because of suppression of *GhACT1* expression, the reduction of F-actin level in transgenic fibers might have a similar effect on fiber cells. With the reduction of actin filaments, the number of organelles (such as Golgi body and endoplasmic reticulum) traveling along the filaments may decrease significantly in the *GhACT1* RNAi transgenic fiber cells. The significant reduction in vesicles may account for the slow elongation of fiber cells in the transgenic plants.

In conclusion, our results provide direct evidence that *GhACT1*, perhaps as well as other *GhACT* genes (such as *GhACT2* and *GhACT5*), is involved in fiber elongation, not fiber initiation. The characterization and expression studies give us novel insights into the role of *GhACT1* in cotton fiber development. Furthermore, the *GhACT1* promoter provides a useful tool to identify transcription regulators confirming its fiber-specific expression and to direct potential target genes for fiber quality improvement.

METHODS

Plant Materials

Cotton (*Gossypium hirsutum* cv Coker312) seeds were surface-sterilized with 70% ethanol for 30 to 60 s and 10% H_2O_2 for 30 to 60 min, followed by washing with sterile water. The sterilized seeds were germinated on half-strength MS medium under a 12-h-light/12-h-dark cycle at 28°C. Cotyledons and hypocotyls were cut from sterile seedlings as explants for transformation as described before (Li et al., 2002). Tissues for DNA and RNA extraction were derived from cotton plants (*G. hirsutum* cv DP5415 and Xuzhou142) grown in a greenhouse.

Construction of Cotton cDNA Libraries

Total RNA was extracted from young fibers, ovules, anthers, petals, leaves, cotyledons, and roots as described previously (Li et al., 2002). Poly(A)$^+$ mRNA was purified from total RNA using an mRNA purification kit (Qiagen, Düsseldorf, Germany). cDNA was synthesized and cloned into the *Eco*RI-*Xho*I sites of the ZAP Express vector and packaged using a ZAP-cDNA Gigapack Gold III cloning kit (Stratagene, La Jolla, CA) according to the manufacturer's instructions.

Isolation of *GhACT* cDNAs and RNA Gel Blot Analysis

More than 300 cDNA clones were randomly selected from the cotton fiber cDNA library for sequencing. Sequence analysis identified one actin clone, *GhACT1*. The 380-bp fragment of the 3′-UTR of *GhACT1* was obtained by PCR amplification using primers *GhACT1*-3′L (5′-AGTTTTG-TAATTGCTTTTGATGGT-3′) immediately downstream the stop codon and *GhACT1*-3′R (5′-AAATCTCGTACAATAATAGCTATT-3′) and used as a gene-specific probe for RNA gel blot analysis as described previously (Li et al., 2002). Then, a 600-bp fragment representing *GhACT1* exon 3 was labeled with [α-^{32}P]dCTP and used as a probe to screen a cotton cDNA library according to standard procedures (Sambrook et al., 1989). cDNA (5×10^6) clones were screened, and 300 clones were identified. Among them, 60 full-length clones were sequenced and analyzed. In total, 15 unique cDNA clones were obtained.

Sequence and Phylogenetic Analysis

Nucleotide and amino acid sequences were analyzed using DNAstar (DNAstar, Madison, WI). For phylogenetic analysis, 15 GhACT peptide sequences and one putative cotton actin sequence (AF059484) were aligned with the ClustalW program (http://www.ebi.ac.uk), then maximum parsimony analysis was performed with the PAUP 4.0 program (Swofford, 1998) using yeast actin ScACT1 as an outgroup. The heuristic search methods were applied and the best parsimonious trees were retained in each search.

RT-PCR Analysis

The expression of the *GhACT* genes in cotton tissues was analyzed by real-time quantitative RT-PCR using the fluorescent intercalating dye SYBR-Green in a LightCycler detection system (Roche, Indianapolis, IN). A cotton polyubiquitin gene (*GhUBI*) was used as a standard control in the RT-PCR reactions. A two-step RT-PCR procedure was performed in all experiments. First, total RNA samples (2 μg per reaction) from leaves, stems, cotyledons, roots, anthers, petals, and fibers were reversely transcribed into cDNAs by AMV reverse transcriptase according to the manufacturer's instructions (Roche). Then, the cDNAs were used as templates in real-time PCR reactions with gene-specific primers (Table 1). The real-time PCR reaction was performed using the LightCycler–FastStart DNA Master SYBR Green I kit (Roche) according to the manufacturer's instructions. The amplification of the target genes was monitored every cycle by SYBR-Green fluorescence. The Ct, defined as the PCR cycle at which a statistically significant increase of reporter fluorescence is first detected, is used as a measure for the starting copy numbers of the target gene. Relative quantitation of the target *GhACT* expression level was performed using the comparative Ct method (Roche LightCycler system). The relative value for expression level of each *GhACT* gene was calculated by the equation $Y = 10^{\Delta Cv3} \times 100\%$ (ΔCt is the differences of Ct between the control *GhUBI* products and the target

GhACT products; i.e., $\Delta Ct = Ct_{GhUBI} - Ct_{GhACT}$). To achieve optimal amplification, PCR conditions for every primer combination were optimized for annealing temperature and Mg^{2+} concentration as recommended by the Roche LightCycler system instructions. PCR products were confirmed on an agarose gel. The efficiency of each primer pair was detected using *GhACT* cDNAs as standard templates, and the RT-PCR data were normalized with the relative efficiency of each primer pair.

DNA Gel Blot Analysis

Genomic DNA was isolated from young cotton (*G. hirsutum* cv DP5415 and Xuzhou142) leaves using a modified method described earlier (Li et al., 2002). Genomic DNA was digested with restriction enzymes and separated on 0.7% agarose gels and transferred onto Hybond N^+ nylon membranes (Amersham Biosciences, Buckinghamshire, UK) by capillary blotting. DNA gel blot hybridization was performed at 68°C overnight using ExpressHyb solution (Clontech, Palo Alto, CA) with ^{32}P-labeled gene-specific DNA probes prepared by the Prime-a-Gene labeling system (Promega, Madison, WI), followed by washing at 68°C in 0.1× SSC and 0.5% SDS for 30 to 60 min. The ^{32}P-labeled membranes were exposed to x-ray film at −80°C for 1 to 3 d.

Isolation of *GhACT* Genes by Screening Cotton Genomic Libraries

Cotton genomic libraries were constructed as described earlier (Li et al., 2002). Approximately 2×10^6 clones were screened with a [α-^{32}P]dCTP-labeled *GhACT1* (0.6 kb of exon 3) probe generated by the Prime-a-Gene labeling system (Promega). The membranes (Hybond N^+; Amersham Biosciences) were hybridized overnight in ExpressHyb solution (Clontech) at 68°C, followed by washing with 0.1× SSC and 0.5% SDS. Autoradiography was performed with x-ray film (Kodak, Rochester, NY), and positive clones were purified and sequenced with the ABI Prism 377 DNA sequencer (Applied Biosystems, Foster City, CA) according to the manufacturer's instructions.

Construction of the *GhACT1*::*GUS* Chimeric Gene and *GhACT1* RNAi

Primers at −816 to −793 bp with an introduced *Sal*I site and from −1 to −27 bp before ATG with an introduced *Xba*I site were used to amplify the *GhACT1* promoter. A 0.8-kb PCR fragment was obtained using pfu DNA polymerase (Stratagene, La Jolla, CA) and digested with *Sal*I and *Xba*I, then subcloned into the *Sal*I/*Xba*I sites of the pBI101 vector (Clontech) to generate a chimeric *GhACT1*::*GUS* gene (named pBI-ACT1-p) (Figure 4B).

To construct *GhACT1* RNAi vector, the first intron (0.2 kb) of the *GhTUB1* gene (Li et al., 2002) was amplified by PCR with two introduced sites, *Xba*I and *Spe*I, using the primer pair TUBint-L, 5′-GGGTCTAGA-GACGTAGTTAGAAAGGAAGCCGA-3′, and TUBint-R, 5′-GGGACTAG-TACGTTCCCATTCCGGAACCCGTT-3′, and inserted into a pBluescript II SK+ vector at the sites *Xba*I and *Spe*I to obtain an intron-containing intermediate construct (pSK-TUBint). The *GhACT1* 3′-terminal sequence (150 bp fragment at 229 to 378 bp downstream the stop codon) was cloned into the 5′ arm with the introduced sites *Bam*HI/*Spe*I and the 3′ arm with the introduced sites *Xba*I/*Sac*I of the intron in pSK-TUBint vector for the sequences encoding the inverted repeat RNA. The constructed RNAi of the *GhACT1* gene was subcloned into the *GhACT1*::*GUS* construct at *Bam*HI/*Sac*I sites to replace the *GUS* gene (named pBI-TUBint-ACT1i) (Figure 4C).

Cotton Transformation

Cotyledon and hypocotyl explants from *G. hirsutum* cv Coker 312 were transformed using *Agrobacterium tumefaciens*–mediated transformation as described previously (Li et al., 2002). Homozygosity of transgenic plants was determined by segregation ratio of the kanamycin selection marker and further confirmed by DNA gel blot analysis.

Histochemical Assay of *GUS* Gene Expression

Histochemical assays for *GUS* activity in transgenic cotton plants were conducted according to Jefferson et al. (1987), with slight modification. Fresh plant tissues were incubated in 5-bromo-4-chloro-3-indolylglucuronide solution at 37°C for 4 to 8 h and then cleared and fixed by rinsing with 100 and 70% ethanol successively. For sectioning, 1 to 3 DPA ovules stained in 5-bromo-4-chloro-3-indolylglucuronide solution were fixed with 2.5% (v/v) glutaraldehyde in 0.1 M sodium phosphate buffer, pH 7.2, overnight at room temperature, then dehydrated through conventional ethanol series, and finally embedded in Historesin (Leica, Wetzlar, Germany) according to the manufacturer's instructions. The samples were cut into 5- to 7-μm-thick sections using a Leica microtome. The sections were examined and photographed under a Leica DMR microscope equipped with dark-field optics.

Protein Gel Blot Analysis

Soluble proteins were extracted from 8 to 10 DPA wild-type and *GhACT1* RNAi transgenic fibers in extraction buffer containing 50 mM Tris-HCl, pH 8.0, 0.5 mM $CaCl_2$, α-mercaptoethanol, 0.5% Nonidet P-40, 1 μg/mL aprotinium, 1 μg/mL leupeptin, and 0.6 μL/mL PMSF. Protein concentration was determined by the Bradford method. Equal amounts of proteins were separated by electrophoresis in a 12% SDS-PAGE gel and transferred onto a nylon membrane by electric transfer (Trans-Blot system; Bio-Rad, Hercules, CA) using semidry transfer buffer. The membrane was blocked with 5% nonfat milk in PBS buffer containing 0.05% Tween-20 at room temperature for at least 1 h and then incubated with affinity-purified goat polyclonal anti-actin IgG (Santa Cruz Biotechnology, Santa Cruz, CA) for 1 h. After washing in PBS buffer for 30 min, the membrane was incubated in PBS containing horseradish peroxidase–conjugated rabbit anti-goat IgG (Pierce, Rockford, IL) for 1 h. After washing in PBS buffer, the membrane was incubated in SuperSignal West Substrate (Pierce) working solution for 5 min and then exposed to x-ray film.

Scanning Electron Microscopy

For examining fiber initiation and elongation, fresh ovules were dissected out and placed on double-sided sticky tape on an aluminum specimen holder and frozen immediately in liquid nitrogen. The frozen sample was viewed with a JSM-5310LV scanning electron microscope (JEOL, Tokyo, Japan).

Observation of F-Actin Structures in Fiber Cells

Ovules dissected out from fresh bolls at 1 to 4 DPA, with or without maleimidoenzoyl-*N*-hydroxysuccinimide ester pretreatment, were fixed in a solution of 2% paraformaldehyde in KMCP buffer (70 mM KCl, 1 mM $MgCl_2$, 1 mM $CaCl_2$, and 100 mM Pipes, pH 6.5) for 1 h. After rinsing in KMCP buffer, the ovules were sectioned into slices of ~1 mm thickness. Thin sections were transferred to slides and treated with 1% cellulase (Sigma-Aldrich, St. Louis, MO), 0.5% hemicellulase (Sigma-Aldrich), 0.5% pectinase (Sigma-Aldrich), and 0.1% BSA in KMCP buffer for 10 min, followed by washing with KMCP buffer. Finally, sections were incubated in a solution of 5 μg/mL Phalloidin-TRITC (Sigma-Aldrich) in KMCP buffer with 0.1% Triton X-100 at room temperature. Excess phalloidin was removed by rinsing with the same buffer. Stained ovule sections were immediately examined with an LSM510 confocal microscope (Zeiss, Jena, Germany).

Sequence data from this article have been deposited with the EMBL/GenBank data libraries under accession numbers AY305723 to AY305737.

ACKNOWLEDGMENTS

This work was supported by Delta and Pine Land Co. and Temasek Holdings (Singapore). The authors appreciate the support of the National Natural Sciences Foundation of China (Project 30340081 and 30470930) to X.-B.L. and the Young Talent Program, Chinese Academy of Sciences to W.-C.Y. We thank Yangsun Chan and Qingwen Lin for technical assistance on electron microscopy and Rajini Sreenivasan for critical reading of the manuscript. We also would like to thank the Sequencing Service for oligo synthesis and DNA sequencing.

Received November 29, 2004; accepted December 27, 2004.

REFERENCES

An, Y.Q., Huang, S., McDowell, J.M., McKinney, E.C., and Meagher, R.B. (1996). Conserved expression of the Arabidopsis ACT1 and ACT3 actin subclass in organ primordia and mature pollen. Plant Cell **8,** 15–30.

Baird, W.V., and Meagher, R.B. (1987). A complex gene superfamily encodes actin in petunia. EMBO J. **6,** 3223–3231.

Baluska, F., Salaj, J., Mathur, J., Braun, M., Jasper, F., Samaj, J., Chua, N.H., Barlow, P.W., and Wolkmann, D. (2000). Root hair formation: F-actin-dependent tip growth is initiated by local assembly of profilin-supported F-actin meshworks accumulated within expansin-enriched bulges. Dev. Biol. **227,** 618–632.

Basra, A.S., and Malik, C.P. (1984). Development of the cotton fiber. Int. Rev. Cytol. **89,** 65–113.

Blancaflor, E.B., and Hasenstein, K.H. (1997). The organization of the actin cytoskeleton in vertical and graviresponding primary roots of maize. Plant Physiol. **113,** 1447–1455.

Chen, C.Y., Chueng, A.Y., and Wu, H.M. (2003). Actin-depolymerizing factor mediates Rac/Rop GTPase-regulated pollen tube growth. Plant Cell **15,** 237–249.

Chen, C.Y., Wong, E.I., Vidalli, L., Estavillo, A., Hepler, P.K., Wu, H., and Cheung, A.Y. (2002). The regulation of actin organization by actin-depolymerizing factor in elongating pollen tubes. Plant Cell **14,** 2175–2190.

Clarke, S.R., Staiger, C.J., Gibbon, B.C., and Franklin-Tong, V.E. (1998). A potential signaling role for profilin in pollen of *Papaver rhoeas*. Plant Cell **10,** 967–979.

Cosgrove, D.J. (1997). Relaxation in a high-stress environment: The molecular bases of extensible cell walls and cell enlargement. Plant Cell **9,** 1031–1041.

Cox, G.M., Rude, T.H., Dykstra, C.C., and Perfect, J.R. (1995). The actin gene from *Cryptococcus neoformans*: Structure and phylogenetic analysis. J. Med. Vet. Mycol. **33,** 261–266.

Chueng, A.Y., Chen, C.Y., Glaven, R.H., Graaf, B.H.J., Vidali, L., Hepler, P.K., and Wu, H.M. (2002). Rab2 GTPase regulates vesicle trafficking between the endoplasmic reticulum and the Golgi bodies and is important to pollen tube growth. Plant Cell **14,** 945–962.

Diet, A., Brunner, S., and Ringli, C. (2004). The *enl* mutants enhance the *lrx1* root hair mutant phenotype of *Arabidopsis thaliana*. Plant Cell Physiol. **45,** 734–741.

Dong, C.H., Xia, G.X., Yang, H., Ramachandran, S., Kost, B., and Chua, N.H. (2001). ADF proteins are involved in the control of flowering and regulate F-actin organization, cell expansion, and organ growth in Arabidopsis. Plant Cell **13,** 1333–1346.

Franklin-Tong, V.E. (1999). Signaling and the modulation of pollen tube growth. Plant Cell **11,** 727–738.

Fu, Y., Li, H., and Yang, Z. (2002). The ROP2 GTPase controls the formation of cortical fine F-actIn and the early phase of directional cell expansion during Arabidopsis organization. Plant Cell **14,** 777–794.

Gilliland, L.U., Kandasamy, M.K., Pawloski, L.C., and Meagher, R.B. (2002). Both vegetative and reproductive actin isovariants complement the stunted root hair phenotype of the Arabidopsis *act2-1* mutation. Plant Physiol. **130,** 2199–2209.

Gilliland, L.U., Pawloski, L.C., Kandasamy, M.K., and Meagher, R.B. (2003). Arabidopsis actin gene *ACT7* plays an essential role in germination and root growth. Plant J. **33,** 319–328.

Hepler, P.K., Vidali, L., and Cheung, A.Y. (2001). Polarized cell growth in higher plants. Annu. Rev. Cell Dev. Biol. **17,** 159–187.

Holmes, K.C., Popp, D., Gebhard, W., and Kabsch, W. (1990). Atomic model of the actin filament. Nature **347,** 44–49.

Huang, S.R., An, Y.Q., McDowell, J.M., McKinney, E.C., and Meagher, R.B. (1996). The *Arabidopsis thaliana ACT4/ACT12* actin gene subclass is strongly expressed throughout pollen development. Plant J. **10,** 189–202.

Jefferson, R.A., Kavanagh, T.A., and Bevan, M.W. (1987). *GUS* fusion: β-Glucuronidase as a sensitive and versatile gene fusion marker in higher plants. EMBO J. **6,** 3901–3907.

John, M.E., and Crow, L.J. (1992). Gene expression in cotton fiber: Cloning of the mRNAs. Proc. Natl. Acad. Sci. USA **89,** 5769–5773.

John, M.E., and Keller, G. (1995). Characterization of mRNA for a proline-rich protein of cotton fiber. Plant Physiol. **108,** 669–676.

John, M.E., and Keller, G. (1996). Metabolic pathway engineering in cotton: Biosynthesis of polyhydroxybutyrate in fiber cells. Proc. Natl. Acad. Sci. USA **93,** 12768–12773.

Kandasamy, M.K., McKinney, E.C., and Meagher, R.B. (1999). The late pollen-specific actins in angiosperms. Plant J. **18,** 681–691.

Kandasamy, M.K., McKinney, E.C., and Meagher, R.B. (2002). Functional nonequivalency of actin isovariants in Arabidopsis. Mol. Biol. Cell **13,** 251–261.

Ketelaar, T., de Ruijter, N.C.A., and Emons, A.M. (2003). Unstable F-actin specifies the area and microtubule direction of cell expansion in Arabidopsis root hairs. Plant Cell **15,** 285–292.

Kost, B., and Chua, N.H. (2002). The plant cytoskeleton: Vacuoles and cell walls make the difference. Cell **108,** 9–12.

Li, H., Lin, Y., Heath, R., Zhu, M., and Yang, Z. (1999). Control of pollen tube tip growth by a Rop GTPase-dependent pathway that leads to the tip-localized calcium influx. Plant Cell **11,** 1731–1742.

Li, X.B., Lin, C., Cheng, N.H., and Liu, J.W. (2002). Molecular characterization of the cotton *GhTUB1* gene that is preferentially expressed in fiber. Plant Physiol. **130,** 666–674.

Malhó, R. (1998). Role of 1,4,5-inositol triphosphate-induced Ca^{2+} release in pollen tube orientation. Sex. Plant Reprod. **11,** 231–235.

Mascarenhas, J.P. (1993). Molecular mechanisms of pollen tube growth and differentiation. Plant Cell **5,** 1303–1314.

Mathur, J., and Hülskamp, M. (2002). Microtubules and microfilaments in cell morphogenesis in higher plants. Curr. Biol. **12,** R669–R676.

Mathur, J., Mathur, N., Kernebeck, B., and Hülskamp, M. (2003b). Mutations in actin-related proteins 2 and 3 affect cell shape development in Arabidopsis. Plant Cell **15,** 1632–1645.

Mathur, J., Mathur, N., Kirik, V., Kernebeck, B., Srinivas, B.P., and Hülskamp, M. (2003a). Arabidopsis *CROOKED* encodes for the smallest subunit of the ARP2/3 complex and controls cell shape by region specific fine F-actin formation. Development **130,** 3137–3146.

Mathur, J., Spielhofer, P., Kost, B., and Chua, N.H. (1999). The actin cytoskeleton is required to elaborate and maintain spatial patterning during trichome cell morphogenesis in *Arabidopsis thaliana*. Development **126,** 5559–5568.

McDowell, J.M., Huang, S., McKinney, E.C., An, Y.Q., and Meagher, R.B. (1996). Structure and evolution of the actin gene family in *Arabidopsis thaliana*. Genetics **142,** 587–602.

McElroy, D., Rothenberg, M., Reece, K.S., and Wu, R. (1990). Characterization of the rice actin gene family. Plant Mol. Biol. **15,** 257–268.

McLean, B.G., Eubanks, S., and Meagher, R.B. (1990). Tissue specific expression of divergent actins in soybean root. Plant Cell **2,** 335–344.

Meagher, R.B., McKinney, E.C., and Kandasamy, M.K. (1999a). Isovariant dynamics expand and buffer the responses of complex systems: The diverse plant actin gene family. Plant Cell **11,** 995–1005.

Meagher, R.B., McKinney, E.C., and Vitale, A. (1999b). The evolution of new structures: Clues from plant cytoskeletal genes. Trends Genet. **15,** 278–284.

Meagher, R.B., and Williamson, R.E. (1994). The plant cytoskeleton. In *Arabidopsis*, E. Meyerowitz and C. Somerville, eds (Cold Spring Harbor, NY: Cold Spring Harbor Laboratory Press), pp. 1049–1084.

Miller, D.D., de Ruijter, N.C.A., Bisseling, T., and Emons, A.M.C. (1999). The role of actin in root hair morphogenesis: Studies with lipochito-oligosaccharide as a growth stimulator and cytochalasin as an actin perturbing drug. Plant J. **17,** 141–154.

Nairn, C.J., Winesett, L., and Ferl, R.J. (1988). Nucleotide sequence of an actin gene from *Arabidopsis thaliana*. Gene **65,** 247–257.

Orford, S.J., and Timmis, J.N. (1998). Specific expression of an expansin gene during elongation of cotton fibers. Biochim. Biophys. Acta **1398,** 342–346.

Otterbein, L.R., Graceffa, P., and Dominguez, R. (2001). The crystal structure of uncomplexed actin in the ADP state. Science **293,** 708–711.

Rinehart, J.A., Peterson, M.W., and John, M.E. (1996). Tissue-specific and developmental regulation of cotton gene FbL2A. Demonstration of promoter activity in transgenic plants. Plant Physiol. **112,** 1331–1341.

Ringli, C., Baumberger, N., Diet, A., Frey, B., and Keller, B. (2002). ACTIN2 is essential for bulge site selection and tip growth during root hair development of Arabidopsis. Plant Physiol. **129,** 1464–1472.

Ruan, Y.L., Llewellyn, D.J., and Furbank, R.T. (2001). The control of single-celled cotton fiber elongation by developmentally reversible gating of plasmodesmata and coordinated expression of sucrose and K^+ transporters and expansin. Plant Cell **13,** 47–63.

Sambrook, J., Fritsch, E.F., and Maniatis, T. (1989). Molecular Cloning: A Laboratory Manual. (Cold Spring Harbor, NY: Cold Spring Harbor Laboratory Press).

Seagull, R.W. (1990). The effects of microtubule and microfilament disrupting agents on cytoskeletal arrays and wall deposition in developing cotton fibers. Protoplasma **159,** 44–59.

Shah, D.M., Highrower, R.C., and Meagher, R.B. (1983). Genes encoding actin in higher plants: Intron positions are highly conserved but the coding sequences are not. J. Mol. Appl. Genet. **2,** 111–126.

Smart, L.B., Vojdani, F., Maeshima, M., and Wikkins, T.A. (1998). Genes involved in osmoregulation during turgor-driven cell expansion of developing cotton fibers are differentially regulated. Plant Physiol. **116,** 1539–1549.

Stranathan, M., Hastings, C., and Trinh, H. (1989). Molecular evolution of two actin genes from carrot. Plant Mol. Biol. **13,** 375–383.

Swofford, D.L. (1998). PAUP*: Phylogenetic Analysis Using Parsimony (*and Other Methods), Version 4.0b1. (Sunderland, MA: Sinauer Associates).

Szymanski, D.B., Marks, M.D., and Wick, S.M. (1999). Organized F-actin is essential for normal trichome morphogenesis in Arabidopsis. Plant Cell **11,** 2331–2347.

Thangavelu, M., Belostotsky, D., Bevan, M.W., Flavell, R.B., Rogers, H.J., and Lonsdale, D.M. (1993). Partial characterization of the *Nicotiana tabacum* actin gene family: Evidence for pollen specific expression of one of the gene family members. Mol. Gen. Genet. **240,** 290–295.

Tiwari, S.C., and Polito, V.S. (1988). Organization of the cytoskeleton in pollen tubes of *Pyrus communis*: A study employing conventional and freeze substitution electron microscopy, immunofluorescence, and rhodamine-phalloidin. Protoplasma **147,** 100–112.

Vitale, A., Wu, R.J., Cheng, Z., and Meagher, R.B. (2003). Multiple conserved 5′ elements are required for high-level pollen expression of the *Arabidopsis* reproductive actin *ACT1*. Plant Mol. Biol. **52,** 1135–1151.

Waller, F., and Nick, P. (1997). Response of actin microfilaments during phytochrome-controlled growth of maize seedlings. Protoplasma **200,** 154–162.

Waller, F., Riemann, M., and Nick, P. (2002). A role for actin-driven secretion in auxin-induced growth. Protoplasma **219,** 72–81.

Whittaker, D.J., and Triplett, B.A. (1999). Gene-specific changes in alpha-tubulin transcript accumulation in developing cotton fibers. Plant Physiol. **121,** 181–188.

Yamamoto, K., and Kiss, J.Z. (2002). Disruption of the actin cytoskeleton results in the promotion of gravitropism in inflorescence stems and hypocotyls of Arabidopsis. Plant Physiol. **128,** 669–681.

Yang, Z. (1998). Signaling tip growth in plants. Curr. Opin. Plant Biol. **1,** 525–530.

Exhibit 12

The Plant Journal (2002) **32**, 985–996

Molecular analysis of the stylar-expressed *Solanum chacoense* small asparagine-rich protein family related to the HT modifier of gametophytic self-incompatibility in *Nicotiana*

M. O'Brien[1], C. Kapfer[1], G. Major[1], M. Laurin[1], C. Bertrand[1], K. Kondo[2], Y. Kowyama[2] and D. P. Matton[1,*]
[1]*Département de Sciences Biologiques, Institut de recherche en biologie végétale, Université de Montréal, 4101 Sherbrooke est, Montréal, Québec, Canada H1X 2B2, and*
[2]*Faculty of Bioresources, Mie University, Tsu 514-8507, Japan*

Received 12 July 2002; revised 20 August 2002; accepted 16 September 2002.
*For correspondence (fax +1 514 872 9406; e-mail mattond@irbv.umontreal.ca).

Summary

Gametophytic self-incompatibility (GSI) systems involving the expression of stylar ribonucleases have been described and extensively studied in many plant families including the Solanaceae, Rosaceae and Scrophulariaceae. Pollen recognition and rejection is governed in the style by specific ribonucleases called S-RNases, but in many self-incompatibility (SI) systems, modifier loci that can modulate the SI response have been described at the genetic level. Here, we present at the molecular level, the isolation and characterization of two *Solanum chacoense* homologues of the *Nicotiana* HT modifier that had been previously shown to be necessary for the SI reaction to occur in *N. alata* (McClure *et al.*, 1999). HT homologues from other solanaceous species have also been isolated and a phylogenetic analysis reveals that the *HT* genes fall into two groups. In *S. chacoense*, these small proteins named ScHT-A and ScHT-B are expressed in the style and are developmentally regulated during anthesis identically to the S-RNases as well as following compatible and incompatible pollination. To elucidate the precise role of each HT isoform, antisense ScHT-A and RNAi ScHT-B lines were generated. Conversion from SI to self-compatibility (SC) was only observed in RNAi ScHT-B lines with reduced levels of ScHT-B mRNA. These results confirm the role of the HT modifier in solanaceous SI and indicate that only the HT-B isoform is directly involved in SI.

Keywords: self-incompatibility, S-RNase, Solanaceae, HT-modifier gene, RNA interference.

Introduction

Self-incompatibility (SI) constitutes an important mechanism for preventing inbreeding through specific pollen recognition and rejection. In the most widespread type of gametophytic self-incompatibility (GSI), the haploid pollen is rejected when the *S*-allele it expresses, matches either of the two *S*-alleles expressed in the sporophytic tissue of the pistil. For *Solanaceae*, the GSI phenotype is specified by a highly multiallelic *S*-locus (de Nettancourt, 1977, 1997) whose only known product is a secreted ribonuclease (McClure *et al.*, 1989) expressed in the transmitting tissue of the style (Anderson *et al.*, 1986; Matton *et al.*, 1998) and called an S-RNase. Gain-of-function experiments in SI plants have shown that expression of an S-RNase transgene is sufficient to alter the SI phenotype of the pistil but not that of pollen (Lee *et al.*, 1994; Matton *et al.*, 1997; Murfett *et al.*, 1994). Furthermore, transgenic plants made to express high levels of S-RNase in pollen did not acquire the new phenotype (Dodds *et al.*, 1999), indicating that the pollen *S* gene (unknown to date) is clearly distinct from the S-RNase (Kao and McCubbin, 1996). In order to determine if expression of an active S-RNase is the sole determinant of SI in styles, transformation of closely related self-compatible (SC) species with S-RNases were attempted. Transformation of SC *Nicotiana tabacum* or *N. plumbaginifolia* with an *S*-allele from the SI species *N. alata* did not result in the acquisition of the SI phenotype (Murfett *et al.*, 1996), nor did the introgression of a chromosome fragment bearing the *S*-locus from the SI *Lycopersicon hirsutum* in SC

L. esculentum (Bernatzky *et al.*, 1995), or the expression of an S-RNase from the SI *L. peruvianum* in the SC *L. esculentum* (Kondo *et al.*, 2002b). Conversely, when an *S*-allele from the SC *Petunia hybrida* was introduced in SI *P. inflata*, it became functional in rejecting its corresponding self-pollen, indicating that factors expressed in the *P. inflata* SI genetic background were needed for the SI reaction to occur (Ai *et al.*, 1991). These results strongly suggest that other factors are necessary for the SI reaction to occur. Some of these factors that affect the SI response have been described in numerous SI systems and often been named *S*-locus inhibitors or modifiers (de Nettancourt, 1977). In *S. chacoense*, an *S*-locus inhibitor (Sli) has been mapped to the distal end of chromosome 12, but has not been cloned yet (Hosaka and Hanneman, 1998a,b). To date, the only modifier functionally characterized at the molecular level is the *HT* gene, a stylar-expressed small asparagine-rich protein in *N. alata* (McClure *et al.*, 1999). The *NaHT* (*Nicotiana alata* HT) cDNA was isolated from a differential screen for SI stylar-specific transcripts, and antisense *Nicotiana* HT plants became SC, although they still expressed normal levels of stylar S-RNases. Recent correlative evidences from mRNA expression studies in *Lycopersicon* species also suggest the involvement of the HT modifier in SI (Kondo *et al.*, 2002a,b). Here, we describe the characterization of HT homologues that are co-ordinately expressed with the S-RNases during pistil development in the SI species *S. chacoense*, and show that only the HT-B isoform is involved in SI.

Results

Isolation of the Solanum HT homologues and sequence comparison

The *ScHT-A*$_1$, *ScHT-A*$_2$ and *S*$_{14}$*-RNase* cDNAs were isolated from a pollinated pistil cDNA library (see Experimental procedures section). The *ScHT-A*$_1$ cDNA codes for a small protein of 99 amino acid residues with a highly predicted N-terminal signal peptide as determined from the SignalP algorithm (Nielsen *et al.*, 1997). The predicted cleavage site for ScHT-A$_1$ is before Arg-25, producing a mature polypeptide of 75 amino acids (8 kDa). The *ScHT-A*$_2$ cDNA is incomplete in the 5′ region, but would comprise all of the mature protein (77 residues, 8.3 kDa) as predicted from the ScHT-A$_1$-deduced cleavage site. Both ScHT-A$_1$ and ScHT-A$_2$ predicted mature proteins are acidic with pIs of 3.98 and 4.11, respectively. Amino acid sequence comparison of the predicted mature polypeptides indicate that ScHT-A$_1$ and ScHT-A$_2$ are 96% identical (93% nucleotide sequence identity) and most probably correspond to allelic variants of the same gene (see linkage analysis of the ScHT-A isoforms below). The ScHT-B$_1$ isoform was obtained by PCR amplification with an upstream primer located in the signal peptide region and a downstream primer located 3′ of the predicted stop codon from the *N. alata* HT and *S. chacoense* HT-A$_1$ isoforms. The ScHT-B$_1$ mature protein comprises 79 amino acids (MW, 8.7 kDa) with an acidic pI of 4.67, and is approximately 51% identical (57% similar) at the amino acid level to the ScHT-A isoforms. No N-glycosylation sites are found on either polypeptides, but six cysteine residues that could be involved in disulfide bonding are conserved between all HT homologues, except from the *S. pinnatisectum* B$_1$ isoform that lacks one cysteine, and are found flanking a striking C-terminal region containing 16–20 Asp (D) or Asn (N) residues. In the mature ScHT proteins, asparagine and aspartic acid residues account for roughly 30% of the total amino acids. A sequence alignment of the deduced amino acid sequences corresponding to the mature protein region of the *S. chacoense* HT isoforms as well as HT homologues from other SI solanaceous plants, including *L. peruvianum*, *N. alata*, *S. pinnatisectum*, *S. bulbocastanum* and from the SI species *S. tuberosum*, is shown in Figure 1(a). All *Solanum* and *Lycopersicon* sequences were obtained by PCR amplification with the same primer pairs as described for the amplification of *ScHT-B*$_1$. Although all the HT sequences share some specific structural features, e.g. a C-terminal Asn/Asp-rich region flanked by conserved cysteine residues, they can be easily classified in two groups when the amino-terminal half of the protein is considered. Based on the CLUSTALX alignment, a phylogenetic analysis was performed to determine if this preliminary classification would hold true. Figure 1(b) shows that all the B isoforms fell into a highly supported cluster, while more sequence data would be needed to determine if the A-type sequences form one or more group. Interspecific amino acid sequence identities between the predicted mature polypeptides ranges from 76 to 86% in the A-isoform group, and 36–92% in the B-isoform group. The ScHT-A$_1$ and ScHT-A$_2$ (94%), SbHT-B$_1$ and SbHT-B$_2$ (98%) and SpHT-B$_1$ and SpHT-B$_2$ (97%) are most probably alleles of the same genes in their respective species. When the only non-*Solanum* sequence is removed (NaHT-B), the B-isoform group sequence identity is in the range of 77–92%. One surprising feature is the very high conservation of the predicted signal peptides between species, as determined from the available complete *HT* cDNA sequences (*ScHT-A*$_1$, *NaHT-B*, *LpHT-A*$_1$ and *LpHT-B*$_1$), ranging from 66 to 100% identity (82–100% similarity), when compared to the mature protein sequences (data not shown). This intriguing situation is also observed with the sporophytic SI (SSI) pollen *S* gene where the signal peptides are also far more similar to each other (mean of 77% identity and 89% similarity) than the mature protein sequences (29% identity and 38% similarity on average) when the sequences of five different SSI pollen *S* genes are compared (Schopfer *et al.*, 1999; Takayama *et al.*, 2000).

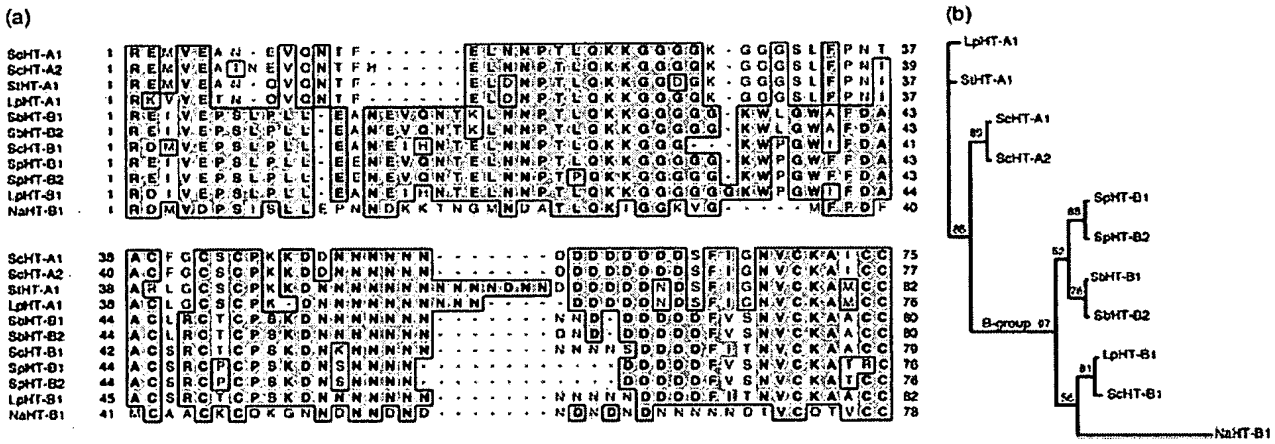

Figure 1. Sequence alignment (a) and phylogenetic analysis (b) of the deduced mature protein sequences of *ScHT-A*$_1$, *ScHT-A*$_2$ and *ScHT-B*$_1$ with related sequences from other solanaceous species.
(a) CLUSTALX alignment was used to produce a phylogenetic analysis of related HT sequences in six solanaceous species.
(b) A jacknife analysis using Paup 4.08b was used to produce the phylogram which is shown.

Tissue-specific and developmental regulation of the ScHT modifiers

Tissue-specific expression of ScHT-A and ScHT-B isoforms was determined using RNA extracted from different tissues of *S. chacoense*. Since the *ScHT-A*$_1$ and *ScHT-A*$_2$ cDNAs are 93% identical at the DNA level, the RNA-gel blot analyses most probably reflect the expression of both genes, although the probe used at all time was *ScHT-A*$_1$. Overall DNA sequence identity between the *ScHT-A* and Sc-HT-B isoforms is around 73%, and long stretches of identity might also produce cross-hybridization. In order to avoid this, an oligonucleotide specific to the B isoform and corresponding to the N-terminal sequence, PSLPLLEA, was synthesized. Both *ScHT-A* and *ScHT-B* isoforms are almost exclusively expressed in styles with very weak expression detected in ovary upon prolonged exposures (data not shown). No *ScHT-A* or *B* mRNAs could be detected in leaf, stem, root, petal, anther, pollen or pollen tube tissues (data not shown). This expression pattern is identical to the one observed for the S-RNases (Matton *et al.*, 1998). Since the S-RNase genes are themselves developmentally regulated during anthesis (Anderson *et al.*, 1986; Cornish *et al.*, 1987), we determined the RNA expression pattern of *ScHT-A* and *ScHT-B*, and compared with the one obtained from *S*$_{14}$*-RNase* (Figure 2a,b). Both ScHT isoforms and the *S*$_{14}$*-RNase* are identically regulated during pistil development and reach a maximum level of expression around anthesis day (Figure 2a,b). Figure 2(a,b) also shows that, in unpollinated flowers, *ScHT-A*, *ScHT-B* and *S*$_{14}$*-RNase* mRNA levels decline from around 2 days after anthesis, coinciding with a reduced fertilization receptivity.

In S-RNase-mediated GSI, rejection of the pollen tubes mostly occurs in the top half of the style. To determine if there could be a correlation with pollen tube arrest and the expression levels of genes involved in SI, mRNA levels of *ScHT-A* and *S*$_{14}$*-RNase* were measured in the upper and lower halves of styles around peak expression time (Figure 2c). Both genes were more strongly expressed in the upper half of the style, consistent with the site of most pollen tube arrest as determined by aniline blue staining in *S. chacoense* styles (Matton *et al.*, 1999).

Effect of compatible and incompatible pollination on ScHT *and* S-RNase *gene expression*

In many species, pollination is known to induce deterioration and death of the secretory cells in the stigmatic region and in the transmitting tissue of the style (Cheung, 1996). We have previously shown that some genes that respond to pollination, also respond to wounding stress and wound hormone treatments, mainly jasmonates (Lantin *et al.*, 1999a,b). Wounding, as well as wound hormone treatment (JA, ABA, MeJA) and elicitors of defense responses (salicylic acid, arachidonic acid), had no effect on either *ScHT-A* or *S*$_{14}$*-RNase* mRNA levels (data not shown, except for wounding in Figure 2d). Expression of these genes thus seemed to be exclusively controlled by developmental cues during pistil maturation, except for a differential response toward the type of pollination. *ScHT-A* and *S-RNases* responded differentially to a compatible or an incompatible pollination. In Figure 2(d), flowers were pollinated with either compatible or incompatible pollen and tissues were harvested 48 h later. For the wounding treatment, the upper part of the style including the stigma was slightly crushed with tweezers and tissues were also harvested 48 h later. Following a compatible pollination, or wounding, both *ScHT-A* and *S*$_{14}$*-RNase* mRNA levels declined similar to

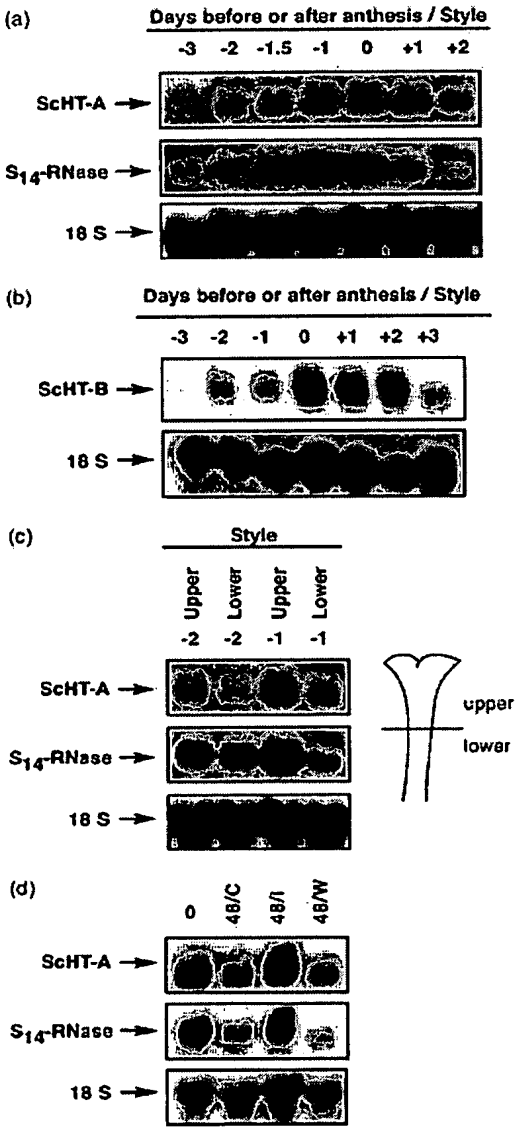

Figure 2. RNA expression analysis of *ScHT* transcript levels in styles.
(a) Developmental expression pattern of *ScHT-A* and S_{14}-*RNase* mRNA levels in unpollinated pistil tissues. ScHT-A and S_{14}-RNase transcript levels were determined by RNA-gel blot analysis of unpollinated pistil tissues, 3 days before anthesis (−3) to 2 days (+2) after anthesis. Ten micrograms of total style RNA from each developmental stage was probed with the *ScHT-A*$_1$ cDNA insert, stripped and re-probed with the S_{14}-*RNase* cDNA insert.
(b) Developmental expression pattern of *ScHT-B* mRNA levels in unpollinated pistil tissues. Same conditions as in (a), except that an identical RNA-gel blot was probed with the *ScHT-B*$_1$ specific oligonucleotide.
(c) Differential expression of *ScHT-A* and S_{14}-RNase transcript levels in upper and lower part of the style. *ScHT-A* and S_{14}-*RNase* transcript levels were determined by RNA-gel blot analysis in upper and lower halves of styles collected 2 (−2) and 1 day (−1) before anthesis. Conditions same as in (a).
(d) Effect of compatible and incompatible pollination on *ScHT-A* and S_{14}-*RNase* transcript levels. *ScHT-A* and S_{14}-*RNase* transcript levels were determined by RNA-gel blot analysis in unpollinated styles at anthesis day (0), in styles collected 48 h after a fully compatible ($S_{11}S_{12} \times S_{13}S_{14}$) pollination (48/C), in styles collected 48 h after a fully incompatible ($S_{13}S_{14} \times S_{13}S_{14}$) pollination (48/I) and in styles collected 48 h after wounding (48/W). Conditions same as in (a). To ascertain equal loading conditions, all RNA-gel blots were stripped and re-probed with an 18S ribosomal cDNA probe from *S. chacoense*.

the developmentally regulated decrease observed in unpollinated flowers (compare Figure 2a,d). An incompatible pollination had the opposite effect. The *ScHT-A* and S_{14}-*RNase* mRNA levels stayed as high as found on anthesis day, indicating that the developmentally programmed decrease in *S-RNase* and *ScHT* mRNA levels could be reversed, at least transiently, following an incompatible pollination.

Polymorphism of the HT modifiers and linkage to the S-locus

Using the *ScHT-A*$_1$ cDNA insert as a probe, an F_1 population from a parental cross ($S_{11}S_{12} \times S_{13}S_{14}$) was tested for polymorphism and linkage to the *S*-locus. A fraction of the F_1 progeny tested is shown in Figure 3. The S-RNase genotype of the progeny had been determined previously (Rivard *et al.*, 1994) and was confirmed by PCR analyses with allele-specific primers (data not shown). The *ScHT-A* gene is highly polymorphic as four different RFLPs could be detected in these plants. Although four different *S*-alleles also segregated in this population, the *ScHT-A* alleles were completely unlinked to the *S*-locus, as any combination of *ScHT-A* alleles could be found with all four S-RNases in this population. The same population was re-probed with the *ScHT-B* cDNA. Two new RFLPs specific to the B form were observed (data not shown). Although cross-hybridization does occur between the *ScHT-A* and *ScHT-B* cDNA probes (data not shown), no single RFLP could be linked with the *S-RNase* gene.

Two-hybrid analysis of ScHT and S-RNase protein interaction

A few putative roles have been proposed for the *N. alata* HT protein (McClure *et al.*, 1999). Recently it was shown that S-RNases, in both compatible or incompatible interactions, are taken up by pollen tubes, but the entry mechanism is still unknown (Luu *et al.*, 2000). One possibility is that other stylar factors involved in SI, such as the HT protein, could accompany or interact directly with the S-RNases as they are being transported into the growing pollen tubes. Since HT proteins from either *S. chacoense* or *N. alata* are fairly acidic proteins with pI around 4, and since S-RNases are basic proteins (S_{14}-RNase mature protein, predicted pI is 9.12), ScHT proteins could interact directly with S-RNases, albeit not in a sequence-specific manner, as determined by the linkage analysis (Figure 3). Another possibility would be that the HT proteins could interact with the pollen tubes and

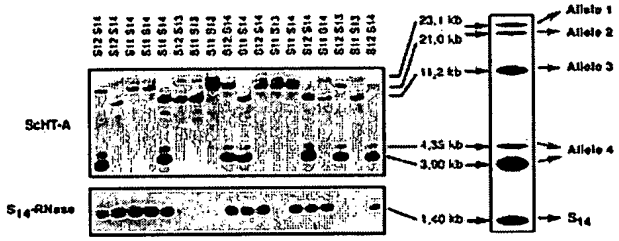

Figure 3. DNA-gel blot analysis of *ScHT-A* and linkage analysis with the *S*-locus.
Left panels: genomic DNA (10 μg) from *S. chacoense* leaves isolated from an F_1 population ($S_{11}S_{12} \times S_{13}S_{14}$) segregating for four *S*-alleles was digested with *Hin*dIII and probed with the *ScHT-A*$_1$ cDNA insert (upper panel). Identitical DNA-gel blots had been previously probed with the corresponding S-RNase cDNAs to determine the genotype of the plants (labeled on top of each lane) and tested by crossing. One *S*-allele hybridization is shown for the *S_{14}-RNase* (lower panel). Molecular sizes of the fragments appear on the right.
Right panel: schematic drawing of the banding pattern of the four *ScHT-A* alleles.

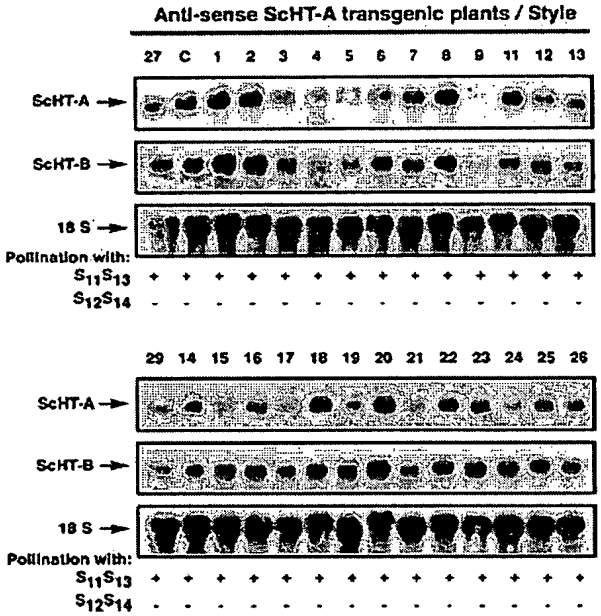

Figure 4. RNA expression analysis of *ScHT* transcript levels in styles of *ScHT-A* antisense transgenic plants and genetic cross results.
ScHT-A and *ScHT-B* transcript levels were determined by RNA-gel blot analysis of unpollinated styles at anthesis day from 27 antisense *ScHT-A*$_1$ transgenic plants. Control plant (C) is the untransformed host (genotype $S_{12}S_{14}$). All crosses were done on at least 10 flowers with pollen from a fully compatible plant (genotype $S_{11}S_{13}$) or a fully incompatible plant (genotype $S_{12}S_{14}$). Ten micrograms of total style RNA from each plant was probed with the *ScHT-A*$_1$ cDNA insert and the *ScHT-B*$_1$ specific oligonucleotide. Equal loading conditions were verified with an 18S ribosomal cDNA probe from *S. chacoense*.

facilitate S-RNase uptake. To test if the HT protein can interact directly with the S-RNase, the *ScHT–A*$_1$ and *ScHT–B*$_1$ cDNAs were PCR amplified with or without the putative signal peptide, and inserted in frame downstream of the yeast GAL4 DNA-binding domain in the pBDGAL4 vector. Since the linkage analysis (Figure 3) showed that all combinations of *ScHTs* and *S-RNases* could be found in the segregating population, this strongly suggested that no allele-specific interactions would be expected. Thus, a single *S-RNase* gene was used to test putative protein–protein interactions between the ScHT and S-RNase protein products. A modified *S_{11}-RNase* that was previously produced by site-directed mutagenesis was fused to the yeast GAL4 activating domain in the pADGAL4 vector. Because of their intrinsic ribonuclease activity, the S_{11}-RNase used in the two-hybrid analysis was mutagenized to remove one histidine residue involved in the active site of the enzyme (C3 domain) and replaced with a leucine, thus abolishing the ribonuclease activity that could have prevented proper growth in yeast cells. No direct interaction could be detected between the *ScHT-A* protein, with or without the predicted signal peptide, or the *ScHT-B* protein without the predicted signal peptide and the modified S_{11}-RNase, as no yeast growth could be observed on histidine-depleted media (data not shown).

Molecular characterization of the antisense Solanum HT-A plants

To determine if the function of the *ScHT* genes is conserved in solanaceous species other than *N. alata*, antisense *HT-A* plants were produced. The *ScHT-A*$_1$ cDNA was inserted in the antisense orientation downstream of the CaMV 35S promoter with doubled enhancer in the pBIN19 vector and flanked by the nopaline synthase terminator. *S. chacoense* plants of $S_{12}S_{14}$ genotype were transformed with *Agrobacterium tumefaciens* LBA4404 strain containing the *ScHT-A*$_1$ antisense construct. Twenty-seven primary transformants were selected. Because *ScHT-A* and *ScHT-B* share 73% nucleotide sequence identity, and since stretches of perfect identity are found between these two sequences, some antisense lines for *ScHT-A* might also be suppressed in *ScHT-B* mRNA accumulation. Figure 4 shows RNA-gel blots of these 27 transgenic plants probed with either the *ScHT-A*$_1$ complete cDNA or the *ScHT-B*$_1$ specific oligonucleotide, and the results of the genetic crosses with either compatible or incompatible pollen are shown below. In some antisense lines where *ScHT-A* mRNA accumulation had been suppressed, *ScHT-B* levels were also affected, albeit to a lesser extent (AS plant #4 and 9). Although numerous plants showed strong reduction in *ScHT-A* mRNA levels (plants #3–5, 9, 29), none set seeds upon self-pollination.

Molecular characterization of the RNAi Solanum HT-B plants

Because antisense *S. chacoense HT-A* plants did not become SC, even with an almost 15-fold reduction in *ScHT-A*

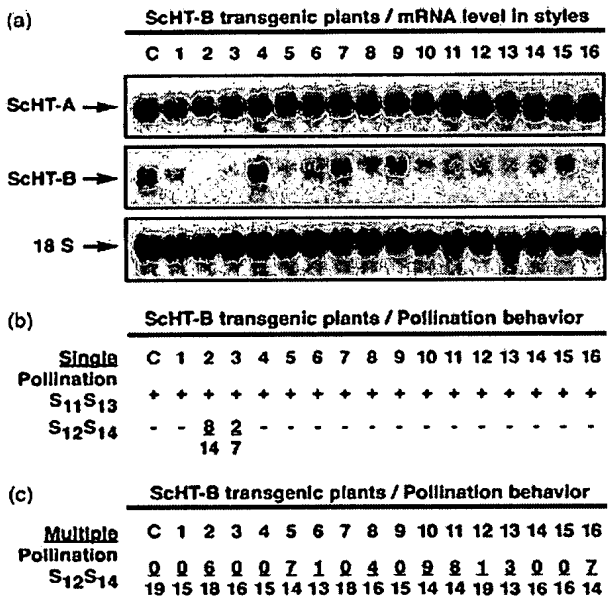

Figure 5. RNA expression analysis of *ScHT* transcript levels in styles of *ScHT-B* RNAi transgenic plants and genetic cross results.
(a) *ScHT-A* and *ScHT-B* transcript levels were determined by RNA-gel blot analysis of unpollinated styles at anthesis day from 16 RNAi *ScHT-B*$_1$ transgenic plants. Control plant (C) is the untransformed host (genotype $S_{12}S_{14}$). Ten micrograms of total style RNA from each plant was probed with the *ScHT-A*$_1$ cDNA insert and the *ScHT-B*$_1$ specific oligonucleotide. Equal loading conditions were verified with an 18S ribosomal cDNA probe from *S. chacoense*.
(b) Genetic cross results with pollen from SI or SC plants. All crosses were done on at least 10 flowers per plant on anthesis day, with pollen from a fully compatible plant (genotype $S_{11}S_{13}$) or a fully incompatible plant (genotype $S_{12}S_{14}$). The plus (+) sign indicates a fully compatible pollination: crosses were successful and seed set occurred in more that 90% of the pollinated flowers. The minus (–) sign indicates a fully incompatible pollination: no crosses were successful and no seed set occurred. For intermediate phenotypes, the number of successful pollination leading to seed set per flower pollinated is indicated.
(c) Genetic cross results with pollen from a SI plant after repeated pollination (multiple pollination). Same as in (b) except that the flowers were repeatedly pollinated with pollen from a fully SI parent (genotype $S_{12}S_{14}$). Pollination was done on anthesis day, and then after 24, 48 and 72 h.

transcripts (*ScHT-A* AS plant #9, as determined by densitometric scans), and since correlative evidences showing weak or complete loss of expression of *HT-B* homologues, but not of HT-A homologues in some SC *Lycopersicon* species, have been recently obtained (Kondo *et al.*, 2002a,b), we also decided to target the *ScHT-B* gene through an RNA interference (RNAi) strategy. The *ScHT-B*$_1$ cDNA was inserted first in the sense orientation downstream of the CaMV 35S promoter, followed by a 327-bp spacer, and by the *ScHT-B*$_1$ cDNA again, but in the antisense orientation. This RNAi construct was then inserted in the *A. tumefaciens* LBA4404 strain and used to transform *S. chacoense* plants of the $S_{12}S_{14}$ genotype. Sixteen primary transformants were initially selected. All *ScHT-B* RNAi lines were cross-pollinated with pollen from fully compatible ($S_{11}S_{13}$) or fully incompatible ($S_{12}S_{14}$) genotypes. Two plants (#2 and #3) sired seeds upon self-pollination (pollen from genotype $S_{12}S_{14}$), and could be scored as partially or semi-compatible (Figure 5b). *ScHT-A* and *ScHT-B* mRNA levels were then determined in mature flowers at anthesis. Figure 5a shows an RNA-gel blot of all the transgenic plants probed with either the *ScHT-A*$_1$ complete cDNA or the *ScHT-B*$_1$-specific oligonucleotide, and the results of the genetic crosses with either compatible or incompatible pollen (Figure 5b). Unlike the *ScHT-A* antisense experiment (Figure 4), the RNA interference strategy specifically targeted the *ScHT-B* transcript as no significant variation in the *ScHT-A* mRNA levels could be observed (Figure 5a). Only the transgenic plants with the most reduced *ScHT-B* mRNA level became partially SC (plants #2 and 3), suggesting that a threshold level of *ScHT-B* is necessary to maintain the SI phenotype, and that only the HT-B isoform is involved in GSI.

The ScHT-B *gene affects flower longevity and stylar abscission following an incompatible pollination*

One intriguing observation, following an incompatible pollination, was that flowers of *ScHT-B* RNAi plants that had lower levels of *ScHT-B* transcripts, stayed much longer on the plant than control or transgenic plants not affected in *ScHT-B* mRNA levels (plants #4, 7, 9 and 15). Under normal conditions, abscission of unpollinated flowers in *S. chacoense* occurs approximately 5 days after anthesis (Figure 6, unpollinated G4). After a compatible pollination, ovary swelling is clearly detectable 3 days after pollination and stylar abscission occurs approximately 4 days after pollination (Figure 6, V22 × G4). Following an incompatible pollination, abscission is delayed by an average of 24 h when compared to unpollinated flowers (Figure 6, G4 × G4). In *ScHT-B*-suppressed lines, flower abscission was further delayed and only occurred after an 8–9-day period following initial pollination (data not shown). This extended flower longevity phenotype caused by a lower than normal *ScHT-B* mRNA level prompted us to re-examine pollination behaviour with SI pollen under a multiple pollination scheme. In this experiment, *ScHT-B* transgenic plants and untransformed control plants were pollinated on anthesis day, and then on the following 3 days with similar pollen load. Fruit formation was then monitored from day 6 to 12 after pollination. As a control, the transformation host genotype was also repeatedly pollinated. Even after multiple pollination, the untransformed plant (control) and the transgenic plants not affected in *ScHT-B* levels (plants #4, 7, 9 and 15) never sired seeds, indicating that multiple pollination alone, even over a 72-h period, was not sufficient to bypass the SI recognition and rejection system (Figure 5c). For the remaining 12 transgenic plants with altered level of *ScHT-B* mRNA, a total of nine plants were scored as

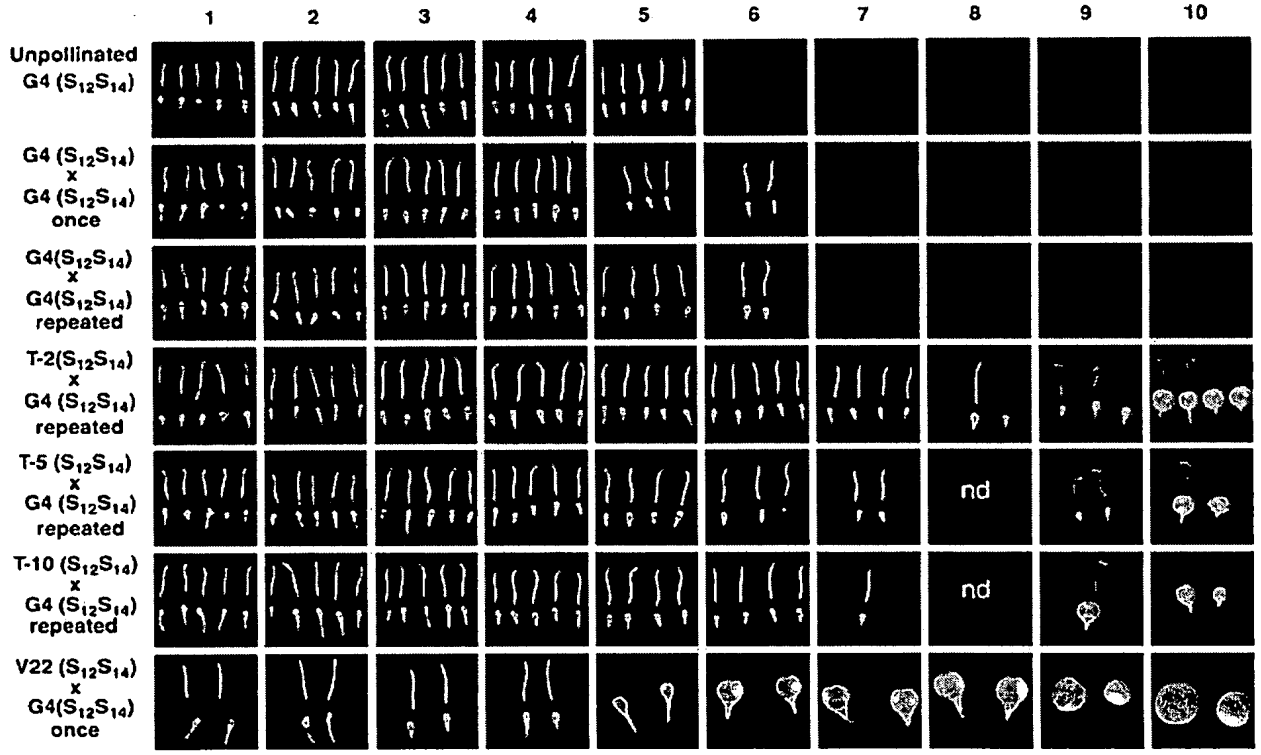

Figure 6. Pistil morphology of *ScHT-B* transgenic and control plants after SI and SC pollination.
Floral and stylar abscission was monitored, from one day after anthesis or from one day after pollination for control plants, and for three transgenic plants (T-2, T-5 and T-10) until day 10. In all cases, pollination was performed with pollen from the G4 line (genotype $S_{12}S_{14}$). Five flowers per plant and per day (except for the V22 × G4 cross) were hand pollinated on consecutive days and, for the remaining flowers, dissected at the end of the time-course. Only the remaining floral parts at the end of the time-course are displayed. ND, not determined. Once, single pollination. Repeated, consecutive pollination on day 0–2 and if possible on day 3, depending on the corolla closure.

semi-compatible (plants #2, 5, 6, 8, 10–13 and 16) upon repeated pollination with fully incompatible pollen (genotype $S_{12}S_{14}$). Floral and stylar abscission were also monitored, from one day after anthesis or from one day after pollination for control plants and three transgenic plants (T-2, T-5 and T-10) that showed a SC behaviour following self-pollination. Five flowers per plant and per day were hand pollinated on consecutive days in order to collect all samples on the same day (except for the unpollinated control plant and the fully compatible cross V22 × G4). As such, with the remaining flowers at the end of the 10-day period, the whole time-course was displayed. Pistil morphology for these plants is shown in Figure 6. Transgenic plants, T-2, T-5 and T-10, clearly showed an increased stylar longevity, with turgid styles that appeared receptive to pollination until day 7 or 8, after pollination. Furthermore, stylar abscission from the developing fruit was also delayed, with some styles still attached even after withering (Figure 6, plants T-2 and T-5 on day 9 and 10; plant T-10 on day 9). When compared to a fully compatible cross (V22 × G4), fruit formation was also delayed in self-pollinated T-2, T-5 and T-10 transgenic plants. These results confirm the involvement of the *ScHT-B* gene in SI and suggest that it might act through an increased flower receptivity period.

Discussion

Mechanisms underlying the breakdown of GSI have been recently reviewed and grouped in three broad categories (Stone, 2002). First, loss of SI occurs following the duplication of the *S*-locus and the presence of heterozygous pollen (heteroallelic for the *S*-locus) (Golz *et al.*, 2000). Secondly, mutations affecting either the expression of the S-RNase or its activity also lead to a SC phenotype (Royo *et al.*, 1994). Thirdly, mutations not affecting the enzymatic activity of the S-RNase have also been described at the genetic level and include many so-called modifier loci. Numerous experiments have demonstrated that although the S-RNase is responsible for pollen recognition and rejection in the style (Lee *et al.*, 1994; Matton *et al.*, 1997; Matton *et al.*, 1999; Murfett *et al.*, 1994), other stylar factors are also necessary for the proper expression of the SI phenotype (Ai *et al.*, 1991; Bernatzky *et al.*, 1995; Kondo *et al.*, 2002b; Murfett

et al., 1996). Such factors, often considered as modifier loci, are present in the genetic background of SI plants, unlinked to the *S*-locus, and have often been lost in SC relatives of SI species. Complementation phenomena of the genetic background have been described in *L. hirsutum* where the F_1 population from two independent SC accessions were all SC, while SI offsprings could be recovered in the F_2 generation from these F_1 plants, strengthening the multigenic nature of the gametophytic SI (Ricks and Chetelat, 1991). One such candidate for a modifier gene is the *N. alata HT* gene (McClure *et al.*, 1999). The *NaHT* gene was cloned based on a differential screen between stylar expressed mRNAs from SC *N. plumbaginifolia* and an SC accession of *N. alata* that is defective in S-RNase expression but that is competent to express SI (Murfett *et al.*, 1996). Anti-sense *NaHT* plants with reduced level of the HT protein but with normal levels of S-RNases were either fully or partially SC (McClure *et al.*, 1999). This strongly suggests that the *NaHT* gene is a good candidate for such a modifier factor necessary for the SI reaction to occur. In the present study, we have characterized *NaHT* homologues from four different *Solanum* species, and have focussed our attention on the putative function of the *S. chacoense HT* homologues (*ScHT-A* and *ScHT-B*) in GSI.

Phylogenetic analyses of the isolated NaHT homologues clearly demonstrated that two different HT isoforms exist and that isoform B is probably the most closely related to the *NaHT* gene. All the HT proteins shared some common features. Firstly, a highly conserved N-terminal region that is strongly predicted to be a signal peptide. The sequence conservation was high enough to originally derive PCR primer pairs from only the *NaHT* and *ScHT-A*$_1$ sequences, and amplify both HT isoforms from numerous *Solanum* (this study) and *Lycopersicon* species (Kondo *et al.*, 2002a,b). Secondly, all HT homologues possess a C-terminal region composed of consecutive stretches of asparagine and aspartic acid residues, flanked by conserved cysteines probably involved in disulfide bridges. Although sequence identity is quite variable, ranging from 36 to 92% in the B-isoform group (77–92% when only *Solanum* sequences are considered), the overall structure conservation combined with identical expression pattern would suggest that the *ScHT-B* isoform and the NaHT protein are probably true orthologues. Both *ScHT-A*, *ScHT-B* and *NaHT* are almost exclusively stylar-expressed as for the *S-RNases*, and all are developmentally regulated during pistil maturation (this study and McClure *et al.*, 1999). Interestingly, we found higher expression levels of both *ScHT* and *S-RNase* genes in the upper style region (Figure 2c), consistent with the pattern of pollen tube arrests that occurs in the top half of the style in *S. chacoense* (Matton *et al.*, 1999). The developmental regulation of S-RNase transcripts accumulation enables the production of selfed progeny in some GSI species when using very young flower buds (bud-pollination), but is very difficult to achieve in *S. chacoense*. One reason could be the elevated level of both S-RNase and HT transcripts, even 2 days before anthesis, and detectable 3 days before anthesis, combined with a preferential upper style accumulation. One intriguing observation was the differential expression pattern of both *S-RNase* and *HT* transcripts following an incompatible pollination compared to an unpollinated or a compatibly pollinated flower (Figure 2d). As the flower ages, *S-RNase* and *HT* transcript levels decreases markedly, but low expression levels coincide with reduced fertilization receptivity, and eventually, flower abscission. Surprisingly, *S-RNase* and *ScHT-A* transcript levels do not decrease following an incompatible pollination (for at least 2 days after pollination, Figure 2d), and this cannot be the result of only stigmatic and transmitting tissue deterioration and death, since this is also induced by a compatible pollination. Furthermore, mechanical wounding or wound hormone treatments had no effect on *S-RNase* and *ScHT-A* transcript levels. This strongly suggests that the presence of dead pollen tubes or molecules liberated from the arrested pollen tubes, either increase the transcription of these genes, or reduce their mRNA turnovers, ensuring that the S-RNases and HT proteins are still present in sufficient amount to reject newly incoming pollen from incompatible genotypes. The maintenance of high steady-state levels of *S-RNases* and *ScHT* mRNAs following an initial incompatible pollination, would also lead to a prolonged reproductive barrier, an important issue since flower senescence is retarded following an incompatible pollination (Figure 6, G4 × G4).

In order to determine the role of the *ScHT* genes in SI, functional analysis of *ScHT-A* and *ScHT-B* protein–protein interactions with an S-RNase were tested in the yeast two-hybrid system, and transgenic plants with strongly suppressed levels of both isoforms were generated. Although *ScHT-A* and *ScHT-B* deduced mature proteins have acidic pIs and the S-RNase is basic (predicted pI = 9.25 for S_{11}-RNase mature protein), no direct interactions based either on specific or electrostatic attractions could be detected in the two-hybrid system, as no yeast growth could be observed, with or without the predicted signal peptide. Such direct interaction had also not been detected with the purified HT protein from *N. alata*, although in that case, the NaHT protein appeared to be unstable in stylar extracts (McClure *et al.*, 1999). Both results suggest that HT proteins and S-RNases do not interact directly.

Recently, correlative evidences for the involvement of the NaHT homologues in *Lycopersicon* species have been obtained (Kondo *et al.*, 2002a,b). In the three *Lycopersicon* SI species tested, all expressed functional S-RNases as well as *HT-A* and *HT-B* mRNAs. In the seven *Lycopersicon* SC species tested, no or low stylar ribonuclease activity was observed. This alone would most probably be sufficient to explain their SC phenotype, since a threshold level of

S-RNase expression is necessary to confer an SI phenotype (Lee *et al.*, 1994; Matton *et al.*, 1997). Intriguingly, in the seven *Lycopersicon* SC species tested, transcription of the HT-B isoform was either weakly or not detected at all, and the HT-B isoform produced had internal stop codons, while the HT-A isoform was strongly expressed at the mRNA level, although some SC species also produced defective (frame-shifted) HT-A transcripts. Apart from the *N. alata* transgenic antisense lines, no other functional analysis had been made prior to the one presented here. In *N. alata*, plants with reduced levels of the NaHT protein were either fully or partially SC, suggesting that the amount of NaHT protein is important (McClure *et al.*, 1999). In the present study, antisense *ScHT-A* and RNAi *ScHT-B* plants were generated. Figure 4 showed that even with a 15-fold decrease in *ScHT-A* mRNA levels, *ScHT-A* AS plant #9 remained SI. *ScHT-B* mRNA levels in that transgenic line were also affected, although to a lesser extent. This could suggest that a threshold level of *ScHT-B* is sufficient to maintain an SI phenotype. In a second series of experiments, *ScHT-B* suppression was achieved through an RNAi strategy. Unlike the antisense plants, the *ScHT-B* RNAi plants were only affected in *ScHT-B* mRNA expression (Figure 5). Plants with severely reduced *ScHT-B* transcripts became SC and sired seeds upon pollination with pollen from an incompatible genotype. RNAi plant #2 had the most severely reduced *ScHT-B* mRNA levels and consistently set seeds upon self-pollination. RNAi plant #3 had a less stable phenotype, and only sired seeds occasionally. Although at first only two plants became partially SC upon selfing, all the transgenic plants with reduced *ScHT-B* mRNA levels also showed an extended, albeit slightly variable, floral longevity upon pollination with incompatible pollen. This observation led to the hypothesis that the *ScHT-B* gene could be involved in modulating the receptivity period of the flower, perhaps through a control over the abscission of the floral organs. This increase in floral longevity, and in particular in stylar turgescence and receptivity might partially explain the SC phenotype since it could increase the chances of pollen tubes to reach the ovary. To test this, repeated pollination were performed on 3–4 consecutive days, on the 16 RNAi *ScHT-B* transgenic plants and control plants. None of the *ScHT-B* transgenic plants unaffected in *ScHT-B* mRNA expression, or the untransformed control plant, had an extended floral longevity and none were fertilized upon selfing. Of the remaining 12 transgenic plants expressing reduced levels of *ScHT-B* mRNA, nine were able to sire seeds. Fruits formed on these plants were smaller than the ones obtained from a compatible cross, and after 10 days, were comparable in size with fruits produced from a compatible pollination after 6 days (Figure 6, compare the fruits from plants T-2, T-5 and T-10 with the ones from the V22 × G4 cross). These results are entirely consistent with our hypothesis that reduced level of *ScHT-B* mRNA affects the receptivity period of the flower and that the SC phenotype observed in *ScHT-B* transgenic plants does not result only from the developmentally regulated decrease in both *S-RNase* and *ScHT-B* mRNA levels (Figure 2a,b), since repeated incompatible pollination could not induce fertilization in control or unaffected *ScHT-B* transgenic plants. Furthermore, in *N. alata HT* antisense plants, pollen tube growth in the style is observed even when the S-RNase level is high, although in that case, fertilization and production of fruits could not be observed because the recipient plant used was a sterile hybrid between *N. alata* and *N. plumbaginifolia* and only pollen tube growth in the style was used to score the SI or SC phenotype.

Our results clearly indicate that there is an increase in flower longevity and pollination receptivity, associated with a decrease in *ScHT-B* transcripts. One possibility would be that the HT-B isoform is involved in a pathway regulating floral abscission. Pollination is known to affect the physiological state of the flower. Pollinated flowers (compatible) senesce rapidly compared to unpollinated flowers or those pollinated by incompatible pollen grains in the case of an SI plant (Gilissen, 1977; Singh *et al.*, 1992). Early studies in *Petunia* ovaries showed an increase in polyribosomes activity, 6–12 h after pollination, well before the arrival of the pollen tubes in the ovary (approximately 50 h) (Deurenberg, 1976). Pollination-induced wilting of the corolla can be prevented if the style is removed early after pollination (Gilissen, 1984). These and other results (Stead, 1992) have led to the hypothesis that a pollination-induced signal is transmitted through the pistil and precedes the growing pollen tube. Ethylene has been shown to have a strong effect on flower abscission in solanaceous species (van Doorn, 2002a,b). Furthermore, pollination itself induces ethylene synthesis (Hall and Forsyth, 1967), and it has been shown that in *P. hybrida*, pollination induces two distinct phases of ethylene production in the flower (Singh *et al.*, 1992). The first phase is common to both self- and cross-pollinated flowers and is dependent on pollen-borne ACC (ethylene precursor). The second phase results from *de novo* synthesis of ethylene from the flower and occurs 18 h after a compatible pollination. Following an incompatible pollination, the production of ethylene is delayed to 3 days after pollination (Singh *et al.*, 1992). Since RNAi *ScHT-B* plants showed delayed floral abscission, we tested these plants for alteration in the expression of ethylene-related genes. No differences could be observed in the expression pattern of two genes involved in ethylene biosynthesis (ACC synthase and ACC oxidase), or in ethylene perception and signal transduction (ethylene receptor ETR1 and EIL-3) in *ScHT-B* transgenic plants (data not shown). Since the ACC synthase and the ACC oxidase genes are part of multigene families (at least eight members for the ACC synthase and four members for the ACC oxidase in *S. lycopersicon*) (Llop-Tous *et al.*, 2000), specific probes will need

to be designed for individual members in order to determine if a given isoform is affected in *ScHT-B* mutant background.

From our results, we propose that the *ScHT-B* isoform is involved in at least two phenomena. Firstly, elevated levels of both S-RNases and *ScHT-B* would be necessary for the SI reaction to occur, as determined from McClure's work (McClure *et al.*, 1999) and from the phenotype of the *ScHT-B* RNAi plant T-2. When the *ScHT-B* mRNA levels are below a threshold level, pollen tubes would be able to reach the ovary and effect fertilization. The developmentally regulated decrease in both *S-RNase* and *ScHT* mRNA levels (Figure 2a,b) would normally lead to an SC phenotype in aged flowers, but is counterbalanced by floral abscission. The increase in both *S-RNase* and *ScHT* mRNA levels following an incompatible pollination (Figure 2d) would also ensure the maintenance of a strong reproductive barrier over a longer period of time. This could be of importance since flowers pollinated with incompatible pollen last longer by an average of 1 day on the plant than unpollinated flowers (Figure 6, G4 × G4), and the receptivity period for a successful pollination is normally limited to the first 2–3 days after anthesis. Secondly, the *ScHT-B* RNAi transgenic plants display a novel phenotype that includes a longer floral longevity with delayed stylar abscission and, perhaps, more relevant for the SC phenotype of those plants, the persistence of turgid styles, even 9 days after anthesis (Figure 6). This phenotype, observed in plants with reduced levels of *ScHT-B* mRNAs, would enable pollen tube growth in older styles with reduced S-RNase level, pass their normal flower lifespan and pollination receptivity period. As suggested by McClure (McClure *et al.*, 1999), the HT protein could interact directly with pollen tubes and facilitate S-RNase uptake. Our two-hybrid results would support the fact that *ScHT-B* does not interact directly with the S-RNase. Furthermore, if the HT-B protein is involved in S-RNase uptake, a reduced level of HT-B protein would increase the number of pollen tubes not affected by the presence of the S-RNase, enabling fertilization to take place. This is entirely consistent with our results, since repeated pollination in *ScHT-B* RNAi plants increase the percentage of fertilized ovules. Although its mode of action still remains unclear, our data demonstrate a specific role for the HT-B isoform in SI and points towards a role in the control of flower senescence and abscission.

Experimental procedures

Plant material and transformation

The diploid ($2n = 2x = 24$) *S. chacoense* Bitt. SI genotypes used included line 314 ($S_{11}S_{12}$), 582 ($S_{13}S_{14}$), G4 ($S_{12}S_{14}$) and V22 ($S_{11}S_{13}$). Plants were grown in greenhouse with 14–16 h of light per day. Transformation was done as described previously and the transformation host plant was line G4 (Matton *et al.*, 1997). The *ScHT-A*$_1$ cDNA was cloned in antisense orientation downstream of a CaMV 35S promoter with doubled enhancers (Skuzeski *et al.*, 1990) and flanked by the nos terminator in the pBIN19 vector (Bevan, 1984). For RNA interference experiments, a new vector was constructed. This new vector, called pDARTH (O'Brien and Matton, unpublished), includes a CaMV 35S promoter with doubled enhancers (Skuzeski *et al.*, 1990), an extended multiple cloning site and a 327-bp intron from a histone deacetylase (*HD2*) gene from *S. chacoense* (our unpublished results). The *ScHT-B*$_1$ cDNA sequence (324 bp) was cloned in sense and antisense orientation separated by the *HD2* intron.

Isolation of the ScHT *cDNAs and PCR amplification of other solanaceous* HT *genes*

The *ScHT-A*$_1$, *ScHT-A*$_2$ and *S*$_{14}$*-RNase* cDNAs were initially isolated from a pollinated pistil cDNA library using virtual subtraction (Li and Thomas, 1998). In this procedure, genes corresponding to low-expressed mRNA species are preferentially isolated. Because the initial screen was for rare mRNA species expressed in ovary tissues, and since the library also contained cDNAs expressed in styles, genes that were highly expressed in styles but only weakly expressed in ovaries were also recovered. A second screening round with a probe derived from stylar mRNAs, uncovered all of the stylar expressed genes, including the *ScHT-A*$_1$, *ScHT-A*$_2$ and *S*$_{14}$*-RNase* cDNAs. For the isolation of the *ScHT-B*$_1$ cDNA and of related sequences in other solanaceous species, three degenerate primers were designed based on the most conserved amino acid sequence of *ScHT-A*$_1$ from *S. chacoense* and HT from *N. alata* (McClure *et al.*, 1999). The sequence of the upstream primers (HT-NS1: 5′-TTT CTT TGG TTC TT(A/T) TGA T(A/T)A TAT CAT CA-3′; HT-NS2: 5′-ATA TCA TCA GA(A/G) GTT ATT GC(A/T) AGG GA(A/T) ATG-3′) are derived from the predicted signal peptide sequence, and the sequences of the downstream primers (HT-C1: 5′-TCC TTT ATT CAA CCA AT(C/T) TCA TAT TA-3′; HT-C2B: 5′-CAA AAA TAT TAC ATA ATA TTT TGT AGT CG-3′) are derived from the C-terminus of the HT protein. The *S. chacoense* HT-B1 isoform was obtained by PCR amplification of cDNAs from a pollinated pistil library while HT isoforms from *S. pinnatisectum*, *S. bulbocastanum* and *S. tuberosum* were obtained by PCR amplification of genomic DNA.

Isolation and gel blot analysis of RNA and DNA

Total RNA was isolated as described previously (Jones *et al.*, 1985). RNA concentration was determined by measuring its absorbance at 260 nm and verified by agarose gel electrophoresis following ethidium bromide staining. To confirm equal loading of total RNA on RNA-gel blots, a 1-kb fragment of the *S. chacoense* 18S RNA was PCR amplified and used as a probe (Lantin *et al.*, 1999a). Genomic DNA isolation was performed via a modified CTAB extraction method (Reiter *et al.*, 1992) or with the Plant DNeasy kit from Qiagen. DNA-gel blot analysis, including restriction, electrophoresis and capillary transfer to a positively charged nylon membrane (Hybond N+, Amersham Pharmacia Biotech, Baie D'Urfé, Québec) were performed as described previously (Sambrook *et al.*, 1989). Hybridization of the membrane was performed under high stringency conditions at 65°C as described previously (Church and Gilbert, 1984) for 16–24 h, and following hybridization, the membrane was washed at room temperature twice with 2X SSC/0.1% SDS for 30 min, twice with 1X SSC/0.1% SDS at 50°C for 30 min and twice with 0.1X SSC/0.1% SDS at 55°C for 10 min (1X SSC is 0.15 M

NaCl, 0.015 M sodium citrate, pH 7.0). RNA-gel blot analyses were performed as described in Sambrook *et al.* (1989), following the formaldehyde denaturing protocol. RNAs were capillary transfered to Hybond N+ nylon membranes and cross-linked (120 mJ cm^{-2}) with a Hoefer UVC 500 UV Crosslinker. Hybridization of the membranes was performed under high stringency conditions at 45°C in 50% deionized formamide, 5X Denhardt solution, 0.5% SDS, 200 µg ml^{-1} denatured salmon sperm DNA and 6X SSC for 16–24 h. Following hybridization, the membranes were washed at room temperature twice with 2X SSC/0.1% SDS for 30 min, twice with 1X SSC/0.1% SDS at 50°C for 30 min and twice with 0.1X SSC/0.1% SDS at 55°C for 10 min. Probes for DNA-gel blot analysis were synthesized from random-labeled isolated DNA inserts (Roche Diagnostic, Laval, Québec) with α-^{32}P dCTP (ICN Biochemicals, Irvine, CA). For RNA-gel blot analyses, cDNA probes were made with α-^{32}P dATP with the Strip-EZ DNA labeling kit (Ambion, Austin, TX) and oligonucleotide probes were labeled with γ-^{32}P dATP (Sambrook *et al.*, 1989). The membranes were autoradiographed at −85°C with one intensifying screen on Kodak Biomax MR film (Interscience, Markham, Ontario).

Site-directed mutagenesis of the S_{11}-RNase and yeast two-hybrid analysis

A mutated S_{11}-RNase gene with the conserved His-114 residue (CAT) located in the C3 active site domain was converted to a leucine residue (CTT) by site-directed mutagenesis using the following oligonucleotide (mutated nucleotide is underlined): 5′-CTAAAGCTTGGATCCTGCTGT-3′ (Altered sites II *in vitro* mutagenesis system, Promega, WI). The original construct contained both the S_{11} intron and 3′ end of the gene, and was expressed in transgenic *S. chacoense* plants (Matton *et al.*, 1997; Matton *et al.*, 1999) under the control of the style specific chitinase promoter (Harikrishna *et al.*, 1996). The spliced His^- S_{11}-RNase cDNA was recovered from reversed transcribed style mRNAs, and the coding region corresponding to the mature protein was PCR amplified (Pwo DNA polymerase, Roche Diagnostics, Laval, Québec) and fused in frame with the DNA-binding domain of the GAL4 protein in the pBDGAL4 yeast vector (TRP1 selection marker) (Stratagene, LaJolla, CA). The *ScHT-A*$_1$ coding region was PCR amplified with or without the predicted signal peptide and inserted in frame with the GAL4 activation domain in the pADGAL4 vector (LEU2 selection marker). For the *ScHT-B* construct, only the coding region without the predicted signal peptide was inserted in frame with the GAL4 activation domain in the pADGAL4 vector. Integrity of the DNA constructs was verified by sequencing. The constructs were transformed sequentially in the yeast strain PJ69-4A (James *et al.*, 1996) and selected through their ability to grow on Trp^- and Leu^- media. Protein–protein interaction assays were performed on media lacking Trp, Leu and His and on media lacking Trp, Leu and Ade.

Acknowledgements

We thank Dr Qin Chen (Agriculture and Agri-Food Canada, Lethbridge Research Centre, AB) for the gift of *S. pinnatisectum* and *S. bulbocastanum* plants; Dr Mario Cappadocia for the segregating population DNA (Université de Montréal, Montréal, Québec); Dr Philip James (University of Wisconsin, Madison, WI) for the gift of the PJ69-4A yeast strain; Mrs Annie Archambault for her help with the phylogenetic analysis and Mr Gabriel Téodorescu for plant care and maintenance. This work was supported by the Natural Sciences and Engineering Research Council of Canada and by Le Fonds pour la Formation des Chercheurs et l'Aide à la Recherce (FCAR, Québec).

References

Ai, Y., Kron, E. and Kao, T.-H. (1991) *S-alleles are retained and expressed in a self-compatible cultivar of* Petunia hybrida. *Mol. Gen. Genet.* **230**, 353–358.

Anderson, M.A., Cornish, E.C., Mau, S.-L. *et al.* (1986) Cloning of cDNA for a stylar glycoprotein associated with expression of self-incompatibility in *Nicotiana alata*. *Nature*, **321**, 38–44.

Bernatzky, R., Glaven, R.H. and Rivers, B.A. (1995) S-related protein can be recombined with self-compatibility in interspecific derivatives of *Lycopersicon*. *Biochem. Genet.* **33**, 215–225.

Bevan, M. (1984) Binary *Agrobacterium* vectors for plant transformation. *Nucl. Acids Res.* **12**, 8711–8721.

Cheung, A.Y. (1996) The pollen tube growth pathway: its molecular and biochemical contributions and responses to pollination. *Sex. Plant Reprod.* **9**, 330–336.

Church, G.M. and Gilbert, W. (1984) Genomic sequencing. *Proc. Natl Acad. Sci. USA*, **81**, 1991–1995.

Cornish, E.C., Pettitt, J.M., Bonig, I. and Clarke, A.E. (1987) Developmentally controlled expression of a gene associated with self-incompatibility in *Nicotiana alata*. *Nature*, **326**, 99–102.

Deurenberg, J.J.M. (1976) *In vitro* protein synthesis with polysomes from unpollinated, cross- and self-pollinated *Petunia* ovaries. *Planta*, **128**, 29–33.

Dodds, P.N., Fergurson, C., Clarke, A.E. and Newbigin, E. (1999) Pollen-expressed S-RNases are not involved in self-incompatibility in *Lycopersicon peruvianum*. *Sex. Plant Reprod.* **12**, 76–87.

van Doorn, W.G. (2002a) Does ethylene treatment mimic the effects of pollination on floral lifespan and attractiveness? *Ann. Bot. (London)*, **89**, 375–383.

van Doorn, W.G. (2002b) Effect of ethylene on flower abscission: a survey. *Ann. Bot. (London)*, **89**, 689–693.

Gilissen, L.J.W. (1977) Style-controlled wilting of the flower. *Planta*, **133**, 275–280.

Gilissen, L.J.W. (1984) Pollination-induced corolla wilting in *Petunia hybrida*. Rapid transfer through the style of a wilting-inducing substance. *Plant Physiol.* **75**, 496–498.

Golz, J.F., Clarke, A.E. and Newbigin, E. (2000) Mutational approaches to the study of self-incompatibility. Revisisiting pollen-part mutants. *Ann. Bot.* **85**, 95–103.

Hall, I.V. and Forsyth, F.R. (1967) Production of ethylene by flowers following pollination and treatment with water and auxin. *Can J. Bot.* **45**, 1163–1166.

Harikrishna, K., Jampates-Beale, R., Milligan, S. and Gasser, C. (1996) An endochitinase gene expressed at high levels in the stylar transmitting tissue of tomatoes. *Plant Mol. Biol.* **30**, 899–911.

Hosaka, K. and Hanneman, R.E. (1998a) Genetics of self-compatibility in a self-incompatible wild diploid potato species *Solanum chacoense*. Part 2. Localization of an *S slocus inhibitor* (*Sli*) gene on the potato genome using DNA markers. *Euphytica*, **103**, 265–271.

Hosaka, K. and Hanneman, R.E. (1998b) Genetics of self-compatibility in a self-incompatible wild diploid potato species *Solanum chacoense*. Part 1. Detection of an *S slocus inhibitor* (*Sli*) gene. *Euphytica*, **99**, 191–197.

James, P., Halladay, J. and Craig, E.A. (1996) Genomic libraries and a host strain designed for highly efficient two-hybrid selection in yeast. *Genetics*, **144**, 1425–1436.

Jones, J.D.G., Dunsmuir, P. and Bedbrook, J. (1985) High-level expression of introduced chimeric genes in regenerated transformed plants. *EMBO J.* **4**, 2411–2418.

Kao, T.-H. and McCubbin, A. (1996) How flowering plants discriminate between self- and non-self pollen to prevent inbreeding. *Proc. Natl Acad. Sci. USA*, **93**, 12059–12065.

Kondo, K., Yamamoto, M., Itahashi, R., Sato, T., Egashira, H., Hattori, T. and Kowyama, Y. (2002a) Insights into the evolution of self-compatibility in *Lycopersicon* from a study of stylar factors. *Plant J.* **30**, 143–154.

Kondo, K., Yamamoto, M., Matton, D.P., Sato, T., Hirai, M., Norioka, S., Hattori, T. and Kowyama, Y. (2002b) Cultivated tomato has defects in both *S-RNase* and *HT* genes required for stylar function of self-incompatibility. *Plant J.* **29**, 627–636.

Lantin, S., O'Brien, M. and Matton, D.P. (1999a) Pollination, wounding and jasmonate treatments induce the expression of a developmentally regulated pistil dioxygenase at a distance, in the ovary, in the wild potato *Solanum chacoense* Bitt. *Plant Mol. Biol.* **41**, 371–386.

Lantin, S., O'Brien, M. and Matton, D.P. (1999b) Fertilization and wounding of the style induce the expression of a highly conserved plant gene homologous to a *Plasmodium falciparum* surface antigen in the wild potato *Solanum chacoense* Bitt. *Plant Mol. Biol.* **41**, 115–124.

Lee, H.S., Huang, S. and Kao, T.-H. (1994) S proteins control rejection of incompatible pollen in *Petunia inflata*. *Nature*, **367**, 560–563.

Li, Z. and Thomas, T.L. (1998) PEI1, *an embryo-specific zinc finger protein gene required for heart-stage embryo formation in* Arabidopsis. *Plant Cell*, **10**, 383–398.

Llop-Tous, I., Barry, C.S. and Grierson, D. (2000) Regulation of ethylene biosynthesis in response to pollination in tomato flowers. *Plant Physiol.* **123**, 971–978.

Luu, D.T., Qin, X., Morse, D. and Cappadocia, M. (2000) S-RNase uptake by compatible pollen tubes in gametophytic self-incompatibility. *Nature*, **407**, 649–651.

Matton, D.P., Bertrand, C., Laublin, G. and Cappadocia, M. (1998) Molecular aspects of self-incompatibility in tuber-bearing *Solanum* species. In *Comprehensive Potato Biotechnology* (Khurana, S.M.P., Chandra, R. and Upadhya, M.D., ed.). New Delhi, India: Malhotra Publishing House, pp. 97–113.

Matton, D.P., Luu, D.T., Xike, Q., Laublin, G., O'Brien, M., Maes, O., Morse, D. and Cappadocia, M. (1999) Production of an S-RNase with dual specificity suggests a novel hypothesis for the generation of new *S*-alleles. *Plant Cell*, **11**, 2087–2097.

Matton, D.P., Maes, O., Laublin, G., Xike, Q., Bertrand, C., Morse, D. and Cappadocia, M. (1997) Hypervariable domains of self-incompatibility RNases mediate allele-specific pollen recognition. *Plant Cell*, **9**, 1757–1766.

McClure, B.A., Haring, V., Ebert, P.R., Anderson, M.A., Simpson, R.J., Sakiyama, F. and Clarke, A.E. (1989) Style self-incompatibility products of *Nicotiana alata* are ribonucleases. *Nature*, **342**, 955–957.

McClure, B.A., Mou, B., Canevascini, S. and Bernatzky, R. (1999) A small asparagine-rich protein required for *S*-allele-specific pollen rejection in *Nicotiana*. *Proc. Natl Acad. Sci. USA*, **96**, 13548–13553.

Murfett, J., Atherton, T.L., Mou, B., Gasser, C.S. and McClure, B.A. (1994) S-RNase expressed in transgenic *Nicotiana* causes *S*-allele-specific pollen rejection. *Nature*, **367**, 563–566.

Murfett, J., Strabala, T.J., Zurek, D.M., Mou, B., Beecher, B. and McClure, B.A. (1996) S-RNase and interspecific pollen rejection in the genus *Nicotiana*: multiple pollen-rejection pathways contribute to unilateral incompatibility between self-incompatible and self-compatible species. *Plant Cell*, **8**, 943–958.

de Nettancourt, D. (1977) *Incompatibility in Angiosperms*. New York: Springler-Verlag.

de Nettancourt, D. (1997) Incompatibility in angiosperms. *Sex. Plant Reprod.* **10**, 185–199.

Nielsen, H., Engelbrecht, J., Brunak, S. and von Heijne, G. (1997) Identitfication of prokaryotic and eukaryotic signal peptides and prediction of their cleavage sites. *Protein Eng.* **10**, 1–6.

Reiter, R.S., Young, R.M. and Scolnik, P.A. (1992) Genetic linkage of the *Arabidopsis* genome: methods for mapping with recombinant inbreds and Random Amplified Polymorphic DNAs (RAPDs). In *Methods in Arabidopsis Research* (Koncz, C., Chua, N.-H. and Schell, J., eds). Singapore: World Scientific Publishing Co., pp. 170–190.

Ricks, C.M. and Chetelat, R.T. (1991) The breakdown of self-incompatibility in *Lycopersicon hirsutum*. In *Solanaceae III: Taxonomy, Chemistry, Evolution* (Hawkes, J.G., Lester, R.N., Nee, M. and Estrada, N., ed.). London: Royal Botanic Garden Kew and Linnean Society of London, pp. 253–256.

Rivard, S.R., Saba-El-Leil, M.K., Landry, B. and Cappadocia, M. (1994) RFLP analyses and segregation of molecular markers in plants produced by *in vitro* anther culture, selfing and reciprocal crosses of two lines of self-incompatible *Solanum chacoense*. *Genome*, **37**, 775–783.

Royo, J., Kunz, C., Kowyama, Y., Anderson, M., Clarke, A.E. and Newbigin, E. (1994) Loss of a histidine residue at the active site of *S*-locus ribonuclease is associated with self-compatibility in *Lycopersicon peruvianum*. *Proc. Natl Acad. Sci. USA*, **91**, 6511–6514.

Sambrook, J., Fritsch, E.F. and Maniatis, T. (1989) *Molecular Cloning: a Laboratory Manual*. Cold Spring Harbor, New York: Cold Spring Harbor Laboratory Press.

Schopfer, C.R., Nasrallah, M.E. and Nasrallah, J.B. (1999) The male determinant of self-incompatibility in *Brassica*. *Science*, **286**, 1697–1700.

Singh, A., Evensen, K.B. and Kao, T.-H. (1992) Ethylene synthesis and floral senescence following compatible and incompatible pollinations in *Petunia inflata*. *Plant Physiol.* **99**, 38–45.

Skuzeski, J.M., Nichols, L.M. and Gesteland, R.F. (1990) Analysis of leaky viral translation termination codons *in vivo* by transient expression of improved β-glucuronidase vectors. *Plant Mol. Biol.* **15**, 65–69.

Stead, A.D. (1992) Pollination-induced flower senescence: a review. *Plant Growth Regul.* **11**, 13–20.

Stone, J.L. (2002) Molecular mechanisms underlying the breakdown of gametophytic self-incompatibility. *Q. Rev. Biol.* **77**, 17–32.

Takayama, S., Shiba, H., Iwano, M., Shimosato, H., Che, F.-S., Kai, N., Watanabe, M., Suzuki, G., Hinata, K. and Isogai, A. (2000) The pollen determinant of self-incompatibility in *Brassica campestris*. *Proc. Natl Acad. Sci. USA*, **97**, 1920–1925.

GenBank accession numbers: *ScHT-A*$_1$ (AF442139), *ScHT-A*$_2$ (AF442140), *ScHT-B*$_1$ (AF442141), StHT-A$_1$ (AF442142), SbHT-B$_1$ (AF442143), SbHT-B$_2$ (AF442144), SpHT-B$_1$ (AF442145), SpHT-B$_2$ (AF442146), LpHT-A$_1$ (AB066582) LpHT-B$_1$ (AB066583), and *S*$_{14}$*-RNase* (AF232304).